Src-Family Kinases Impact Prognosis and Targeted Therapy in Flt3-ITD^{+} Acute Myeloid Leukemia

by

Ravi K. Patel

Bachelor of Science, University of Minnesota, 2013

Submitted to the Graduate Faculty of

School of Medicine in partial fulfillment

of the requirements for the degree of

Doctor of Philosophy

University of Pittsburgh

2019

UNIVERSITY OF PITTSBURGH

SCHOOL OF MEDICINE

This dissertation was presented

by

Ravi K. Patel

It was defended on

May 31, 2019

and approved by

Qiming (Jane) Wang, Associate Professor Pharmacology and Chemical Biology

Vaughn S. Cooper, Professor of Microbiology and Molecular Genetics

Adrian Lee, Professor of Pharmacology and Chemical Biology

Laura Stabile, Research Associate Professor of Pharmacology and Chemical Biology

Thomas E. Smithgall, Dissertation Director, Professor and Chair of Microbiology and Molecular Genetics

Src-Family Kinases Play an Important Role in Flt3-ITD Acute Myeloid Leukemia Prognosis and Drug Efficacy

Ravi K. Patel, PhD

University of Pittsburgh, 2019

Acute myelogenous leukemia (AML) is a disease characterized by undifferentiated bone-marrow progenitor cells dominating the bone marrow. Currently the five-year survival rate for AML patients is 27.4 percent. Meanwhile the standard of care for most AML patients has not changed for nearly 50 years. We now know that AML is a genetically heterogeneous disease and therefore it is unlikely that all AML patients will respond to therapy the same way. Upregulation of protein-tyrosine kinase signaling pathways is one common feature of some AML tumors, offering opportunities for targeted therapy. Important examples include activating mutations in the FLT3 receptor or overexpression of SRC-family kinases expressed in myeloid cells (HCK, FGR, LYN). Inhibition of HCK with the pyrrolopyrimidine kinase inhibitor A-419259 reversed AML cell bone marrow engraftment in patient-derived xenograft mice. Here we show that A-419259 inhibits not only HCK but also FGR, LYN and FLT3 bearing an activating internal tandem duplication (ITD). To investigate the relationship of FLT3, HCK and FGR to the A-419259 response, we generated TF-1 human myeloid cell populations expressing FLT3-ITD either alone or in combination with HCK or FGR. FLT3-ITD alone sensitized TF-1 cells to growth arrest by A-419259, supporting direct action on the FLT3 kinase domain. Cells transformed with inhibitor-resistant FLT3-ITD mutants (D835Y, F691L) were insensitive to A-419259, while co-expression of wild-type HCK or FGR with these FLT3 mutants restored inhibitor sensitivity. Expression of HCK or FGR mutants with engineered A-419259 resistance also decreased inhibitor sensitivity of TF-1/FLT3-ITD cells. To investigate how resistance to A-419259 evolves de novo, we developed populations of FLT3-ITD+ AML cell lines via long-term dose escalation. Whole exome sequencing identified only a single FLT3-ITD kinase domain mutation (N676S) among all A-419259 target kinases in each of six independent resistant cell populations. Thus, the anti-AML activity of A-419259

involves inhibition of FLT3-ITD, HCK and FGR, suggesting that clinical inhibitors targeting all three kinases may enhance efficacy while reducing the probability of acquired resistance.

Table of Contents

List of Tables

List of Figures

List of Abbreviations

ALL- Acute Lymphoid Leukemia

allo-HSCT - allogeneic hematopoietic stem cell transplant

A-Loop- activation loop

AML- Acute Myeloid Leukemia

APL/APML- Acute Promyeloid Leukemia

Ara-C – cytarabine

ATO- Arsenic trioxide

BFLS- Börjeson-Forssman-Lehman syndrome

CAMK- calcium/calmodulin-dependent kinases

CAR-T cells- chimeric antigen receptor T cells

casein kinase like- CK1

CLL- Chronic Lymphoid Leukemia

CML- Chronic Myeloid Leukemia

CR- complete remission

DFG- aspartatae, pheylalanine, glycine motif on the A-loop of kinases

ELN- European LeukemiaNet

ePK- Eukaryotic protein kinase domain

FAB- French American British

FISH- Fluorescence in situ hybridization

FLAG-IDA- fludarabine, cytarabine, G-CSF and idarubicin

FPKM- fragments per kilobase of transcript per million mapped reads

GO- gemtuzumab ozaogamicin

HiDAC - high-dose cytarabine

HSCs- hematopoietic stem cells

IF- immunofluorescence

ITD- internal tandem duplication

KI- kinase insert domain

LSC- Leukemic stem cell

MPD- Myeloproliferative disorder

MPN- myelo-proliferative neoplasm

MRC- myelodysplasia-related changes

MRD- minimal residual disease

nRTK- non-receptor tyrosine kinase

PB- peripheral blood

pTyr- phosphorylated tyrosine

pY416- phospho-tyrosine 416

RTK- Receptor tyrosine kinase

t-AML- therapy-related AML

TCGA- The Cancer Genome Atlas

TKD- tyrosine kinase domain (mutants)

TKL- tyrosine kinase-like

VCF- variant calling file

WES- Whole exome sequencing

WGS- Whole genome sequencing

Acknowledgements

I would like to thank everyone who has helped me in graduate school.

First, I would like to thank my mentor Dr. Thomas Smithgall. Your guidance and mentorship have been immensely helpful during the writing of this thesis and before that. Aside from all of the science lessons I have learned from you, there are many other lessons I have learned. The most important lesson I learned from you early on is separating lab results from your general mood or wellbeing. I always appreciated how much you were open to trying new experimental techniques and how open you were when I brought new ideas or explanations to the table. I appreciate that you encouraged my new ideas, even when after a short discussion we concluded that they were not always the greatest ideas. Continuing with this open mindedness you supported with my future career aspirations even though they may not be the typical path.

I would also like to thank every member of my committee, Dr. Jane Wang, Dr. Vaughn Cooper, Dr. Adrian Lee and Dr. Laura Stabile. Each of you has had more of an impact on my project than you know. You have given very valuable input related to various aspects of my project and I am unsure what direction we would have without all of you.

To everyone in the Smithgall lab, you were all amazing co-workers. It is truly amazing how well everyone in this group gets along. The support you have offered me has been invaluable. Everyone is always willing to do things like offer advice or consolation for failed experiments, but it goes much further than that. I would like to particularly thank Dr. Mark Weir and Dr. Sabine Hellwig for your training in many of the methods that I employed through graduate school. I also would like to thank Kecey Shen for preparation of materials for my project, in particular the difficult to purify FGR proteins. I would also like to thank Winson Li

for help finishing the last few experiments for the paper that will come out of Chapter 3 of this thesis. I would also like to thank Ryan Staudt. It would have been much more difficult to make my codon mutagenesis library if we weren't both making our own libraries at the same time. It was great that we could do the subsequent deep sequencing experiment together too. All the other lab members have been great for advice, ideas and great company.

To all my friends and family, thank you for helping me take my mind of graduate school when experiments aren't working. A particular shout out to my brother Yash, who has helped immensely with coding related problems I have had along the way, especially related to generation of codon mutagenesis primers and current help with analysis of deep sequencing of my codon mutagenesis library.

Lastly, a thank you to my wife, Valerie. Though we have been living apart for the last portion of my graduate career, your help has been great. Especially during the writing of this thesis you have visited me many weekends just to help me pack, clean and cook just so I could focus on writing for a few extra hours. You also put things in perspective whenever I was finishing up writing and needed the emotional support. Thank you so much for your continued support as I move to San Francisco!

1.0 Introduction

1.1 Acute Myeloid Leukemia (AML)

1.1.1 History of AML

The earliest published description of leukemia is from 1827 by Alfred-Arman-Louis Marie Velpeau, who describes a patient with an illness consisting of fever, weakness, urinary stones, and enlargement of liver and spleen. Velpeau was also able to discern that the blood of the patient had a "gruel" like consistency[1]. Eighteen years later, pathologist J.H. Bennet reported a condition called "leucocythemia" to describe a a series of patients with enlarged spleens and differences in the color and consistency of their blood[2].

The first major advances for understanding the disease were made by German pathologist Rudolf Virchow. He used the light microscope to find that the disease, previously described by Velpeau and Bennet, is an excess of white blood cells. Virchow was the first to use the phrase "leukemia"[3]. Further advances that defined AML were made by Wilhelm Ebstein, who distinguished "acute" or fast progressing from "chronic" or indolent leukemia[4], and Otto Naegeli, who separated the leukemias into myeloid and lymphocytic origins[5]. The first breakthrough treatment for AML was developed in 1973 by Yates and Colleagues. This treatment, known as the 7+3 chemotherapy regimen,[6] remains as the stand of care treatment for most AML patients today and is discussed further in section 1.1.7.1.

1.1.2 Epidemiology of AML

Acute Myeloid Leukemia (AML) is a rare, but deadly type of cancer. There are approximately 20,000 new cases of AML every year in the USA and approximately 11,000 deaths[7]. This means that AML accounts for one-third of all adult leukemia cases, but accounts for nearly one-half of all leukemia-related deaths[7]. While AML is a common type of leukemia in adults, it is much rarer in children. The median age of AML onset is 63 years of age, and AML tends to be more lethal in the elderly population due to limitations of chemotherapy in older patients. In fact, in the 65 and older population, there is only a 10% five-year survival rate[8]. Approximately 10-20% of AML cases are believed to be therapy-onset AML, which are believed to be caused by previous administration of chemotherapy to the patient for another form of cancer[9].

1.1.3 Morphology and classification of AML

Acute Myeloid Leukemia (AML) is distinguished from other leukemias by its morphology. Further, many AML classification systems rely of the morphology of the tumor to make subtypes. AML typically appears as an overpopulation of morphologically normal, immature white blood cells within the bone marrow, blood stream and spleen. These cells are much larger than normal, functional and differentiated white blood cells. AML cells may contain multiple nucleoli and often have large cytoplasms. Azurophilic granules, as well Auer rods formed from their fusion, are present within the cytoplasm of approximately 50% of AML cases and represent one of the definitive ways to diagnose AML. Therapeutic responses and cytogenetic changes also vary greatly with morphology..

In this section we will dive deep into the different method used to classify AML. The French-American-British system (FAB) is based solely on cellular morphology, while the World Health Organization (WHO) classification is based on both morphology and cytogenetics. The European LeukemiaNet (ELN) classification system relies on cytogenetics and mutations to assign optimal treatment and expected prognosis.

1.1.3.1 French-American-British classification

The French-American-British Classification (FAB) is primarily based on histochemical staining and immunologic phenotyping, and are related to certain cytogenetic patterns or correlated to response to therapy. FAB classification was initially introduced in 1976[10] with six classifications identified, while later iterations of the FAB classification system now include between nine and twelve classifications[11–13].

The first FAB class is M0, which is minimally differentiated AML[12]. This includes approximately 7% of all AML cases. This class can easily be confused with Acute Lymphocytic Leukemia (ALL) because it is negative for many histochemical stains. Immunologic staining is often the only way to differentiate AML FAB M0 from ALL. M0 tumors are often even negative for the cell-surface marker CD34, which is associated with most normal hematopoietic progenitors as well as malignant blast cells that are more “stem cell-like”. M0 AML is not associated with any particular cytogenetic profile and is typically resistant to chemotherapy[12,14].

FAB M1 and M2 are quite similar to each other, differing only in how much the tumor cells are differentiated. In M1 AML less than 10% of the cells have differentiated beyond the promyelocyte. There is no association of cytogenetic feature, age, gender or clinical feature with M1 AML. About 25% of M2 AML has a translocation between chromosomes 8 and 21 [t(8;21)(q22;22)]. This translocation is almost exclusive to M2 AML and associated with

favorable response to chemotherapy. The translocation results in fusion of the *RUNX1* and *RUNX1T1* genes[15]. The translocation blocks differentiation by removing the ability of *RUNX1* to induce transcription, while still allowing for the recruitment of co-repressors[16].

AML with the M3 FAB classification is also known as Acute Promyelocytic Leukemia (APL/APML). APL is characterized by translocations involving the retinoic acid receptor α (RARα). These translocations result in an accumulation of granulocytes and promyelocytes. The disease was first characterized in 1957[17], with median survival times of less than one week[18]. Now the disease is treated with All-trans-retinoic acid (ATRA; tretinoin) and 10-year survival rates are 90%[19]. This drug has an interesting mechanism of action, in that it induces terminal differentiation of the leukemic blasts.

FAB M4 AML is called myelomonocytic AML. In this subtype, greater than 20% of the tumor cells are monocytic in nature[20]. This subtype is also not associated with particular cytogenetic changes or clinical outcomes.

When patients with acute myelomonocytic leukemia also have 5-10% eosinophils within their tumor, they are described as FAB M4EO. Almost all M4EO AMLs have a pericentric inversion or homologous translocation involving chromosome 16q22[21,22]. The resulting fusion protein is between Core Binding factor β (CBF-β) and the smooth muscle myosin heavy chain. The fusion protein probably recruits nuclear co-repressors which likely results in prevention of transcription of genes required for myeloid differentiation, similar to the t(8;21) discussed for M2 AML. Patients with inv16 respond very well to chemotherapy, but its unclear why[23].

There are two variants of monocytic leukemia, M5 FAB. M5a blasts have rounder nuclei and less signs of differentiation. M5b blasts are at least 20% promonocytes and show some degree of differentiation. Patients with M5 AML tend to present with a high blast count at

diagnosis and are much less likely to respond to therapy. Those patients with M5 AML that do respond to therapy are more likely to relapse. The most frequent translocation in M5 AML involves chromosome 11 band q23 at the lysine methyl transferase 2A (KMT2A/MLL1) gene. KMT2A is a transcriptional coactivator involved in differentiation and development in early hematopoietic cells[24].

Erythroleukemia is known as M6 AML. There are two subtypes of M6 AML. This disease is rarely purely erythrocytic (M6b), but rather a mixture of myeloid and erythroid blasts (M6a). The erythroid cells frequently have abnormalities such as megablastosis, multi-nuclearity, karyorrhexis and frequent mitosis. There are no distinct clinical or karyotypic features associated with FAB M6.

A particularly rare type of leukemia is M7 FAB. These tumors are predominantly of the megakaryocytic lineage. Not much is known about the linkage of this subtype to karyotype, but FAB M7 is associated with poor prognosis.

Lastly, FAB M8 is the designation for Acute basophilic leukemias. These are difficult to classify as they have features of both myeloid and lymphoid cells. These tumors are believed to be even less differentiated than M0 tumors[13]. In many cases M8 AML is treated with the ALL protocol instead.

Table 1 shows a summary of FAB classification of AML. The percentages of AML cases with each subtype are taken from Seiter et al.[25], but that study did not count the instances of FAB M8 AML.

Table 1. FAB subtypes summary

Type	Name	Affiliated Cytogenetics	Percentage of adult AML within this Type
M0	Acute myeloblastic leukemia, minimally differentiated	None	5%
M1	Acute myeloblastic leukemia, without maturation	None	15%
M2	Acute myeloblastic leukemia with granulocytic maturation	t(8;21)(q22;q22), t(6;9)(p22;q34)	25%
M3	Promyelocytic, or acute promyelocytic leukemia (APL)	t(15;17)(q24;q21)	10%
M4	Acute myelomonocytic leukemia	inv(16)(p13q22), del(16q)	20%
M4eo	Myelomonocytic with bone marrow eosinophilia	inv(16)(p13q22), t(16;16)	5%
M5	Acute monoblastic leukemia (M5a) or acute monocytic leukemia (M5b)	del(11q), t(9;11)(p21;q23), t(11;19)(q23;p13)	10%
M6	Acute erythroid leukemias, subtypes include erythroleukemia (M6a) and the very rare pure erythroid leukemia (M6b)	None	5%
M7	Acute megakaryoblastic leukemia	t(1;22)(p13;q13)	5%
M8	Acute basophilic leukemia	None	unknown

1.1.3.2 The World Health Organization (WHO) classification

The world health organization (WHO) specifies AML disease entities by focusing on molecular genetic and cytogenetic subgroups. WHO defines six major classes of AML and each class has several subclasses. The WHO Blue handbook gives a preferred treatment for each subtype as well[26]. While the WHO classification system is more comprehensive than FAB system, it still leaves out many prognostically relevant mutations, including prognostically

relevant activating mutations to FLT3 receptor tyrosine kinase or the transcriptional regulator, ASXL1.

The first major group identified is AML with recurrent genetic abnormalities. The different types of cytogenetic changes and mutations recognized by WHO are listed in Table 2.

Table 2. WHO AML with recurrent genetic abnormalities

Genetic abnormality recognized
t(8;21)(q22;q22.1);RUNX1-RUNX1T1 inv(16)(p13.1q22) or t(16;16)(p13.1;q22);CBFB-MYH11
APL with PML-RARA
t(9;11)(p21.3;q23.3);MLLT3-KMT2A
t(6;9)(p23;q34.1);DEK-NUP214
inv(3)(q21.3q26.2) or t(3;3)(q21.3;q26.2); GATA2, MECOM
Megakaryoblastic AML with t(1;22)(p13.3;q13.3);RBM15-MKL1
BCR-ABL1
mutated NPM1
biallelic mutations of CEBPA
mutated RUNX1

The next WHO classification is AML with myelodysplasia-related changes (AML-MRC), which is associated with poor prognosis. There are several known cytogenetic changes that occur within AML-MRC, but most of these indicate that the disease was likely preceded by myelodysplastic syndrome (MDS)[26].

WHO recognizes therapy-related myeloid neoplasms (t-MN) as another category of AML. Although the mechanism is yet to be proven, it is believed that t-MN is caused by previous exposure to chemotherapy. The therapy-related AML (t-AML) can take months or years to arise, depending on the dose and type of chemotherapy used. NQO1, which encodes an

NAP(P)H quinone dehydrogenase, is mutated more frequently in t-AML than in *de novo* AML[27]. In general, though it is very difficult to study the t-AML since it is rare, and often not immediately linked to previous chemotherapy. There may be a lot to discover about the differences between t-AML and *de novo* AML.

The next WHO class of AML is "not otherwise specified" (NOS). NOS AML cases do not fit within the cytogenetic changes, AML-MRC or t-AML. The NOS-AML class is further subdivided in a manner similar to the FAB system[28]. The subclasses are listed in Table 3.

Table 3. AML-NOS subclasses.

NOS-AML Subclasses
AML with minimal differentiation
AML without maturation
AML with maturation
Acute myelomonocytic leukemia
Acute monoblastic/monocytic leukemia
Pure erythroid leukemia
Acute megakaryoblastic leukemia
Acute basophilic leukemia
Acute panmyelosis with myelofibrosis

The remaining WHO AML classes are quite unique. Myeloid sarcoma is a type of AML that includes a solid tumor, as well as peripheral blood (PB) and bone marrow involvement. Myeloid sarcomas can be present *de novo* or be present in a relapsed AML. Myeloid sarcomas

can also be a result of a prior myelodysplastic syndrome (MDS) or myelo-proliferative neoplasm (MPN)[26,29].

The last WHO category includes myeloid proliferation related to Down syndrome. The two subclasses include transient abnormal myelopoiesis (TAM) and myeloid leukemia associated with Down syndrome. TAM occurs at birth or within a few days of birth and is usually resolved within a matter of months. Myeloid leukemia associated with Down syndrome occurs later but still during infancy[30,31]. Both subclasses usually have a megakaryoblastic phenotype and are characterized by mutations in the GATA1 transcription factor and JAK-STAT signaling pathway[32].

1.1.3.3 European LeukemiaNet (ELN) classification

The European LeukemiaNet (ELN) is another set of guidelines for diagnosing and managing AML. While similar to the WHO classification, there is more emphasis on the genetics of the cancer. ELN describe that a full two-thirds of the variation of patient prognosis can be explained by genetic lesions alone[33]. Most of the translocations have already been discussed in the FAB and WHO sections so they will not be discussed again here. The mutations will be discussed in the next section. In general, the ELN classification system is easy to understand and the summary table from Döhner *et al*., Blood 2017 is presented in Table 4.

While the ELN system is the easiest to understand and the most comprehensive classification system in terms of the information considered, it is still not perfect. As I will discuss in Chapter 2, gene expression changes can also be highly predictive of patient prognosis.

1.1.4 Genomic landscape of AML

Until now this thesis has focused mainly on cytogenetic changes within AML. However, in the last 10 years there has been an explosion of molecular genetic information reported for AML. This began in 2008 when the first whole cancer genome was sequenced. Ley et al. were able to sequence an entire cancer genome of a cytogenetically normal AML case and matching DNA from skin cells of the same patient[34]. Since that time AML has somewhat lagged behind in sequencing information compared to the more common cancer types, such as breast or colon. Regardless, there have been some major breakthroughs.

Table 4. ELN risk classification summary

Risk Category	Genetic Abnormality
Favorable	t(8;21)(q22;q22.1); RUNX1-RUNX1T1 inv(16)(p13.1q22) or t(16;16)(p13.1;q22); CBFB-MYH11 Mutated NPM1 without FLT3-ITD or with FLT3-ITDlow Biallelic mutated CEBPA
Intermediate	Mutated NPM1 and FLT3-ITDhigh Wild-type NPM1 without FLT3-ITD or with FLT3-ITDlow (without adverse-risk genetic lesions) t(9;11)(p21.3;q23.3); MLLT3-KMT2A Cytogenetic abnormalities not classified as favorable or adverse
Adverse	t(6;9)(p23;q34.1); DEK-NUP214 t(v;11q23.3); KMT2A rearranged t(9;22)(q34.1;q11.2); BCR-ABL1 inv(3)(q21.3q26.2) or t(3;3)(q21.3;q26.2); GATA2,MECOM(EVI1) -5 or del(5q); -7; -17/abn(17p) Complex karyotype, monosomal karyotype| Wild-type NPM1 and FLT3-ITDhigh Mutated RUNX1 Mutated ASXL1 Mutated TP53

The first large-scale genomic study of AML was published in 2011 by Marcucci et al. This group used a microarray platform to determine mutation status and gene expression profiles of AML tumors[35]. This was the first ever attempt to correlate expression of certain genes to clinical outcomes in AML. Unfortunately, this study did not make clear how many tumors were processed, what proportion of tumors carried each mutation, or how often mutations co-occur within the same tumor. Furthermore, there are the downsides of array-based systems, such as sensitivity and saturation of signal when measuring gene expression. In 2012, Patel and colleagues published a study in which 18 AML-associated genes were sequenced in nearly 400 patients. The goal of this study was to correlate specific mutations with clinical data, such as survival or whether the patient responded better to a higher dose of chemotherapy. This study yielded a clearer picture of the distribution and co-occurrences of mutations in these 18 genes. Remarkably, they were able to find somatic alterations in 97.3% of patients in just the 18 genes they targeted, plus the cytogenetic profiles[36].

The next large-scale functional genomic study of AML was published in 2013 as part of The Cancer Genome Atlas (TCGA)[37] project. TCGA was a very comprehensive study that included whole genome sequencing (WGS) of 50 AML cases, whole exome sequencing (WES) of 150 cases, mRNA sequencing of 163 cases (from both the WGS and WES cohorts), micro-RNA sequencing (miRNAseq) and DNA methylation analysis. WGS and WES sequencing in 200 patients gave a clearer picture of exactly how many genes were recurrently mutated in AML. While 237 genes were found to be mutated in more than one AML patient, only 23 genes showed significant mutations in excess of random variation. TCGA also reveals that AML genomes in general have far fewer mutations in the exome than other adult cancers. In fact, the average AML case has only 13 mutations, with only 5 in genes recurrently mutated in AML. Similar to Patel *et*

al., TCGA also reported co-occurrence and mutual exclusivity analysis of mutations. Broadly speaking, the mutations fall into 9 distinct classes and mutations within a particular class are mutually exclusive. For example, 59% of the tumors had mutations predicted to cause activated signaling, but it is unlikely that any single tumor had multiple mutations that caused activated signaling. In other words, it is highly unlikely that a given tumor would have activating mutations in both *FLT3* and *RAS*[37]. Shortly after the TCGA study was published, Papaemmanuil *et al*. published a study in which the driver mutations and cytogenetics were distributed into 11 unique molecular groups in AML[38]. However, aside from IDH2 and PML-RARα, the molecular subtypes do not necessarily represent groups that may respond to a particular targeted therapy. For example, internal tandem duplications in the FLT3 receptor tyrosine kinase (FLT3-ITD), widely believed to define a useful drug target[39], are represented in 9 of the 11 classes.

In 2018, the Therapeutically Applicable Research to Generate Effective Treatments (TARGET) AML group published a study comparable to TCGA, but for pediatric AML. This study, in which nearly 1000 AML cases were analyzed, confirmed on the molecular level that AML varies considerably with age. The types of mutations in infants are different than those found in children or young adults. All pediatric AML differs greatly from adult AML. For example, gene fusions involving the splicing factor MBNL1 and the transcriptional regulators, ZEB2 and ELF1, were much more prevalent in pediatric AML compared to adult AML. Additionally, DNMT3A and TP53 mutations, which are among the most common mutations in adult AML, were almost completely absent from pediatric AML[40]. These differences may account for the large difference in survival and prevalence of pediatric and adult AML. We will focus on adult AML for the remainder of this thesis.

In 2013, Kandoth *et al*. published a comparative study of TCGA data from 12 distinct tumor types. Strikingly AML tumors had far fewer mutations per tumor than any other tumor type. Interestingly, AML does not have less mutations in frequently mutated genes per tumor. On average, AML tumors have 2 mutations in significantly mutated genes, which is the same as breast cancer, ovarian cancer, glioblastoma, and kidney renal cell carcinoma. Furthermore, aside from TP53, KRAS and NRAS, the genes that were most frequently mutated in AML were mostly uniquely mutated in exclusively AML[41].

The most recent landmark AML genomic study was the first publication from the BEAT AML master clinical trial. This study's goal was to link genetic lesions and gene expression to *ex vivo* drug sensitivity to 122 different therapies. The ultimate goal of BEAT AML is to predict which therapy a given tumor will respond to before the patient is given any treatment. They performed WES, RNAseq and *ex vivo* drug screening for 672 tumors from 562 AML patients. As a validation of targeted therapy in AML, they were able to link mutations with response to particular targeted therapy. For example, the strongest association was the presence of FLT3-ITD mutations with response to FLT3 kinase inhibitors such as sorafenib, quizartinib, and crenolanib. They were also able to link gene expression with drug sensitivity. For example, sensitivity to the kinase inhibitor Ibrutinib is correlated with the expression of seventeen different genes[42]. Interestingly, mutations seem to give a yes or no indicator as to whether the tumor will respond to the drug, whereas gene expression has some predictive power as to what the extent of the response will be.

Table 5 has a summary of the frequency of specific types of mutations according to TCGA[37].

Table 5. Frequency of commonly mutated genes in AML TCGA

Category	Gene Mutated (or fusion)	Mutation Frequency (%)
Transcription factor fusions	PML-RARα	6.5
	MYH11-CBFβ	5.0
	RUNX1-RUNX1T1	4.8
	PICALM-MLLT10	1.1
NPM1	NPM1	27.8
Tumor suppressors	TP53	7.5
	WT1	6.4
	PHF6	3.2
DNA methylation	DNMT3A	23.5
	DNMT3B	1.1
	DNMT1	0.5
	TET1	1.1
	TET2	8.0
	IDH1	9.6
	IDH2	10.2
Activated signaling	FLT3	28.9
	Kit	3.7
	Other Tyr kinases	4.5
	Ser-Thr kinases	12.5
	KRAS/NRAS	12.3
	Protein tyrosine phosphatases	6.3
Myeloid transcription factors	RUNX1	9.1
	CEBPA	6.4
	Other myeloid Transcription factors	6.5
Chromatin modifiers	MLL-X fusions	3.7
	MLL-PTD	1.6
	NUP98-NSD1	0.5
	ASXL1	2.7
	EZH2	1.6
	KDM6A	1.6
	Other modifiers	14.5
Cohesion	Cohesion	12.5
Spliceosome	Spliceosome	13.5

The remainder of section 1.1.4 will focus on what is known about individual genes that commonly undergo translocations or are mutated in AML.

1.1.4.1 Recurrently translocated transcription factor genes

PML-RARα

As discussed previously, translocation of Chr15q24 with Chr17q21 results in the fusion of the PML and retinoic acid receptor alpha (RARα) coding sequences. The resulting translocation product, PML-RARα, causes acute promyelocytic leukemia (APL). Because chromosomes 15 and 17 are very similar in size and the q arms have very similar banding, it is preferable to diagnose this translocation using fluorescence *in situ* hybridization (FISH). This translocation is found in approximately 10% of AML patients. There have also been translocations of RARα with other genes, but they all have the same effect. PML is by far the most common translocation partner[43].

Normally RARα is dependent on retinoic acid for its function as a transcription factor (TF). However, the PML- RARα fusion protein has enhanced ability to bind DNA but does not initiate transcription. In fact, both the DNA binding domain and ligand binding domain of RARα are intact in the fusion gene[44]. PML-RARα enhances interaction of nuclear co-repressor (NCORs) and Histone de-acetylases (HDACs), which effectively blocks transcription of genes requires for granulocyte differentiation[45]. While untreated APL is particularly deadly, the targeted therapies ATRA and ATO drastically mitigate this disease. It is now one of the most survivable cancers and the most survivable form of AML. The treatment of APL will be discussed further in the targeted therapies section.

MYH11-CBFB

As discussed previously, an inversion in chromosome 16 results in the translocation of Core binding factor subunit beta (CBFB) and myosin 11 (MYH11). This translocation results in a fusion protein that acts in a dominant-negative fashion against the transcription factor core binding factor (CBF). CBF is considered to be one of the master regulators of hematopoiesis[46]. Interestingly, the MY11-CBFB translocation is associated with a favorable prognosis, even though 90% of cases co-occur with altered Ras signaling[47].

RUNX1-RUNX1T1

Runt related transcription factor 1 (RUNX1) is also known as acute myeloid leukemia 1 protein (AML1) or core-binding factor subunit alpha 2 (CBFA2). RUNX1 is a transcription factor normally involved with the differentiation of hematopoietic cells[48]. The translocation with RUNX1T1 (ETO/AML1T1/CBFA2T1) results in a protein that is able to bind DNA and recruit HDACs and corepressors, but not able to activate gene expression related to cell differentiation. This effectively blocks differentiation[16]. This is mechanism is very similar to the MYH11-CBFB translocation, but the phenotype is different. RUNX1-RUNX1T1 is associated with FAB M2, while MYH11-CBFB is associated with FAB M4eo. Together RUNX1- and CBFB-translocated AMLs are known as core binding factor (CBF) AMLs, since they both cause dysregulation of CBF.

PICALM-MLLT10

The PICALM-MLLT10 translocation is primarily present in T-ALL but is rarely found in AML cases that also express T-cell markers. PICALM is a clatherin assembly protein that recruits clathrin and AP-2. The normal functions of MLLT10 are not well studied. While it is a

transcription factor, the main reason it is known is because it is involved in translocation in several leukemias.

1.1.4.2 Recurrently mutated myeloid transcription factors

RUNX1

I previously discussed the RUNX1 translocation causing FAB M2 AML. However, RUNX1 mutations are also associated with MDS and AML. It is thought that RUNX1 mutations alone can cause MDS, but an additional mutation in genes encoding signaling proteins such as MLL, FLT3 or JAK2 may result in full transformation to AML. *RUNX1* mutations are also associated with other diseases such as Fanconi anemia and congenital neutropenia.

CEBPA

CCAAT enhancer binding protein alpha (CEBPA) is a transcription factor that is required for granulocyte maturation[49]. Most patients that have CEBPA mutations have biallelic mutations that reduce function. This results in cells that are stuck in early differentiated states (FAB M1 or M2). *CEBPA* methylation is also one way in which the gene is inactivated in AML. Both *CEBPA* mutation and methylation are associated with a favorable prognosis[49,50]. Currently, several groups are working towards developing compounds that can induce myeloid differentiation to treat CEBPA-mutant AML[51].

1.1.4.3 NPM1

Nucleophosmin 1 (NPM1) is involved in various cellular processes such as centrosome duplication, ribosome biogenesis, histone assembly, protein chaperoning, cell proliferation and regulation of p53 and ARF[52]. While mutations are known to change the localization of NPM1 to

be only cytosolic[53], the effect of these mutations on NPM1 functions is not completely clear. *NPM1* is one of the most frequently mutated genes in AML. Almost one-third of AML tumors have NPM1 mutations. NPM1 mutations also co-occur with FLT3-ITD and DMT3A mutations[36,37]. NPM1 mutations in general are a positive prognostic indicator, and can even shift the prognosis of FLT3-ITD+ AML from unfavorable to intermediate[33,36].

1.1.4.4 Recurrently mutated DNA methylation genes

DNMT3A and DNMT3B

DNA (cytosine-5)-methyltransferase 3A (DNMT3A) and DNA (cytosine-5)-methyl-transferase 3B (DNMT3B) are two of the three members of the DNMT3 family. DNMT3A is much more frequently mutated in AML than DNMT3B, but both are thought to work in a similar fashion. The normal function of both of these enzymes is transfer of a methyl group to DNA to inactivate genes while the cell is undergoing differentiation, embryonic development, transcriptional regulation, heterochromatin formation, X-chromosome inactivation, imprinting and genome stability[54].

DNMT3A mutations are more frequent in younger patients, and indicate a poor prognosis[55]. DNMT3A mutations likely result in loss of function. These somatic mutations occur as nonsense, frameshift or missense mutations at R882. Mutations of R882 have been shown to decrease DNA binding ability and reduce catalytic function, resulting in continued expression of genes that prevent cell differentiation[56]. DNMT3A mutations co-occur with NPM1, FLT3 and IDH1 mutations[36,37,57]. *DNMT3A* mutations typically occur in only one allele, which suggests that haploinsufficiency is enough to contribute to AML pathogenesis or the mutated gene can function in a dominant negative fashion[58].

TET1 and TET2

The ten eleven translocation genes (TET1, TET2, TET3) encode iron and α-ketoglutarate-dependent methylcytosine dioxygenase enzymes that catalyze the conversion of 5-methylcystine (5-mC) to 5-hydroxymethylcytosine (5-hmC) in DNA[59]. This function of TET1 and TET2 seems to block the binding of DNA methyl transferases to methylated DNA[60]. This is associated with increased expression of the affected gene, especially in embryonic stem cells[61]. TET2 is more frequently mutated in AML, MDS and MPN. AML is the only disease however that TET2 mutations are correlated with a slightly negative prognosis[36]. TET2 mutations typically happen in only one allele, but still result in the loss of function of TET2. The normal TET2 allele is still retained and expressed[60]. Therefore it seems that haploinsufficiency is enough to drive the AML phenotype caused by TET2 mutations[36,37]. Experimental suppression of TET2 activity by shRNA or by knockout results in loss of the ability of hematopoietic cells to differentiate, consistent with a CMML phenotype[62].

IDH1 and IDH2

Isocitrate dehydrogenase 1(IDH1) and isocitrate dehydrogenase 2 (IDH2) are $NADP^+$-dependent enzymes normally involved in the Krebs cycle, where they function to convert isocitrate to α-ketoglutarate. The two enzymes are localized to different part of the cell. IDH1 is found in the cytosol and peroxisomes, while IDH2 is found in mitochondria. IDH1 mutations have been found in many cancer types including glioblastoma, chrondrosarcoma, cholangiocarcinoma, colorectal cancer, thyroid cancer and AML[63]. Based on the discovery of IDH1 mutations, subsequent studies also found IDH2 mutations in AML[64]. IDH mutations occur at conserved arginine residues. IDH1 mutations occur at arginine 132 and IDH2 mutations occur at arginine 140 and 172. While all of these mutations result in a decrease in α-ketoglutarate

production they also result in a new enzymatic activity that converts α-ketoglutarate to 2-hydroxyglutarate (2-HG)[65,66]. As a result, 2-HG is found to be elevated in the serum of AML patients with IDH mutations[65].

When the genomic methylation of IDH mutant AML tumors was studied, it was found that mutations in IDH1/2 correlate with similar methylation patterns as mutations in TET2[67]. Furthermore, mutations in IDH1/2 seem to be mutually exclusive to TET2[37,67]. These data suggest that IDH1/2 and TET2 mutations affect the same pathway. It is now known that 2-HG actually inhibits TET2 and α-ketoglutarate is an essential cofactor of TET2[68,69]. Additionally, 2-HG inhibits α-ketoglutarate-dependent lysine demethylases[68,70]. This agrees with the fact that IDH mutations result in a similar phenotype to TET2 knockdown or knockout[69]. There are other enzymes that require α-ketoglutarate as a cofactor, including enzymes involved in DNA and RNA demethylation, hypoxia sensing, collagen biosynthesis, and lipid biosynthesis[70]. This may mean that IDH mutations may have further reaching consequences than TET2 mutations.

Because IDH mutations are a gain-of-function, it is possible to block altered IDH activity in AML with a small molecule inhibitor. These inhibitors will be discussed further in section 1.1.5.

1.1.4.5 Recurrently mutated tumor suppressor genes

TP53

TP53 encodes p53, the well-known tumor suppressor protein of 53 kDa. *TP53* is one of the most frequently mutated genes in all of cancer, with more than 50% of all tumors (of all types) having *TP53* mutations[71]. While *TP53* mutations are frequent in solid tumors, they are less frequent in AML. The p53 protein can trigger DNA repair at genomic lesions or induce

apoptosis. In AML, Mutations in *TP53* are associated with older patients, but mutations have been observed in all FAB subtypes[72]. There is no gene expression pattern associated with *TP53* mutation[37]. *TP53* mutations are associated with some resistance to chemotherapy, but some patients still respond. *TP53* mRNA is expressed in nearly all patients[37,42] suggesting that loss of p53 function is not the dominant mechanism for AML progression as in several solid tumors.

WT1

Wilms Tumor 1 (*WT1*) is a tumor suppressor gene named after the pediatric kidney malignancy. About 20% of Wilms tumors have mutations in WT1[73]. In addition, WT1 is mutated in other types of cancer including desmoplastic small cell tumor, breast cancer, retinoblastoma, lung carcinoma, and AML[74]. The WT1 protein contains an N-terminal transactivation domain, involved in protein-protein interactions. The C-terminus of WT1 consists of four zinc finger domains. WT1 interacts with many other proteins including p53[75], HSP90[76], STAT3[77], TET2 and TET3[78].

WT1 is expressed in $CD34^+$ $CD38^-$ early undifferentiated hematopoietic progenitor cells[79]. WT1 expression is undetectable in lineage-committed progenitor cells[80]. Overexpression of WT1 in human $CD34^+$ cells results in enhanced differentiation, while overexpression in $CD34^+$ $CD38^-$ cells increased the proportion of cells committed to quiescence[80]. In colony forming assays in methylcellulose, overexpression of WT1 reduced myeloid and erythroid colony formation, while not affecting cell viability[81].

WT1 is overexpressed in both myeloid and lymphoid leukemias[82,83] and MDS[84]. In addition to overexpression of WT1 in the majority of AML cases, it is also frequently mutated in AML[37,85,86]. The vast majority of WT1 mutations result in a stop codons or frameshifts, resulting in loss-of-function and expression of WT1 lacking the zinc-finger domains[36,37,86] and therefore

the ability to bind to DNA. Large-scale genomic studies have revealed that *WT1* mutations are mutually exclusive to TET2 and IDH1/2 mutations[36,37]. Furthermore, WT1-mutated AMLs have a gene methylation profile that overlaps that of TET2-mutated and IDH1/2-mutated AML[87]. Subsequently, WT1 was found to bind to TET2 and enhance its function in the conversion of 5-mC to 5-hmC on DNA. Loss of functional WT1 also greatly reduces TET2 activity[87].

PHF6

PHD finger protein 6 or PHF6, contains 4 nuclear localization signals and two PHD zinc fingers[88]. PHF6 has a proposed role in transcription regulation or chromatin binding[89], but it is the least studied of tumor suppressor genes listed here. Mutations in PHF6 were originally discovered in Börjeson-Forssman-Lehman syndrome (BFLS), a X-linked disease that causes mental retardation[90]. It was later found that PHF6 is mutated in AML cases, predominantly in males[91]. PHF6 mutations occur primarily as nonsense or frameshift mutations, but occasionally point mutations are observed[91]. Mutations in PHF6 are associated with adverse prognosis[36].

1.1.4.6 Recurrently mutated chromatin modifying genes

KMT2A-X Fusions and KMT2A-PTD

Histone-lysine N-methyltransferase 2A (KMT2A), also known as acute lymphoblastic leukemia 1 (ALL-1) or myeloid/lymphoid/mixed-lineage leukemia 1 (MLL1), is a positive global regulator of gene transcription. Specifically, KMT2A tri-methylates histone 3 at Lysine 4. One study found that deletion of KMT2A results in decreased H3K4me3 at 318 genes[92]. This gene has been frequently been shown to be involved with cognition and emotion[92], but mutations in KMT2A have been found in ALL and AML[37].

In frame-translocations involving KMT2A are found in 5-10% of all AML cases and are an indicator of poor prognosis[93,94]. In frame-partial tandem duplications (PTDs) in KMT2A are found in 5-7% of AML and are also associated with a worse prognosis[95–97]. Interestingly, KMT2A rearrangements are much more common in pediatric AML than adult AML[40]. More than 80 different gene fusion partners for KMT2A have been described, but only 6 are frequent[98]. Interestingly, the N-terminal fragment of KMT2A does not recapitulate disease, and the fusion partner is needed[99,100]. The most frequent KMT2A fusion partners are nuclear proteins involved in transcriptional elongation, or proteins that bind to nuclear proteins[101–105]. The most frequent KMT2A fusion partners are ALL1-fused gene from chromosome 4 (AF4), ALL1-fused gene from chromosome 9 (AF9), eleven-nineteen leukemia (ENL), ALL1-fused gene from chromosome 10 (AF10), and ALL1-fused gene from chromosome 17 (AF17)[106].

There have been several hypotheses as to the mechanism by which KMT2A rearrangements drive AML pathogenesis, but none have held up to experimentation. It has been noted that tumors with rearrangements in KMT2A have a unique gene expression profile[107–109], but the exact mechanism is still unknown. The most commonly overexpressed genes in KMT2A-rearranged tumors encode the HOX family of proteins[110]. The HOX gene family encodes transcription factors that are important in early hematopoiesis[111]. Therefore it is thought that the expression of the HOX genes are important in maintaining the 'stemness' of the leukemic blasts in KMT2A-rearranged AML[112,113].

NUP98-NSD1

NUP98 is a component of the nuclear pore complex (NPC), which mediates trafficking between the cytoplasm and the nucleus[114]. NUP98 is anchored to the center of the NPC[115] where it plays a role in protein import[116] and mRNA export[117]. NUP98 also plays a role in transcription.

It is recruited to the promoters of development-related genes in human embryonic stem cells[118]. There are 72 NUP98 fusions present in AML according to atlasoncology.org, of which NSD1 is the most common. NUP98 has an N-terminal GLFG (Glycine-leucine-phenylalanine-glycine) repeat domain which is always preserved in NUP98 fusions[119]. The GLFG domain can act as a transcriptional co-activator[120] or co-repressor[121]. The fusion partners of NUP98 are mainly homeodomain transcription factors, or histone modifying enzymes that contain PHD fingers or SET domains[122]. Some of the fusion partners are from the HOX family of proteins discussed in the KMT2A section[123]. This raises the question of whether the HOX family is central to the role of NUP98 fusions as well.

ASXL1

The additional sex-comb like 1 (ASXL1) locus is mutated in 3-10% of AML cases[37,124]. ASXL1 normally activates or represses HOX genes and also recruits histone methylases to the promoters of certain genes. Furthermore, ASXL1 has been described as a co-activator for the retinoic acid receptor[125]. ASXL contains an N-terminal ASX homology domain and a C-terminal PHD domain[126]. All of the mutations in ASXL1 cause a truncation in the gene that preserve the ASX domain but delete the PHD domain. These mutations are thought to result in a gain of function[127]. The truncated ASXL1 protein can bind to and activate BRD4[128]. This activation of BRD4 causes the acetylation of histones and the activation of gene transcription[129]. This BRD4 activity is thought to drive disease progression in ASXL1-mutant AML. In fact, BET bromodomain inhibitors show some efficacy against ASXL1-mutant AML in vivo[128]. ASXL1 mutations tend to be mutually exclusive of FLT3-ITD or NPM1[36,37,130], but still confer a poor prognosis[36,130].

EZH2

Enhancer of zeste homolog 2 (EZH2) encodes the catalytic subunit of polycomb repressive complex 2 (PRC2). PRC2 is responsible for the repression of target gene expression via tri-methylation of histone 3 lysine 27 (H3K27me3)[131]. PRC2 is required in normal hematopoiesis for replication of adult hematopoietic stem cells (HSCs)[132]. In many lymphomas, there are instances of gain-of-function EZH2 mutations[133], while in AML EZH2 loss of function mutations are more common[134]. It seems that too much EZH2 activity would hold the tumor in a state that is too de-differentiated to rapidly proliferate and therefore loss of some EZH2 activity adds to leukemogenesis[134]. There are inhibitors of EZH2 under development[135], but these are not useful for AML since they are meant to reduce EZH2 activity, not restore it.

1.1.4.7 Spliceosome protein mutations

The spliceosome is an incredibly complex molecular machinery responsible for splicing mRNA to its final form. The spliceosome consists of five small ribonucleoproteins and at least 150 other proteins that recognize the elements that separate intron/exon boundaries. Analysis of TCGA data from multiple tumors reveals that AML has the highest number of alternative splicing events among tumor types[136]. It should be noted that that spliceosome mutations have been found in the peripheral blood of otherwise healthy aging individuals, so it may be that some of these spliceosome mutations confer a selective growth advantage even in the context of normal hematopoiesis[137]. Several mutations in particular spliceosome components have an effect on overall survival in AML[138]. All studied models of spliceosome mutations in mice seem to result in an MDS phenotype, therefore it is likely that spliceosome mutations only contribute to AML rather than drive the disease[138].

1.1.4.8 Cohesion mutations

The cohesion complex is a group of proteins that regulate the separation of sister chromatids during cell division in both mitosis and meiosis. It is well known that mutations in the cohesion complex contribute to chromosomal instability[139]. Mutations in cohesion complex genes are either missense or frameshift mutations[37,140], which implies a loss of function. The clinical outcomes of patients with cohesion mutations are slightly favorable. Mutations in the cohesion complex have no effect on overall survival, but have a slightly favorable effect on relapse-free survival[140].

1.1.4.9 Recurrently activated signaling pathway mutations

FLT3

FMS-related tyrosine kinase 3 (*FLT3*) encodes a receptor tyrosine kinase that is one of the top 3 mutated genes in AML, along with DMT3A and NPM1[36,37,141]. In early stage myeloid and lymphoid cells, FLT3 plays an important role in survival, proliferation and differentiation[142]. The ligand for FLT3 (FLT3 ligand) binds to the extracellular domain of the receptor and activates intracellular signaling[142]. Mutation in *FLT3* predominantly occur as internal tandem duplications (ITDs) in the juxtamembrane domain (JM), which allow for ligand independent activity[143]. FLT3-ITD expression is associated with a very poor prognosis[141], and therefore has been the target of many drug discovery and development efforts[144]. The other type of FLT3 mutation are tyrosine kinase domain point mutations (TKDs), the most common of which is D835Y[36,37]. D835 is located on the activation loop of the kinase domain of FLT3. This mutation also activates FLT3 in a ligand-independent manner, but it should be noted that the extent of activation is much lower than ITD mutations and results in less aggressive tumors[145,146]. This

probably explains why FLT3-D835Y mutations are not prognostically relevant. The biology of FLT3 and the treatment of FLT3-mutated AML will be discussed extensively in chapter 1.2.1.

Kit

The Hardy-Zuckerman 4 Feline Sarcoma Viral Oncogene-Like Protein (better known as KIT) is a receptor tyrosine kinase that is commonly mutated in cancer. Most notably, Kit is mutated in 85% of gastrointestinal stromal tumors (GISTs)[147]. Mutations in Kit also occur in 52% of the Core binding factor (CBF) subtype of AML[148,149] (Table 5). In AML, Kit mutations are most commonly observed in the activation loop of the kinase domain (exon 17) or the extracellular domain, near the transmembrane domain (exon 8). Both of these types of mutations have activating functions[150,151]. Although Kit is an established drug target in AML, there are no FDA approved Kit inhibitors for AML[152], even though there are several approved KIT inhibitors for GIST[153–155]. There have been comparatively few studies studying the efficacy of Kit inhibitors in the clinic compared to FLT3 inhibitors in AML, despite being mutated in 4-10% of AMLs[36,37]. Hopefully trials such as BEAT AML can address the lack of attention to KIT mutations in AML[42].

KRAS/NRAS

The RAS family of small GTPases are expressed in every animal cell type. There are three RAS genes in humans, HRAS, KRAS and NRAS. All three are proto-oncogenes and together they are mutated in 25% of all human cancers, making them the most frequently mutated oncogene [156,157]. In AML, KRAS and NRAS are the RAS genes that are normally expressed. Unlike other cancer types, Ras mutations do not have an association with poor prognosis in adult AML. It should be noted that Ras mutations are associated with a poor

prognosis in childhood AML[158]. RAS activates several signaling pathways including MAP kinase cascades and the PI3K/AKT/mTOR pathway, both of which contribute to its oncogenic activity[159].

While there have not been any successful targeted therapies that act on RAS itself, there are some approaches to inhibit RAS. One strategy is to inhibit kinases that are constitutively active downstream of mutated RAS, such as MEK[160], ERK[161], AKT[162], mTOR[163] or PI3K[164]. Another strategy is to use oncolytic viruses to destroy cancer cells with over-active RAS. These approaches include the use of reovirus[165] or a modified herpes simplex virus[166]. The last approach is to disrupt the farnesylation[156] or palmitoylation[167] of RAS, which interferes with its association with the plasma membrane, thereby disrupting its activity. None of these approaches have been studied in AML, but are actively being pursued in solid tumors with RAS mutations.

In AML, RAS mutations are less frequent than most solid tumors[157], but remains a challenge nonetheless. It should be noted that Ras mutations are associated with certain FAB subtypes[168] and certain cytogenetic changes[168,169].

Protein tyrosine phosphatases

The last class of signaling pathway mutations that we will discuss are protein-tyrosine phosphatases (PTPs). PTPs play a variety of roles in healthy cells. In the context of cancer, PTPs can either be tumor suppressor like or oncogenic[170]. For example, hypermethylation can cause the loss of the expression of two receptor PTPs, PTPRK[171] and PTPRO[172], that act as tumor suppressors in AML. PTPRK acts as a tumor suppressor because it limits the activity of AKT[173], EGFR[174] and STAT3[175]. PTPRO may function by limiting the same pathways as PTPRK[172,176].

The SH2-domain containing phosphatase SHP2 functions as a PTP oncogene in AML and can be activated by overexpression[177] or by mutation[178]. Rather than acting upstream of

many oncogenes, like other PTPs, SHP2 is actually activated by EGFR[179] and contributes to the activation of the RAS/MAP kinase pathway[180].

In general, PTPs are understudied in AML and much of what we know about how they function comes from studies in other tumors. There are no therapies available that act directly on PTPs.

1.1.5 Current treatment paradigms in AML

Treatment of AML is usually thought of in two phases. Induction therapy is meant to 'induce' remission. The standard of care is currently '7+3' for induction therapy. For those 60-80% of patients that achieve complete remission (CR)[181], the second phase of therapy is consolidation. Consolidation is designed to remove any minimal residual disease (MRD), as the tumor is all but guaranteed to relapse if no consolidation therapy is administered. The options for consolidation therapy are currently allogeneic hematopoietic stem cell transplant (allo-HSCT) or high-dose cytarabine (HiDAC). Allo-HSCT is the replacement of a patient's HSC with cells transplanted from a matching donor. HiDAC is very high dose cytarabine (ara-C) and is given for 3-4 weeks. Both options are not easy on the patient and can be life-threatening. Which consolidation therapy is best depends on the patients cytogenetic risk profile and age. For those with a favorable profile, HiDAC is just as effective as allo-HSCT[182,183]. While the best consolidation in intermediate risk AML is still being determined[184], there is little doubt that allo-HSCT is the best option for adverse risk AML patients[185–187]. As important as cytogenetic risk is age of the patient. Both HiDAC and allo-HSCT are too risky for many patients older than 65, which make up more than 50% of the AML patient population[7].

1.1.5.1 Chemotherapy regimens with cytarabine and anthracycline (7+3)

The standard of care induction therapy in AML is 7+3 therapy for all patients except those with APL. This therapy is called 7+3 because it is a sequence of cytarabine given as a continuous IV infusion for seven days followed by an anthracycline given for 3 days as an IV push. The anthracycline can be either daunorubicin or idarubicin[188–190]. About 70% of AML patients receive this standard protocol[191]. The original 7+3 protocol was established in 1973 and has not changed much in the last 45 years[192]. There have been improvements in AML survival since the 7+3 protocol was developed, but that is mainly due to improvements in supportive care, and minor tweaks to the 7+3 protocol.

There are some changes that can be made to the standard 7+3 protocol, mainly by changing the dosing of the anthracycline. For example, a subset of patients with mutations in KMT2A and DNMT3A benefit from higher doses of daunorubicin[36]. While increasing the dose of ara-C is an approach that is effective at killing the disease, it also greatly increases toxicity. As such, attempts to change to ara-C dosage during induction therapy have been largely abandoned[188,193,194]. Another alternative approach that has been proposed is the combination of fludarabine, cytarabine, G-CSF and idarubicin (FLAG-IDA) for induction therapy[195]. Normally FLAG-IDA is reserved for treating relapsed AML. Yet another approach is the combination of 7+3 with a tyrosine kinase inhibitor (TKI) in the case of FLT3 mutated AML[196].

The mechanisms of action of the ara-C portion of treatment and the anthracycline portion are different. Cytarabine is converted into cytarabine triphosphate. Cytarabine triphosphate can stall DNA polymerase[197]. The mechanisms of resistance against cytarabine can be the upregulation of deaminases which metabolize cytarabine[198], activity of nucleoside

transporter 1 which is induced by the bone marrow[199], or upregulation of SAMHD1[200] which removes the polyphosphate group. Anthracyclines have more diverse mechanisms of action. Anthracyclines can insert in between adjacent base pairs of DNA (intercalation) which can inhibit transcription and DNA replication[201]. In addition to intercalation, anthracyclines also form DNA adducts[202]. Anthracyclines also inhibit topoisomerase-II activity[203]. Lastly, anthracyclines also generate reactive oxygen species (ROS), although this may have more to do with its side effects rather than its anti-tumor activity[204]

Like every chemotherapy, 7+3 is associated with many side effects. According to the package inserts for cytarabine and daunorubicin the most frequent expected adverse reactions are anorexia, hepatic dysfunction, nausea, fever, vomiting, rash, diarrhea, thrombophlebitis, oral and anal inflammation/ulceration, bleeding (all sites), nausea, vomiting, myelosuppression, cardiotoxicity, reversible alopecia, rash, contact dermatitis, urticaria, abdominal pain, tissue necrosis, severe cellulitis, or thrombophlebitis[205,206]. These adverse reactions are all the more reason to pursue targeted therapy, which presumably will be safer to use. The remainder of this chapter is dedicated to targeted therapies currently in use or being investigated in AML.

1.1.5.2 All-trans-retinoic acid (ATRA) and arsenic trioxide (ATO)

The only type of AML in which 7+3 is not the standard of care is APL. Both ATRA and ATO are meant to treat APL. They both target the PML-RARα translocation that is diagnostic of this AML subtype. Both drugs work by inducing degradation of the PML-RARα protein, but their mechanisms of action are distinct. ATRA degrades the protein via the ubiquitin-proteasome pathway[207]. Meanwhile, ATO uses a sumoylation and caspase-dependent pathway[208]. As of 2013, the standard treatment for PML-RARα+ APL involves co-administration of ATRA and ATO (ATRA-ATO)[209]. Rather than killing APL cells, ATRA-ATO induces terminal

differentiation[45]. ATRA and ATO represent the biggest breakthroughs in AML treatment since 7+3[192].

1.1.5.3 Therapies targeting mutant IDH1 and IDH2

Since IDH1 and IDH2 are some of the more frequently mutated genes in AML, and these mutations result in a gain-of-function, they are good candidates for targeted therapy. The first IDH2 inhibitor was AGI-6780 which was found to induce terminal differentiation of an IDH2 mutant erythroleukemia cell line, TF-1[210]. Later screens for IDH2 inhibitors, and significant medical chemistry efforts, led to the discovery of AG-221. AG-221 is orally bioavailable and has much better pharmacology than AGI-6780[211]. Both AG-221[211] and AGI-6780[210] are allosteric inhibitors that act on the IDH2 homodimer interface. In clinical trials, AG-221 resulted in a complete response by some patients with IDH2 mutations[212]. Importantly, AG-221 caused a decrease in 2-HG levels in peripheral blood and differentiation of IDH2 mutant myeloblasts into neutrophils[213]. Most patients that did not respond to AG-221 were found to have *RAS* mutations[213], which may interfere with differentiation. AG-221 was FDA-approved and is now the recommended therapy for IDH2 mutant AMLs[214]. There are also several IDH1 therapies under investigation[215].

1.1.5.4 Therapies targeting CD33

CD33, sialic acid binding Ig-like lectin 3, is a transmembrane protein found predominantly on myeloid lineage cells and is upregulated in some AMLs[216]. Although downstream signaling by this CD33 is unclear[217], it is thought to be a good target for immunotherapy in AML. The most frequent way that CD33 has been targeted is with antibody-drug-conjugates (ADC)[218]. Initially, the success of CD33-targeted therapy was limited[219,220]. The

first major success in CD33 targeted therapy was gemtuzumab ozaogamicin (GO), an ADC that delivers calicheamicin, a potent DNA damaging agent, to $CD33^+$ cells[221]. Initially the approval of GO was controversial[222], but after several more clinical trials, GO was approved in 2017[221]. While many CD33 ADCs have been investigated in clinical trials, only GO has advanced past phase II[223].

Other than ADCs, chimeric-antigen-receptor T-cells (CAR-T cells) are another strategy for targeting CD33+ AMLs. There have been many CAR-T strategies for targeting CD33[224–227], but all have been highly cytotoxic in humans, probably because healthy myeloid cells also express CD33[228]. To mitigate toxicity from CD33 targeted CAR-T cells, the strategy of grafting HSCs with genetic inactivation of CD33 prior to CAR-T cell treatment has been proposed. A proof of concept experiment of this strategy was successful in rhesus macaques[229].

1.1.5.5 Brief introduction to FLT3-targeted therapy

Kinase inhibitors of FLT3 are the largest area of focus for current drug development in AML. There are currently two FDA-approved FLT3 inhibitors, midostaurin (PKC412)[230] and gilteritinib (ASP2215)[231]. These inhibitors and many other FLT3 inhibitors that are currently in the pipeline will be discussed extensively in chapter 1.2.

1.2 Aberrant tyrosine kinase signaling in AML

1.2.1 FLT3 receptor tyrosine kinase

1.2.1.1 Normal functions of FLT3 linked to AML etiology

FLT3 is a transmembrane receptor tyrosine kinase consisting of an intracellular kinase domain, intracellular juxtamembrane domain, transmembrane domain, and an extracellular immunoglobulin-like domain. FLT3 is a member of the class III receptor tyrosine kinase family, members of which all share the same domain architecture. This family also includes the platelet-derived growth factor receptor (PDGFR), macrophage colony-stimulating factor receptor (FMS) and stem cell factor receptor (c-KIT).

In healthy bone marrow, FLT3 is only expressed on $CD34^+$ HSCs and immature hematopoietic progenitors, including myeloid and lymphoid progenitors[232–234]. Interestingly FLT3 is virtually absent from erythroid precursors[234]. This is consistent with the fact that FLT3 mutations occur in every FAB subtype of AML except acute erythroid leukemia (FAB M6)[141]. The level of FLT3 expression in $CD34^+$ bone marrow cells can determine what type of cells they differentiate into. Those cells expressing high levels of FLT3 follow the granulocyte-macrophage lineage, while those that express low levels become erythroid cells[235]. FLT3 is also expressed in other organs such as spleen, liver, thymus, lymph nodes, gonads and brain[236].

The FLT3 protein is synthesized in the endoplasmic reticulum and undergoes glycosylation in the Golgi. The active protein is localized to the plasma membrane. The monomeric protein remains in its downregulated in active state until it binds to FLT3 ligand, which induces dimerization, promotes autophosphorylation and activation of the intracellular kinase domain[237].

The FLT3 ligand comes from a family of transmembrane protein growth factors that stimulate differentiation and proliferation of hematopoietic cells[238,239]. Alternative splicing results in three FLT3 ligand isoforms. The most common is a 30 kDa transmembrane protein. The next most common is a soluble form, which is identical to the extracellular portion of the transmembrane protein. The last form from a premature stop codon that results in an inactive protein[240]. Unlike the expression of FLT3, FLT3-ligand is expressed in most tissues, suggesting the expression of FLT3 is normally the limiting factor in FLT3 activation[241].

FLT3, like many other receptor tyrosine kinases, activates a wide variety of signaling pathways[242,243]. The phosphorylated tyrosines on the juxta-membrane domain of Flt serve as docking sites for SH2-containing adapter proteins, such as SHIP, SHP2, GRB2 and SHC[244]. Through these adapters, FLT3 can activate the PI3K/AKT[245], RAS/MAPK[246,247], and STAT[247] pathways along with several others.

1.2.1.2 Structure and activation of FLT3

FLT3 consists of an N-terminal extracellular region of 541 amino acids, a 21 amino acid transmembrane domain, a 98 amino acid juxtamembrane domain and a 333 amino acid kinase

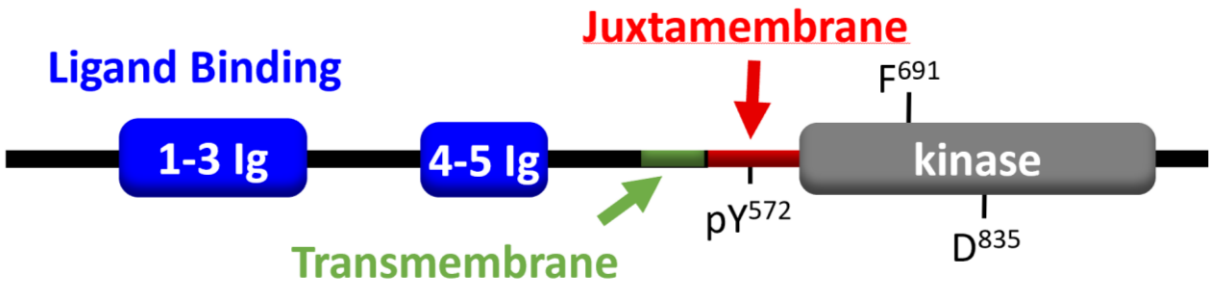

Figure 1. The overall domain organization of FLT3.

Also shown are the relative positions of the gatekeeper residue (Phe338), the autophosphorylation site in the juxtamembrane region (pTyr572), and a common site of resistance mutation in the activation loop (Asp835).

domain[248]. A summary of the domain architecture of FLT3 is shown in Figure 1. The extracellular domain consists of five immunoglobulin-like sub domains, but only the three most N-terminal sub-domains are involved in FLT3L binding. This extracellular region is also heavily glycosylated, which may relate to ligand binding activity[249]. The non-glycosylated isoform of FLT3 has a molecular weight of 130 kDa and the glycosylated form is 160 kDa. Only the glycosylated form is associated with the plasma membrane, but plasma membrane association is not required for the activity of the AML-associated FLT3-ITD mutant[250].

The majority of what is known about FLT3 structure and comes from X-ray crystallography studies of the intracellular portion of FLT3[143,251–253], the extracellular portion of FLT3[254] and the FLT3 ligand[237]. From these structures we have a good idea of how FLT3 is activated, and how mutations may activate FLT3[143,237,254] or lead to drug resistance[251–253]. The FLT3 ligand exhibits two FLT3 binding sites[237], which forces the dimerization of two FLT3 molecules[254]. The mode in which FLT3 ligand binds to FLT3 is somewhat unique, in that FLT3 ligand and FLT3 only interact on the surface, while most class III receptor tyrosine kinases bind their ligand in such a way that parts of the ligand are buried within the extracellular domain of the receptor[254]. It is not completely clear how this translates to the displacement of the juxtamembrane domain away from the kinase domain inside the cell, but that seems to be required for activation[143,254]. In the inactive state, FLT3 juxtamembrane residues Tyr572-Met578 are buried within the N-lobe of the kinase domain, residues Val579-Val592 make contacts with the exterior of the C-lobe of the kinase domain, and Asp593-Trp603 are bound to the outside of the α-C helix in the N-lobe[143]. When active, several residues within the juxtamembrane domain are autophosphorylated including Tyr572, Tyr589, Tyr591, Tyr597, and Tyr599[255]. Based on the structure of inactive FLT3, Tyr572 is critical as it is deeply buried within the N-lobe of the

kinase domain and forms a polar contact with Glu661 as well as several non-polar contacts which push the α-C helix away from the body of the kinase. When Tyr572 is phosphorylated all of these contacts are expected to disappear[256]. The phosphorylated juxtamembrane residues also serve as docking sites for SH2-containing proteins, some of which then serve as substrates for active FLT3[257,258].

The FLT3 kinase domain is considered 'split' because of the extra-long 'kinase insert' between the N-lobe and C-lobe of the kinase domain. Because of this, the N-lobe of the kinase is sometimes referred to as the TKD1 and the C-lobe is TKD2, while the kinase insert is called KI[143]. This extra-long KI is unique to class III and class IV receptor tyrosine kinases[257]. Like many other kinases the activation loop (A-loop) is lodged in between the N-lobe and C-lobe at the substrate binding site when the kinase is inactive[143,257]. The A-loop is moved outside of this substrate binding pocket when the kinase is active or bound to an inhibitor[143,251–253].

All of the inhibitors of FLT3 that are currently under investigation bind to the catalytic site of the kinase domain[251–253,259], which explains why there is substantial structural information about this domain. For the most part, the entirety of the kinase domain of the inhibitor-bound structure looks the same as the autoinhibited FLT3 structure. The notable exception is the A-loop which can take on a wide variety of confirmations depending on the inhibitor that is bound. The A-loop also has the lowest resolution in all of the inhibitor structures, implying a large degree of flexibility of this structural feature even when the inhibitor is bound[143,251–253]. In all of the structures with inhibitors bound to date, the kinase domain adopts the so-called 'Type-II' conformation, in which a highly conserved Asp-Phe-Gly (DFG) motif at the N-terminal end of the activation loop is rotated outward. Because this 'DFG-out' conformation is often characteristic of inactive kinase domains, it is not surprising that portions of the juxtamembrane

domain bound to the kinase domain are also also observed in these crystal structures[251–253]. It would be extremely interesting to see a structure of FLT3 bound to a 'Type-I' inhibitor, in which the DFG motif is rotated inward as observed in active kinase domain structures. In this case, the juxtamembrane domain may not be visible because it is predicted to moved away from its regulatory position as described above. Without these kinase domain contacts, it is likely to become unstructured and therefore will not be visible in the electron density. Signal transduction of FLT3 in AML

FLT3 mutations significantly alter the signaling behavior in AML, and are a major driver of the disease[260]. Because of this, both the NCCN and the ELN recommend FLT3 genotyping be performed early in the diagnosis of AML[33,261]. FLT3 mutations occur as internal tandem duplications (ITDs)[262] or tyrosine kinase domain mutations (TKDs)[263] as described above. Both mutations are known to activate FLT3[264,265], but only FLT3-ITD is consistently associated with a poor prognosis[36,37,42,141,266]. FLT3-TKD are associated with worse survival in some studies[141], but not in others[36,37,42,267]. Interestingly it seems that when TKD mutations co-occur with PML-RARα, FLT3-ITD or MLL-PTD, the presence of FLT3-TKD mutations does in fact correlate with worse survival[36,267]. It is also important to note that FLT3-ITD and FLT3-D835Y signal differently. For example FLT3-ITD activates the non-receptor tyrosine kinase Fes downstream, whereas FLT3-D835Y does not[268]. Even when not mutated, FLT3 expression is upregulated in almost all AML samples[269] and overexpression of wild-type FLT3-WT induces AML in mice[244]. This may mean FLT3 targeted therapy has greater utility beyond just FLT3 mutant tumors. Indeed, the BEAT AML study found that FLT3 mutations correlated very strongly with response to FLT3 targeted therapy, but there remains a subset of patients wild type for FLT3 who do respond to FLT3-targeted therapy[42].

The FLT3-ITD mutations are in-frame genetic insertions within one copy of the FLT3 gene. The insertion varies in length and location. The insert is usually derived from genetic material in exon 11 of FLT3, hence the name internal tandem duplication, but can contain some exonic material as well[270]. The size of insertion can range from 1 to 60 amino acids, with a median length of 54[141]. The length of the insertion has a small prognostic effect. Longer insertions do correlate with worse outcome, but that is assuming all patients receive standard 7+3 treatment[271,272]. There is currently no consensus on the effect that length or location of the insert on efficacy of TKIs against FLT3. However, inclusion of non-exon 11 material within the ITD correlates with less efficacy of TKIs[270]. The ITD is almost always inserted within the juxtamembrane domain. The FLT3-ITD mutation usually includes Asp593-Trp603, and is inserted somewhere in between Gln575 and Gly613[141]. This insertion in the juxtamembrane domain disrupts critical interactions between the juxtamembrane domain and the kinase domain which hold the kinase in an auto-inhibited state in the absence of ligand as described above[143,264]. Occasionally, the ITD mutation occurs within the kinase domain. These instances are associated with even worse prognosis that juxta-membrane ITDs[266]. The ITD mutation also results in the trans-activation of wild type FLT3[264]. Knock-in mouse models of FLT3-ITD result in aggressive MPN in mice[273]. FLT3-ITD signaling is similar to that of the wild type kinase, except that FLT3 is constitutively active. This leads to overactivation of the RAS/MAPK and PI3K/AKT pathways[274]. FLT3-ITD also induces STAT5 phosphorylation, resulting in activation of this transcription factor and subsequent upregulation of anti-apoptotic and cell-cycle genes[247].

FLT3-TKD mutations were first reported 5 years after the ITD was discovered[263]. The most common mutation results in substitution of Asp835 with tyrosine, histidine or glutamate. TKD mutations have been found at other residues as well such as Ile836. These mutations are

almost exclusive to the A-loop[37,42,275]. The proposed mechanism by which A-loop mutations activate the kinase is by disrupting interactions between the A-loop and the catalytic site of the kinase which may allow for some kinase activity. The FLT3-D835Y does not transform myeloid cells on its own, but the presence of one of the many additional AML related mutations contributes to transformation[265]. While a FLT3-D835Y knock-in mouse model does lead to a myeloproliferative syndrome, it is notably less aggressive than the FLT3-ITD model[146]. Many of the TKD mutations, including D835Y/H/E, are also resistant to most FLT3 inhibitors[276]. Together with the complicated prognostic relevance and lower frequency of TKDs, most FLT3 inhibitor development has been focused on FLT3-ITD[277].

1.2.1.3 Targeted therapies against FLT3 in AML

While outcomes for FLT3-ITD AML are worse than AML overall, the outlook for FLT3 mutant AML seems to be improving since the integration of FLT3 inhibitors into treatment[278]. While some FLT3 inhibitors have been FDA approved in recent years, there are many more FLT3 inhibitors in the clinical trial pipeline and treatment outcomes should continue to improve with time.

Early-generation FLT3 inhibitors

The earliest FLT3 inhibitors that were studied in clinical trials were mostly broad spectrum kinase inhibitors developed for other cancers such as lestaurtinib[279], sunitinib[280,281], sorafenib[282], and midostaurin[283]. While many early clinical trials with these inhibitors showed very little or no efficacy as single agents, some of these therapies gave a slight benefit when combined with standard 7+3 treatment, though this was often accompanied by additional toxicity as well[281,282]. Specifically, lestaurtinib did not improve patient outcomes at all, even when

combined with chemotherapy[284,285]. Sunitinib did elicit short-lived partial responses[286], but induced dose-limiting toxicities when combine with 7+3[281]. For sorafenib, monotherapy actually brought some patients all the way to complete remission[287]. When sorafenib was combined with chemotherapy, higher event-free survival was observed with no change in overall survival. This can be explained by toxicity due to the combined treatment[282,288]. Further analysis of the data from the sorafenib and 7+3 trials revealed that the FLT3 mutant patient population was not more likely to respond to treatment compare to patients with wild-type FLT3[282,288]. However, when sorafenib was combined with 7+3 in patients that received no prior treatment, almost all FLT3-ITD patients had at least a partial response[289,290]. Furthermore, sorafenib was successful in maintaining remission after allo-HSCT[291].

Midostaurin was the most successful of the early FLT3 inhibitors. As monotherapy, midostaurin had similar efficacy to sunitinib and sorafenib, but with less toxicity[283,292]. Midostaurin plus 7+3 resulted in slightly improved event-free survival and overall survival[293]. Based on these trials, midostaurin (Rydapt; Novartis) was approved by the FDA in 2018 for use with 7+3 in FLT3-mutant AML[294]. The European approval also included a designation for use of midostaurin for maintenance of remission[295]. A retrospective analysis of the midostaurin phase III trial revealed that the efficacy of the drug is highly dependent on whether or not the tumor also contains NPM1 mutations and the FLT3-ITD:FLT3-WT allelic ratio[296]. The approval of midostaurin remains somewhat controversial to this day, however. Because patients who were FLT3-WT, FLT3-TKD or FLT3-ITD all benefitted from the treatment and as the fact that midostaurin, a staurosporine derivative, inhibits many different kinases, it is possible that midostaurin efficacy comes from the inhibition of other oncogenic kinase pathways in addition to FLT3 inhibition[277]. The phase III trial, RATIFY, that led to the approval of midostaurin is

highly controversial. For example, 23% of patients enrolled in RATIFY were FLT3-TKD, which is much larger than the proportion of FLT3-TKD mutations reported in the overall AML patient population[36,37,42]. Further, patients with FLT3-TKD mutations tend to have a less aggressive disease and a better prognosis than FLT3-ITD[36,37,42,267]. The RATIFY trial also enrolled a much younger population than the median AML age, while no age restriction was put on midostaurin upon approval[297].

Current FLT3 inhibitor developments

In general, the early FLT3 inhibitors were not effective as monotherapy, while all of them were too toxic when combined with 7+3 except midostaurin[292]. In contrast, newer FLT3 inhibitors have evolved that are much more specific and potent for FLT3 inhibition[259,298], resulting in stronger efficacy in clinical trials even as monotherapy[299,300]. The FLT3 inhibitors under clinical investigation that meet these criteria are quizartinib, crenolanib and gilteritinib. Quizartinib is a Type II inhibitor that binds to an inactive conformation of the FLT3 kinase domain[251,252]. Meanwhile crenolanib and gilteritinib are Type I inhibitors that bind to a DFG-in, active conformation of FLT3, but still maintain specificity[301].

Quizartinib has been studied the longest of these newer FLT3 inhibitors. It is highly active in clinical trials, with over 50% of relapsed patients responding[300,302]. While responses to quizartinib alone tend to be more durable than midostaurin plus 7+3, most patients do eventually relapse, especially if they do not transition to allo-HSCT [293,300,302]. This short duration of treatment may be related to the many mechanisms of resistance against quizartinib[39,303]. The extraordinary selectivity of quizartinib is thought to be partially due to its Type II binding mode[251,252,259], but paradoxically this binding mode is also likely responsible for the many FLT3

mutations that can confer resistance[39]. In 2018, the FDA granted break-through status for quizartinib for the treatment of relapsed or refractory AML[304].

While it is now thought of a FLT3 inhibitor, crenolanib was originally developed as an inhibitor for the related receptor tyrosine kinase, PDGFR [305]. Even though it is a Type I inhibitor, crenolanib still retains a high degree of specificity according to its KINOMEscan profile[306]. This inhibitor gained a lot of interest because it retains efficacy against most of the mutations that confer quizartinib resistance, especially those in the A-loop[301]. However, clinical trials with this compound were somewhat disappointing, with lower response rates than quizartinib even in treatment-naïve patients[307,308].

The most successful FLT3 inhibitor in clinical trials is gilteritinib. This Type I inhibitor had a higher response rate and longer remission time than quizartinib in clinical trials[299]. Unfortunately, not much has been published about this inhibitor, but we know from kinome-wide profiling that the primary target is FLT3[309] and a secondary target is the receptor tyrosine kinase, AXL[310]. The FLT3 inhibition profile of gilteritinib is very similar to crenolanib, and initial studies would suggest that the same mechanisms of resistance will apply[309]. However, gilteritinib has a more durable response in the clinic[299], which may be partially explained by its inhibitory activity against the AXL kinase[310].

Resistance to FLT3 inhibitors

As opposed to CML, where tyrosine kinase inhibitors such as imatinib and dasatinib have long lasting impacts, the best inhibitors for AML only have efficacy for 3-6 months[311]. The primary cause of resistance to FLT3 inhibitors in AML are additional kinase domain mutations, but activation of parallel signaling pathways and bone marrow microenvironment mediated

resistance are also big concerns. In terms of resistance, quizartinib is probably the best studied compound in AML, but resistance is a major issue for all FLT3 inhibitors.

The most frequent cause of resistance to FLT3 inhibitors involves acquired mutations in the FLT3 kinase domain. With midostaurin for example, those patients that initially responded and then relapsed most frequently had mutations at the kinase domain residue Asn676[312,313]. For some of the more selective FLT3 inhibitors, much more is known about mechanisms of resistance since the FLT3 kinase domain sequence is now routinely examined in resistant tumors. Resistance to quizartinib, for example, can be achieved with mutations to residues Asp835, Asp842, Phe691, and Glu608[39]. Furthermore, there is the possibility of multiple quizartinib resistance mechanisms evolving concurrently[303]. Meanwhile, crenolanib and gilteritinib have a different resistance profile. The potency of both inhibitors can be reduced by mutations to the FLT3 gatekeeper residue, Phe691, but this resistance effect is much less for these compounds than quizartinib[301,309]. In fact for crenolanib, two FLT3 mutations are probably required for complete resistance[301]. In general, when looking at FLT3 inhibitor resistance as a whole, a trend emerges. For Type II inhibitors like quizartinib, there are many mutations that confer resistance. Many of those mutations are on the A-loop or within the inhibitor binding pocket[39,303]. This makes sense from a structural point of view, because the selectivity of quizartinib lies in its ability to bind and stabilize a very specific kinase domain configuration that can be disrupted by a multitude of mutations. Meanwhile resistance mutations against Type I FLT3 inhibitors, such as midostaurin or crenolanib, map to the kinase domain N-lobe, the gatekeeper residue, or involve mutations in alternative pathways[301,309,312]. There have also been inhibitors that have been developed with FLT3 resistance mutations explicitly in mind. For example PLX3397 and

pontatinb, repurposed from CML, both have potent activity against common FLT3 gatekeeper mutations (e.g., Phe691Leu)[251,314,315].

Exposure to FLT3 inhibitors does not guarantee the mitigation of activity by downstream effectors, including ERKs, STATs, AKT and S6 kinase[316,317]. In fact, for sorafenib, there is significant synergy between FLT3 inhibition and ERK or AKT inhibition[316]. The presence of bone marrow stroma also increases the activity of the ERK pathway[318] which is likely due to FGF2 present in the bone marrow microenviornment[319]. Because of these findings, a dual FLT3/ERK kinase inhibitor, E6201, is under investigation[320].

FLT3 inhibitors have a greater impact on peripheral AML blasts compared to blasts within the bone marrow[311]. One explanation is that FLT3 activity promotes the migration to some bone marrow factors including CXCL12, which is produced by stem cells in the bone marrow. FLT3 promotes migration to CXCL12 via to activation of CXCR4 signaling[321,322]. In fact the co-inhibition of FLT3 and CXCR4 with two compounds does mitigate most of the resistance to sorafenib and increases survival dramatically when co-administered with sorafenib in a cell-line xenograft mouse model[323]. Furthermore, co-administration of a CXCR4 inhibitor with sorafenib was able achieve a 70% response rate[323], which is better than any FLT3 inhibitor alone or in combination with chemotherapy.

A more recent analysis of the Type-I inhibitor crenolanib demonstrated the diversity of resistance mechanisms[324]. While there are some FLT3 mutations that confer partial resistance to crenolanib, multiple mutations are required for cells to survive in the presence of greater than 100 nM of the inhibitor *in vitro*[301]. Therefore, it was interesting to see how patients would respond in the clinic and how resistance may arise. The results of the clinical trial were disappointing in that most patients who had received prior tyrosine kinase inhibitors did relapse

or did not respond to crenolanib at all. Zhang et al. followed the progression of the tumors with crenolanib treatment with whole exome sequencing (WES). Mutations of one of the many other AML-associated genes seems to be the main mechanism of resistance to crenolanib. The most frequent additional mutations were in NRAS, TET2 and IDH1/2. Interestingly these additional mutations often arise in subpopulations of the tumor that do not even have the FLT3-ITD mutation[324].

Immunotherapy targeting FLT3

Currently the only approved immunotherapies in AML are allogenic hematopoietic stem cell transplant (allo-HSCT) and the CD33 targeting ADC called GO described above. Allo-HSCT was discussed extensively in chapter 1.1.5, but as a reminder this therapy requires a bone marrow donor and is dangerous for the patient. Allo-HSCT is typically not recommended for patients over 65, a group that includes more than half of the AML patient population. While CD33 targeted ADCs provide specificity for myeloid cells, it took a long time to determine that these therapies had any efficacy when co administered with 7+3[222]. GO and other CD33 targeted therapies are discussed extensively in chapter 1.1.5.4. There have also been several immunotherapies investigated that directly target FLT3 as described below.

Anti-FLT3 monoclonal antibodies (MABs)[325,326] and more recently chimeric antigen receptor T cells (CAR-T cells) have been engineered to target FLT3[327,328]. Specifically, the anti-FLT3 MAB IMC-EB10 was able to reduce the extent of FLT3 ligand binding and downstream activation of STAT5, AKT, and ERK by both FLT3-ITD and FLT3-WT *in vitro*. Further, in NOD/SCID mice, IMC-EB10 reduced the presence of engrafted FLT3-ITD^{+} MOLM-14 cells in bone marrow and peripheral blood, while greatly increasing the survival of the mice. Meanwhile the CD34^{+} population from human cord blood remained normal when treated with IMC-EB10[325].

Unfortunately the phase-I trial of IMC-EB10 in AML patients was discontinued due to lack of efficacy[329]. The trial was never followed up with only FLT3-ITD^{+} patients. Interesting it was later shown that IMC-EB10 also has efficacy against ALL, which is also known to overexpress FLT3[326]. The latest anti-FLT3 MAB is 4G8SDIEM. This antibody seems to have more potent binding to FLT3, while also maintaining selectivity for those cells that over-express FLT3 vs. those that express a normal level of FLT3 (300 molecules/cell). This was partially attributed to better engineering of the Fc portion of the antibody[330]. However, there has not been any in vivo efficacy data for this MAB since it was initially reported more than 7 years ago.

More care was taken in the pre-clinical investigation of FLT3-targeted CAR-T cells compared to anti-FLT3 MABs. The CAR-T cells were able to reduce the tumor burden of both Molm13-engrafted and AML patient PBMC-engrafted immunocompromised (NSG) mice. Notably in these experiments the tumors were allowed to engraft for days or weeks before the CAR-T cells were administered. Tumor burden reduction was accompanied by survival of all treated mice until the end of the experiment. The CAR-T cells also did not become activated in the presence of healthy PBMCs which implies a great degree of selectivity[327]. Subsequent study with this CAR-T cell strategy revealed that the treatment also has efficacy against AML cells expressing wild type FLT3, but the therapy also disrupts normal hematopoiesis. This is not surprising since the differentiation and proliferation of multiple cell types is dependent on FLT3. The authors propose a CAR-T cell depletion strategy at the end of treatment, followed by allo-HSCT[328]. Interestingly, treatment with the FLT3 kinase inhibitor crenolanib was found to increase cell surface expression of FLT3. This could mean that CAR-T cells and crenolanib could work synergistically. In fact, mice treated with both survived longer, with smaller tumors, than mice treated with either CAR-T cells or crenolanib alone[328].

1.2.2 Non-receptor tyrosine kinases in AML and multi-targeted inhibitors

1.2.2.1 AXL

AXL was previously discussed in section 1.2.1.4 in relation to gilbertinib, a dual FLT3/AXL inhibitor. AXL is a receptor tyrosine kinase from the Tyro3, Axl, Mer (TAM) family. AXL is a therapeutic target in AML independent of FLT3 because its expression is associated with poor prognosis, and knockdown of AXL increases survival[331]. Further treatment with the kinase inhibitor BGB234 reduced AXL activity, slowed tumor growth, and slightly prolonged survival. BGB234 treatment also resulted in attenuation of ERK activity so it remains unclear if this is due to on-target effects due to AXL inhibition or off-target effects due to inhibition of another kinase[331]. AXL was later shown to be activated upon treatment with midostaurin or quizartinib, especially in those patients that do not respond to treatment. Furthermore, Molm13 cells that were selected to be midostaurin resistant were found to be highly sensitive to the AXL inhibitor TP-0903, and could be re-sensitized to midostaurin or quizartinib by as little as 5 nM TP-0903 or shRNA targeting AXL[332]. AXL has also been previously shown to be involved in resistance to TKIs targeting $HER2^+$ breast cancer[333,334], EGFR or PI3K in lung cancer[335,336], KIT in GIST[337] and BCR-ABL in CML[338]. In summary, AXL targeted therapy is somewhat effective alone[331], but FLT3 and AXL targeted therapy is much more effective[332]. Furthermore, the AXL inhibitory activity of gilberitinib may account for its more durable response in patients[299].

1.2.2.2 SYK

Most of what is known about SYK in AML comes from the Stagmaeir group in two papers published in *Cancer Cell*[339] and *Oncotarget*[340]. SYK is a non-receptor tyrosine kinase

expressed in all AML cells, however it is only active in some patients. Phospho-SYK/total-SYK staining by immunofluorescence (IF) has been used to study the extent of SYK activity within the AML cells. Higher SYK activity measured by IF is correlated with worse prognosis in AML patients[340], but SYK expression by mRNA is not correlated with prognosis[37]. Furthermore, the only cell lines that were positive for phospho-SYK also contain ITD mutations in FLT3[340].

SYK is occasionally translocated in MDS with the TEL gene (SYK-TEL)[341]. The forced expression of SYK-TEL in AML cell lines increases the phosphorylation of several other kinases, including FLT3 and several SRC-family kinases. Further investigation revealed that wild type SYK directly phosphorylates and activates FLT3. Mice engrafted with FLT3-ITD$^+$ tumor cells survived longer when SYK was knocked down. The AML cell lines that are most sensitive to pharmacologic SYK inhibition were all FLT3-ITD positive. When FLT3-ITD$^+$ AML cells were engineered to co-express SYK-TEL, they exhibited a more aggressive and lethal phenotype compared to those made to express wild-type SYK or no SYK. When the SYK phosphorylation site on FLT3-ITD (Tyr955) was mutated to an alanine, SYK-TEL no longer resulted in a more aggressive tumor. Furthermore, treatment of engrafted mice with the FLT3-ITD inhibitor quizartinib and the SYK inhibitor PRT062607 resulted in prolonged survival with FLT3-ITD$^+$, SYK-WT and FLT3-ITD$^+$ SYK-TEL tumors[339]. These results indicated that SYK represents an important drug target in FLT3-ITD$^+$ AML, which could potentiate FLT3 targeted therapy.

It has long been known that SYK can bind to multi-phosphorylated receptor tyrosine kinases via its dual SH2 domains[339,342]. However, recent data suggests that the SRC-family kinase LYN may activate SYK more potently than receptor tyrosine kinases[343]. Since SYK can

activate FLT3[339] and LYN, and possibly other SRC-family kinases, can activate SYK[343], SRC-family kinases must be considered drug targets in FLT3-ITD$^+$ AML as well.

1.2.2.3 FES and FER

FES and FER make up a unique non-receptor tyrosine kinase family linked to growth, differentiation, and oncogensis in a wild variety of tumor sites, including AML. Both FES and FER have been implicated in downstream signaling of FLT3-ITD to PI3K and STAT5[127]. This interaction between FLT3 and the FES family of kinases seems to be preserved across all class III receptor tyrosine kinases[344]. FES knockdown only seems to relevant for AML survival in FLT3-ITD$^+$ AML[127]. Recently, Weir *et al*. did a comparative analysis of kinase inhibitors selective for FES/FER or inhibitors that have activity against both FLT3-ITD and FES/FER. They found that those inhibitors that acted on both FLT3-ITD and FES had much greater activity against FLT3-ITD$^+$ AML cell lines than those that acted on FES alone[268].

1.2.2.4 SRC-family kinases

A major focus of my thesis research concerned the role of the SRC kinase family in the pathogenesis of AML, especially as it relates to FLT3 in kinase inhibitor efficacy and acquired resistance. For this reason, a detailed history of SRC-family kinase biology, structure and signaling is presented below.

SRC-Family kinases history

In 1911 Peyton Rous discovered the Rous sarcoma virus (RSV), an acutely transforming retrovirus which reproducibly causes sarcomas in infected chickens[345,346]. This was the first ever

model to study cancer and was involved in many discoveries about cancer and virology in subsequent years. In 1966, Rous was awarded the Nobel prize in physiology or medicine for the discovery of "tumor inducing viruses". Work in the late fifties and early sixties by Harry Rubin and Howard Temin revealed that there was genetic component in RSV that caused the transformation of cells. This work later revealed the v-SRC, named for the viral sarcoma caused by this gene, is the cause of the cancer[347]. In 1976, Harold Varmus and J. Michael Bishop showed that normal chicken cells possessed a homologous gene, which they named c-SRC for cellular-SRC[348,349]. The discovery of c-SRC, the first example of a proto-oncogene, completely changed the paradigm for how we thought cancer can form. Now we knew that cancer could be caused by changes in endogenous genes and proteins within our cells, whereas before many researchers believed that a foreign agent was required for the formation of cancer. For this discovery, Varmus and Bishop were awarded the 1989 Nobel prize in Physiology or Medicine[350].

We now know that there are 7 additional kinases with very high homology to SRC in mammals (SRC, YES1, FYN, FGR, LYN, BLK, HCK and LCK). These eight kinases make up the SRC family. All 8 kinases are associated with cancer in some way, but SRC[347], YES1[351] and FGR[352] were all discovered as homologs of viral oncogenes. SRC, YES1 and FYN are ubiquitously expressed in human cells, while the other SRC-family kinases are expressed in various subsets of hematopoietic cells.

Structure and Function of SRC-family kinases

All kinases in the SRC-family contain the same domain architecture. From N- to C-terminus, there is the SH4 domain, unique region, SH3 and SH2 domains, an SH2-kinase linker, the SH1 (or kinase) domain and a C-terminal tail[353,354]. See Figure 2A for a visual representation

of this domain architecture and Figure 2B for the downregulated structure of HCK as an example for how these domains assemble in the inactive kinase. SH stands for SRC-homology domain. Many kinases (and other proteins) outside of the SRC-family also contain one or more of these domains, which are involved in protein-protein interactions related to diverse signaling events.

The SH4 domain is involved in kinase association with the membrane via one or two types of post-translational modifications. In all SRC-family members, the initiating methionine is removed by methionine aminopeptidase. All the SRC-family members are then co-translationally myristoylated at glycine 2 by N-myristoyltransferase. Every SRC-family member except SRC and BLK are also post-translationally palmitoylated at cysteine 3, 5 or 6. Those kinases that contain two lipid modification appear to require both for membrane association[355,356]. While the plasma membrane localization of SRC-family kinases is thought to be critical for their signaling, at least some of the SRC family kinases can also be localized to the inside of the nuclear membrane[357]. This nuclear localization is not well understood, but may be related to the DNA damage response to UV irradiation[358].

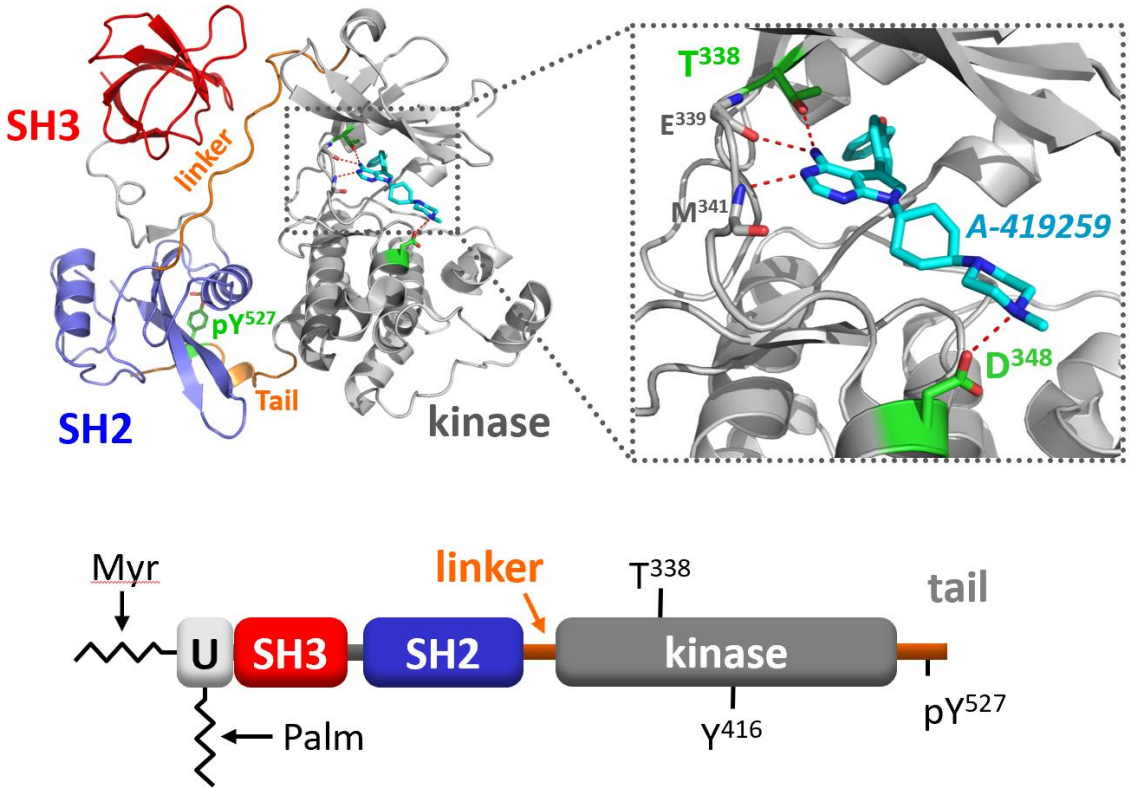

Figure 2. X-ray crystal structure of downregulated HCK bound to the Type-I inhibitor, A-419259.

(A) The overall structure of HCK is shown at the top left, with the SH3 and SH2 domains packed against the back of kinase domain. In this inactive conformation, the SH3 domain engages the SH2-kinase linker, while the SH2 domain binds to the tail when phosphorylated on Tyr527. A close up of the kinase domain active site is shown at right, with the carbon skeleton of A-412959 modeled in cyan. The 4-amino group of the pyrrolopyrimdine makes a hydrogen bond with Thr388, the so-called gatekeeper residue, and together with a ring nitrogen contacts main chain residues Glu339 and Met341 in the hinge region. One of the A-419259 piperidine nitrogens also contacts the catalytic aspartate, Asp348. (B) The overall domain organization of Hck is shown at the bottom, to illustrate the N-terminal unique domain (U; not present in the crystal structure) and its post-translational modification with myristate (Myr) and palmitate (Palm). Also shown are the relative positions of the gatekeeper residue (Thr338) as well as the autophosphorylation site in the activation loop (pY416; not resolved in this crystal structure). Model based on PDB 4LUE and rendered using PyMol.

The unique domain, as implied by its name, is the least conserved domain among the SRC-family. Neither the length nor the sequence of the unique domain is conserved. The unique domain is not present in proteins used for crystallization or not resolved in crystal structures of these proteins. The function of this domain is similarly elusive. The unique domain that is most understood structurally is from LCK, for which a partial solution structure has been reported in complex with the cytoplasmic tails of the T-cell receptors CD4 and CD8. This interaction requires zinc, which induces a zinc-finger motif in the LCK unique domain, and masks the di-leucine motif that is required for internalization of CD4 and CD8[359]. The interaction between FYN, LYN and SRC and cell surface receptors is also known to require the unique domain[360–362]. Furthermore, mutations and phosphorylation events in the unique domain are known to be involved in the regulation and function of the kinase[363,364]. In general the unique domain is highly flexible and disordered[365], but does seem to form weak intramolecular interactions with the SH3domain[366]. Further, a recent in-depth NMR study revealed that the unique domain may have some type of pre formed "fuzzy" structure even when not attached to the SH3 domain[353].

SH3 is a small (approximately 60 amino acid) domain involved binding to protein containing proline-rich regions that form Type II polyproline (PPII) helices. SH3 domains are found in many non-receptor tyrosine kinases as well as adapter proteins and even other enzymes, such as the guanine nucleotide exchange factors and GTPase activating proteins that regulate RAS and other small GTPases[367]. There are around 300 proteins that contain SH3 domains, which play central roles in protein-protein interactions[368]. The structure of the SH3 domain involves five or six antiparallel β-sheets that form a barrel. The linkers in between each β-strand may contain small α-helices. This fold is thought to be very ancient in evolutionary terms, since it is even found in prokaryotes[369]. The hydrophobic pocket of SH3 binds to specific

protein sequences. The consensus SH3 binding site is X-P-p-X-P, where X represents an aliphatic amino acid, P represents proline and p often but not always represents proline[370]. However, other SH3 binding sites have also been described, such as R-X-X-K[371]. In the inactive SRC-family kinase structure, SH3 interacts in *cis* with the linker (between SH2 and kinase domain) which forms a sub-optimal PPII helix[372]. Abl, a non-receptor kinase related to SRC, has "SRC-like core" which also contains a similar arrangement of SH3, SH2, linker and kinase domains. In this SRC-like core, the ABL SH3 to linker interaction is also preserved. Work from our lab shows that the interaction between the ABL SH3 and its linker can be enhanced by the introduction of additional prolines within the binding site on the linker. These changes enhanced the strength of the interaction between the SH3 and the linker, favoring the downregulated kinase state. Enhanced SH3-linker interaction also increased the apparent potency of Type-II kinase inhibitors such as imatinib, which require a specific inactive kinase domain conformation for binding[373]. Additional work in our lab demonstrated that the interaction between SH3 and the linker can also be disrupted by peptides as well as small molecules in ABL as well as HCK and other SRC-family members[358,374]. These studies along with many others have clearly established an essential role for intramolecular SH3-linker interaction in the regulation of SRC-family kinase activity.

SH2 domains bind to short peptide sequences bearing phosphorylated tyrosines (pTyr) and like SH3 domains are also found in many signaling adapter proteins and kinases[375]. Proteins containing this domain are most commonly associated with signaling from receptor tyrosine kinases[376]. SH2 domains are approximately 100 amino acids in length and typically consist of two α-helices and seven β-strands. 115 human proteins contain this domain[377,378]. The specificity of this domain for target phosphopeptides can vary somewhat, but usually depends on the 3-6

amino acids C-terminal to the pTyr[379]. The SH2 domain has only been found in Eukaryotes[378]. In downregulated SRC-family kinases, the SH2 domain interacts with the phosphorylated tyrosine 527 on the C-terminal tail of the kinase. This brings the C-lobe of the kinase domain directly adjacent to the SH2 domain[372,380]. Tyr527 is phosphorylated by C-terminal SRC kinase (CSK) or C-terminal SRC kinase-homologous kinase (CHK)[381–383]. Work from our lab has shown that mutation of Tyr527 to phenylalanine in HCK prevents the phosphorylation of this residue by CSK, dramatically increases kinase activity in HCK, allows HCK to phosphorylate STAT3, and transforms Rat-2 fibroblast cells in a colonyforming assay[384–386]. This observation is consistent with mechanism of activation of v-SRC, which lacks a C-terminal tail and the attendant regulatory tyrosine for CSK.

The SRC kinases are just one group of more than 500 kinases encoded by the human genome (often referred to as the 'kinome'). All kinases share the ability to transfer phosphate from ATP to a substrate. Of the 518 kinases that make up the kinome, 20 are lipid kinases. Of the remaining kinases, an additional 20 are atypical protein kinases which lack the conserved eukaryotic protein kinase domain. The remaining kinases can be subdivided into 8 groups, which include the tyrosine kinases (TK), tyrosine kinase-like kinases (TKL), STE20/STE11/STE7 related kinases (STE), casein kinase like kinases (CK1), the protein kinase A/G/C related group (AGC), calcium/calmodulin-dependent kinases (CAMK), the CDK/MAPK/GSK related kinases (CMGC), and the receptor guanylyl cyclase related group (RGC)[387]. A prototypical protein kinase domain is around 300 amino acids in length but can be much longer if there is an insertion within the kinase domain as described above for FLT3. The TKs are the largest subfamily with 90 members and phosphorylate substrate proteins exclusively on tyrosine, while all other kinases phosphorylate serine, threonine or both. TKs are much more highly regulated than Ser/Thr

kinases, which may reflect their critical roles in cellular growth regulation. The total phosphotyrosine content within a given cell is one-thousand times less than phosphoserine and one hundred times less than phosphothreonine [388,389].

SRC-family kinase domain architecture is structurally conserved, consisting of a smaller N-lobe with five β-sheets and 1-2 α-helices, connected via a "hinge region" to a larger C-lobe, which is predominantly α-helical. Kinases bind to substrate and ATP in the cleft between the N- and C-lobes[390–392]. The N-lobe has several residues that are very important in catalysis. In between β1 and β2 there is glycine-rich loop which contains an important basic residue, usually lysine, that is critical for the coordination of the third phosphate in ATP[390–392]. The conserved α-helix in the N-lobe is called the α-C helix. This helix makes several contacts with the C-lobe of the kinase and is held in place by a loop preceding the 4th β-strand and a portion of the fifth β-strand. The loop preceding the fifth β-strand forms the activation loop (A-loop). The A-loop often sits in the space in between the N- and C-lobes when the kinase is inactive[390]. The A-loop contains several residues of importance, the most N-terminal of which is the conserved DFG motif (aspartate, phenylalanine, glycine) described above in relation to inhibitor action. This position of this dynamic motif indicates whether or not the kinase is in an active state. If the phenylalanine is pointed toward the catalytic aspartate in the C-lobe of the kinase (the DFG-in conformation described above), then the kinase is properly configured for the phosphotransfer reaction[390,392]. The position of this phenylalanine upon inhibitor binding also determines whether an inhibitor is Type-I (DFG-in preference; e.g. midostaurin) or Type-II (DFG-out preference; e.g. quizartinib). The A-loop also contains one or more tyrosine residues that are autophosphorylated upon kinase activation. In all eight SRC-family kinases, the tyrosine autophosphorylation site is located at position 416 (Y416), and phosphospecific antibodies for

this site provide a very useful tool to monitor SRC-family kinase activity in vitro or in cells . Near the end of β-strand 5 there is a residue known as the "gatekeeper residue". This residue controls access to a hydrophobic "back-pocket" of the N-lobe and is the most frequent residue mutated in kinase inhibitor resistance[390–393]. In SRC-family kinases this residue is always threonine, and is located at position 338. After β-stand 5 is the hinge region that connects the N and C-lobes. The C-lobe is predominantly α-helical but contains four β-strands. Between β-strand 6 and 7 there is the catalytic loop, which contains much of the catalytic machinery, including the Y/HRD motif (Tyr/His-Arg-Asp). The aspartate in the Y/HRD motif is responsible for orienting the hydroxyl acceptor of the substrate, while H/Y makes a hydrophobic contact with the phenylalanine in the DFG motif during phosphotransfer.

SRC-family kinase expression is critical in AML

SRC-family kinases have a long history of being associated with cancer[394]. Specifically in human cancer over-expression and upregulation of SRC-family kinase activity has been linked to poor prognosis in colorectal[395], breast[396], and prostate[397] cancer, even though these genes are rarely mutated in those cancers. These kinases represent unique drug targets in AML because unlike the other tyrosine kinases discussed in this section (AXL, SYK, FES, FER) they are good drug targets even without the presence of a FLT3-ITD mutation. This is due to the revelation by Dos Santos *et al*. that SRC-family kinases are both over-expressed and hyperactive, as measured by immunoblot, in AML cells compared to healthy $CD34^+$ hematopoietic progenitor cells[398]. Dos Santos *et al*. also found that among the SRC-family members expressed in myeloid cells (FYN, HCK, FGR and LYN), LYN was expressed at the highest level, leading them to conclude LYN was the most relevant drug target. However, their assay for SRC-family kinase activity did not resolve which SRC-family member was active in a given patient sample. This is because the

antibody for phosphotyrosine 416 recognizes all SRC-family members due to sequence conservation around the activation loop. Therefore, it is very possible that multiple SRC-family members are involved in AML pathogenesis. Furthermore, HCK, FGR, and FYN were also shown to be consistently expressed in AML patients, and even strongly overexpressed in a subset of the cases[398]. In a follow-up publication, the same group found that siRNA knockdown of LYN, HCK or FGR individually, or pan-inhibition with the pan-SRC inhibitor dasatinib, reduced the proliferation and increased apoptosis of primary AML cells[399]. In Chapter 2, I will also discuss the mRNA expression of SRC-family kinase in AML patients from the TCGA cohort, and how SRC-family kinase expression is linked to prognosis.

HCK and leukemic stem cells

The most critical evidence for HCK as an AML drug target comes from the idea that it is involved in the maintenance of leukemic stem cells (LSCs). LSCs and HSC both are $CD34^+$ and $CD38^-$. Saito *et al*. isolated LSCs from AML patients and compared gene expression to HSC isolated from cord blood. They found 25 genes to be significantly upregulated in LSCs compared to HSCs. The largest differences were observed for CD25 and CD32, followed by the WT1 tumor suppressor and then HCK, which was an exciting observation because HCK represents druggable target[400]. In a subsequent study, this same group screened for HCK inhibitors and re-discovered the HCK inhibitor, A-419259. This inhibitor was highly effective in treating mice with AML patient-derived xenografts. A-419259 also reduced the LSC burden, consistent with the idea that HCK is required for LSC survival[401]. Subsequent studies[402], and our own work (chapter 2), revealed that A-419259 has efficacy against other SRC-family members and FLT3. These results raise some questions about HCK as the primary drug target of A-419259.

Our lab has previously shown that substitution of the gatekeeper residue of HCK (T338) with methionine results in resistance to A-419259. Expression of HCK-T338M also confers resistance to A-419259 in BCR-ABL-transformed CML cells[403]. Further studies revealed that overexpression of wild type HCK in CML cells results in a strong resistance phenotype to the BCR-ABL inhibitor imatinib. This resistance could be overcome with selective co-inhibition of HCK and ABL[404]. This study also showed that the mechanism of resistance is likely due to transphosphorylation of the BCR-ABL SH3 domain by HCK, resulting in linker displacement and a shift to the DFG-in mode incompatible with imatinib binding. We were interested to see if a similar effect was found with HCK and other oncogenes, such as FLT3-ITD. See Chapter 2 for some experiments related to this idea.

LYN and AML

LYN was found to be the highest expressed SRC-family kinase in AML patients[398]. However, LYN is highly expressed in other types of hematopoietic cells including B-cells and T-cells[405] and is especially important in negative regulation of the B-cell receptor[406]. Thus, inhibition of LYN in the context of AML may produce unwanted effects in B cells. It should be noted that LYN has been implicated in many AML-related signaling pathways, such as phosphorylation of STAT3/STAT5[407] and activation of AKT[408]. Inhibition of LYN, with pan-SRC-family kinase inhibitors, reduced STAT3/5 phosphorylation. Additionally, treatment of primary AML cells with the FDA-approved pan-SRC-family kinase inhibitor dasatinib (Sprycel; Bristol-Myers Squibb) reduced proliferation and increased apoptosis[399]. It should be noted that dasatinib also inhibits many other kinases and therefore it is difficult to conclude that dasatinib activity against LYN is solely responsible for its anti-leukmic effects[298].

FGR inhibition as a strategy for AML treatment

FGR is arguably the least studied SRC-family kinase but appears to be one of the most interesting. Our lab is heavily involved in studying FGR as an AML drug target. We found FGR to be upregulated in a subset of AML patients (see chapter 2). Further, we found that wild type FGR has much higher intrinsic kinase activity than other SRC-family members. Unlike HCK or SRC, wild type FGR can transform Rat-2 fibroblasts and increase the colony forming efficiency of the AML cell line, TF-1. Further, peptides that bind to and displace the regulatory SH2 or SH3 domains do not increase the kinase activity of FGR, like they do for HCK or SRC[385]. Our lab also recently described TL02-59, a Type-II inhibitor with unique selectivity for FGR. The growth inhibitory efficacy of TL02-59 against primary AML bone marrow cells correlates with FGR mRNA expression. In fact, the primary cells that responded best to this kinase inhibitor were wild type for FLT3, which suggests that FLT3 is not the primary target for this inhibitor[409]. While our published data strongly link FGR to the efficacy of TL02-59, this compound also inhibits other SRC-family members and FLT3 albeit with lower potency.

Summary of pharmacologic inhibition of SRC-Family kinases in AML

Thus far I have discussed several studies that use small molecules to inhibit SRC-family kinases in AML where the authors imply that inhibitor efficacy is due to inhibition of one particular kinase, such as LYN, FGR or HCK. To be clear, A-419259[401], dasatinib[399], TL02-59[409] and other SRC inhibitors[407] all have strong anti-AML efficacy, but they all have at least some activity against HCK, LYN and FGR making it difficult to decipher which kinase is the true target. In fact, inhibition of all three of these kinases by a single compound may be of therapeutic benefit, given that knockdown of any one of these kinases individually results in growth arrest of AML patient-derived bone marrow cells in vitro. SRC-family kinases appear to be relevant

AML drug targets, even without the presence of a FLT3-ITD mutation. This is supported by the observation that all AML patient-derived xenograft mice respond to A-419259[401] (although the FLT3 mutational status of each donor was unfortunately not reported in this study). Furthermore, the AML bone marrow samples most sensitive to TL02-59 were wild-type for FLT3-WT[409]. Lastly, dasatinib, which has no activity against FLT3[298], still had strong efficacy against AML primary cells in vitro[399].

1.2.3 Serine/Threonine kinases in AML and multi-targeted inhibitors

1.2.3.1 MAP kinases

While, additional mutations in the FLT3 kinase domain remain the predominant mechanism of resistance to selective FLT3 inhibitors, upregulation of downstream pathways such as AKT or ERK are alternative mechanisms of reisstance[311]. To address these concerns a dual FLT3/ERK inhibitor, E6201, is under investigation[320]. This inhibitor has great efficacy in mouse models against AML driven by FLT3-ITD[410]. In the clinic, E6201 has demonstrated some efficacy for melanoma patients[411], but these results are very early and no results have been published for FLT3-ITD AML patients.

1.2.3.2 PIM kinases

One of the most exciting drug targets in FLT3-ITD AML are the PIM kinases. PIM1 and PIM2 are found to be frequently upregulated in FLT3 inhibitor-resistant tumors[412–414]. Furthermore, inhibition of PIM1/2 seemed to re-sensitize FLT3 inhibitor-resistant AML to FLT3 inhibition[413]. These findings have resulted in the development of several dual FLT3/PIM inhibitors[415,416]. It remains to be seen how effective these inhibitors are in the clinic, but there is

reason to be optimistic. The rationale for PIM inhibition is very similar to AXL, and dual FLT3/AXL inhibitors are the most successful FLT3 inhibitors in the clinic currently available[299].

1.2.3.3 Cyclin dependent kinases 4 and 6

Another promising area of research regarding multi-targeted FLT3 inhibitors is dual CDK and FLT3 inhibitors. CDK4 is downstream of FLT3-ITD and regulators of CDK4, such as p15 are downregulated in AML[417]. Additionally there is synergy in the inhibition of CDK4 and FLT3-ITD in AML cell lines[418]. The dual CDK4/FLT3 inhibitor AMG925 was rationally designed based on crystal structures of CDK4 bound to inhibitors and existing FLT3 structures[419]. AMG925 (also called FLX925) was highly effective in preclinical studies, especially in xenograft mice[420]. AML cells that are resistant to sorafenib or quizartinib, remained responsive to selective CDK4 inhibition. All the mutations that typically confer FLT3 inhibitor resistance, only conferred partial resistance to AMG925. Furthermore, in a screen in which mutagenized cells (treated with ENU) were incubated with high concentrations of AMG925, resistant clones were observed only 1% of the time, whereas quizartinib-resistant clones were found in 7.6% of wells[421]. Unfortunately, AMG925 was not effective in the clinic due to poor pharmacokinetics[422].

1.3 Two hit model for leukemogenesis

The AML tumor cell population within a given patient is heterogeneous, with different subgroups of cells containing different mutations or expressing different genes. By extension, it is reasonable to assume that LSCs also reflect this heterogeneity. There is evidence for LSCs

being heterogeneous in acute lymphocytic leukemia (ALL), where engraftment of the same initial ALL cell population in different mice can result in different subpopulations of the tumor propigating[423]. There is also evidence of the requirement of a series of genetic changes in order to lead to AML progression. In fact there is evidence of cells in the blood containing MLL rearrangement in utero[424] and in cord blood[425], which increases the risk of AML, but do not necessarily predict it. The presence of AML-associated mutations in the blood is not unique to infants, as 6% of women over age 65 were found to have detectable TET2 mutation in their blood[426]. Clones carrying these mutations proliferate enough to become the dominant group of cells within the bone marrow and blood, but do not result in a cancer phenotype. The presence of these mutations (or others) does not definitively predict the occurrence of cancer, but do significantly increase the risk[427]. Therefore, there is the idea that multiple 'classes' of mutations are required for AML pathogenesis. Class I mutations confer a proliferative and survival advantage, while class II mutations lead to impaired differentiation. An example of a class I mutation is FLT3-ITD. A possible reason why FLT3 expression is retained in AML may be due to the presence of a class II mutation, because FLT3 is normally expressed only in early hematopoietic cells. Class II mutations include all of the defective transcription factors associated with AML[428].

1.4 Hypothesis and specific aims

1.4.1 Hypothesis

AML is a deadly disease with only a 10-25% survival rate. The disease etiology is very heterogeneous. Unlike CML, where 95% of cases can be explained by a single translocation, there are multiple types of mutations that drive AML. To make matters more complex, a single tumor likely has multiple AML-related mutations, and the disease tends to be multi-clonal, that is different driver mutations can be in different cells. One mutation that has consistently been shown to be associated with poor prognosis is FLT3-ITD. Inhibitors against FLT3-ITD result in efficacy for a short period of time, but patients will almost always relapse with drug-resistant disease. The most promising inhibitors for combatting the acquired drug resistance thus far are the multi-kinase inhibitors against FLT3-ITD and either AXL, CDK4 or PIM1/2. Therefore, we believe that multi-kinase inhibitors may be required for a durable response to FLT3 inhibition.

An additional group of drug targets in AML are the myeloid members of SRC kinase family, including HCK, LYN and FGR, which are upregulated and overactive in a substantial subset of AML patients. Transcript levels of these SRC-family members in the TCGA cohort is correlated with poor prognosis. The efficacy of SRC-family kinase inhibitors such as A-419259, TL02-59 or dasatinib validates SRC-family kinases as drug targets in AML. Furthermore, the efficacy of at least one of these inhibitors, TL02-59, is not dependent on the presence of a FLT3-ITD mutation.

Based on these observations, I propose a multi-targeted strategy that may result in more durable responses against FLT3 inhibition. Targeting multiple pathways may reduce the propensity of compensatory pathways conferring resistance. In this thesis, I investigated the

mechanism of action of a promising dual SRC/FLT3 inhibitor called A-419259. In Chapter 2, I applied the techniques of engineered inhibitor resistance, based on X-ray crystal structures of HCK bound to A-419259, along with in vitro evolution of *de novo* resistance, to better understand the efficacy of this compound. In Chapter 3, I describe a codon mutagenesis approach to identify possible A-419259 resistance mutations HCK in an unbiased way. My thesis research consisted of the following Specific Aims:

1.4.2 Specific aims

1.4.2.1 Aim 1: Examine the relationship of SRC-family kinase expression on AML patient survival

SRC-family kinase inhibition with A-419259, TL02-59 and dasatinib have all been shown to reduce growth of primary AML cells, with efficacy in vivo. In some cases, the expression of SRC-family kinases is correlated with efficacy of these compounds. Each of the myeloid SRC-family member has independent attributes making them ideal drug targets as well. HCK is upregulated in leukemic stem cells. LYN can directly phosphorylate STAT5. FGR has oncogenic properties when overexpressed. Therefore, we wanted to understand the expression patterns and prognosis of AML patients expressing high levels of SRC-family kinases. First, we confirmed that HCK, LYN and FGR expression was higher than the other SRC-family kinases in AML patient samples. We also found that the expression of these kinases was independent of FLT3 mutations. We found that high levels of HCK, LYN or FGR expression was highly correlated to poor prognosis. Furthermore, HCK, LYN and FGR expression was strongly correlated. This may indicate that there is a subset of AML patients with high levels of HCK, LYN and FGR expression that may benefit from SRC-family kinase inhibitors.

1.4.2.2 Aim 2: Determine the effect of SRC-family kinase expression on AML cell responses to kinase inhibitors

In order to study the SRC-family kinase inhibitor A-419259 in the context of FLT3-ITD$^+$ AML, we generated stable TF-1 myeloid leukemia cells that expressed FLT3-ITD either alone or together with either HCK or FGR. We discovered that A-419259 was effective against TF-1 cells transformed with FLT3-ITD, and that the expression of wild type HCK or FGR with FLT3-ITD in TF-1 cells did not change sensitivity to A-419259. We then engineered resistance to the inhibitor by introducing canonical FLT3 inhibitor resistance mutations into FLT3-ITD. Expression of these FLT3-ITD mutants, D835Y and F691L, in TF-1 cells resulted in a resistance phenotype that was partially mitigated by co-expression of HCK or FGR. Similarly, engineered HCK or FGR inhibitor resistance mutations also generated partial resistance to A-419259 in TF-1 cells transformed with wild type FLT3-ITD. These results indicate that in FLT3-ITD$^+$ AML the main drug target is likely the FLT3 kinase domain, but that SRC-family kinases do play a role in A-419259 efficacy as well as resistance.

1.4.2.3 Aim 3: Investigate *de novo* mechanisms of A-419259 resistance in FLT3-ITD+ AML

To understand how resistance to A-419259 may evolve in an unbiased way, we generated A-419259-resistant cell lines by passaging FLT3-ITD$^+$ AML cells in gradually higher concentrations of the compound over a period of more than one year. Our resistant cell lines maintained resistance even after a 4-week drug holiday, which implied a genetic change that caused resistance. Subsequent whole exome sequencing revealed that six independently derived resistant cell populations all had mutations of N676 in the FLT3 kinase domain. No mutations were observed in HCK, LYN or FGR. We confirmed that FLT3-N676S conferred a strong resistance phenotype against A-419259 in TF-1 cells. Importantly, even co-expression of HCK

or FGR could not re-sensitize TF-1 FLT3-ITD-N676S cells to A-419259. These results suggest that the pathway to acquired resistance with A-419259 is distinct from that observed with other FLT3 inhibitors, and that its activity against SRC-family kinases may influence the timing and route to resistance.

1.4.2.4 Aim 4: Determine HCK mutations that are highly resistant to A-419259

In FLT3 wild-type AML, the main mechanism of action of A-419259 is HCK kinase inhibition. To investigate HCK as an A-419259 target we need to develop highly resistant mutants. We used a codon-mutagenesis approach, in which we created every possible mutation at all codons in HCK-Y527F. The HCK-Y527F mutation results in a highly active kinase that is able to induce colony formation of Rat-2 fibroblast cells in soft agar. We expressed our HCK-Y527F codon mutagenesis library in Rat-2 cells and selected for the drug resistant mutants by plating the cells in soft agar and looking for colony formation. We found that a mutation of the gatekeeper residue of HCK (T338) to histidine was enough to confer strong resistance to A-419259. We further confirmed that this mutation was resistant in AML cells. HCK-T338H will prove to be a valuable tool for studying HCK as an A-419259 drug target in FLT3 wild-type AML.

2.0 Expression of myeloid SRC-family kinases is associated with poor prognosis in AML and influences FLT3-ITD$^+$ kinase inhibitor acquired resistance

2.1 Chapter 2 summary

Unregulated protein-tyrosine kinase signaling is a common feature of AML, often involving mutations in FLT3 and overexpression of myeloid SRC-family kinases (HCK, FGR, LYN). Here we show that high-level expression of these SRC kinases predicts poor survival in a large cohort of AML patients. To test the therapeutic benefit of FLT3 and SRC-family kinase inhibition, we used the pyrrolo-pyrimidine kinase inhibitor A-419259. This compound potently inhibits HCK, FGR, and LYN as well as FLT3 bearing an activating internal tandem duplication (ITD). FLT3-ITD expression sensitized human TF-1 myeloid cells to growth arrest by A-419259, supporting direct action on the FLT3-ITD kinase domain. Cells transformed with the FLT3-ITD mutants D835Y and F691L were resistant to A-419259, while co-expression of HCK or FGR restored inhibitor sensitivity. Conversely, HCK and FGR mutants with engineered A-419259 resistance mutations decreased sensitivity of TF-1/FLT3-ITD cells. To investigate *de novo* resistance mechanisms, A-419259-resistant FLT3-ITD$^+$ AML cell populations were derived via long-term dose escalation. Whole exome sequencing identified a distinct FLT3-ITD kinase domain mutation (N676S/T) among all A-419259 target kinases in each of six independent resistant cell populations. These studies show that HCK and FGR expression influences inhibitor sensitivity and the pathway to acquired resistance in FLT3-ITD$^+$ AML.

2.2 Introduction

Acute myeloid leukemia (AML) is characterized by unchecked expansion of undifferentiated myeloid blast cells that ultimately take over the bone marrow, resulting in suppression of normal hematopoiesis. Currently, AML patients have only a 40% five-year survival rate[7] and most are limited to a chemotherapy regimen that has changed little over the past 45 years[429]. While multiple genetic changes are associated with AML, upregulation of protein-tyrosine kinase signaling is a common theme that offers an opportunity for targeted therapy. One important example involves the FMS-like tyrosine kinase 3 (FLT3) receptor tyrosine kinase, which is often over-expressed[430] or mutated in AML[141]. FLT3 and its associated ligand regulate normal hematopoiesis and are expressed by progenitor cells of the myeloid and lymphoid lineages[243,431]. Mutations in FLT3 result in ligand-independent kinase activity and leukemogenesis[432], defining FLT3 as a classic proto-oncogene in AML. Activating FLT3 mutations occur as either internal tandem duplication (ITD) events in the cytosolic juxtamembrane region[141,143] or as point mutations in the tyrosine kinase domain [145]. FLT3-ITD mutations are more common[37,38,42] and associated with a worse prognosis[36,38,141,433].

The identification of FLT3-ITD as a common driver mutation in AML led to the development of FLT3 kinase inhibitors as an approach to precision therapy. FLT3 inhibitors have had some success in clinical trials[196,292,434,435] although low response rates and acquired resistance remain as vexing problems[196,300,436,437], even for the recently FDA-approved FLT3 inhibitor midostaurin[313]. Most patients develop resistance to FLT3 inhibitors through mutations in the kinase domain that affect inhibitor binding but not kinase activity[251,276,312,313,438,439]. For example, midostaurin resistance can arise from substitution of kinase domain residue Asn676, which forms a network of hydrogen bonds to stabilize inhibitor binding[312,313,439]. Quizartinib is

another promising FLT3 inhibitor currently in clinical trials as an FDA-designated breakthrough therapy for AML. While quizartinib is a potent and highly selective FLT3 inhibitor, single kinase domain point mutations can also confer complete resistance including F691L, D835Y and Y842C[276]. Other mechanisms of FLT3 inhibitor resistance have been reported including upregulation of Stat5[440] and FLT3 ligand[441] expression as well as enhanced flux through the Ras/Erk[317], PI3K/Akt[317] and PIM kinase families[413,442]. The rapid evolution of FLT3 kinase inhibitor resistance underscores the need for strategies that limit emergence of mutations that acutely evade treatment and thus minimize the prospect of recurrent disease.

One promising approach to suppress the emergence of inhibitor resistance is to use compounds that target not only FLT3, but also other AML-associated tyrosine kinases linked to disease. Myeloid SRC-family kinases, including HCK, LYN and FGR, are frequently over-expressed in AML leukemic stem cells[398,399] and are known to interfere with FLT3 maturation[443]. Our group has recently shown that HCK, LYN and FGR are commonly overexpressed in bone marrow cells from AML patients, consistent with these findings[409]. In addition, AML stem cells have much higher SRC-family kinase activity than normal hematopoietic stem cells and myeloid cells[398,399]. High expression and kinase activity suggest that selective inhibitors of HCK, LYN and FGR will reduce AML cell viability. This idea is reinforced by RNAi-knockdown studies of these SRC-family members, where reduced kinase expression correlates with growth arrest and increased apoptosis in primary AML cells[399].

Strong evidence specifically implicates HCK in AML. Saito *et al*. found HCK to be overexpressed in leukemic stem cells from patients who had relapsed from chemotherapy[444] and showed that shRNA-mediated knockdown of HCK arrested growth of blast cells from AML patients[399,401]. This group went on to show that the pyrrolopyrimidine SRC-family kinase

inhibitor A-419259 (referred to as RK-20449 in Saito *et al.*[401]) completely eliminates chemotherapy-resistant AML patient xenografts in mice[401]. Subsequent work has shown that A-419259 is also an inhibitor of FLT3 kinase activity in vitro, suggesting that its activity against multiple AML-associated tyrosine kinases may account for its efficacy against primary patient cells in the mouse xenograft model[402]. In addition to HCK, recent evidence has identified FGR as an oncogene and a therapeutic target in AML. In contrast to HCK, expression of wild-type FGR without mutation induces oncogenic transformation of rodent fibroblasts in vitro, and reduces the cytokine dependence of the human myeloid leukemia cell line, TF-1[385]. In addition, an *N*-phenylbenzamide kinase inhibitor, TL02-59, potently inhibits FGR kinase activity in vitro and in vivo. This compound suppresses proliferation of bone marrow cells from AML patients that express high levels of FGR[409].

In this present study, we combined the use of kinases with engineered inhibitor resistance mutations and *in vitro* selection of resistance to determine the roles of FLT3, HCK and FGR in the sensitivity of AML cells to A-419259 treatment. Human myeloid leukemia cells transformed with FLT3-ITD acquired remarkable sensitivity to A-419259 in the presence or absence of HCK or FGR. Cells transformed with mutants of FLT3-ITD (D835Y and F691L), known to cause resistance to other kinase inhibitors, completely lost their A-419259 sensitivity, validating FLT3-ITD as a direct target for this compound in cells. When HCK or FGR were co-expressed with these FLT3-ITD mutants, A-419259 sensitivity was partially restored. Conversely, co-expression of wild-type FLT3-ITD with engineered A-419259-resistant mutants of HCK or FGR resulted in partial resistance to A-419259. In an unbiased approach, we experimentally evolved A-419259-resistant populations of FLT3-ITD^{+} AML cell lines (which also express endogenous active HCK and FGR) through gradual dose escalation, which required many months. Subsequent whole

exome sequence analysis revealed a distinct resistance mutation at a single position in the FLT3 kinase domain (N676 only), but not in HCK, FGR, or any other A-419259 target kinase domains identified by KINOMEscan analysis. Together, our results show that HCK and FGR expression influences both A-419259 sensitivity and the pathway to acquired resistance to this compound in FLT3-ITD^{+} AML.

2.3 Results

2.3.1 Myeloid SRC-family kinase expression is predictive of patient survival in AML

Knockdown of HCK, LYN and FGR expression has been shown to decrease proliferation of patient AML cells, suggesting that the activity of these kinases is essential for disease progression[399]. However, the extent to which these kinases are expressed in AML as well as their relationship to disease outcome has not been analyzed in detail. To address these important issues, we first examined mRNA expression data in 163 AML patient samples publicly available from the Cancer Genome Atlas (TCGA) database. This analysis revealed that the SRC-family kinases HCK, LYN and FGR are most highly expressed in AML patients in comparison to the other five SRC-family members (Figure 3). HCK and FGR showed a broad distribution of expression across the samples, while the levels of LYN were more tightly clustered. Furthermore, pairwise analysis of HCK, FGR and LYN transcript levels revealed that expression of these kinases is highly correlated within individual patients (Figure 4). To determine whether myeloid SRC-family kinase expression correlated with prognosis, we performed Kaplan-Meier

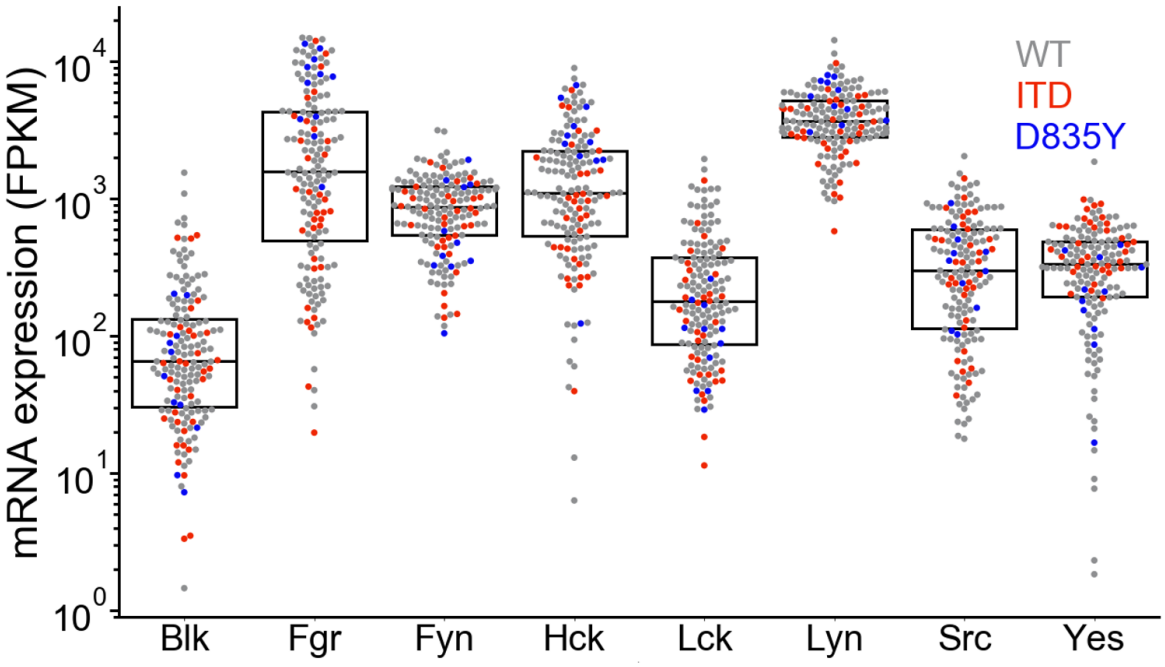

Figure 3. Expression profiles of Src-family kinases in AML.

Gene expression of the eight mammalian Src-family members in samples from all AML patients in The Cancer Genome Atlas (TCGA) cohort (n = 163). Transcript data are shown as the number of kinase cDNA fragments per kilobase of transcript per million mapped reads (FPKM). Dots represent individual patient expression data, with the dot color representing Flt3 mutational status (grey, wild type; red, ITD; blue, D835Y). The boxplot shows the mean and quartile (25-75%) expression values for each kinase.

analysis on the 150 AML patient samples from TCGA where survival data was available. HCK, FGR and LYN expression were all strongly predictive of patient prognosis. The 20% of patients with the highest levels of HCK, LYN or FGR expression showed the worst survival outcomes compared to the 20% with the lowest expression (Figure 5). In contrast, expression levels of FLT3 did not correlate with significant differences in survival. However, when other clinical features are taken into account in a multivariate analysis, clinical features such as ethnicity, race and cytogenetics are much more predictive of a given patient's survival (Figure 6). It should be noted that Hck, Fgr and Lyn expression did not correlate strongly with any single clinical feature

(Figure 7). Furthermore, HCK, FGR and LYN are most highly expressed in AML compared to other cancer types, with the exception of diffuse large B-cell lymphoma (DBLC; Figure 8). Taken together, these results provide strong support for the idea that HCK, LYN and FGR are viable inhibitor targets for AML therapy, and that selective inhibitors of these kinases may provide therapeutic benefit without the toxicity associated with broad-spectrum kinase inhibitors.

2.3.2 A-419259 targets multiple AML-associated kinases *in vitro* and in cells

Previous studies have shown that the pyrrolopyrimidine tyrosine kinase inhibitor A-419259 (also known as RK-20449) has potent anti-tumor efficacy against AML cells both in vitro and in vivo. While initial studies suggested that HCK is the primary inhibitor target for A-

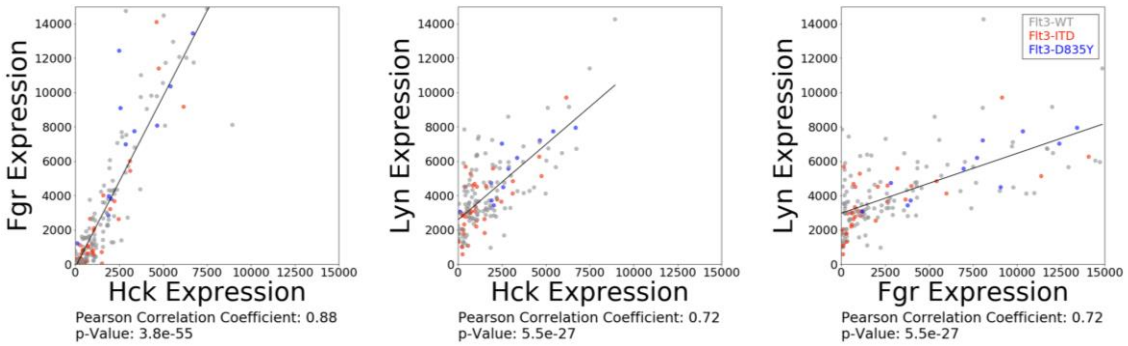

Figure 4. Pairwise correlation analysis of Hck, Fgr and Lyn transcript levels across all AML samples in the TCGA cohort.

Hck, Fgr, and Lyn transcript levels are shown as the number of kinase cDNA fragments per kilobase of transcript per million mapped reads for all AML patients in the TCGA cohort (n=163). Dots represent individual patient expression data, with the dot color representing Flt3 mutational status (grey, wild type; red, ITD; blue, D835Y). The plots compare Fgr vs. Hck (*left*), Lyn vs. Hck (*middle*) and Lyn vs. Fgr (*right*). Shown below each plot is the Pearson correlation coefficient and p-value for each comparison. Code used to generate these plots is available on github (see Materials and Methods).

419259 in AML[401], additional SRC-family kinases as well as FLT3 may also be inhibited by this compound. Whether inhibition of a single kinase or multiple kinases is responsible for its potent anti-AML effects is unknown. To begin to address these questions, we first determined the A-419259 target kinase profile compound[402]. This raises the important issues of the overall kinase specificity profile for A-419259 by KINOMEscan, an indirect binding assay that provides kinome-wide assessment of inhibitor specificity[445]. A-419259 was analyzed at the relatively high concentration of 1 μM against 468 kinase targets and showed remarkable overall selectivity with just 19 interactions, indicating that just 4% of the tested kinases bound to the compound. A-419259 interacted most strongly with SRC-family kinases, including HCK, FGR and LYN, and to several class III receptor tyrosine kinases, including FLT3 (wild-type, ITD and D835Y forms), Kit, the CSF-1 receptor as well as the α and β forms of the PDGF receptor (Figure 9A; complete KINOMEscan results are presented in Appendix A). To validate these results, each of the AML-associated kinases that scored as hits were tested for sensitivity to A-419259 using the Z'Lyte in vitro kinase assay (see Experimental Procedures). A-419259 inhibited all three AML-associated SRC-family members as well as the wild-type and mutant forms of the FLT3 kinase domain (Figure 9B). The potency of A-419259 or HCK, FGR, LYN and FLT3-ITD varied by three-fold or less, suggesting that inhibition of each of these kinases may contribute A-419259 anti-AML efficacy.

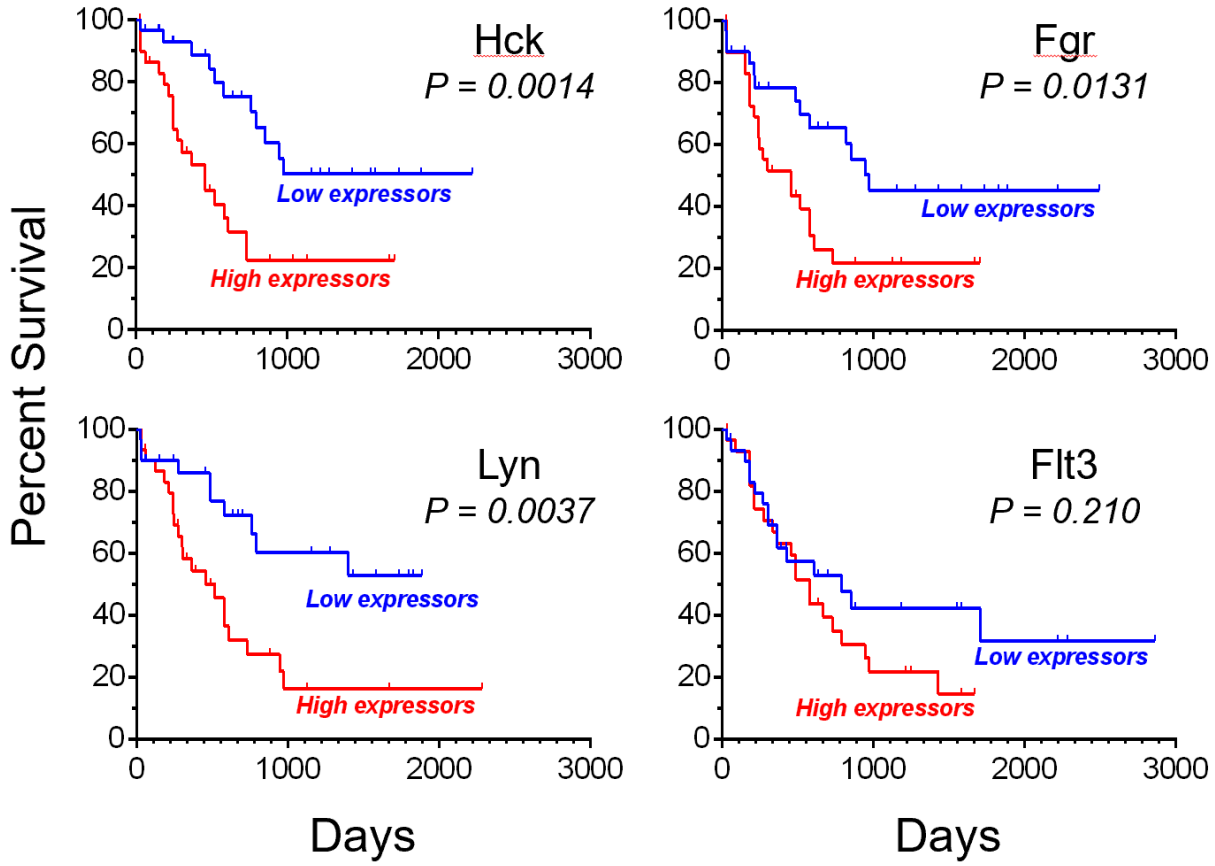

Figure 5. Survival of AML patients based on Src family kinase expression.

Kaplan-Meier survival analysis for AML patients with the highest (top 20%; red) and lowest (bottom 20%; blue) mRNA levels for *FGR*, *HCK*, *LYN* and *FLT3* (30 patients per group from 150 cases where survival data was available). The survival difference between patients with high vs. low expression is significant for the Src-family kinases but not *FLT3* (P value shown from Mantel-Cox test).

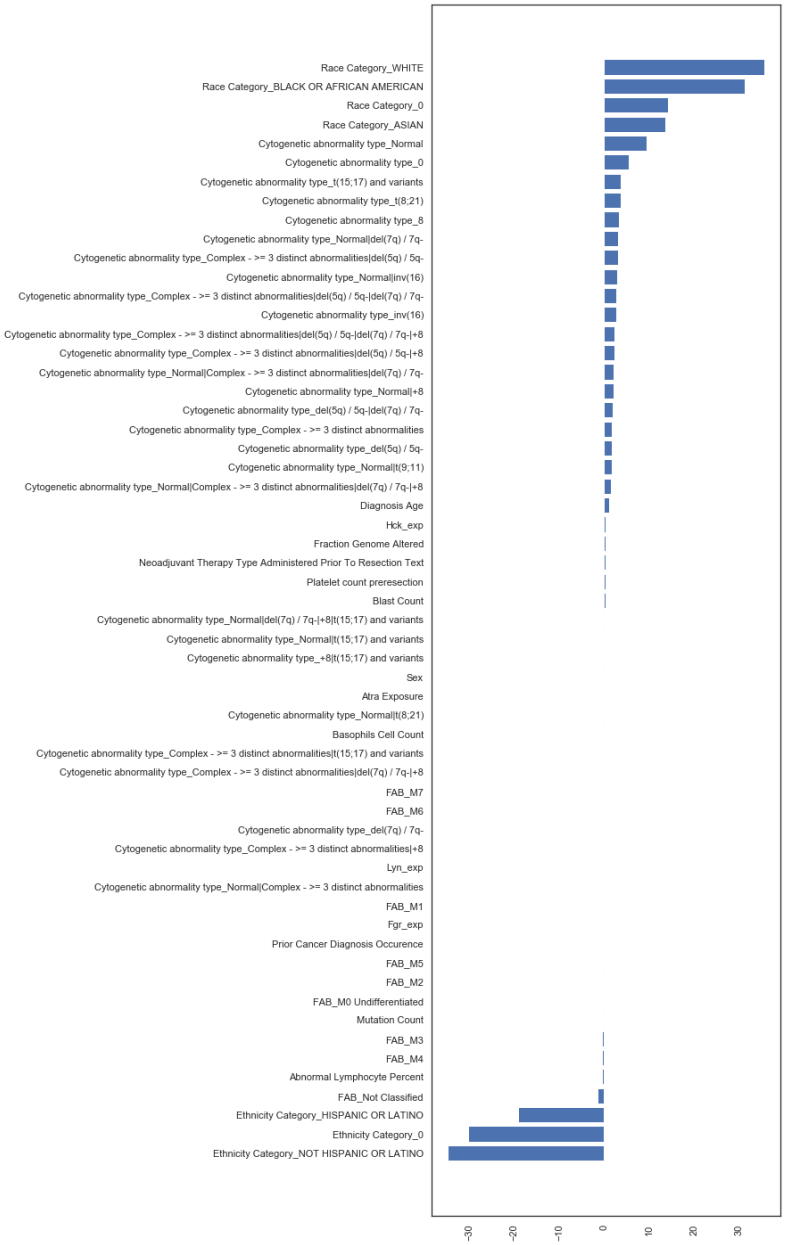

Figure 6. Cox-proportional hazard's model reveals that clinical features are more informative than Hck, Fgr and Lyn expression.

A Cox-proportional hazard's model to look at multi-variate survival analysis for AML patients based on clinical features and Hck, Fgr and Lyn expression. The feature weights on the model are shown. Code used to generate these plots is available on github as described under Materials and Methods.

Figure 7. Correlation matrix of AML clinical features

The correlation plot of all clinical features and Hck, Fgr and Lyn expression from patients in the TCGA AML cohort. Red indicates positive correlation between clinical features. Code used to generate these plots is available on github as described under Materials and Methods.

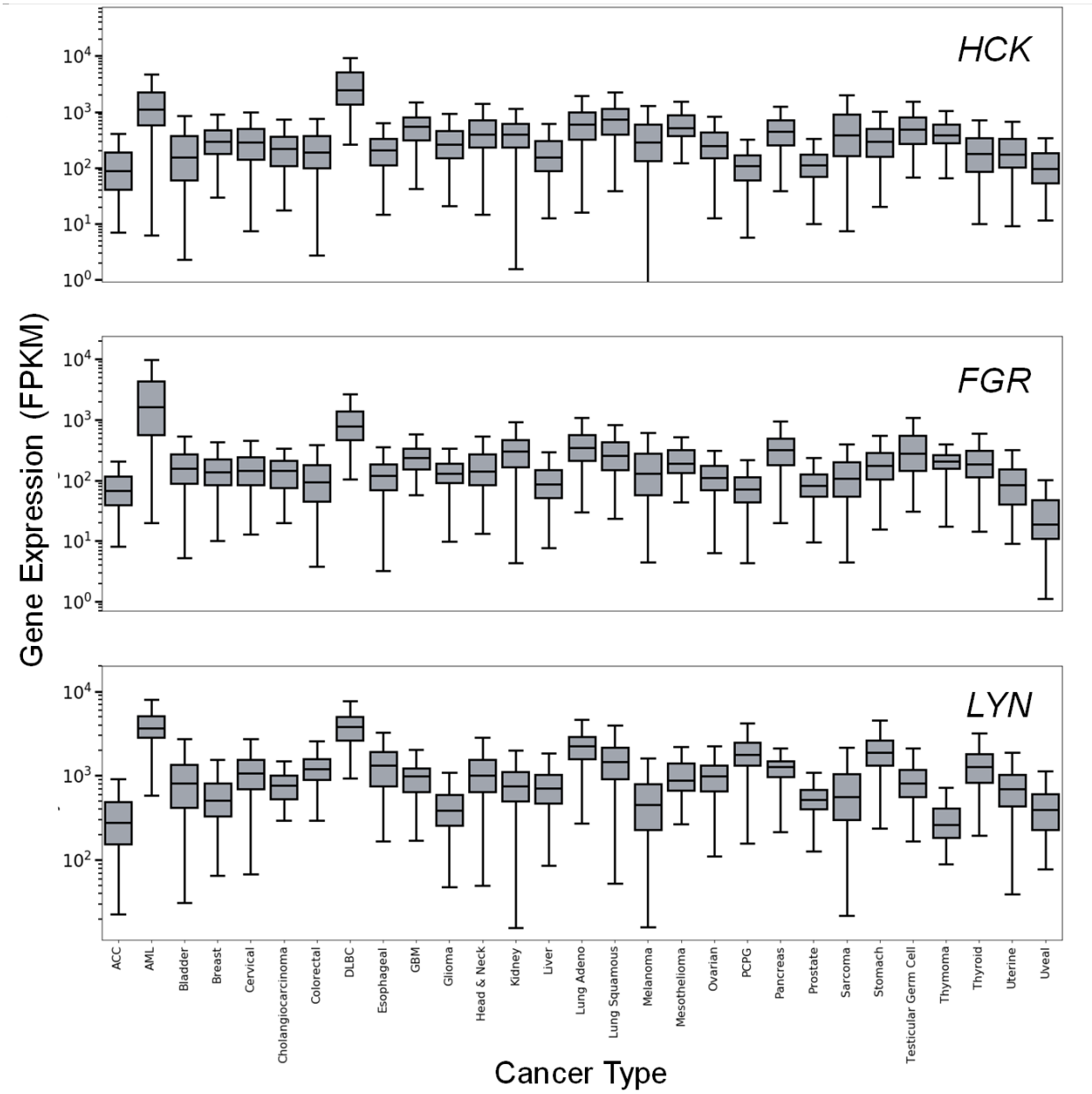

Figure 8. Comparison of Hck, Fgr and Lyn transcript levels across all tumors in the TCGA cohort.

Transcript levels for Hck, Fgr and Lyn were downloaded for all tumors available on cBioPortal from the TCGA database. Data are shown as the number of cDNA fragments per kilobase of transcript per million mapped reads (FKPM). Each box and whisker plot shows the mean (middle line in box), 25th-75th percentiles (edges of box), and outliers (whiskers) for each data set. Code used to generate these plots is available on github as described under Materials and Methods.

2.3.3 FLT3-ITD is a target for A-419259 in transformed AML cells

Our observation that A-419259 potently inhibits FLT3-ITD kinase activity *in vitro* led us to explore whether FLT3-ITD alone is a target for this compound in AML. To test this hypothesis, we used the human myeloid leukemia cell line TF-1 which is dependent on the cytokine GM-CSF for growth[446]. TF-1 cells do not express endogenous HCK, FGR or FLT3, and are transformed to GM-CSF-independent growth by the expression of FLT3-ITD but not wild-type FLT3[268]. In this way, TF-1 cells provided an ideal system for analysis of the contributions of FLT3-ITD, as well as HCK and FGR, to A-419259 responsiveness.

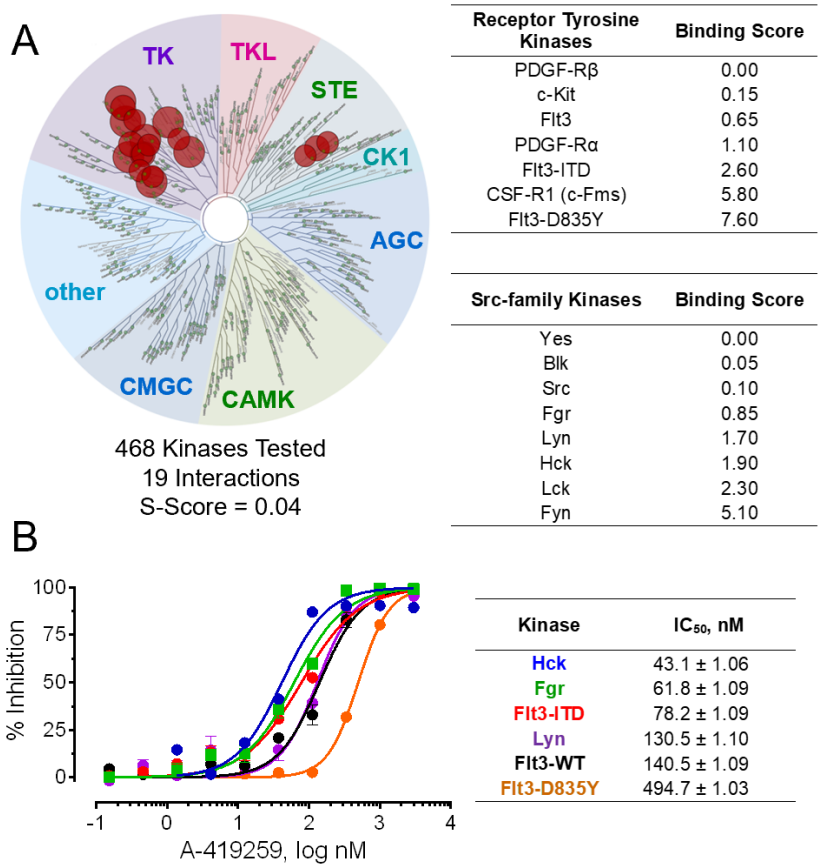

Receptor Tyrosine Kinases	Binding Score
PDGF-Rβ	0.00
c-Kit	0.15
Flt3	0.65
PDGF-Rα	1.10
Flt3-ITD	2.60
CSF-R1 (c-Fms)	5.80
Flt3-D835Y	7.60

Src-family Kinases	Binding Score
Yes	0.00
Blk	0.05
Src	0.10
Fgr	0.85
Lyn	1.70
Hck	1.90
Lck	2.30
Fyn	5.10

Kinase	IC_{50}, nM
Hck	43.1 ± 1.06
Fgr	61.8 ± 1.09
Flt3-ITD	78.2 ± 1.09
Lyn	130.5 ± 1.10
Flt3-WT	140.5 ± 1.09
Flt3-D835Y	494.7 ± 1.03

Figure 9. Target kinase specificity profile for the pyrrolopyrimidine tyrosine kinase inhibitor, A-419259.

(**A**) KINOMEscan profile of A-419259 tested against 468 kinases at a final concentration of 1 µM. TreeSpot diagram (*left*) shows all test kinases on a circular dendrogram of the human kinome, with interacting kinases shown as red circles; non-interacting kinases are represented as small green dots. Interacting kinases include class III receptor tyrosine kinases and Src-family kinases, and their individual binding scores are summarized in the tables (*right*). Each value represents the percent of residual kinase binding to the immobilized probe compound (i.e., a value of 0 represents 100% probe displacement by A-419259). Overall, 19 kinase interactions were observed for an S-Score of 0.04, indicative of a very selective inhibitor. Complete KINOMEscan results are provided in the Supporting Information (Appendix A). (**B**) *In vitro* kinase assays. Recombinant Flt3 kinase domains (wild type, ITD and D835Y) as well as near-full-length Hck, Lyn and Fgr were assayed using the Z'-LYTE *in vitro* kinase assay in the presence of a range of A-419259 concentrations, and the resulting data are plotted as percent inhibition relative to the DMSO control (*left*). The concentration-response curves were best-fit by non-linear regression analysis, and the resulting IC_{50} values are shown in the table as the mean of four replicates ± SE (*right*).

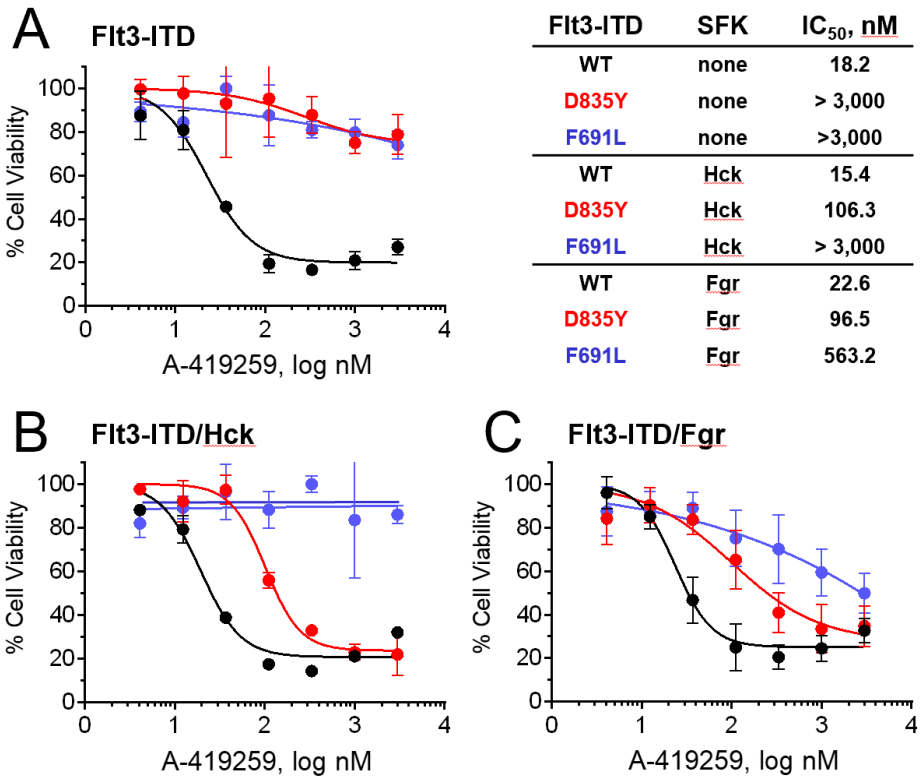

Flt3-ITD	SFK	IC_{50}, nM
WT	none	18.2
D835Y	none	> 3,000
F691L	none	>3,000
WT	Hck	15.4
D835Y	Hck	106.3
F691L	Hck	> 3,000
WT	Fgr	22.6
D835Y	Fgr	96.5
F691L	Fgr	563.2

Figure 10. Transformation of by Flt3-ITD sensitizes TF-1 myeloid cells to growth suppression by A-419259.

TF-1 myeloid cells were transformed to cytokine independence by expression of Flt3-ITD with wild type, D835Y or F691L mutant kinase domains. These mutations are associated with clinical resistance to quizartinib and other Flt3 kinase inhibitors (see main text). (**A**) TF-1 cells expressing each form of Flt3-ITD (wild-type, black; D835Y, red; F691L, blue) were incubated in the presence of a range of A-419259 concentrations or DMSO alone as control. Cell viability was determined 72 hours later using the CellTiter Blue cell viability assay. Results were normalized to DMSO control values, and are presented as mean percent control ± SD for triplicate determinations. (**B**, **C**) Hck and Fgr were co-expressed in the TF-1/Flt3-ITD cell populations from part A, and sensitivity to growth arrest by A-419259 was determined as before. IC_{50} values for each experiment were determined by non-linear regression analysis and are summarized in the table (*upper right*).

TF-1 cells transformed by FLT3-ITD became very sensitive to A-419259 treatment, with an IC_{50} value for growth inhibition of 18.2 nM (Figure 10). By contrast, growth of parent TF-1 cells cultured in the presence of GM-CSF was unaffected by A-419259 treatment (highest concentration tested was 3.0 µM; data not shown). Co-expression of FLT3-ITD with HCK or FGR did not substantially alter the sensitivity of TF-1 cells to the inhibitor, with IC_{50} values of 15.4 and 22.6 nM, respectively. TF-1 cells were then transformed with two established FLT3-ITD inhibitor resistance mutants, D835Y and F691L. These cell populations were completely resistant to A-419259, supporting direct action of the compound on the FLT3-ITD kinase domain. Interestingly, co-expression of HCK with FLT3-ITD-D835Y (but not F691L) partially re-sensitized the cells to growth arrest by A-419259, with an IC_{50} value just over 100 nM. Co-expression of FGR re-sensitized both FLT3-ITD-D835Y and FLT3-ITD-F691L cells to A-419259, although the effect on the FLT3-ITD-F691L cells was less pronounced. These results suggest that the presence of HCK and FGR may suppress the evolution of the FLT3-ITD resistance mutations D835Y and F691L.

To explore the relationship between inhibitor action on cell growth and kinase function, FLT3-ITD was immunoprecipitated from each of the cell lines in Figure 10 after A-419259 treatment and immunoblotted for phosphotyrosine content with anti-phosphotyrosine antibodies. Recovery of FLT3-ITD was determined by immunoblotting for FLT3 protein, and activity was expressed as a ratio of the antiphosphotyrosine to FLT3 immunoblot signal intensities following LI-COR imaging (Figure 11). As expected, tyrosine phosphorylation of FLT3-ITD was observed

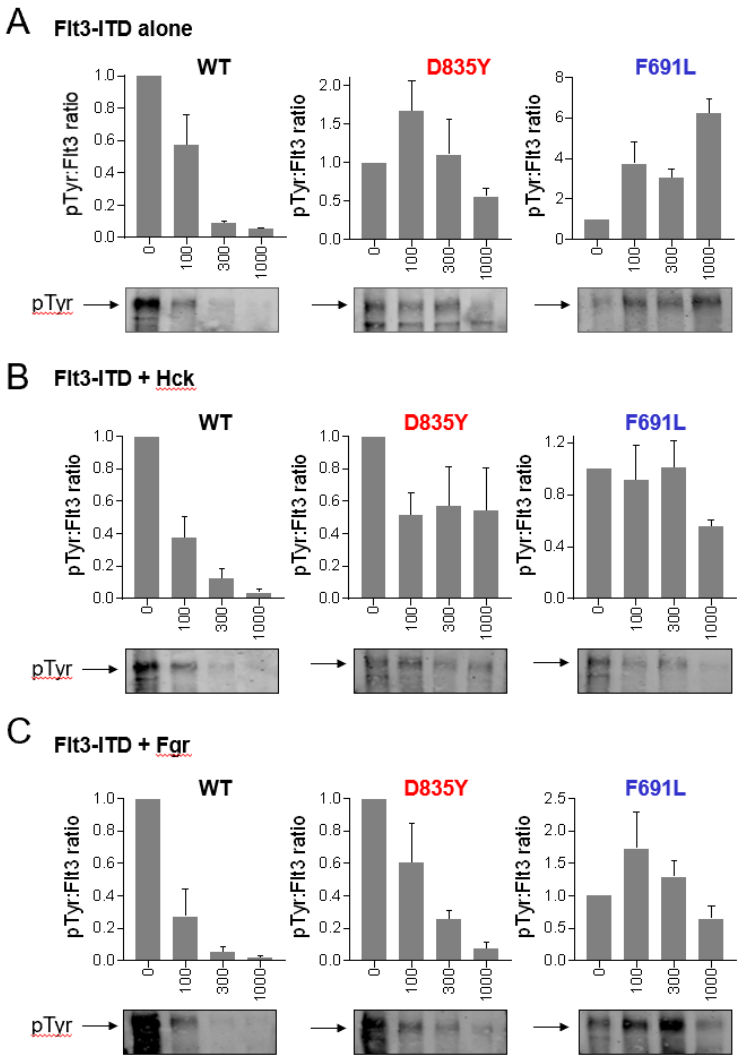

Figure 11. Analysis of Flt3-ITD phosphotyrosine content in TF-1 cells following A-419259 treatment.

Each TF-1 cell population from Figure 3 was treated with A-419259 at the concentrations shown or with DMSO as control. Following overnight incubation, Flt3 was immunoprecipitated and analyzed for phosphotyrosine (pTyr) content and Flt3 protein recovery by immunoblotting. Flt3 and pTyr immunoreactivity were quantified using the Odyssey infrared imaging system, and data are expressed as mean pTyr:Flt3 protein ratios ± SE for three independent experiments. (**A**) Results from TF-1 cells expressing Flt3-ITD wild type (WT), as well as the inhibitor-resistant D835Y and F691L mutants. Ratios are shown in the bar graphs, with representative Flt3 pTyr blots shown below the graphs; the phosphorylated form of Flt3 used for imaging is indicated by the arrow. (**B**, **C**) Results from TF-1 cells co-expressing each form of Flt3-ITD with Hck or Fgr, respectively.

in all three TF-1 cell populations transformed with the wild-type form of the kinase (FLT3-ITD alone and in the presence of HCK or FGR), and phosphorylation was completely inhibited by A-419259 treatment in a concentration-dependent manner in all three cases. Interestingly, FLT3-ITD phosphotyrosine content was strongly enhanced in cells co-expressing FGR, suggesting that FLT3-ITD may serve as substrate for FGR in cells. FLT3-ITD remained phosphorylated in immunoprecipitates from cells transformed by the D835Y and F691L mutants in the presence of the inhibitor, consistent with the lack of growth inhibition in response to the compound by these cell populations. Co-expression of HCK partially restored the sensitivity of the D835Y mutant of FLT3-ITD to A-419259 in terms of phosphotyrosine content, consistent with the rescue effect of HCK expression on growth suppression. Co-expression of FGR also restored FLT3-ITD-D835Y sensitivity to A-419259 treatment, as well as FLT3-ITD-F691L to a lesser extent, consistent with the growth inhibitory responses of these cell populations to inhibitor treatment. As with wild-type FLT3-ITD, co-expression of FLT3-ITD-D835Y (but not F691L) with FGR led to a marked increase in phosphotyrosine content. Direct phosphorylation of FLT3-ITD-D835Y by FGR may alter its responsiveness to the inhibitor in cells. More generally, these studies with TF-1 cells suggest that FLT3-ITD is the primary inhibitor target for A-419259 in FLT3-ITD$^+$ AML, although the presence of HCK and FGR may modulate FLT3-ITD inhibitor sensitivity especially in the presence of FLT3-ITD kinase domain mutations.

2.3.4 Mutants of HCK and FGR with engineered resistance reduce AML cell sensitivity to A-419259

If HCK, FGR or other myeloid SRC-family members are involved in A-419259 efficacy in FLT3-ITD$^+$ AML, then mutations in their drug-binding pockets would be anticipated to confer

resistance to A-419259 in AML cells. To test this idea, we engineered A-419259-resistant mutants of HCK and FGR. The crystal structure of HCK bound to A-419259 (PDB code: 4LUE) reveals that the kinase domain gatekeeper residue (Thr338) has a major role in binding to the compound, forming a hydrogen bond with the 4-amino group on the pyrrolopyrimidine heterocycle[447]. In general, kinase domain gatekeeper residues are well known to confer resistance to many ATP-site kinase inhibitors and can be substituted with alternative amino acids without loss of activity. In the case of HCK, Thr338 is just small enough to allow access of the 4-phenoxyphenyl group of A-419259 to the hydrophobic pocket adjacent to the ATP-binding site. Previous work from our group showed that substitution of T338 in HCK with methionine resulted in resistance to A-419259 both in vitro and in cell-based assays[403]. Here we extended this work by substituting Thr338 in both HCK and FGR with larger, more hydrophobic residues, including phenylalanine and leucine in addition to methionine. All of these gatekeeper substitutions are predicted to disrupt hydrogen bonding with the compound and to introduce steric clash, resulting in impaired binding and hence resistance. The position of the gatekeeper residue in the ATP binding site of the HCK kinase domain and the predicted effect of these substitutions are modeled in Figure 12.

First, we expressed and purified recombinant near-full-length HCK, FGR and LYN with each of these gatekeeper mutations, and assessed their kinase activity and inhibitor sensitivity in vitro using the Z'Lyte assay. The wild-type and mutant forms of all 12 recombinant kinases were active, although the gatekeeper mutations altered the K_m for ATP in some cases (Figure 13). With the ATP concentration set to the K_m value for each kinase, we then determined the IC_{50} values for A-419259 (Table 6). For HCK, substitution of the gatekeeper threonine with methionine or phenylalanine reduced kinase sensitivity to A-419259 by 2-fold and nearly 5-fold,

respectively, while leucine substitution was without an effect. For FGR, all three substitutions resulted in resistance, ranging from 2.5-fold for methionine to nearly 5-fold for phenylalanine. However, none of the LYN gatekeeper mutants displayed resistance to A-419259, suggesting a different binding mode for the inhibitor with this kinase (data not shown). For this reason, LYN was not explored further in cell-based assays.

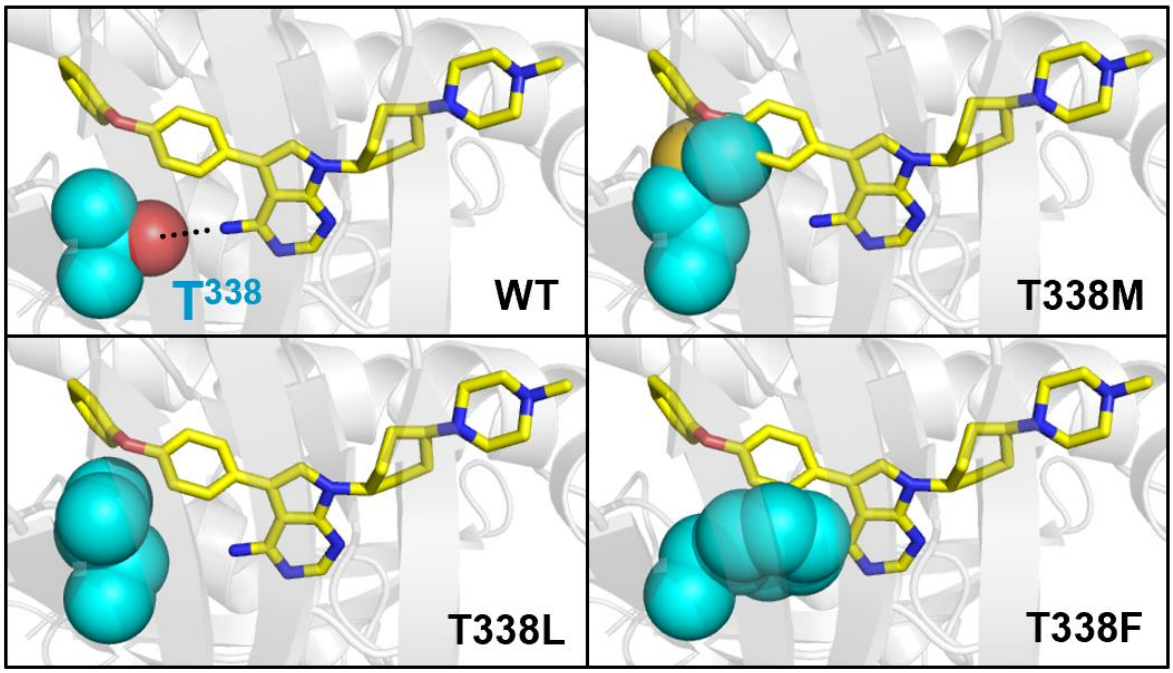

Figure 12. Hck and Fgr gatekeeper mutants modeled.

Close-up view of the A-419259 binding pocket in the crystal structure of Hck bound to A-419259 (PDB: 4LUE). The carbon backbone of A-419259 is shown in yellow. The side chain of the Hck gatekeeper residue (Thr338; cyan) and forms a hydrogen bond with the primary amine on the pyrrolopyrimidine core of A-419259 (dotted line). Using PyMOL, T338 was substituted with methionine, leucine, and phenylalanine as shown, resulting in loss of the H-bond and steric clash predicted to interfere with inhibitor action.

Table 6. IC_{50} values of A-419259 against recombinant Hck gatekeeper mutants

Kinase	Form	ATP K_m, µM	A-419259 IC_{50}, nM
Hck	Wild-type	26.0	43.1 ± 1.06
	T338M	6.9	94.9 ± 1.14
	T338L	17.2	41.0 ± 1.02
	T338F	42.0	201.0 ± 1.03
Fgr	Wild-type	17.9	61.8 ± 1.09
	T338M	5.3	160.6 ± 1.05
	T338L	10.0	218.4 ± 1.06
	T338F	95.7	282.9 ± 1.07

We next determined whether expression of wild type or mutant forms of HCK and FGR affected the growth and survival of TF-1 cells. TF-1 cell populations expressing each kinase were grown in the presence or absence of GM-CSF, and cell viability was assayed daily for five days Figure 14). Neither wild type nor any of the gatekeeper mutants of HCK promoted GM-CSF independent growth under these conditions. Expression of wild type FGR, as well as the T338L gatekeeper mutant, also failed to promote cytokine-independent growth. However, the T338F and T338M mutants of FGR both transformed TF-1 cells to cytokine-independent growth. This observation may be related to changes in intrinsic kinase activity resulting from these gatekeeper mutations (Figure 13). TF-1 cells expressing FLT3-ITD (but not wild type FLT3) grew equally well in the presence or absence of GM-CSF as expected, providing a positive control for this experiment.

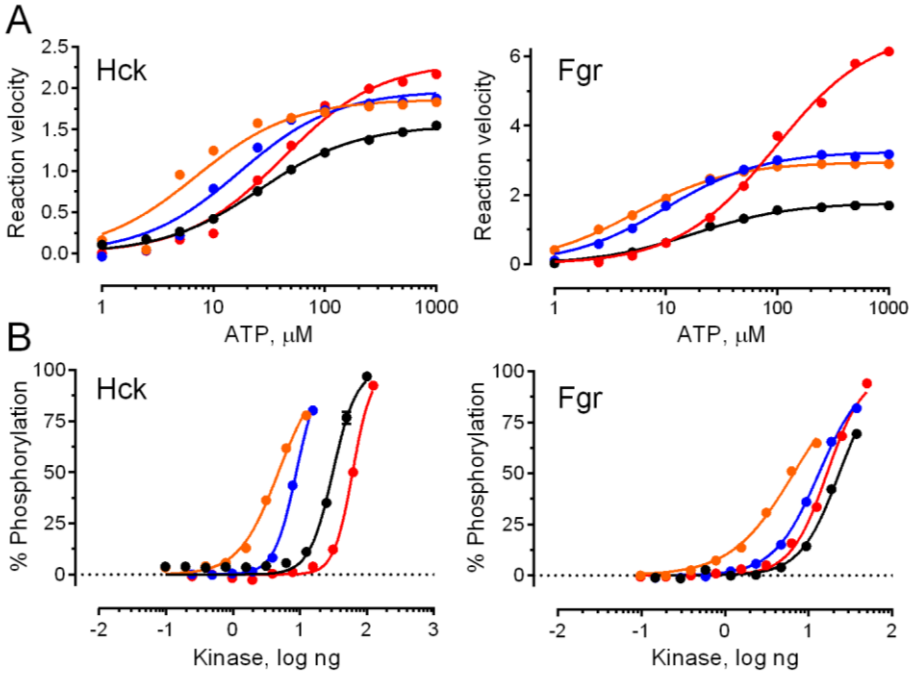

Kinase	Form	ATP K_m, μM	Kinase EC_{50}, ng
Hck	Wild-type	26.0	31.1
	T338M	6.9	4.8
	T338L	17.2	8.9
	T338F	42.0	61.4
Fgr	Wild-type	17.9	23.3
	T338M	5.3	6.6
	T338L	10.0	13.3
	T338F	95.7	16.6

Figure 13. In vitro kinetics analysis of wild-type and gatekeeper mutants of Hck and Fgr.

Recombinant near-full-length kinases, consisting of the SH2, SH3 and kinase domains plus the negative regulatory tail, were expressed in *E. coli* in the presence of Csk (to phosphorylate the tail tyrosine) and PTP1B (to keep the activation loop dephosphorylated). Purified kinases were assayed in vitro using the Z'-LYTE kinase assay (ThermoFisher) and the Tyr-2 peptide substrate (final concentration of 1.0 μM). **A**) Determination of Km values for ATP. Kinase activity was determined over the range of ATP concentrations shown. Reaction velocities were determined by quenching each reaction at various time points. The resulting curves were fit the Michaelis-Menten equation using GraphPad Prism v7.0, and the resulting K_m values are shown in the Table below. Colors as in Table. **B**) Determination of intrinsic kinase activity. Each kinase was assayed over a range of input amounts with the ATP concentrations

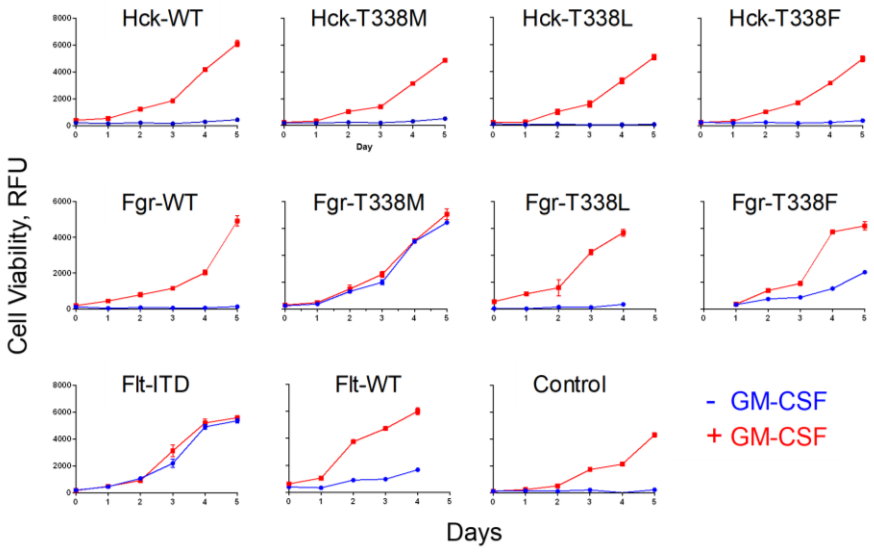

Figure 14. Fgr but not Hck gatekeeper mutants transform TF-1 myeloid cells to cytokine-independent growth.

Wild-type and gatekeeper mutants of Fgr and Hck were stably expressed in TF-1 cells. After selection with G418, cells were cultured in the presence or absence of GM-CSF and viability was monitored daily using the CellTiter Blue assay (Promega). Data are presented as relative fluorescence units, which increase as a function of cell proliferation. TF-1 cells transformed with Flt3-ITD served as a positive control, while cells transduced with an empty vector served as negative control. Expression of each kinase was confirmed by immunoblotting (*data not shown*). TF-1 cells expressing Fgr-T338M showed GM-CSF-independent proliferation to the same extent as Flt3-ITD, while Fgr-T338F produced a partial cytokine-independent phenotype.

The wild-type and gatekeeper mutant forms of HCK and FGR were then stably expressed in TF-1 cells previously transformed by FLT3-ITD. With HCK, expression of each of the three gatekeeper mutants resulted in about a 3-fold decrease in cell sensitivity to A-419259 (Figure 15A). With FGR, the T338M and T338L mutants also produced about 3-fold resistance to the inhibitor. However, the FGR-T338L mutant resulted in a much more robust resistance phenotype in the cell-based assay, with an IC_{50} value > 1,000 nM (Figure 15B). By contrast, expression of wild-type HCK or FGR had no effect on inhibitor sensitivity.

We next assessed wild-type and mutant HCK and FGR activity in each of the TF-1 cell populations in the presence of A-419259 by immunoblotting for phosphorylation of Tyr416 (pY416), the major site of activation loop phosphorylation found in all SRC-family members. HCK and FGR were immunoprecipitated from each cell population and blotted for both pY416 and kinase protein recovery. The signal intensities of each band were quantified using LICOR infrared imaging and are expressed as pY416/kinase ratios (Figure 16). TF-1/FLT3-ITD cells co-expressing wild-type HCK and FGR showed concentration-dependent decreases in Tyr416 phosphorylation in response to A-419259 treatment (Figure 16). The IC_{50} values for inhibition of the wild-type kinases were less than 30 nM in each case, in agreement with the potency for growth suppression. Gatekeeper mutants of HCK expressed in TF-1/FLT3-ITD cells remained phosphorylated in the presence of A-419259 in the 100 to 300 nM range, also consistent with the degree of inhibitor resistance observed in terms of cell growth. For the FGR mutants, pY416 phosphorylation also persisted in the presence of A-419259 treatment. This effect was particularly marked for the T338L mutant, which is consistent with the strong resistance phenotype observed in this cell population. This cell-based observation is in contrast to the results with recombinant FGR-T338L in vitro and may reflect differences in the sensitivity of this mutant to inhibition when expressed as a full-length kinase in the context of the plasma membrane. Taken together, these data show that inhibition of HCK and FGR, in addition to FLT3-ITD, is important to the mechanism of action of A-419259.

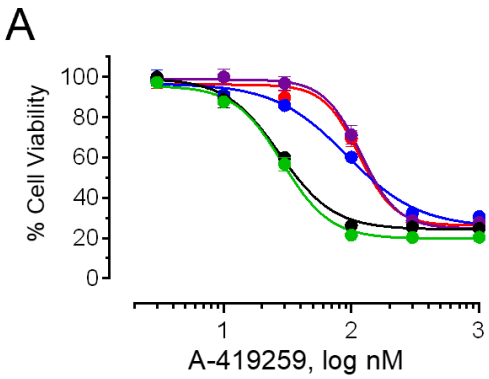

TF-1/FLT3-ITD +	IC_{50}, nM
Control	28.7 ± 1.1
Hck-WT	27.7 ± 1.1
Hck-T338M	119.0 ± 1.1
Hck-T338L	92.0 ± 1.1
Hck-T338F	114.9 ± 1.1

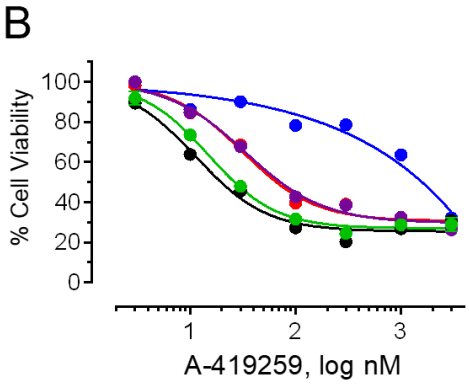

TF-1/FLT3-ITD +	IC_{50}, nM
Control	15.0 ± 1.1
Fgr-WT	11.3 ± 1.2
Fgr-T338M	33.5 ± 1.2
Fgr-T338L	> 1,000
Fgr-T338F	29.0 ± 1.4

Figure 15. Hck and Fgr gatekeeper mutants confer resistance to A-419259 in TF-1 Flt3-ITD+ cells.

TF-1 cells co-expressing Flt3-ITD together with wild-type and gatekeeper mutants of Hck (**A**) or Fgr (**B**) were incubated over a range of A-419259 concentrations or DMSO alone as control. Cell viability was determined 72 hours later using the CellTiter Blue cell viability assay. Results were normalized to DMSO control values, and are presented as mean percent control ± SD for triplicate determinations. IC_{50} values for each experiment were determined by non-linear regression analysis of the resulting concentration-response curves and are summarized in the tables (*right*).

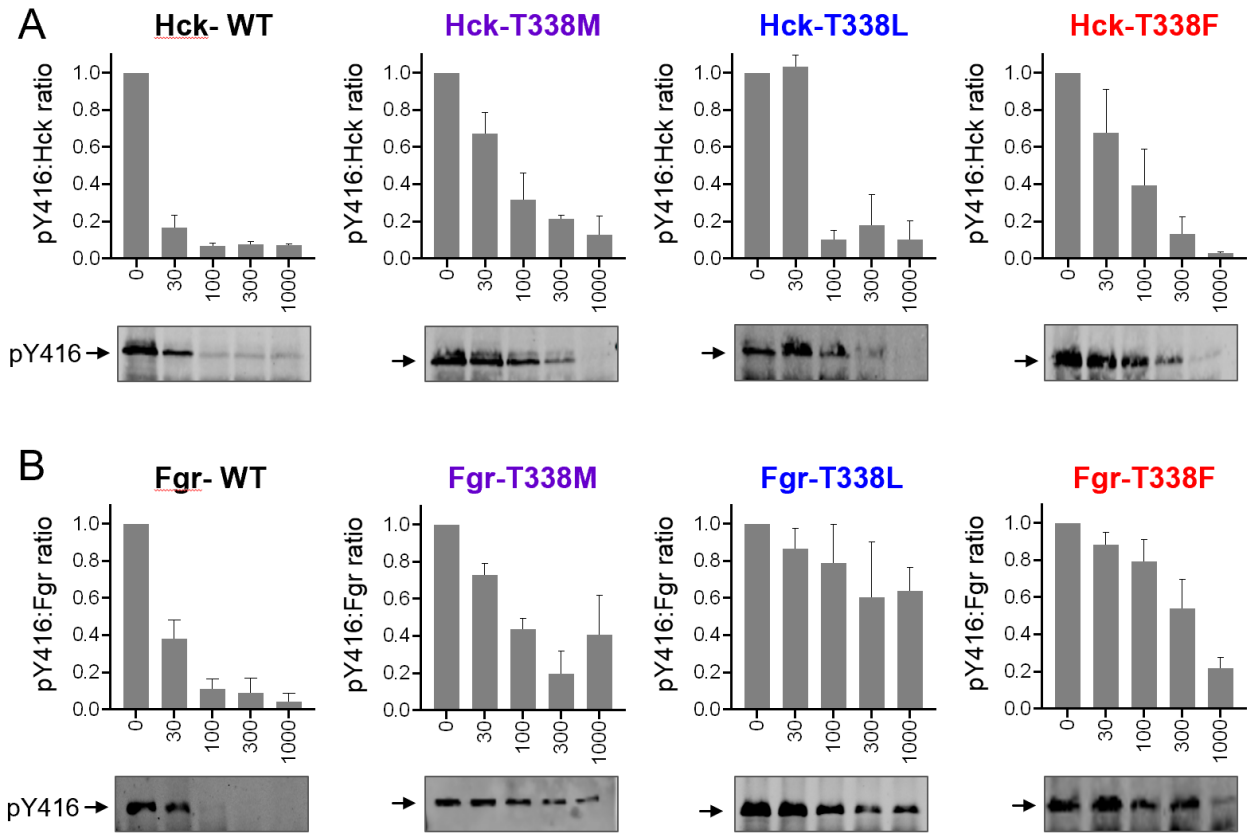

Figure 16. Hck and Fgr gatekeeper mutants remain phosphorylated in the presence of A-419259.

TF-1 cells co-expressing Flt3-ITD together with wild-type and gatekeeper mutants of Hck (**A**) or Fgr (**B**) were incubated overnight with A-419259 at the concentrations shown. Hck and Fgr were immunoprecipitated from clarified cell extracts and immunoblotted for kinase protein recovery as well as activation loop phosphorylation as a marker for kinase activity (pY416). Kinase and pY416 immunoreactivity were quantified using the Odyssey infrared imaging system, and data are expressed as mean pY416:kinase protein ratios ± SE for at least three independent experiments (bar graphs). Representative pY416 blots are also shown.

2.3.5 Acquired resistance to A-419259 involves mutations to FLT3-ITD but not SRC-family kinases in AML cell lines

To begin to understand how resistance to A-419259 may evolve in vivo, we sequentially passaged a series of FLT3-ITD$^+$ AML cell populations with acquired resistance to A-419259. For these studies, we used the human FLT3-ITD$^+$ AML cell lines MV4-11, MOLM13 and MOLM14. Importantly, each of these cell lines expresses HCK, FGR, and other A-419259 target kinase transcript levels that closely mirror those observed in primary bone marrow cells from AML patients (Figure 17). To generate inhibitor-resistant cell populations, three independent cultures of each cell line were cultured in the presence of A-419259 at a starting concentration of 10 nM. The cultures were incubated until viable cell outgrowth was observed, at which point the concentration of A-419259 was increased by 50%. This process was repeated until outgrowth was observed in the presence of the inhibitor at a concentration of 1 µM, which required 50-80 passages over the course of almost one year. We ultimately obtained two resistant populations from MV4-11, one from MOLM13, and three from MOLM14. IC_{50} values for A-419259 were then determined for each of the resistant cell populations (Figure 18A and Table 7). The selected cells were 5- to 25-old less sensitive to growth inhibition by A-419259 compared to the parental cell line. To determine whether A-419259 resistance was due to genetic changes, each resistant cell population was passed eight additional times over four weeks in the absence of the inhibitor, followed by re-determination of the IC_{50} values. No significant changes were observed in the degree of inhibitor resistance, consistent with the idea that each population acquired mutations or other fixed genetic changes that are responsible for resistance as opposed to temporary changes in gene expression, drug efflux or drug metabolism (Figure 18B and Table 7).

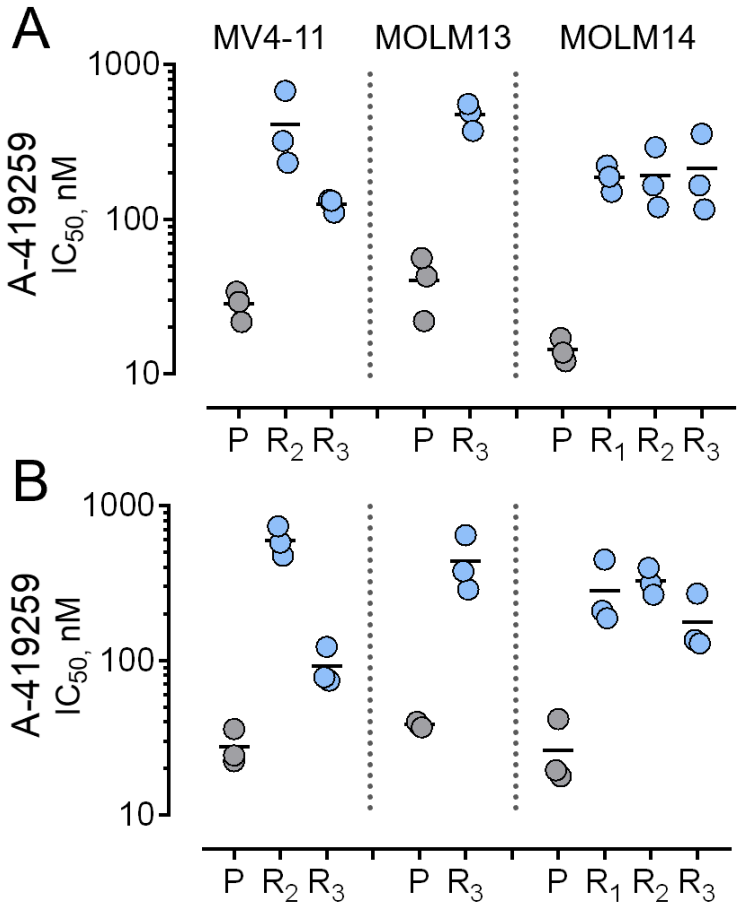

Figure 17. Acquired resistance to A-419259 in the Flt3-ITD+ AML cell lines MV4-11, MOLM13 and MOLM14 is a heritable trait.

Three independent populations of each AML cell line were passaged in the presence of increasing concentrations of A-419259 until outgrowth was observed in the presence of an inhibitor concentration of 1 µM. MV4-11 yielded two resistant populations (R_2, R_3), MOLM13 yielded one (R_3), while three were obtained from MOLM14 (R_1, R_2, R_3). P, parent cell line. (**A**) Three replicates of the parent and resistant cell populations were incubated over a range of A-419259 concentrations or DMSO alone as control. Cell viability was determined 72 hours later using the CellTiter Blue cell viability assay. Results are shown relative to the DMSO control values, and IC_{50} values were determined by non-linear regression analysis of the resulting concentration-response curves and are plotted for each cell line. The mean IC_{50} value for each cell population is shown as the black bar, and IC_{50} values for all resistant populations were significantly higher than those for the corresponding parent cell line ($p < 0.05$ by Student's t-test). (**B**) Resistant cell populations from part A were passaged 8 times over the course of 4 weeks in the absence of A-419259, followed by re-determination of the IC_{50} values for A-419259. IC_{50} values from parts A and B are summarized in Table 7.

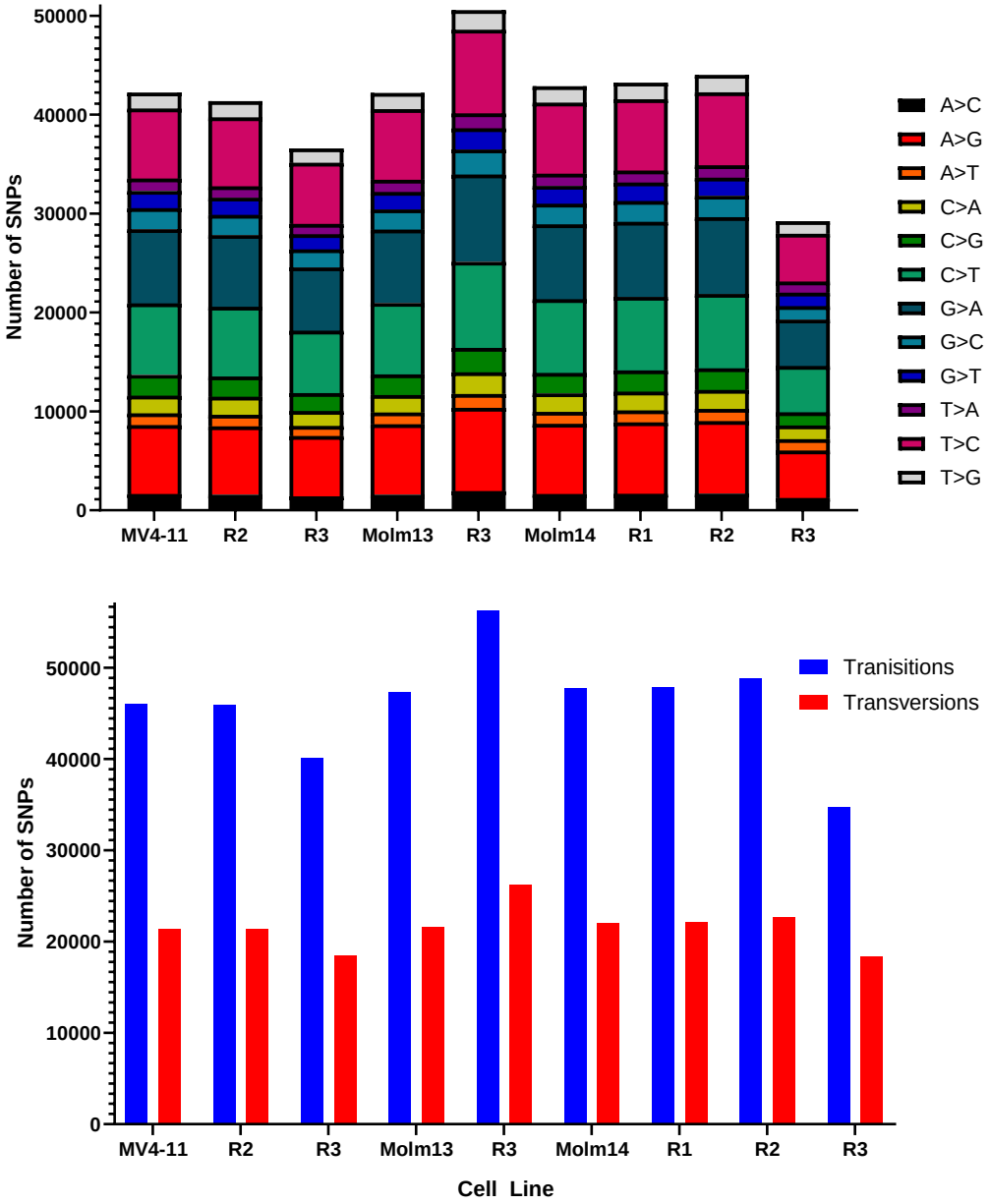

Figure 18. SNPs in the Exomes of all the resistant cell lines

Three independent populations of each AML cell line were passaged in the presence of increasing concentrations of A-419259 until outgrowth was observed in the presence of an inhibitor concentration of 1 µM. MV4-11 yielded two resistant populations (R_2, R_3), MOLM13 yielded one (R_3), while three were obtained from MOLM14 (R_1, R_2, R_3). P, parent cell line. (**A**) All single nucleotide substitutions in each of the resistant and parent cell lines. Colors shown on the right. (**B**) Transitions and transversions of resistant cell lines and parent cell lines.

Table 7. Acquired resistance to A-419259 in Flt3-ITD+ AML cell lines.

Three independent cultures of each parent AML cell line were grown in increasing concentrations of A-419259 until proliferation was observed in the presence of 1 µM compound. Two resistant populations emerged from MV4-11 cells, MOLM-13 produced one, while MOLM-14 produced three. Initial A-419259 IC_{50} values were then determined from concentration-response curves using the CellTiter-Blue assay. The cells were then passaged for 4 weeks in the absence of inhibitor, and IC_{50} values determined again (Post-holiday). IC_{50} values are presented as the mean value ± SE (n = 3). Whole exome sequencing revealed Flt3 mutations in all of the resistant populations, whereas no mutations were observed in Hck, Fgr or other AML-associated tyrosine kinases. Flt3 Asn676 mutations were confirmed in individual clones of Flt3 kinase domain transcripts by Sanger sequencing.

Cell Population		**A-419259 Sensitivity (IC_{50}, nM)**		**Flt3 mutations**	
		Initial	**Post-holiday**	**Exome Seq**[a]	**Sanger (clones)**[b]
MV4-11	Parent	28.3 ± 3.5	27.5 ± 4.3	none	13/13 WT
	R2	409.8 ± 135.6	596.8 ± 76.3	Asn676 → Ser	6/14 N676S
	R3	125.3 ± 7.3	91.6 ± 15.6	Asn676 → Thr Asp839 → Tyr	8/10 N676T 0/10 D839Y
MOLM13	Parent	40.3 ± 9.9	38.4 ± 0.9	none	14/14 WT
	R3	473.1 ± 53.9	436.4 ± 107.3	Asn676 → Ser	3/13 N676S
MOLM14	Parent	14.3 ± 1.5	26.4 ± 7.7	none	14/14 WT
	R1	186.7 ± 20.8	282.6 ± 84.2	Asn676 → Ser	5/13 N676S
	R2	192.6 ± 51.4	325.7 ± 38.4	Asn676 → Ser	10/15 N676S
	R3	213.1 ± 73.7	178.3 ± 46.1	Asn676 → Ser	3/11 N676S

To explore possible mutations involved in acquired resistance to A-419259, we performed whole exome sequencing of genomic DNA isolated from each parent cell line and the inhibitor-resistant cell populations derived from them. We found that the resistant cell lines contained a similar number of mutations and types of mutations relative to the reference genome as the parent cell lines (Figure 19). Upon closer inspection, we found that all six A-419259-resistant cell populations acquired missense mutations in FLT3 residue Asn676 while one resistant cell line (MV4-11 R3) also exhibited a FLT3 D839Y mutation, both of which map to the kinase domain (Table 7). To confirm the presence of these FLT3 mutations in each cell population, we amplified FLT3 kinase domain transcripts by RT-PCR from the parent and resistant cells and performed Sanger sequencing on 10-15 individual clones. This analysis confirmed the presence of the FLT3 N676S mutation in all six resistant populations, but not in any FLT3 clones from the parent cells. In contrast, the FLT3 D839Y mutation observed by whole exome sequencing of MV4-11 R3 cells was not present in any of ten independent clones.

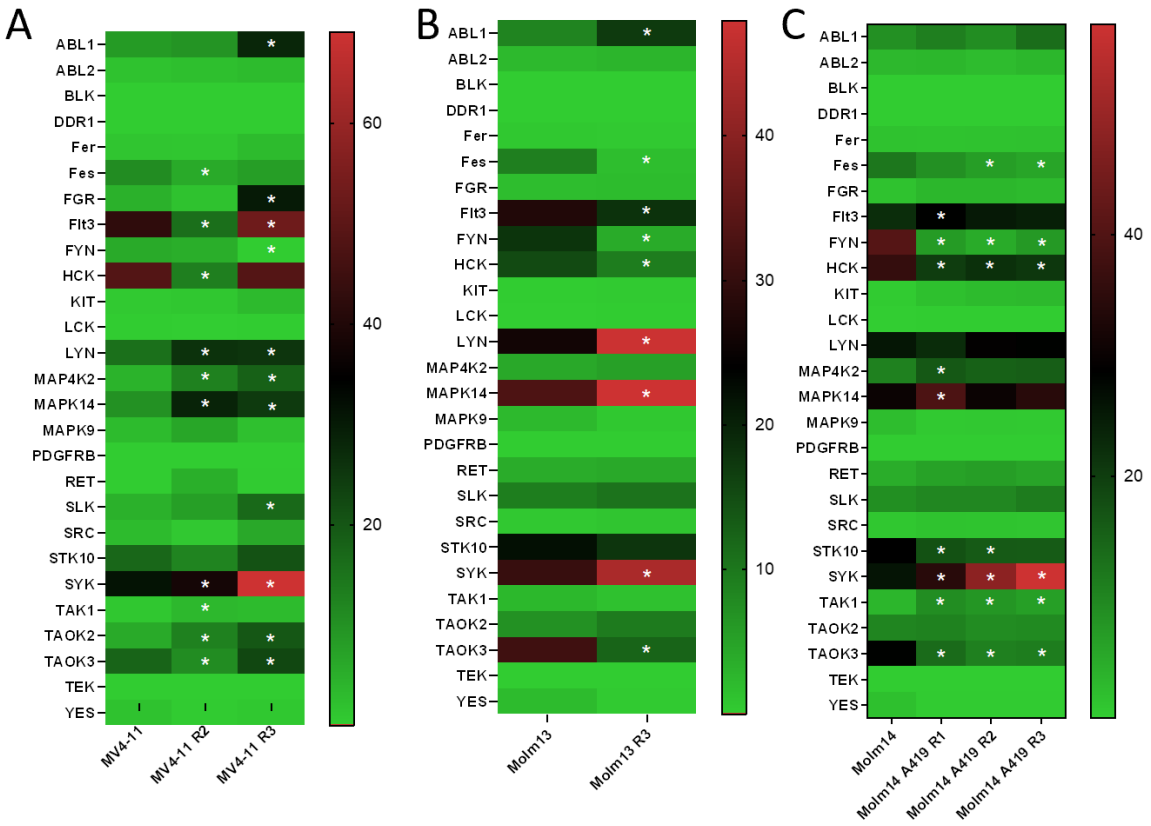

Figure 19. SYK expression is upregulated in A-419259 resistant AML cell populations.

Heat map of relative mRNA expression levels in parent and inhibitor-resistant MV4-11, MOLM13, and MOLM14 cells as determined by qPCR of A-419259 target kinases identified by KINOMEscan analysis. Of the 27 kinases examined, only Syk expression was consistently increased in at least one resistant population from all three cell lines. Relative expression values were calculated as the base 2 antilog of the qPCR ΔCt values relative to GAPDH for each kinase. These values were then plotted as a distribution relative to the mean value for all 27 kinases analyzed in each sample. All determinations were made on at least three independent RNA samples from each cell line. * indicates $p < 0.0001$ compared to parent cell line.

Whole exome sequencing revealed an average of 25,050 mutations in each resistant cell population relative to the corresponding parent cell line. Of these, an average of 15,738 mutations localized to protein coding sequences, although only a few non-synonymous mutations were observed in other A-419259 target kinases identified in the KINOMEscan profile. MOLM14 R1 had an S1060C mutation in the receptor tyrosine kinase, Erbb3. This mutation is

C-terminal to the kinase domain of Erbb3 and is therefore unlikely to be involved in inhibitor resistance. MV4-11 R3 had an R428N mutation in Mknk2, which is also C-terminal to the kinase domain. Finally, MV4-11 R2 had a C280S mutation in SRC, which localizes to the non-catalytic SH2 domain. Our qPCR analysis shows that SRC is expressed at very low levels in parental MV4-11 cells and even lower levels in MV4-11 R2 cells (Figure 20). While a mutation in the SRC SH2 domain could potentially influence A-419259 sensitivity through an allosteric mechanism, the low overall SRC expression argues against a role for SRC in A-419259 action and resistance in these cells. No mutations were observed in any other A-419259 target kinases identified by KINOMEscan analysis and expressed in these AML cell lines, including HCK and FGR.

To determine whether the FLT3 N676S point mutation was sufficient to confer resistance to A-419259, FLT3-ITD N676S was expressed in TF-1 cells. This FLT3-ITD mutant transformed TF-1 cells as efficiently as wild-type FLT3-ITD, indicating that kinase activity and transforming potential are not attenuated by this substitution. Each cell population was then compared to control TF-1/FLT3-ITD cells for sensitivity to growth arrest by A-419259. Cells expressing the FLT3-

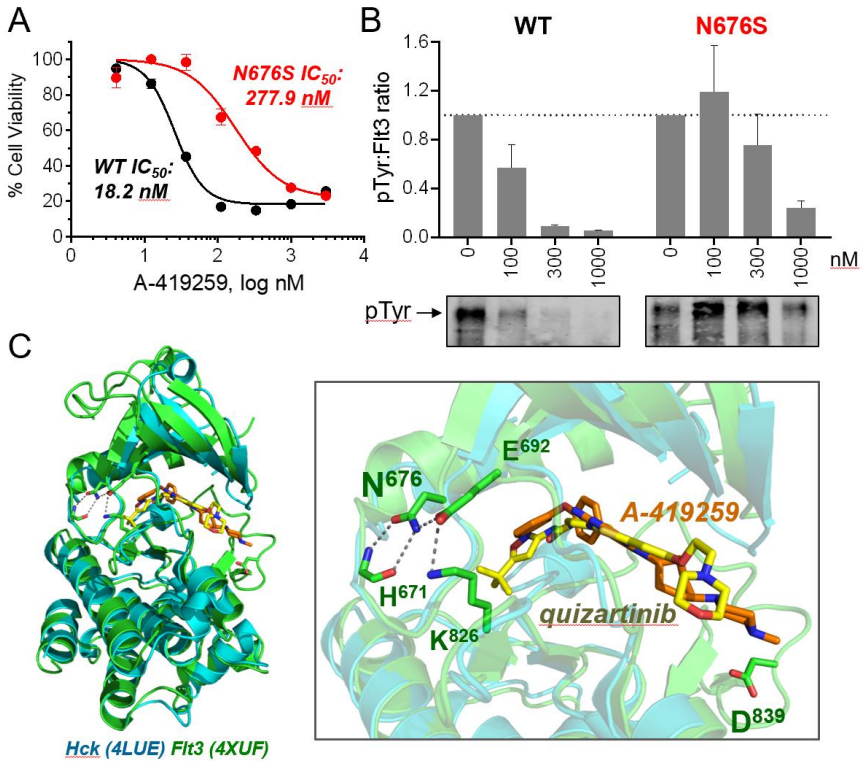

Figure 20. Flt3-ITD N676S mutation confers resistance to A-419259 in TF-1 cells.

(**A**) TF-1 cells expressing Flt3-ITD wild type (WT) or the N676S mutant were incubated over a range of A-419259 concentrations or DMSO alone as control. Cell viability was determined 72 hours later using the CellTiter Blue cell viability assay. Results are shown relative to the DMSO control values, and IC_{50} values were determined by non-linear regression analysis of the resulting concentration-response curves. (**B**) Cell populations from part A were incubated overnight in the presence of the A-419259 concentrations shown. Flt3 was then immunoprecipitated and analyzed for phosphotyrosine (pTyr) content and Flt3 protein recovery by immunoblotting followed by Odyssey infrared imaging. Data in the bargraphs represent the mean pTyr:Flt3 protein ratios ± SE for three independent experiments, with representative pTyr blots shown below the graphs; phosphorylated Flt3 is indicated by the arrow. (**C**) Model of A-419259 bound to the Flt3 kinase domain. The crystal structure of the Flt3 kinase domain bound to quizartinib (PDB: 4XUF; green) was aligned with the crystal structure of the Hck kinase domain bound to A-419259 (PDB: 4LUE; blue) using PyMol. The overall alignment is shown at left, and a close-up of the inhibitor binding site is shown at right. Significant overlap was observed in the positions of quizartinib (yellow) and A-419259 (orange) in the ATP-binding site. In the Flt3 structure, residue Asn676 forms a web of polar contacts with the side chains of Glu692, Lys826 and the main chain of His671. Acquired mutations in this residue were associated with resistance to A-419259 in AML cell lines. Whole exome sequencing also identified a substitution of Flt3-ITD Asp839 (shown) in MV4-11 population R_3; this mutation was not verified in subsequent Sanger sequencing of individual clones (Table 7).

ITD N676S mutant were 15-fold less sensitive to A-419259 (Figure 21A). The mutant kinase also showed reduced sensitivity to A-419259 in terms of phosphotyrosine content, consistent with the

resistant phenotype (Figure 21B). Asn676 is located near the active site in a crystal structure of the FLT3 kinase domain (Figure 21C) and is positioned to impact inhibitor binding (see Discussion). We also evaluated the impact of HCK and FGR on TF-1 cells expressing the FLT3-ITD N676S resistance mutation for A-419259. Neither HCK nor FGR co-expression affected the inhibitor sensitivity of TF-1 cells expressing the FLT3-ITD N676S mutant, which remained phosphorylated following A-419259 treatment (data not shown).

2.3.6 Evaluation of A-419259 target kinase gene expression in resistant AML cells

While mutation of FLT3-ITD N676 was consistently observed across six independent A-419259-resistant AML cell populations, the possibility exists that changes in the expression of HCK, FGR, or other target kinases for this inhibitor may also contribute to the resistant phenotype. To address this possibility, we used quantitative real-time RT-PCR to determine the relative expression profiles of all A-419259 target kinases identified by KINOMEscan analysis in each parent and resistant cell population. We also profiled several additional kinases previously identified as targets for TL02-59, another AML-active kinase inhibitor with a slightly broader target specificity profile than A-419259[409]. Of the 27 kinases profiled, only the non-receptor tyrosine kinase SYK was consistently upregulated in the A-419259-resistant cell populations (Figure 20). Previous studies have implicated SYK in the pathogenesis of AML, and upregulation of SYK is known to confer resistance to other FLT3 inhibitors[339]. To determine whether the upregulation of SYK kinase activity contributes to A-419259 resistance, we used the

SYK inhibitor PRT 062607[448]. All three parent AML cell lines, as well as their resistant counterparts, were sensitive to growth suppression by this SYK inhibitor, with IC_{50} values in the 0.5 to 2.0 µM range (Figure 22, Table 8). We then performed concentration-response studies with A-419259 in the presence of fixed concentrations of the SYK inhibitor (50, 100 and 200 µM) using the CellTiter-Blue cell viability assay. Overall, addition of PRT 062607 did not affect sensitivity to A-419259, suggesting that upregulation of SYK expression does not contribute to A-419259 resistance. One exception was the R2 population of A-419259-resistant MV4-11 cells, where a subtle but significant leftward shift in the A-419259 concentration-response curve was observed with increasing concentrations of the SYK inhibitor.

Table 8. A-419259 resistant cells are not resistant to PRT062607.

Cell Line	Population	PRT062607 IC_{50}, nM
MV4-11	Parent	453.2 ± 90.7
	R_2	1717.0 ± 93.5
	R_3	794.6 ± 128.4
MOLM13	Parent	1377.7 ± 123.6
	R_3	1991.0 ± 377.4
MOLM14	Parent	1328.4 ± 183.1
	R_1	2033.5 ± 1085.4
	R_2	1644.7 ± 153.6
	R_3	1195.7 ± 128.0

The IC_{50} values for growth suppression was determined for parent and resistant cells using the CellTiter-Blue assay

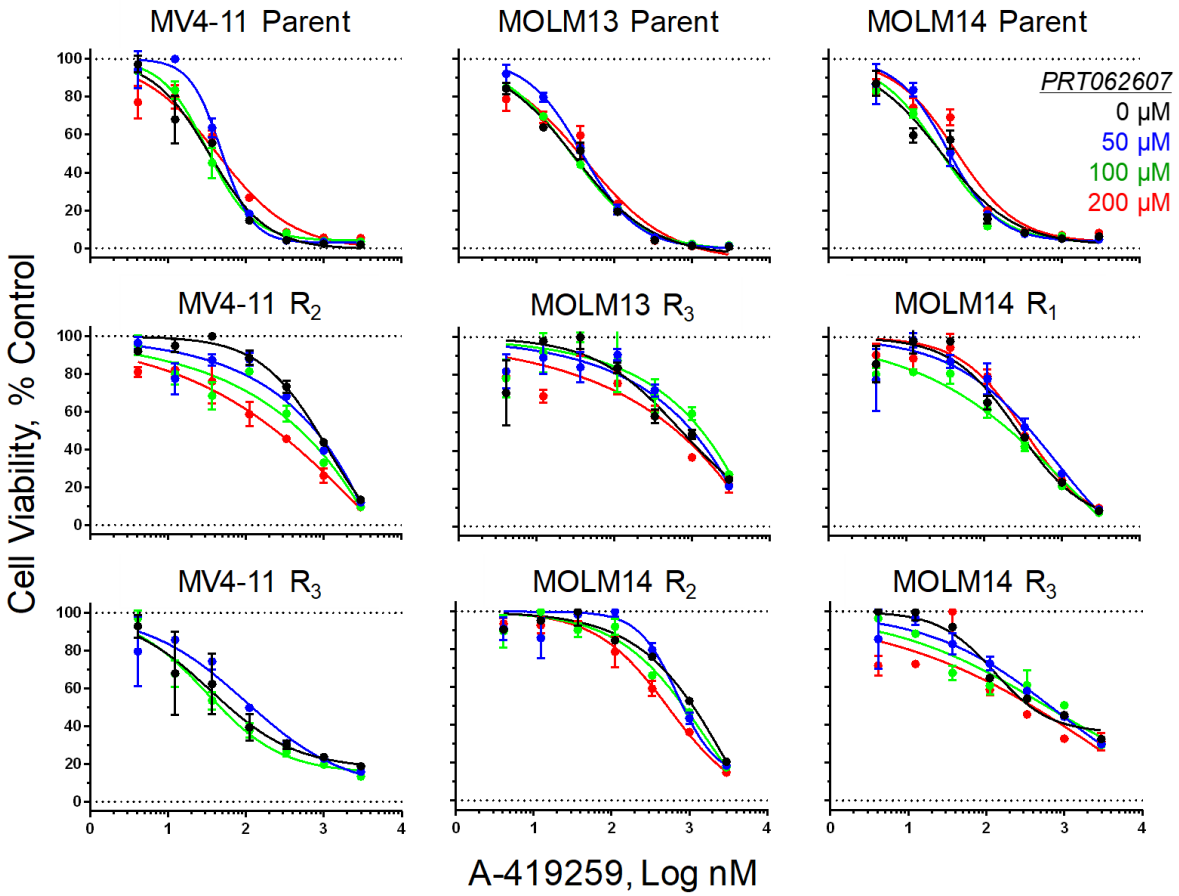

Figure 21. Inhibition of Syk kinase activity does not affect resistance to A-419259.

These experiments used the Syk-selective inhibitor PRT062607 (P505-15) to probe the role Syk kinase activity in acquired resistance to A-419259 in our inhibitor resistant AML cell populations. In an initial experiment, the IC_{50} values for growth suppression was determined for parent and resistant cells using the CellTiter-Blue assay (values in Table 8). Based on these results, we then tested the effect of submaximal concentrations PRT062607 on A-419259 inhibitory activity in each cell population. Each population was treated with 0 μM (black), 50 μM (blue), 100 μM (green) or 200 μM (red) PRT062607 over a range of A-419259 concentrations as shown. Cell viability was determined 72 h later using the Cell-titer Blue assay. Each value is normalized to the no-drug control, and the resulting concentration-response curves are shown below (non-linear curve fitting performed with Prism v7.0). If Syk over-expression and activity contributes to A-419259 resistance, then addition of the Syk inhibitor would be predicted to result in a shift of the concentration-response curve to left (re-sensitization) in the A-419259 resistant populations. However, no significant PRT062607-dependent shifts were observed in the resistant cell populations with enhanced Syk expression, suggesting that Syk does not contribute to the A-419259-resistant phenotype.

2.4 Discussion

FLT3 is a bona fide proto-oncogene in the context of AML, which has led to the development of multiple FLT3 kinase inhibitors as targeted therapy[39,196]. The myeloid SRC-family kinases HCK, LYN and FGR have been independently described as relevant AML drug targets, and inhibition of these kinases is also a promising strategy for AML treatment[385,399–401,409]. In the present study, we demonstrate that these myeloid SRC-family members are highly expressed in a substantial subset of AML patients (Figure 3). Furthermore, HCK and FGR expression are highly correlated (Figure 4), suggesting that the subset of AML patients dependent on SRC-family kinase signaling will be most susceptible to selective inhibitors of these kinases. Along these lines, HCK and FGR as well as LYN mRNA expression are strong predictors of AML patient prognosis, while FLT3 expression per se is not (Figure 5). These observations led us to investigate the efficacy of SRC-family kinase inhibition in the context of FLT3-ITD^{+} AML. We focused primarily on HCK and FGR since their expression is limited to myeloid cells, while LYN is more ubiquitously expressed.

HCK expression is upregulated in chemotherapy-resistant AML leukemic stem cells[400], and inhibition of HCK with the ATP-competitive kinase inhibitor A-419259 prevented the engraftment of primary AML cells in genetically immunocompromised mice[401]. Here we show that that A-419259 inhibits not only HCK, but also FGR and other SRC-family kinases in addition to FLT3 (Figure 9). This observation raised the question of whether or not A-419259 efficacy could be attributed solely to HCK inhibition. To explore this question, we developed a model system based on the human myeloid cell line, TF-1. These cells do not express detectable HCK or FGR but are readily transformed to cytokine-independent growth following retroviral transduction with FLT3-ITD. We found that TF-1 cells transformed with FLT3-ITD became

very sensitive to A-419259 treatment, while those expressing two common FLT3 inhibitor resistance mutants (D835Y and F691L) were completely insensitive to this compound (Figure 10). Interestingly, co-expression of HCK partially re-sensitized TF-1/FLT3-ITD-D835Y cells to A-419259, while co-expression of FGR re-sensitized cells expressing either of these inhibitor-resistant FLT3-ITD mutants. These data demonstrate that the anti-AML efficacy of A-419259 is dependent on inhibition of FLT3-ITD and myeloid SRC-family kinases when they are co-expressed in the same AML cell population. D835Y and F691L are among the most frequent FLT3-ITD clinical resistance mutations for highly selective FLT3 inhibitors such as quizartinib, which does not inhibit myeloid SRC-family kinases (data not shown). Our findings with A-419259 suggest that combined inhibition of FLT3-ITD and SRC-family kinases may delay the appearance of resistance in the clinic by simultaneously inhibiting the activity of both kinase families.

As a second approach to validate HCK and FGR as relevant targets for A-419259 in AML, we developed kinase mutants with engineered resistance to this inhibitor (Figure 12). Using the crystal structure of HCK bound to A-419259 (PDB 4LUE) as a guide[447], we substituted the gatekeeper residue in each kinase domain (Thr338) with methionine, leucine or phenylalanine. Each mutation conferred resistance in in vitro kinase assays, most likely due to loss of a hydrogen bond with the inhibitor and increased steric bulk at the binding site. Expression of the inhibitor-resistant HCK and FGR mutants in TF-1 cells transformed with FLT3-ITD decreased their sensitivity to A-419259 (Figures 15 and 16), providing direct evidence that these SRC-family members are important for inhibitor action. These results are reminiscent of earlier studies of this compound in the context of CML cell lines. In this case,

gatekeeper mutants of HCK also resulted in A-419259 resistance, establishing a role for this kinase in Bcr-Abl signaling as well[403].

To investigate possible pathways to A-419259 resistance in an unbiased manner, we generated de novo resistance to A-419259 using the FLT3-ITD$^+$ AML cell lines MV4-11, MOLM13 and MOLM14. Each cell line was incubated with increasing concentrations of A-419259 over many months, resulting in six independent cell populations able to grow in the presence of 1 μM A-419259, which is 25-70 times the IC_{50} value for growth suppression of the parent cell lines. Repeated passage of each resistant population in the absence of A-419259 did not result in loss of resistance, suggesting that acquired heritable mutations are responsible for the resistant phenotype (Table 7).

To explore the genetic basis of resistance, whole exome sequencing analysis was performed on each parent cell line and their inhibitor-resistant progeny. All six resistant cell lines exhibited missense mutations of FLT3 Asn676, while HCK, FGR and almost all other A-419259 target kinases identified by KINOMEscan analysis were wild-type. The FLT3 Asn676 mutations were validated by Sanger sequencing of individual FLT3 clones isolated by RT-PCR from each resistant population; no mutations were observed in the parent cell lines. Transformation of TF-1 cells with FLT3-ITD bearing the N676S mutant showed significant resistance to A-419259, validating this mutation as a likely mechanism of acquired resistance to A-419259.

Experiments with TF-1 cells transformed by FLT3-ITD bearing the clinical inhibitor resistance mutations D835Y and F691L were completely resistant to A-419259 (Figure 10). However, we were unable to detect either of these mutations in AML cell populations with acquired resistance to A-419259. One possible explanation may relate to our observation that TF-1 cells expressing FLT3-ITD D835Y or F691L are re-sensitized to A-419259 by co-

expression of HCK or FGR. Unlike TF-1 cells, MV4-11, MOLM13 and MOLM14 cells all express endogenous HCK and FGR, which may suppress the evolution of resistance via FLT3-ITD D835Y and F691L mutations. In contrast, the A-419259 resistance of TF-1 cells transformed by FLT3-ITD N676S is unaffected by HCK or FGR co-expression, consistent with this idea.

The FLT3 Asn676 mutation has been linked to clinical resistance to quizartinib, midostaurin, and other FLT3 inhibitors[251,313,439,449,450]. In the crystal structure of quizartinib bound to the FLT3 kinase domain (PDB: 4XUF), Asn676 forms a hydrogen bond network with three adjacent residues near the inhibitor binding site: His671, Glu692, and Lys826[251]. This structure led to the hypothesis that mutation of Asn676 disrupts this hydrogen bond network to favor the active, 'DFG-in' state of the active site, thus resulting in resistance to quizartinib and other so-called 'Type II' inhibitors with conformationally sensitive binding modes[251]. Alignment of the kinase domains from the crystal structure of HCK bound to A-419259 (PDB: 4LUE)[447] with quizartinib-bound FLT3 shows remarkable overlap in the position of the two inhibitors (modeled in Figure 21C). This alignment suggests that Asn676 mutations may affect A-419259 binding to the FLT3 kinase domain in a manner similar to that as quizartinib.

In summary, our study provides new evidence that the level of HCK, LYN and FGR expression has strong prognostic power in AML. We also demonstrate that the anti-leukemic efficacy of the tyrosine kinase inhibitor A-419259 is dependent on inhibition of myeloid SRC-family kinases as well as FLT3 in the context of FLT3-ITD^{+} AML. Importantly, the ability of A-419259 to inhibit both FLT3-ITD and myeloid SRC family kinases may suppress the evolution of common resistance mutations seen for other FLT3 inhibitors, including D835Y and F691L, although the N676S mutation is still a liability with A-419259. Combination therapy with FLT3

inhibitors that display non-overlapping acquired resistance profiles may suppress a broader range of resistance mutations. For example, quizartinib and A-419259 have minimally overlapping resistance profiles, since quizartinib resistance primarily involves D835Y and F691L mutations while A-419259 resistance primarily involves substitution of Asn676 as established here.

2.5 Materials and methods

2.5.1 Kinase inhibitors

A-419259 was obtained from Sigma-Aldrich. Quizartinib (AC220) was purchased from LC laboratories. TL02-59 was custom synthesized by A Chemtek, Inc. The SYK inhibitor, PRT062607, was purchased from Selleckchem.

2.5.2 KINOMEscan analysis of A-419259 target specificity

The target kinase specificity of A-419259 was profiled using the KINOMEscan scanMAX service from Eurofins/DiscoverX as previously described[298,445,451]. KINOMEscan is a competitive binding assay in which a DNA-tagged kinase is incubated with a compound of interest in the presence of immobilized, non-selective ATP analogs. Kinase retention to the immobilized ligand is then measured using quantitative real-time PCR for each kinase-specific DNA barcode. Results are reported as the percent of each kinase that remains bound to the immobilized ATP analog. Data were visualized using the TREEspot™ profile visualization tool

version 5.0 (Eurofins) which overlays the interacting kinases on a circular dendrogram representing the entire human kinome.

2.5.3 Recombinant protein kinases

Recombinant purified FLT3 wild-type, FLT3-ITD and FLT3-D835Y kinase domains were purchased from ThermoFisher. Recombinant near-full-length HCK and FGR were co-expressed with Csk and PTP1B in BL21Star (DE3) E. coli in 1 L terrific broth. Once the culture reached an OD_{600} of 1.0, protein expression was induced with 0.5 mM IPTG for 16 h at 16 °C. The bacterial cell pellet was lysed using a Microfluidics M-110P microfluidizer and clarified by ultracentrifugation. Recombinant kinases were purified through sequential HisTrap HP, HiTrap Blue and HiLoad 26/600 Superdex columns using an ÄKTA Explorer automated chromatography system (GE Healthcare Life Sciences).

2.5.4 Z'-LYTE in vitro kinase assay

The Z'Lyte in vitro kinase assay (Life Technologies) is described in detail elsewhere[452,453]. Assays were performed in quadruplicate in 384-well low volume, non-binding, black polystyrene microplates (Corning) according to the manufacturer's instructions. Briefly, this assay measures phosphorylation of the Tyr2 peptide substrate which is tagged with coumarin and fluorescein on its N- and C-termini, respectively, to form a FRET pair. After the kinase reaction, a development step involves site-specific proteolytic cleavage of the unphosphorylated but not the phosphorylated peptide. Peptide cleavage results in loss of the FRET signal. Kinase reactions were initiated by the addition of ATP at the K_m for each kinase and Tyr2 peptide

substrate (1 μM). Following incubation for 1 h, reactions were quenched by addition of the development protease, and coumarin and fluorescein fluorescence were measured 1 h later on a Molecular Devices SpectraMax M5 plate reader. Data are expressed as a ratio of the coumarin (445 nm) to fluorescein FRET (520 nM) emissions normalized to signals observed in the absence of ATP (negative control) and with a positive control peptide in the absence of kinase (Tyr2 that is 100% phosphorylated). For experiments with inhibitors, compounds were preincubated with the kinase for 30 min prior to initiation of the reaction by the addition of ATP.

2.5.5 Cell culture

TF-1 and MV4-11 cells were obtained from the American Type Culture Collection (ATCC) and cultured in RPMI 1640 medium supplemented with 10% fetal bovine serum (FBS), 100 units/ml of penicillin, 100 μg/ml of streptomycin sulfate, and 0.25 μg/ml of amphotericin B (Antibiotic-Antimycotic; Gibco/ThermoFisher). TF-1 cells also require recombinant human GM-CSF (1 ng/mL; ThermoFisher). MOLM13 and MOLM14 cells were obtained from Leibniz Institute Deutsche Sammlung von Mikroorganismen (DSMZ) and grown in RPMI 1640 medium containing 20% FBS and Antibiotic-Antimycotic. Human 293T cells were obtained from ATCC and cultured in Dulbecco's modified Eagle's medium (DMEM) containing 10% FBS and Antibiotic-Antimycotic.

2.5.6 Generation of TF-1 cell lines stably expressing FLT3, HCK, or FGR

Full-length cDNA clones of each kinase were subcloned into the retroviral expression vectors pMSCV-neo or pMSCV-puro (Clontech). High-titer retroviral stocks were produced in

293T cells co-transfected with each pMSCV construct and an amphotropic packaging vector. TF-1 cells (10^6) were resuspended in 5.0 mL of undiluted viral supernatant and centrifuged at 1,000 × g for 4 h at 18 °C in the presence of 4 μg/mL Polybrene (Sigma-Aldrich) to enhance viral transduction. Forty-eight hours after infection, the cells began a two-week selection period with 400 μg/ml G-418 (neo vectors) or 3 μg/mL puromycin (puro vectors). Following selection, cells were maintained with 200 μg/ml G418 or 1 μg/mL puromycin. For double transduction experiments, TF-1 cells were first infected with the pMSCV-neo-FLT3-ITD virus, selected with G418, followed by the pMSCV-puro virus carrying HCK or FGR and puromycin selection.

2.5.7 Cell titer blue cell viability assay

Cells were seeded at 10^5 per mL in the presence or absence of inhibitors with DMSO as carrier solvent (0.1% final). Cell viability was assessed using the CellTiter-Blue reagent according to the manufacturer's instructions (Promega). Fluorescence intensity, which correlates directly with viable cell number, was measured using a SpectraMax M5 microplate reader. Each experiment included three technical replicates per condition, and each experiment was repeated at least three times.

2.5.8 Immunoprecipitation and immunoblotting

Cells (3 x 10^6 per 5 mL medium) were cultured with inhibitors or DMSO alone for 16 h. Cells were then lysed in RIPA buffer (50 mM Tris-HCl, pH 7.4, 150 mM NaCl, 1 mM EDTA, 1% Triton X-100, 0.1% SDS, 1% sodium deoxycholate) supplemented with 2.5 mM sodium orthovanadate, 25 mM sodium fluoride, 5 units/mL Benzonase (Novagen), and a protease

inhibitor cocktail (cOmplete EDTA-Free tablets; Sigma). Protein concentrations in the lysates were determined using Protein Assay Dye concentrate (BioRad).

FLT3, HCK and FGR were immuno-precipitated using anti-FLT3 (CST #3462), anti-HCK (CST #14643S), anti-FGR (CST #2755S) antibodies (Cell Signaling Technologies). Each immuno-precipitation reaction contained 1 mg lysate protein, 2 µg antibody, and 20 µL of protein G-Sepharose beads (Invitrogen) in RIPA buffer with supplements as described above. Immuno-precipitation reactions were incubated overnight at 4 °C. Immunoprecipitates were collected by micro-centrifugation, washed two times by resuspension in 1.0 mL RIPA buffer, separated by SDS-PAGE and transferred to nitrocellulose membranes. FLT3 was blotted with anti-FLT3 (Cell Signaling Technologies #3462) and anti-phosphotyrosine (pY99; Santa Cruz sc-7020) antibodies. HCK was blotted with anti-HCK (Cell Signaling Technologies #14643S) and anti-phospho-SRC (pTyr416) clone 9A6 (EMD Millipore) antibodies. FGR was blotted with anti-FGR (Cell Signaling Technologies #2755S) and anti-phospho-SRC (pTyr416) clone 9A6. Secondary antibodies included anti-mouse or anti-rabbit IgG conjugated to 680 nM and 800 nM fluorophores, respectively (LI-COR). Blots were scanned using a LI-COR Odyssey imager, and signal intensities were quantified using the Image Studio Lite software. Data are shown as ratios of the phosphoprotein to total protein signals and in the case of inhibitor treatment the ratios are normalized to the vehicle-treated cells.

2.5.9 Experimental evolution of A-419259-resistant populations of MV4-11, MOLM13, MOLM14 cells

Populations of MV4-11, MOLM13 and MOLM14 cells with de novo resistance to A-419259 were initiated by culturing 10^6 cells in 5.0 mL of medium containing A-419259 at a

starting concentration of 10 nM. Viability of each cell population was measured three times per week using the CellTiter-Blue assay. Once cell viability crossed a threshold of 4000 RFU over background in this assay, 10^6 cells were subcultured into 1.0 mL fresh medium containing 50% more compound (i.e. cells growing in 10 nM would be passed into 15 nM). Cells were sub-cultured in this way until outgrowth was observed in the presence of 1 µM A-419259.

2.5.10 Exome sequencing and analysis

Genomic DNA was prepared for sequencing using the Illumina TruSeq Rapid Exome kit, and 150 bp paired-end sequencing was performed with a mid-output flowcell (Illumina FC-404-2003) on an Illumina NextSeq-500 sequencer. Data analysis was performed at the University of Pittsburgh Center for Research Computing using the Genome analysis Toolkit (GATK) best practices[454]. Contaminating 5' and 3' adapter sequences were removed with Trimmomatic version 0.33[455], resulting in ~135 bp paired-end reads with greater than 30-fold average coverage of the exome for each sample. Sequence reads were aligned to human reference genome hg37 with Burrows-Wheeler aligner maximal exact matches (BWA-MEM) algorithm version 0.7.15[456]. Samtools version 1.3.1 was used to convert the sam file to bam. Duplicates were removed and base scores were recalibrated with Picard Mark Duplicates version 2.11.0[457]. Variant calling files (VCFs) were generated using GATK version 3.8.1 Haplotypecaller[458]. SnpEff version 4.3 was used to annotate the VCF[459]. Finally, Cancer-specific High-throughput Annotation of Somatic Mutations (CHASM) was used to rank the variants[460,461]. All software code is freely available at this link: https://github.com/RaviKPatel-PhD/HCK-and-FGR-Regulate-Sensitivity-of-FLT3-ITD-AML. Raw sequencing data are available via the NCBI sequence read archive (SRA).

2.5.11 RNA Isolation, cDNA preparation, qPCR

Total RNA was isolated from cells using the RNeasy Plus Mini Kit (Qiagen). cDNA was prepared from total RNA using the RETROscript kit (ThermoFisher/Invitrogen). Real-time quantitative RT-PCR assays were performed on total RNA using SYBR Green detection and gene-specific QuantiTect primers (Qiagen) on an Applied Biosystems StepONE plus real-time PCR instrument.

3.0 Codon mutagenesis reveals a single gatekeeper mutation as the sole source of SRC-family kinase resistance to a Type I inhibitor

3.1 Chapter 3 summary

Understanding acquired drug resistance to protein-tyrosine kinase inhibitors, which often arises from binding site or allosteric mutations in the target kinase, is an issue central to the development of more durable therapies.

Experimental systems that reveal the potential path to resistance for a given inhibitor and target have an important role in preclinical develop of kinase inhibitor drugs. Here we employed a codon mutagenesis approach to define the mutational landscape of acquired resistance in HCK, a myeloid member of the SRC tyrosine kinase family with untapped therapeutic potential in acute myeloid leukemia (AML). Using PCR-based saturation mutagenesis, we created a library in which all codon substitutions are represented at every amino acid position with the HCK open reading frame. This HCK mutant library was used to transform Rat-2 fibroblasts, followed by selection for resistant colonies with A-419259, a pyrrolopyrimidine HCK inhibitor and drug lead for AML. Remarkably, only a single resistance mutation was discovered by this approach, despite representation of nearly all possible missense mutations in the HCK open reading frame as confirmed by deep sequencing. This observation predicts that A-419259, which binds to HCK kinase domain through a conformationally independent Type I mechanism, may have a much narrower path to acquired resistance compared to inhibitors that function via conformationally sensitive, Type II mechanisms.

3.2 Introduction

SRC-family kinases have been implicated in many forms of cancer, including myeloid leukemias and other hematologic malignancies. In chronic myeloid leukemia (CML), the myeloid SRC-family member HCK cooperates with BCR-ABL in signaling pathways related to CML cell survival and also influences sensitivity to imatinib and other tyrosine kinase inhibitors[1,2]. More recently, HCK has also attracted attention as a therapeutic target in the context of acute myeloid leukemia (AML). Comparison of gene expression signatures in normal hematopoietic stem cells vs. leukemic stem cells (LSCs) from AML patients identified HCK as a LSC-specific transcript[3]. Selective knockdown of HCK expression with siRNAs resulted in decreased cell proliferation and increased apoptosis in primary AML cells[4]. A recent analysis of SRC-family kinase expression in AML identified HCK as one of the most highly expressed SRC-family members and showed that HCK expression levels correlate with poor outcomes in terms of AML patient survival. These data support the development of selective inhibitors of HCK as a new approach to precision AML therapy in patients that express high levels of this kinase.

One promising inhibitor candidate for HCK is the pyrrolopyrimidine compound, A-419259, which was originally developed as part of medicinal chemistry campaign to identify selective, orally active inhibitors of the closely related T cell kinase, LCK[5]. Initial studies showed that A-419259 selectively induced growth arrest and induced apoptosis of Philadelphia chromosome-positive CML cells at concentrations that did not directly inhibit BCR-ABL[6]. HCK

mutants with engineered resistance to A-419259 reversed its anti-CML effects, demonstrating that HCK is a primary target for A-419259 in CML[7]. More recently, A-419259 was rediscovered in a high-throughput screening campaign for HCK inhibitors, and shown to have potent activity against in mice bearing AML patient-derived xenografts following oral administration[8]. As for CML, mutants of HCK with engineered resistance to A-419259 rescued its anti-leukemic activity in FLT3-ITD^{+} AML cell lines, providing further support for HCK as a viable drug target in the subset of AML cases that over-express this kinase[9].

A-419259 inhibits HCK by binding to a pocket near the ATP-site in the kinase domain through a so-called 'Type I' mechanism, in which a conserved Asp-Phe-Gly (DFG) motif at the N-terminal end of the activation loop as well as the α-C helix are both rotated inward[10]. This binding mode is observed in an X-ray crystal structure of HCK bound to A-419259, which also shows contacts between the pyrrolopyrimidine core and the side chain of the gatekeeper residue (Thr338; SRC numbering) and the main chain of the hinge residues, Glu339 and Met341 (Figure 2)[11]. In addition, the piperidine moiety of A-419259 makes a polar contact with the catalytic aspartate (Asp348). Because the structural features of active tyrosine kinase domains are similar, Type I inhibitors are often considered to lack target kinase specificity. However, KINOMEscan analysis shows that A-419249 exhibits a remarkably narrow specificity profile for a Type I compound, with the most likely targets confined to the HCK, other SRC-family members, as well as FLT3 and other Class III receptor tyrosine kinases relevant to AML[9]. This specificity profile makes A-419259 a promising candidate for further development against AML cases that are associated with over expression of HCK and other myeloid SRC-family kinases, as well as mutants of FLT3.

Development of precision therapies targeting tyrosine kinases in myeloid leukemias has exploded over the past two decades. This effort was spawned by the success of imatinib, a relatively selective inhibitor for the BCR-ABL tyrosine kinase associated with CML. Imatinib owes its specificity in part to its ability to trap a unique inactive conformation of the ABL kinase domain, in which the DFG motif is rotated outward while the α-C helix is rotated inward[12]. This 'Type II' binding mode is more conformationally sensitive than Type I and is therefore more sensitive to allosteric effects on the overall conformation of the kinase domain. Random mutagenesis studies with BCR-ABL followed by imatinib selection in vitro revealed a diverse array of mutations that can produce inhibitor resistance, including many outside of the inhibitor binding pocket[13]. Many of these mutations have also been observed in the clinic[14,15], illustrating the power of this approach in the identification of potential pathways to resistance during the drug development process. A similar approach has also been used to find clinically relevant resistance mutations against the Flt3-ITD inhibitors quizartinib[16] and crenolanib[17], which are currently in development for FLT3-ITD^{+} AML.

Given the therapeutic potential of A-419259 described above, herein we performed a forward genetic screen designed to identify all possible mutations that may give rise to resistance using HCK as the inhibitor target. Using PCR-based codon mutagenesis, we generated an HCK cDNA library in which all possible codons are represented across the entire HCK open reading frame with the exception of those essential to function. The library was used to transform Rat-2 fibroblasts, followed by selection of clones resistant to A-419259. Despite the extensive diversity of this library, the only resistance mutations identified mapped to the gatekeeper residue in the inhibitor binding pocket. This remarkable finding suggests that AML cells treated

with A-419259 may have a much narrower path to inhibitor resistance compared to inhibitors that function via conformationally sensitive, Type II mechanisms.

3.3 Results

3.3.1 A forward genetic screening strategy to identify potential A-419259 resistance mutations in HCK

HCK is one of eight mammalian SRC-family members that share a similar architecture consisting of four domains (Figure 2). These include the N-terminal unique domain, which is myristoylated and palmitoylated for membrane anchoring. The unique domain is followed by the SH3, SH2, and kinase domains as well as a C-terminal tail with a conserved tyrosine (Tyr527) essential for kinase regulation. Phosphorylation of Tyr527 by the regulatory kinase CSK induces intramolecular engagement of the SH2 domain. This contact, together interaction of SH3 with the SH2-kinase linker, hold HCK and other SRC-family kinases in an inactive, assembled conformation. Mutation of Tyr527 to phenylalanine (HCK-YF mutant) prevents tail phosphorylation, leading to constitutive kinase activity and oncogenic transformation following ectopic expression in Rat-2 fibroblasts[18–20]. This Rat-2 transformation assay forms the basis of the codon mutagenesis screen for A-419259 resistance described below.

In order generate a fully diverse library of HCK mutants, we used a PCR-based saturation mutagenesis procedure covering the entire open reading frame of the p59 form of human HCK. This method involves a large set of overlapping PCR primers with a central degenerate codon

flanked by adjacent coding sequences. The primers are then combined, and subsequent annealing and low-cycle PCR results in a single product in which every possible codon is theoretically represented at each position along the sequence. In the case of HCK, we excluded codons for residues critical to HCK activity and subcellular localization, while substituting Tyr527 with phenylalanine to ensure transformation in Rat2 fibroblasts (see Methods). In total, 488 of 505 codons underwent mutagenesis; with 64 codons possible at each position, the maximum theoretical diversity of the *HCK* mutagenesis library is 488 codons x 64 possible codons = 31,232 individual clones. Following PCR, the final PCR product was subjected to large-scale ligation into the retroviral vector for subsequent gene transfer. The resulting ligation reaction was used to transform *E. coli*, and subsequent plating produced approximately 100,000 individual bacterial colonies. This outcome suggests that more than 95% of the possible codon substitutions are represented in at least one clone within our library.

To assess the diversity of the HCK codon mutagenesis library, twenty individual clones were picked at random and analyzed by Sanger sequencing in their entirety. Nucleotide changes were observed in all three positions within each codon, with a slight bias towards single nucleotide substitutions (Figure 23A). This bias may reflect the enhanced PCR efficiency of primers with single nucleotide substitutions, although errors generated during PCR may also contribute. Next, we compared the number of mutations in each clone to the expected Poisson distribution (Figure 23B). The expected distribution was observed for clones with zero or one mutation, while fraction observed for 2 and 3 mutations per clone was somewhat skewed. This result may reflect the relatively small sample size. On average, we observed about two mutations per clone, with 72% of the clones exhibiting at least one mutation. We also examined the cumulative distribution of observed mutations across the *HCK-YF* coding sequence (Figure

23C). Perfectly distributed mutations would yield a cumulative distribution plot that follows a straight line. However, PCR-based codon mutagenesis tends to bias for mutations at the beginning and end of the gene, an effect that is more pronounced as a function of target sequence length. This effect is observed in our cumulative distribution plot, although mutations are present across the entire length of the coding sequence as desired.

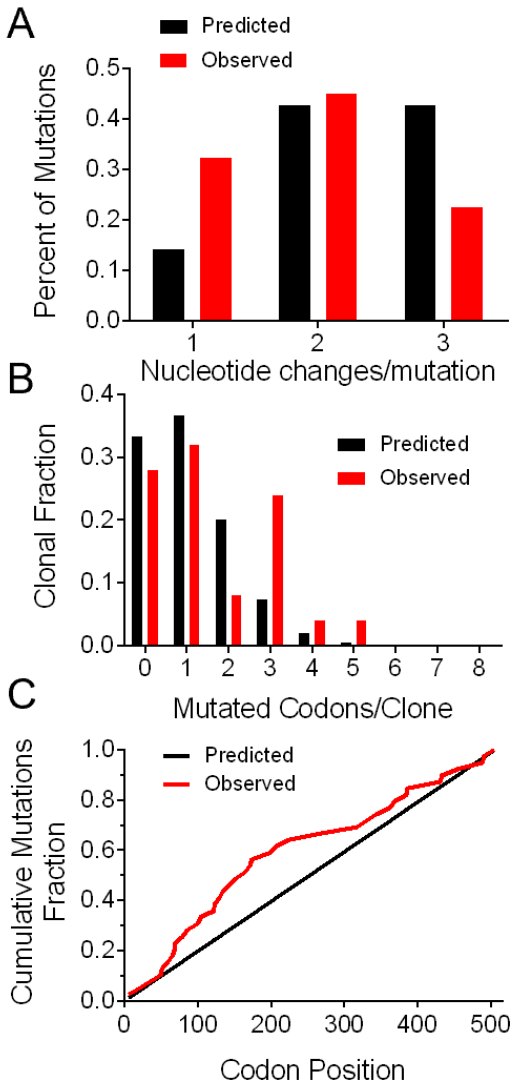

Figure 22. HCK-YF codon mutagenesis library contains mutations across the entire gene.

Analysis of 20 codon mutagenesis clones by sanger sequencing. The expected distribution is shown in black and the actual distribution is in red. **A.** The number of nucleotide substitution in each codon substitution found across the 20 clones. **B.** Distribution of the number of mutations per clone. **C.** Cumulative distribution of mutations across the entire Hck-YF gene. The expected value here is an equal distribution of mutations across the gene.

To better understand if every possible codon substitution is represented in our library we deep sequenced the library (details in methods). We are currently working on plotting the substitutions on a sequence logo[21]. The distribution of all substitutions sequenced is as expected, although some codons are more represented than others.

3.3.2 Transformation of Rat-2 cells with the HCK-YF mutant library and selection of A-419259-resistant clones

Recombinant retroviruses carrying the HCK-YF codon mutagenesis library were produced in 293T cells and used to infect Rat-2 fibroblasts. Following G-418 selection, the transduced Rat-2 cell population was plated in soft-agar colony-forming assays in the presence of A-419259. Rat-2 cells expressing HCK-YF grow in an anchorage- independent fashion that is dependent on HCK kinase activity, forming tight colonies amenable to subsequent isolation and subculture[18–20]. To ensure complete coverage of the library, 40 plates were prepared with 5,000 cells per plate, for a total of 200,000 individual cells that underwent selection which represents more than six times the possible number of individual clones present. Selection was performed at a final concentration of 1 µM A-419259, which completely blocked colony formation by control cells expressing HCK-YF. Following two weeks of selection, 13 colonies appeared over 5 of the selection plates. These colonies were picked and expanded in the absence of agarose and inhibitor under regular culture conditions. Eight of the thirteen original colonies regrew and were subsequently retested for colony formation in the presence of A-419259 (Figure 24). Of these, only a single clone retained the ability to form equal numbers of large colonies in the presence or absence of A-419259. This verified resistant clone (R5-1) was analyzed in detail as described below.

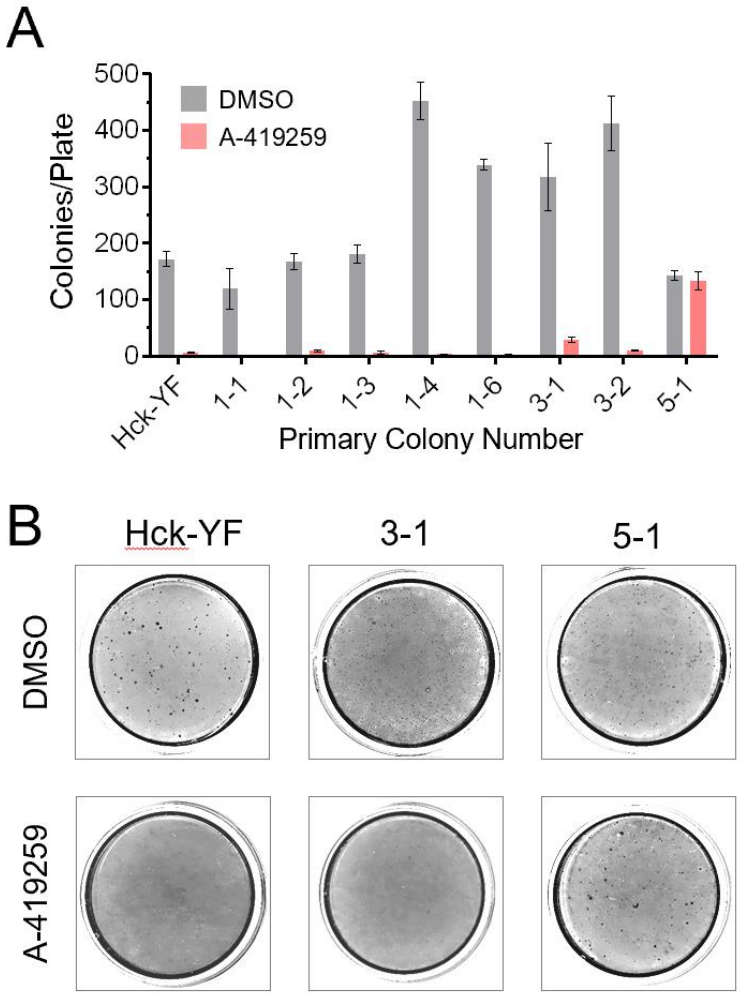

Figure 23. Isolation of an A-419259 resistant colony of Rat-2 fibroblasts transformed with a HCK-YF mutant library.

Rat-2 cells were infected with recombinant retroviruses carrying a HCK-YF codon mutagenesis library, followed by selection with G418. The transduced cell population was then plated in colony-forming assays in semi-solid medium in the presence of A-419259. Resistant colonies were picked and expanded in 2D culture, followed by re-assay for colony-forming activity in the presence of A-419259 or DMSO as control. A) Of eight colonies assayed, only one (colony 5-1) produced the same number of colonies in the presence and absence of A-419259. B) Images of representative culture plates from part A. A-419259 (1 µM) completely suppressed colony formation by control cells expressing HCK-YF (*left*). Colonies 3-1 and 5-1 both formed colonies in the absence of A-419259, but only 5-1 formed equivalent colony numbers in the presence of the inhibitor.

Genomic DNA was isolated from resistant clone R5-1, and the integrated *HCK-YF* coding sequence was amplified by PCR and analyzed by Sanger sequencing. Missense mutations were observed at the codons for Pro32 in the unique domain, Asp158 in the SH2 domain, and Met302, Ile334, and Thr338 in the kinase domain (Table 9). To determine whether these mutations were linked in individual clones, the *HCK-YF* PCR product from colony R5-1 was subcloned, and individual bacterial colonies were picked for subsequent nucleotide sequencing. This analysis revealed two variants of the *HCK-YF* coding sequence within the resistant R5-1 Rat-2 cell population. The first clone contained three mutations, P32H-D158I-T338H, while the second encoded a stop codon at position 34, along with the two other missense mutations (M302W and I334S). These results are consistent with a single Rat-2 cell being transduced by two independent retroviruses, each carrying one of the triple mutant clones.

3.3.3 The HCK gatekeeper mutant T338H confers strong resistance to A-419259

Analysis of the HCK-YF coding sequence from A419259-resistant clone R5-1 identified seven missense mutations that were distributed across two independent clones. The M302W and I334S were linked to a stop codon upstream, making this mutant very unlikely to be expressed or to contribute to the resistant phenotype. Nevertheless, each of the five missense mutations observed was reintroduced individually into wild-type HCK for subsequent analysis. To evaluate the effect of the mutations on HCK protein stability, we first expressed each single mutant in 293T cells and blotted for HCK protein expression relative to actin as a control (Figure 25). This analysis revealed that several of the mutations resulted in reduced levels of full-length HCK relative to the wild-type kinase, including P32H, and D158I. The HCK-I334S mutant protein

underwent a significant shift in mobility on the western blot, consistent with proteolytic cleavage. Cultures expressing HCK were also treated with A-419259, which enhanced the levels of the P32H, D158I mutants relative to the untreated cells. This observation suggests that the presence of the inhibitor may alter the conformation of HCK in such a way as to make the protein less susceptible to proteolytic degradation. Indeed, a recent study has shown that ATP-site inhibitors have long range effects on overall Src-family kinase conformation[22]. In contrast, the M302W and T338H mutants were at least as stable as wild-type HCK, and the presence of A-419259 did not alter their expression levels. We also compared the stability of the T338H mutant to that of a previously characterized gatekeeper mutant, T338M[9]. Whereas T338H was very stable, expression of T338M was reduced, and the presence of A-419259 appeared to accentuate this effect. These differences in HCK mutant protein stability may influence the overall sensitivity of cells to A-419259 as described in the next section.

Table 9. Mutations associated with A-419259 resistance in Rat-2 cells transformed with the HCK-YF codon mutagenesis library.

Nucleotide sequence analysis was performed on human HCK present in A-419259 resistant colony 5-1 (see Figure 4 and main text). Six codons were modified in two independent HCK clones isolated from these cells, resulting in the amino acid changes shown. Note that the nucleotide and amino acid numbering for the HCK unique domain mutation (P32 position) is based on the human p59 HCK coding sequence due to lack of homology with SRC in this region; all other numbering is based on homology to SRC as per convention.

Mutation	Amino Acid Change	Domain
$C^{95}G$ to AT	P32H	Unique
$G^{394}AC$ to ATA	D158I	SH2
$A^{826}T$ to TG	M302W	Kinase
$A^{922}TC$ to TCC	I334S	Kinase
$A^{934}CG$ to CAC	T338H	Kinase

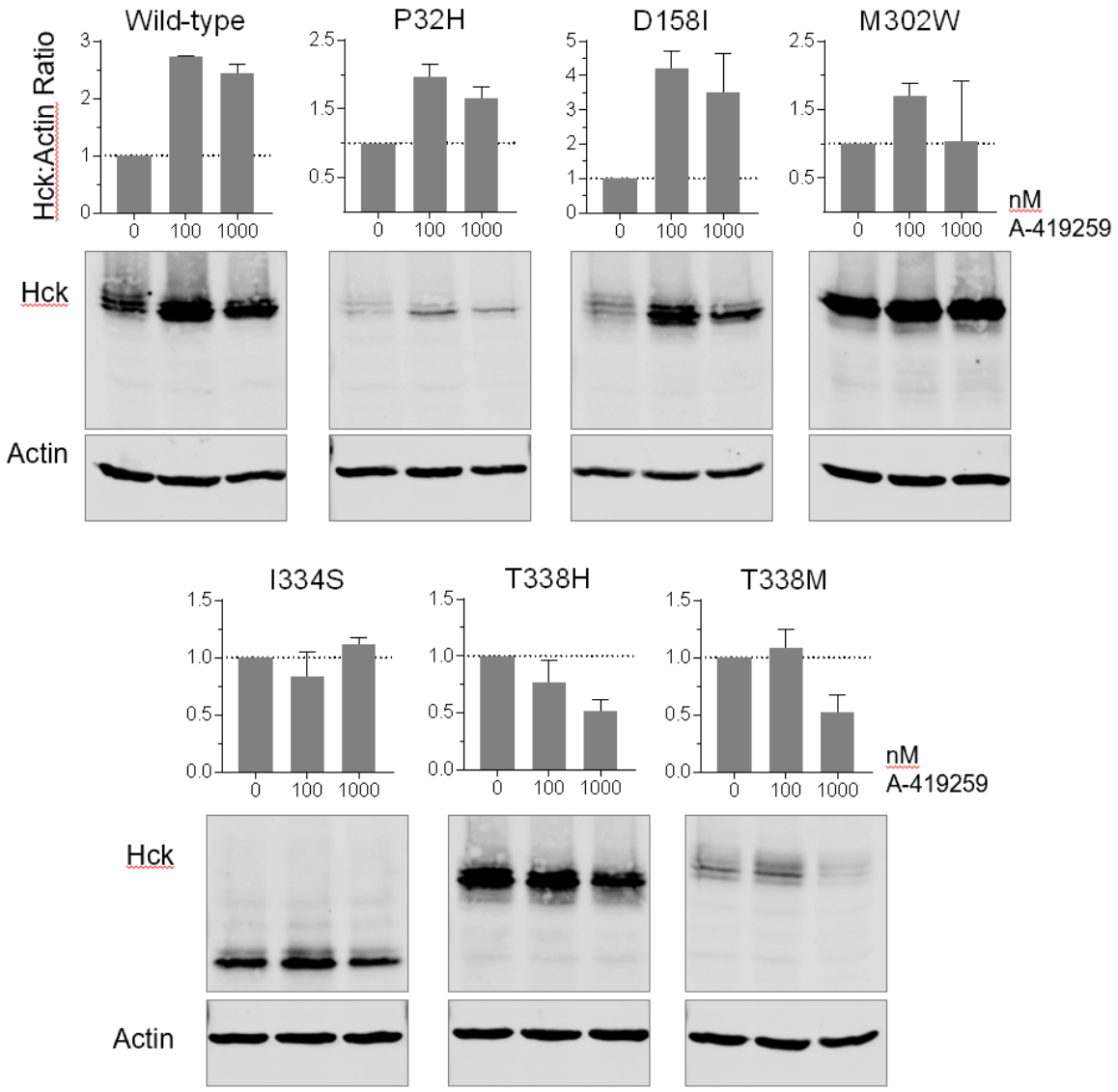

Figure 24. Assessment of wild-type and mutant HCK expression in 293T cells.

293T cells were transfected with wild-type HCK or the six mutants associated with acquired A-419259 resistance from the Rat-2 cell codon mutagenesis screen (P32H, D158I, M302W, I334S and T338H). An engineered gatekeeper mutant of HCK (T338M) was also included for comparison. Cells were then treated with A-419259 at the concentrations shown. Cells lysates were analyzed for HCK expression by immunoblotting, along with actin as a loading control. Immunoreactive proteins were visualized using secondary antibodies conjugated to infrared dyes and imaged using the LI-COR Odyssey system. Bar graphs above each set of images show the ratio of the HCK to actin signal intensities from two independent experiments. Ratios from each experiment were normalized to the DMSO control, and the average value ± S.E. is presented.

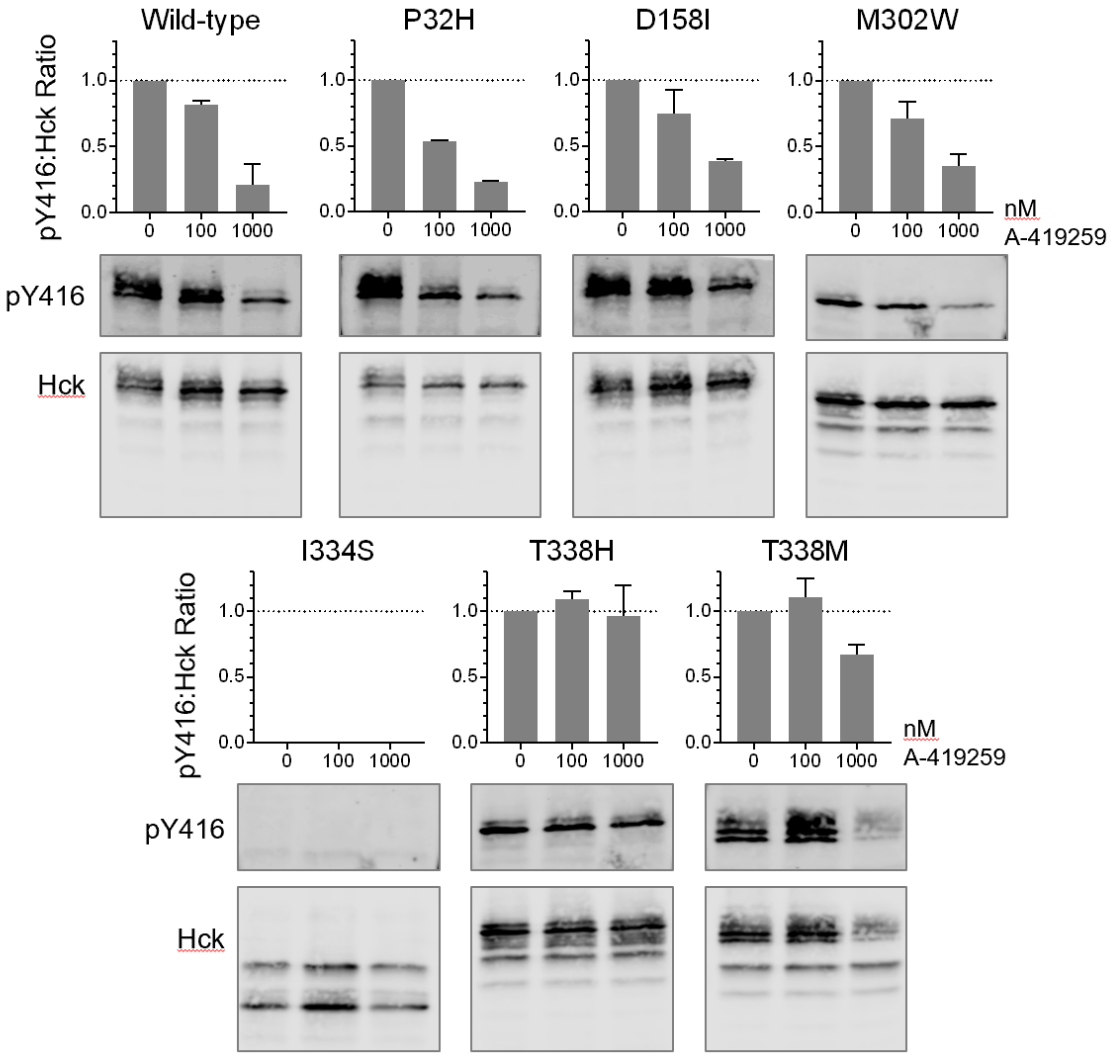

Figure 25. HCK-T338H is resistant to A-419259 following transient expression in 293T cells.

293T cells were transfected with wild-type HCK or the six mutants associated with acquired A-419259 resistance from the Rat-2 cell codon mutagenesis screen (P32H, D158I, M302W, I334S and T338H). An engineered gatekeeper mutant of HCK (T338M) was also included for comparison. Cells were then treated with A-419259 at the concentrations shown, followed by immunoprecipitation of HCK and blotting to assess activation loop phosphorylation (pY416) and HCK protein recovery. Immunoreactive proteins were visualized using secondary antibodies conjugated to infrared dyes and imaged using the LI-COR Odyssey system. Bar graphs above each set of images show the ratio of pY416 to HCK signal intensities from two independent experiments. Ratios from each experiment were normalized to the DMSO control, and the average value ± S.D. is presented.

To determine the effect each mutation on HCK sensitivity to A-419259, transfected 293T cells were treated in the presence or absence of A-419259 at final concentrations of 100 and 1,000 nM. HCK proteins were immunoprecipitated followed by immunoblotting for the autophosphorylated activation loop as a measure of kinase activity (pY416 antibody) as well as HCK protein recovery (Figure 26). Of the five mutants tested, only the gatekeeper mutant (T338H) was resistant to A-419259, with no change in activation loop phosphorylation at either inhibitor concentration. In comparison, the HCK-T338M gatekeeper mutant showed complete resistance to A-419259 at 100 nM but only partial resistance at 1,000 nM. In addition, the HCK-T338M protein is less stable in the presence of the higher concentration of the inhibitor, while HCK-T338H remains stable. Taken together, this analysis suggests that the T338H gatekeeper mutant alone generates A-419259 resistance without affecting protein stability, which together may explain the emergence of this mutant from the codon mutagenesis screen.

To control for codon mutants that may only be resistant in the context of HCK-YF and not HCK-WT we performed the same 293T cell experiment with all the codon mutants in the context of HCK-YF (Figure 27). The results were similar to HCK-WT, in that all the mutants are sensitive to the inhibitor except HCK-T338H-YF and HCK-T338M-YF. We again see a similar effect of stabilization of the HCK-YF protein after addition of A-419259. Interesting HCK-I334S-YF does not degrade as HCK-D158I does.

3.3.4 Human FLT3-ITD^{+} AML cells expressing HCK-T338H are resistant to A-419259

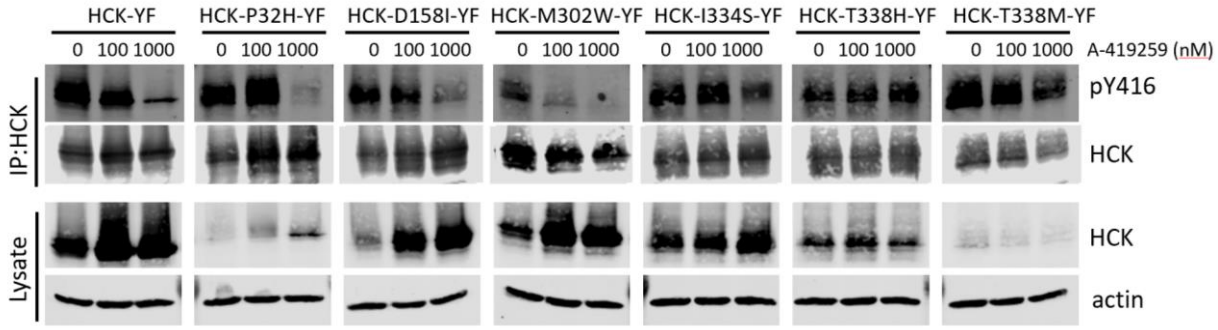

Figure 26. Hck-T338H-Y527F is resistant to A-419259.

293T cells were transfected with HCK-Y527F or the six mutants associated with acquired A-419259 resistance from the Rat-2 cell codon mutagenesis screen (P32H, D158I, M302W, I334S and T338H). An engineered gatekeeper mutant of HCK (T338M) was included for comparison. Cells were then treated with A-419259 at the concentrations shown, followed by immunoprecipitation of HCK and blotting to assess activation loop phosphorylation (pY416) and HCK protein recovery. Immunoreactive proteins from the immunoprecipitate and the lysate were visualized using secondary antibodies conjugated to infrared dyes and imaged using the LI-COR Odyssey system. No quantification is shown because this experiment has only been done once so far.

To determine whether the HCK-T338H gatekeeper mutation is solely responsible for resistance to A-419259 in a cellular context relevant to AML, we turned to the human TF-1 myeloid cell line. TF-1 cells require GM-CSF to support their proliferation and survival in culture and can be transformed to a cytokine-independent phenotype by retroviral transduction of the AML-associated receptor tyrosine kinase mutant, FLT3-ITD[23,24]. TF-1 cells were transformed with FLT3-ITD, followed by stable expression of wild-type HCK and each of the mutants recovered from the codon mutagenesis screen. Each population of cells was then tested for sensitivity to growth inhibition by A-419259 over a range of inhibitor concentrations (Figure 28). Of all the mutants tested, only expression of HCK-T338H resulted in reduced sensitivity of TF-1/FLT3-

ITD cells to the inhibitor, and the effect was greater than that that observed with the previously described gatekeeper mutant, HCK-T338M[9].

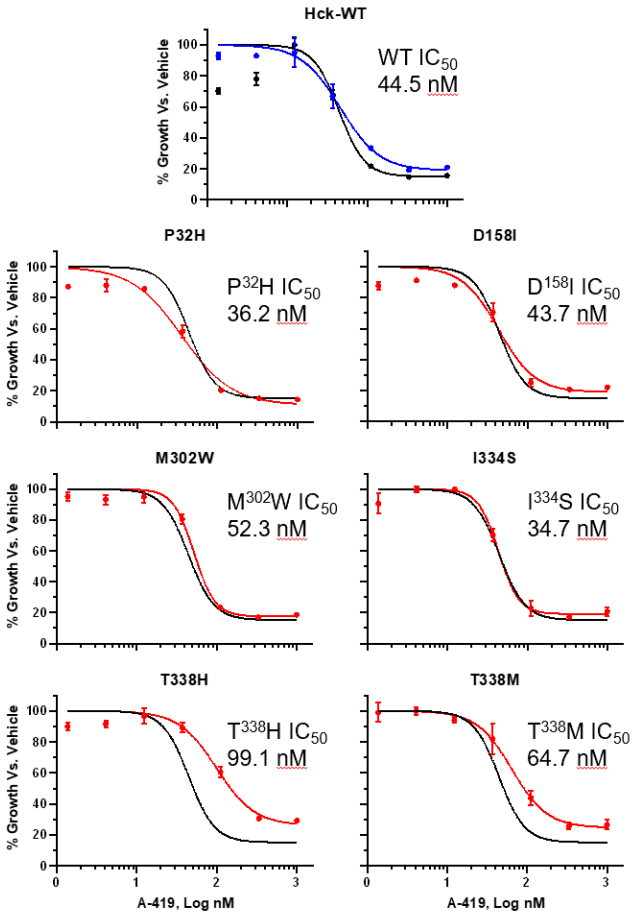

Figure 27. The HCK-T338H gatekeeper mutant confers resistance to A-419259 in TF-1 myeloid cells transformed with FLT3-ITD.

TF-1 cells were transformed to cytokine-independent growth by stable expression of the FLT3-ITD receptor tyrosine kinase mutant associated with AML. Wild-type HCK (WT), as well as the six HCK mutants associated with acquired resistance in the Rat-2 cell codon mutagenesis screen (P32H, D158I, M302W, I334S and T338H), we then expressed in the TF-1/FLT3-ITD cells. Viability of each cell population over the range of A-419259 concentrations shown was then assessed by CellTiter-Blue assay, and the resulting concentration-response curves were best-fit by non-linear regression analysis (GraphPad Prism v8) to estimate the IC_{50} values shown. The upper right panel compares responses of TF-1 cells expressing FLT3-ITD and HCK-WT (black curve) vs. FLT3-ITD alone (blue curve). All other panels compare responses of TF-1 cells expressing FLT3-ITD and each HCK mutant (red curves); the FLT3-ITD + HCK-WT curve is plotted on each panel for reference. TF-1/FLT3-ITD cells expressing a previously described engineered resistance mutant, HCK-T338M, were also included for comparison (lower right panel). Each condition was performed in triplicate, and the average values are shown.

To correlate growth suppression with effects on kinase activity in the presence of A-419259, HCK was immunoprecipitated from each cell population and immunoblotted for activation loop phosphorylation and HCK protein recovery as before (Figure 29). In all TF-1/FLT3-ITD cell populations, HCK was expressed and constitutively active, with the exception of the I334S mutant which underwent proteolytic cleavage as observed in 293T cells. In cells expressing wild-type HCK, A-419259 potently inhibited autophosphorylation with an IC_{50} value of less than 30 nM, consistent with previous observations in this system as well as established FLT3-ITD^{+} AML cell lines[9]. The P32H, D158I, and M302W mutants of HCK all remained sensitive to A-419259, with IC_{50} values similar to wild-type. However, HCK-T338H remained phosphorylated on Tyr416 in the presence of A-419259 at concentrations up to 100 nM, consistent with the reduced sensitivity of cells expressing this gatekeeper mutant to growth suppression by the inhibitor. Cells expressing T338M were also assayed for comparison and showed somewhat higher resistance than T338H in terms of activation loop phosphorylation. However, the T338M was expressed at much lower levels than T338H, suggesting that mutant protein stability as well as inhibitor resistance may contribute to the overall sensitivity of the cells to the compound.

To determine whether the differences in HCK protein expression observed with the different mutants was due to protein stability rather than mRNA expression levels, we performed quantitative real-time RT-PCR analysis of HCK transcript levels in each TF-1 cell population (Figure 30). This analysis revealed that HCK transcript levels were very similar across all of the TF-1 cell populations, with the exception of the I334S mutant which was somewhat reduced. Thus, the differences observed in HCK protein expression levels are most likely related to effects of the mutations on protein stability.

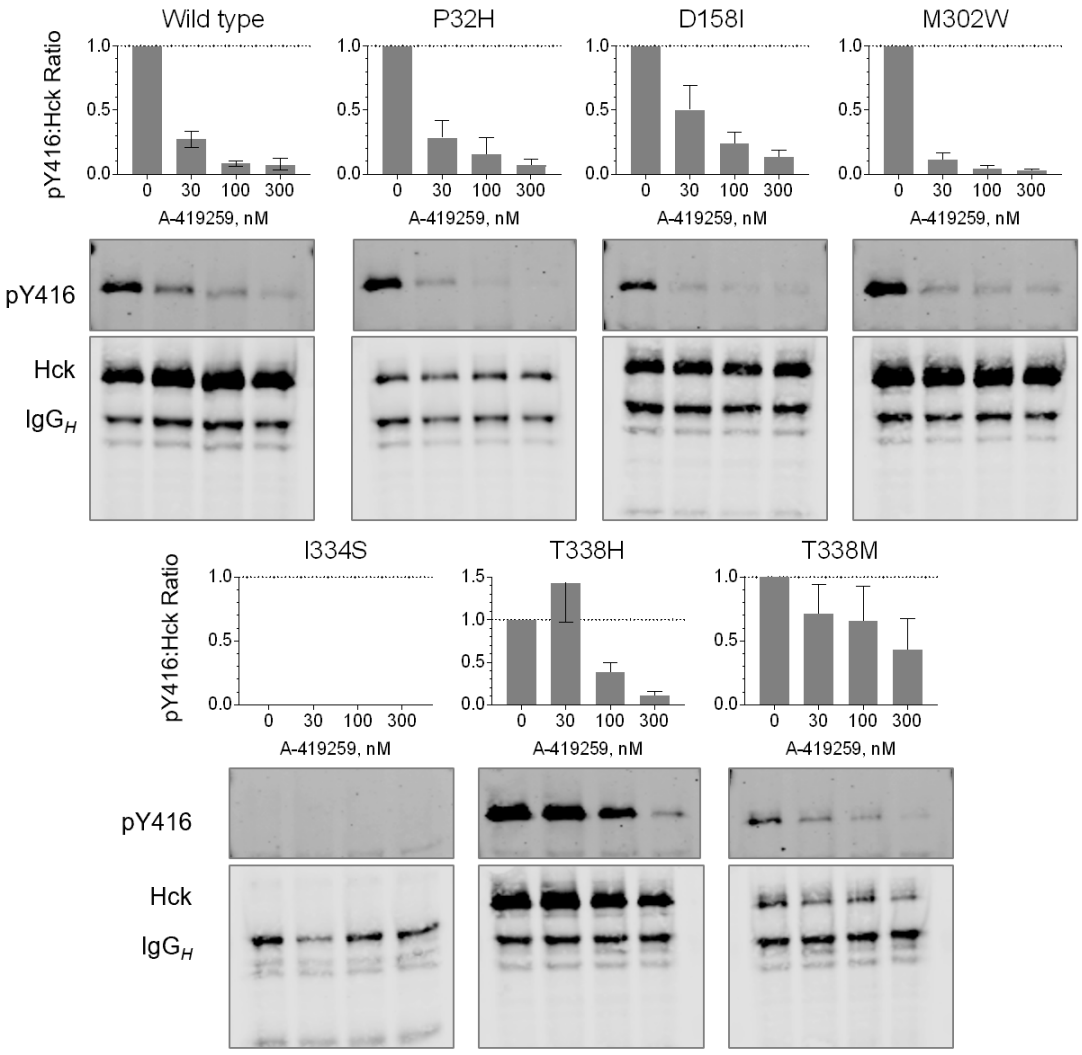

Figure 28. HCK-T338H is resistant to A-419259 following expression in TF-1 cells transformed by FLT3-ITD.

TF-1 cells were transformed with FLT3-ITD, followed by expression of wild-type HCK or the six mutants associated with acquired A-419259 resistance from the Rat-2 cell codon mutagenesis screen (P32H, D158I, M302W, I334S and T338H). An engineered gatekeeper mutant of HCK (T338M) was also included for comparison. Cells were treated with A-419259 at the concentrations shown, followed by immunoprecipitation of HCK and blotting to assess activation loop phosphorylation (pY416) and HCK protein recovery. Immunoreactive proteins were visualized using secondary antibodies conjugated to infrared dyes and imaged using the LI-COR Odyssey system. Bar graphs above each set of images show the ratio of pY416 to HCK signal intensities from three independent experiments. Ratios from each experiment were normalized to the DMSO control, and the average value ± S.E. is shown.

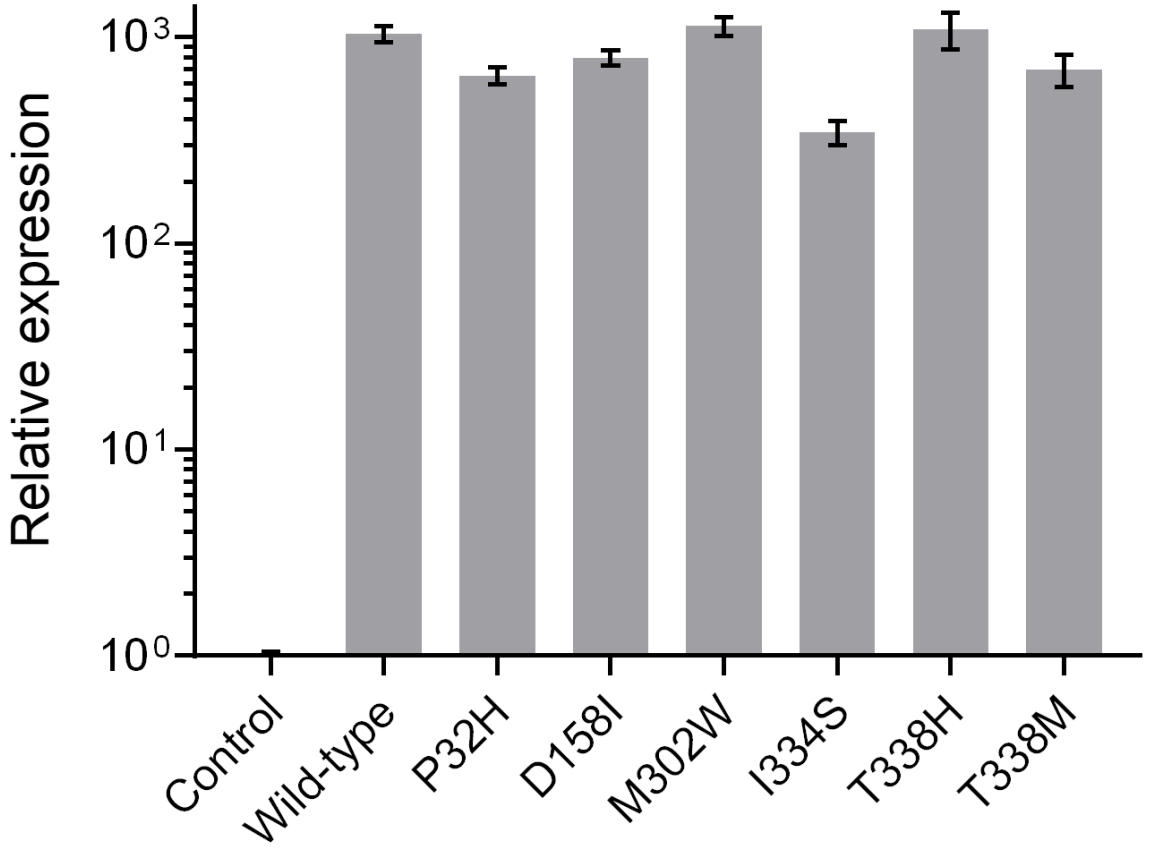

Figure 29. Analysis of wild-type and mutant HCK transcript levels in TF-1/FLT3-ITD cell populations.

Total RNA was isolated from TF-1 cells transformed with FLT3-ITD and co-expressing wild-type HCK or the six mutants associated with acquired A-419259 resistance from the codon mutagenesis screen (P32H, D158I, M302W, I334S and T338H) as well as an engineered gatekeeper mutant (T338M). HCK transcript levels were analyzed by quantitative real-time RT-PCR, and relative expression levels are presented as the base 2 antilog of the ΔC_t values relative to GAPDH. Parental TF-1 cells which do not express HCK were included as a negative control. Each cell population was analyzed in duplicate, with triplicate determinations per sample, and the mean value ± S.E. is presented.

3.4 Discussion

HCK is a promising kinase target for inhibitor development as precision therapy for AML, especially in cases where this kinase is expressed at high levels[3,4,8,9,25]. Our study focused on the pyrrolopyrimidine tyrosine kinase inhibitor A-419259, which potently inhibits HCK and shows significant promise against AML both *in vitro* and in patient-derived xenograft mouse models [8,9,26]. However, the spectrum of possible HCK mutations that have the potential to cause A-412959 resistance have not been investigated. This question is important, because acquired resistance mutations have been a significant clinical limitation of many other tyrosine kinase inhibitors developed to date, especially those that target the AML-associated receptor tyrosine kinase mutant, FLT3-ITD. Using a combinatorial PCR-based approach, we constructed a complex library of mutants in which each codon was represented at all 488 non-critical amino acid positions within the human HCK open reading frame. The mutant library was created in the background of an active form of HCK (HCK-YF) and used to transform Rat-2 fibroblasts and therefore enabled rapid selection of resistant clones. Remarkably, this approach yielded only a single confirmed resistant colony, despite over 6-fold coverage of the library during the selection phase. Subsequent DNA sequence analysis and biochemical studies in two different cellular contexts revealed that a single gatekeeper mutation, Hck-T338H, was solely responsible for the A-419259-resistant phenotype. This observation suggests that clinical use of A-419259 may be less prone to acquired resistance in AML cases dependent upon HCK, because this amino acid change appears to be the only mutational pathway to resistance and is dependent upon two nucleotide substitutions.

X-ray crystallography of near-full-length HCK bound to A-419259 shows that this compound targets the kinase active site through a Type-I, DFG-in mechanism (see Introduction).

Inhibitors in this class tend to be insensitive to allosteric effects of mutations at other sites in the kinase or regulatory domains, because the DFG-in state is associated with the active kinase conformation. Type-II inhibitors, on the other hand, achieve their specificity by stabilizing an inactive, DFG-out conformation of the active site. Resistance to Type-II inhibitors, such as imatinib for BCR-ABL in CML or quizartinib for FLT3-ITD in AML, can result from a wide variety of mutations both within and outside of the drug binding site. Allosteric loss of inhibitor binding relates to conformational changes that bias the kinase active site toward the DFG-in conformation, which is no longer capable of high-affinity inhibitor recognition due to steric clashes at the binding site[16,27]. In this way, Type-I inhibitors may display a narrower profile of mutations because of this lack of conformational dependence. In addition to A-419259, this is also true for the FLT3-ITD inhibitor crenolanib, for which an extensive screen revealed that no single amino acid change confers resistance to the inhibitor and only partial resistance can be achieved through dual mutations of both D698 and Y693[17].

The critical role for the HCK gatekeeper residue, Thr338, is also highlighted in the crystal structure of A-419259 complex. T338 forms a hydrogen bond with C4 amino group on the pyrrolopyrimdine of A-419259 and orients the piperazinyl moiety in the catalytic pocket where it makes a polar contact with the catalytic aspartate (Asp348; Figure 31A). Substitution of T338 with histidine, the sole resistance mutation isolated in the codon mutagenesis screen, is anticipated to result in steric and electrostatic clash with the ligand (modeled in Figure 31B). Importantly, substitution with histidine at the gatekeeper position did not alter HCK protein stability or kinase activity, demonstrating that this missense mutation does not impair a fitness cost in terms of kinase function.

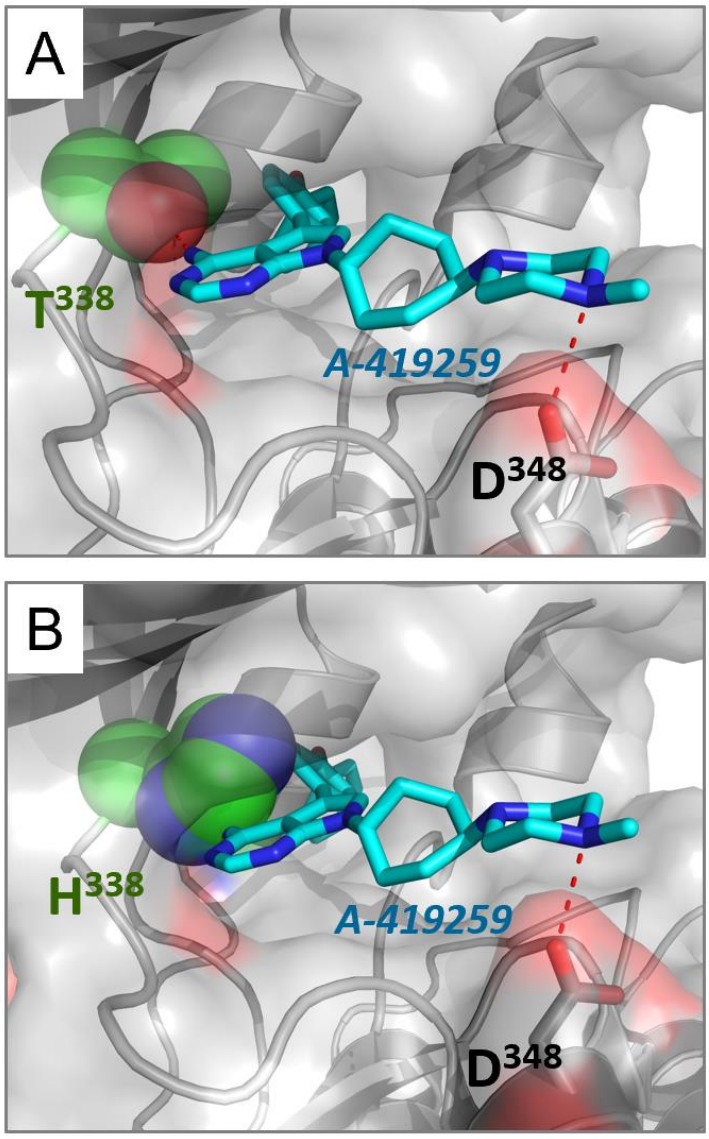

Figure 30. Molecular model of the HCK-T338H gatekeeper mutant in complex with A-419259.

A) Close-up view of the active site of HCK bound to A-419259. The side chain of the wild-type gatekeeper residue (T338), highlighted with spheres, makes a hydrogen bond with the C4 amino group of the pyrrolopyrimidine moiety in A-419259, positioning the piperidnyl group for hydrogen binding with the catalytic aspartate (D348). B) *In silico* mutagenesis of T338 to histidine removes this critical H-bond, creating electrostatic and steric clash predicted to disrupt inhibitor action.

3.5 Materials and Methods

3.5.1 Generation of HCK Codon Mutagenesis library

PCR-based codon mutagenesis was performed according to the method of Bloom[28] using primers designed with software freely available from the Bloom laboratory (https://github.com/jbloomlab/CodonTilingPrimers). First, the complete cDNA coding sequence of *HCK-YF* (Y527F tail mutant) was amplified using primers containing 5' restriction sites for subsequent subcloning into a retroviral vector for gene transfer. The *HCK-YF* PCR product was purified by agarose gel electrophoresis and used as a template in fragment PCR reactions. One fragment PCR reaction consisted of the 488 forward-facing codon mutagenesis primers and the reverse end primer. A second fragment PCR reaction was set up which consisted of the 488 reverse-facing codon mutagenesis primers and the forward end primer. The full list of overlapping codon mutagenesis primers is provided in Appendix B. The following sites were not targeted for mutagenesis because they are critical to HCK functionality: the first seven codons (required for N-terminal myristoylation and membrane anchoring), Lys295 (coordinates ATP), Glu310 (forms critical salt bridge with Lys295 when the kinase is active), Asp386 (catalytic residue), Asp404-Phe405-Glu406 ('DFG motif' involved in phosphotransfer reaction), Tyr416 (activation loop auto-phosphorylation site), and Tyr527Phe (mutation required for kinase activity and transformation of Rat-2 cells). After three cycles of fragment PCR, the two mutagenized fragments were joined in a final PCR reaction which yielded a single PCR product

of the expected molecular weight. This fragment was digested with *Eco*RI and *Sbf*I for ligation into the retroviral expression vector, pSRαMSVtkneo[29]. The ligation reaction was incubated overnight at 16° C and used to transform *E. Coli* XL10-Gold Ultracompetent cells (Agilent). The transformed cells were plated on forty x 10 cm LB/ampicillin agar plates for a total of about 100,000 discrete colonies. Twenty colonies were picked at random, and individual plasmids isolated for DNA sequence analysis. The remainder of the colonies were combined, and the library plasmid DNA was isolated for retrovirus preparation.

3.5.2 Deep sequencing of codon mutagenesis library

The HCK codon mutagenesis library, in the pSRαMSVtkneo backbone, was prepared for Illumina sequencing using reagents and PCR conditions as described elsewhere[28]. The *HCK-YF* library inserts were first amplified using the same primers used in the joining PCR step described above. Sub-amplicons were then PCR-amplified using a primer set which also added unique barcodes sequences and Illumina adapter fragments. A subsequent PCR step added the full Illumina adapter fragments, as well as a six base pair index sequence. The sequences of the primers for the sub-amplicon PCR and the Illumina adapter PCR step are shown in Table 10. Sequencing was performed on an Illumina MiSeq platform using the MiSeq reagent kit V3 600-cycle (#MS-102-3003). This kit results in 300 base pair paired-end reads. The resulting FASTQ files were analyzed using code freely available at the following website: https://github.com/jbloomlab/Perth2009-DMS-Manuscript/blob/master/analysis_code/analysis_notebook.ipynb.

Table 10. Primers used to generate samples for deep sequencing of codon mutagenesis library.

(Above) Each of 4 sub amplicons of HCK-YF is generated with a forward and reverse primer pair. Lowercase sequence binds to HCK-YF, uppercase sequence is the partial Illumina adaptor. N indicates the 8-nucleotide barcode added to the sub amplicons. (Below) The primer sequences for the addition of the Illumina adapters. Each experimental sample is associated with one of these index sequences (lowercase) for multiplexing all experimental samples to a single flowcell.

Primer	Sequence
HCK-YF.subamp1.Fwd	CTTTCCCTACACGACGCTCTTCCGATCTNNNNNNNNcgaggtcgaattcatggg
HCK-YF.subamp1.Rev	GGAGTTCAGACGTGTGCTCTTCCGATCTNNNNNNNNgctgatgcccttgaaaaacc
HCK-YF.subamp2.Fwd	CTTTCCCTACACGACGCTCTTCCGATCTNNNNNNNNctatgtcgcccgcgttgactctc
HCK-YF.subamp2.Rev	GGAGTTCAGACGTGTGCTCTTCCGATCTNNNNNNNNccaaactgcccagctccaag
HCK-YF.subamp3.Fwd	CTTTCCCTACACGACGCTCTTCCGATCTNNNNNNNNaatccctcaagctggagaag
HCK-YF.subamp3.Rev	GGAGTTCAGACGTGTGCTCTTCCGATCTNNNNNNNNcgagccgtgtactcgttgtc
HCK-YF.subamp4.Fwd	CTTTCCCTACACGACGCTCTTCCGATCTNNNNNNNNccgggtcattgaggacaacg
HCK-YF.subamp4.Rev	GGAGTTCAGACGTGTGCTCTTCCGATCTNNNNNNNNcgtagcagatctcctgcaggtcatgg

Primer	Sequence
UniversalRnd2for	AATGATACGGCGACCACCGAGATCTACACTCTTTCCCTACACGACGCTCTTCC
index01Rnd2rev	CAAGCAGAAGACGGCATACGAGATacatcgGTGACTGGAGTTCAGACGTGTGCTCTTCCGATCT
index03Rnd2rev	AAGCAGAAGACGGCATACGAGATcactgtGTGACTGGAGTTCAGACGTGTGCTCTTCCGATCT
index08Rnd2rev	CAAGCAGAAGACGGCATACGAGATgcctaaGTGACTGGAGTTCAGACGTGTGCTCTTCCGATCT
index09Rnd2rev	CAAGCAGAAGACGGCATACGAGATtcaagtGTGACTGGAGTTCAGACGTGTGCTCTTCCGATCT

3.5.3 Cell Culture

TF-1, 293T and Rat-2 cells were obtained from the American Type Culture Collection. TF-1 cells were cultured in RPMI 1640 medium supplemented with 10% fetal bovine serum (FBS), 100 units/ml of penicillin, 100 μg/ml of streptomycin sulfate, and 0.25 μg/ml of

amphotericin B (Antibiotic-Antimycotic; Gibco/ThermoFisher). TF-1 cells require recombinant human GM-CSF (1 ng/mL; ThermoFisher). The 293T and Rat-2 cell lines were cultured in Dulbecco's modified Eagle's medium (DMEM) containing 10% FBS and Antibiotic-Antimycotic.

3.5.4 Selection of resistant clones from Codon mutagenesis library

The HCK-YF codon mutagenesis library was packaged in recombinant retroviruses by co-transfecting 293T cells with the pSRαMSVtkneo library plasmids and an ecotropic packaging vector. The viral supernatant was collected daily for three days, and then filtered through an 0.22 µm filter. Undiluted viral supernatant was used to infect Rat-2 cells in the presence of 4 µg/ml Polybrene (Millipore Sigma). Infection was enhanced by low speed centrifugation (1500 x g) for 4 h at room temperature. The viral supernatant was then aspirated and replaced with fresh medium. Forty-eight hours later, infected Rat-2 cells were placed under selection with G-418 (800 µg/ml; ThermoFisher/Invitrogen) for two weeks.

To select for inhibitor-resistant colonies, Rat-2 cells transduced with the HCK mutant library were plated in culture medium containing 0.33% SeaPlaque agarose (Lonza) in the presence of 0.1, 0.3 and 1.0 µM A-419259 or the carrier solvent DMSO as control. To ensure complete coverage of the library, a total of 200,000 infected cells were plated (5,000 cells per 60 mm plate x 40 plates). Rat-2 cells expressing wild-type HCK were included as a negative control for colony formation, while cells expressing HCK-YF were included as a positive control. Cultures were incubated for two weeks at which point colony formation was observed in the HCK-YF control cultures in the absence of A-419259. Colony formation by cells expressing HCK-YF was completely suppressed in the presence of A-419259 at 1.0 µM.

Therefore, colonies from Rat-2 cells expressing the HCK-YF mutant library in the presence of 1 µM A-419259 were picked and expanded in regular 2D culture on plastic.

3.5.5 Site-directed mutagenesis

Individual HCK codon mutations were made in the mammalian expression vector pCDNA3.1 with a wild-type HCK insert, and then subcloned into pMSCVpuro. Site directed mutagenesis was performed using 10 µL 2X KOD Hot Start master mix (Millipore Sigma; cat. #71842), 20 ng template DNA, overlapping forward and reverse primers containing the desired mutation at a final concentration of 0.5 µM and water to bring the final volume to 20 µL. The resulting PCR reaction was purified from the template by the addition of 0.5 µl DpnI (New England BioLabs; #R0176) directly into the PCR reaction and subsequent incubation at 37° C for two hours. XL-10 Gold Ultracompetent *E. coli* cells were transformed with the PCR reaction and subsequent colonies were picked for plasmid isolation and subsequent confirmation of the mutations (Stratagene, cat. #200314).

3.5.6 Transfection of 293T cells

For transient expression studies, 293T cells (10^6) were seeded in 6-well plates and transfected 24 h later with X-tremeGENE 9 DNA Transfection Reagent (Millipore Sigma) and 2 µg of each pCDNA3.1-HCK expression plasmid. Transfected cells were treated with inhibitor 24 h after transfection and harvested after an additional 24 h incubation period.

3.5.7 Generation of TF-1 cell populations stably expressing FLT3-ITD and HCK

Full-length cDNA clones of each wild-type and mutant form of HCK, as well as FLT3-ITD, were subcloned into the retroviral expression vectors pMSCV-puro or pMSCV-neo, respectively (Clontech). High-titer retroviral stocks were produced in 293T cells co-transfected with each pMSCV construct and an amphotropic packaging vector as described above. TF-1 cells (10^6) were resuspended in 5.0 mL of undiluted viral supernatant and centrifuged at 1,000 × g for 4 h at 18 °C in the presence of 4 µg/mL Polybrene to enhance viral transduction. Forty-eight hours after infection, the cells began a two-week selection period with 400 µg/ml G-418 (neo vectors) or 3 µg/mL puromycin (puro vectors). Following selection, cells were maintained with 200 µg/ml G418 or 1 µg/mL puromycin. For double transduction experiments, TF-1 cells were first infected with the FLT3-ITD virus, selected with G418, followed by HCK virus and puromycin selection.

3.5.8 Immunoprecipitation and Immunoblotting

TF-1 (3 x 10^6 per 5 mL medium) or 293T cells (0.5 x 10^6 per 5 mL medium) were cultured with inhibitors or DMSO alone for 16 h. Cells were then lysed in RIPA buffer (50 mM Tris-HCl, pH 7.4, 150 mM NaCl, 1 mM EDTA, 1% Triton X-100, 0.1% SDS, 1% sodium deoxycholate) supplemented with 2.5 mM sodium orthovanadate, 25 mM sodium fluoride, and a protease inhibitor cocktail (cOmplete EDTA-Free tablets; Millipore Sigma) with sonication. Protein concentrations in the lysates were determined using Protein Assay Dye concentrate (BioRad).

HCK was immunoprecipitated using an anti-HCK antibody (Cell Signaling Technologies #14643S). Each 1.0 mL sample contained 1 mg lysate protein, 2 µg antibody, and 20 µL of protein G-Sepharose beads (Life Technologies/Invitrogen) in RIPA buffer with supplements as described above. Following overnight incubation at 4 °C, immunoprecipitates were collected by micro-centrifugation and washed twice by resuspension in 1.0 mL RIPA buffer. Precipitated proteins were separated by SDS-PAGE, transferred to nitrocellulose membranes, and probed with anti-HCK (Cell Signaling Technologies #14643S) and anti-phospho-SRC (pTyr416 clone 9A6; EMD Millipore) antibodies. Lysate blots were also probed with anti-actin antibodies (Millipore Sigma #MAB1501R). Secondary antibodies included anti-mouse or anti-rabbit IgG conjugated to 680 nM and 800 nM fluorophores, respectively (LI-COR). Blots were scanned using a LI-COR Odyssey imager, and signal intensities were quantified using the Image Studio software. Data are shown as ratios of the phosphoprotein to total protein signals and in the case of inhibitor treatment the ratios are normalized to the vehicle-treated cells. For assessment of HCK protein levels in cell lysates, HCK protein signals were normalized to actin signals.

3.5.9 RNA Isolation, cDNA preparation, and real-time quantitative RT-PCR

Total RNA was isolated from cells using the RNeasy Plus Mini Kit (Qiagen). cDNA was prepared from total RNA using the RETROscript kit (ThermoFisher/Invitrogen). Real-time quantitative RT-PCR assays were performed on total RNA using SYBR Green detection and gene-specific QuantiTect primers (Qiagen) on an Applied Biosystems StepONE Plus real-time PCR instrument. Relative HCK transcript levels were determined from the base 2 antilog of the ΔC_t values relative to GAPDH.

3.5.10 Cell viability assay

TF-1 cells were seeded at a density of 10^5 per mL in the presence or absence of inhibitors with DMSO as carrier solvent (0.1% final). Cell viability was assessed using the CellTiter-Blue reagent according to the manufacturer's instructions (Promega). Fluorescence intensity, which correlates directly with viable cell number, was measured using a SpectraMax M5 microplate reader. Each experiment included three technical replicates per condition, and each experiment was repeated at least three times.

4.0 Overall Discussion

4.1 Summary of findings and significance

4.1.1 SRC family kinases in AML pathogenesis

In my thesis research, I found that SRC-family kinases play an important role in AML pathogenesis and a more nuanced role in determining the efficacy of the tyrosine kinase inhibitor, A-419259. We found that the myeloid SRC family members HCK, LYN and FGR are the three highest expressed SRC kinases in AML patients in the TCGA cohort. FYN is also highly expressed. There are data in literature that support these findings. Dos Santos, *et al.*, found that LYN is the highest expressed SRC family member in AML patients, but HCK and FGR are also highly expressed[398]. Saito *et al.*, found that HCK is overexpressed in leukemic stem cells compared to healthy hematopoietic stem cells[400].

We then compared survival of the highest and lowest SRC family kinase-expressing AML patients in the TCGA cohort. To our surprise we found that expression of HCK, LYN and FGR strongly correlated with poor prognosis. FLT3 expression, on the other hand, did not correlate strongly with patient prognosis. If we assume that kinase expression is correlated with kinase activity, then we can conclude that SRC family kinases are viable drug targets in AML, even though they are rarely mutated. We did find from a multivariate analysis that clinical features, especially race/ethnicity and cytogenetics, were more informative predictors of patient survival. Interestingly Hck, Fgr and Lyn expression was not strongly correlated with any single

clinical feature which supports the idea that the expression of these genes is independently predicative of patient survival.

4.1.2 FLT3 and SRC family kinases in the efficacy of A-419259

From the KINOMEscan of A-419259, we found that both SRC family kinases and class III receptor tyrosine kinases bind to A-419259 strongly. We later found that A-419259 inhibits FLT3 activity *in vitro* and in cells. This agrees with a recent publication, in which it was discovered that A-419259 has activity against both FLT3 and HCK[402]. These finding questions whether the efficacy of A-419259 was due to the inhibition of FLT3 or HCK. This issue is very important because it raises questions about selective HCK inhibition as a strategy for AML treatment.

To determine which kinase was the main target of A-419259 efficacy, we generated TF-1 cells expressing FLT3-ITD containing resistance mutations and wild-type SRC-family kinases, or vice versa. We then tested the survival of these cells in the presence of A-419259 and immunoblotted for kinase activity. We found that FLT3-ITD resistance mutations conferred strong resistance phenotypes, but some of this proliferative advantage could be reversed by co-expression of SRC family kinases. These findings suggest that the specific SRC family kinases expressed in FLT3-ITD^{+} AML will tune which FLT3 mutations arise to produce resistance to A-419259. AML cells normally express HCK, LYN, FGR and FYN, suggesting that the canonical FLT3 inhibitor resistance mutations, F691L and D835Y, will not emerge against A-419259. In this way, A-419259 is superior to selective inhibitors of FLT3 such as quizartinib, where F691L, D835Y and many other mutations can confer complete resistance. The exact mechanism by which co-expression of HCK or FGR can re-sensitize cells with the resistance mutations is still

unknown. One possibility is that SRC kinase bind and/or *trans*-phosphorylate the FLT3 kinase domain, resulting in conformational changes that reduce quizartinib efficacy. Previous work from our group has shown an analogous relationship between HCK and BCR-ABL in CML, where phosphorylation of BCR-ABL by HCK on its SH3 domain and activation loop results in reduced sensitivity to imatinib[404]. It would be interesting to see if other dual SRC family and FLT3 inhibitors have the same effect.

4.1.3 De novo resistance to A-419259

Based on the resistance experiments discussed in Section 4.1.2, we might expect that complete resistance to A-419259 in FLT3-ITD$^+$ AML patients would require mutations in both FLT3-ITD and SRC-family kinases. To understand how resistance may arise *de novo*, we generated A-419259 resistant cells by long-term evolution experiments with the workhorse FLT3-ITD$^+$ cell lines MV4-11, MOLM13 and MOLM14. When we sequenced the exomes of the resistant cells we found that they all had mutations in FLT3-ITD at the same amino acid position, N676, and no mutations in SRC family members. This finding was remarkable in that six independently derived cell populations from three different cell lines all led to the same FLT3-ITD resistance mutation, despite selection with A-419259 for more than one year. This finding strongly suggests that FLT3-ITD, not HCK, LYN or FGR is the true target of A-419259 in AML cases where all of these kinases are co-expressed.

FLT3-N676S was previously described as resistance mutant against midostaurin, a type-I inhibitor. Interestingly, midostaurin also inhibits many other kinases, as it is a staurosporine analog. It is possible that this off-target activity prevents the development of resistance via F691L or D835Y mutations. The KINOMEscan data do show that midostaurin can bind to HCK,

LYN and FGR[462]. It is also not immediately obvious how mutations to N676 would confer resistance against A-419259. N676 does form a hydrogen bond network involving three other residues. This hydrogen bond network is proposed to help hold FLT3 in a downregulated conformation. Mutation of N676 would disrupt this hydrogen bond network and cause FLT3 to favor an active confirmation. This would make sense as a mechanism of resistance except A-419259 is a Type-I inhibitor and known to bind to the active conformation of HCK. We would expect that A-419259 also binds to the active conformation of FLT3, and therefore favoring an active conformation of the kinase may increase A-419259 binding. X-ray crystallography of the FLT3 kinase domain in complex with A-419259 would help to clarify this issue.

4.1.4 Resistance to the Type-I inhibitor A-419259 is limited to the gatekeeper residue

In FLT3-WT AML, HCK is still thought to be the main target of A-419259[401,402]. Therefore, it is important to understand how resistance to A-419259 may arise in HCK. We used a codon mutagenesis approach to introduce every possible codon substitution at almost every residue within HCK. From this codon mutagenesis library, A-419259 selection identified HCK-T338H as the most resistant clone from the whole library. It was reassuring to see gatekeeper mutations come through the screen as we have previously made engineered A-419259 resistance mutations at that HCK residue based on the co-crystal structure.

The fact that only one mutation, T338H, came through the screen indicates that the pathway to A-419259 resistance in HCK is very limited. This is not unexpected since A-419259 has a type-I binding mode, and therefore binds to the active confirmation of HCK. Because this active conformation is highly conserved, most other mutations in the A-419259 binding pocket would likely also disrupt kinase activity and therefore carry a significant fitness cost. This is a

desirable feature of A-419259, especially if T338H is the most resistant mutant. T338H would be highly unlikely to occur in nature since it requires mutation of all three nucleotides within the codon.

HCK-T338H is the ideal mutation to study HCK as a drug target for A-419259, but in our hands only FLT3-ITD^{+} cell lines are sensitive to this inhibitor. We need to gain a better understanding of how HCK works in AML patients before continuing to study HCK as a drug target.

4.2 Future directions

4.2.1 A-419259 efficacy in AML patients

One question that is not addressed by my project is how A-419259 works in FLT3-wildtype AML. Saito *et al*. showed this compound had strong efficacy in AML patient-derived xenograft mice[401]. In that study, the genetics of individual AML cases used to generate the mice was not reported, but the majority of the xenografts responded strongly to the compound. This implies that A-419259 is effective in the majority of AML patients regardless of FLT3 status. To study A-419259 efficacy we can profile AML primary cells based on gene expression and mutational information, then test the efficacy of A-419259. Presumably A-419259 efficacy would correlate with expression of SRC family kinases. From personal communication we know that A-419259 is highly toxic in humans, even though such toxicity does not exist in mice.

Along the lines of SRC family kinase inhibition in AML, our group recently reported that the efficacy of the small molecule kinase inhibitor TL02-59 against primary AML cells was most

strongly correlated with myeloid SRC-family kinase expression rather than FLT3 expression or mutational status[409]. To extend this work we can test the efficacy of A-419259 against a panel of AML cell lines and look for markers of A-419259 efficacy. If we were to take a broad approach we could do something similar to the cancer cell line encyclopedia[463] or BEAT AML[42], where high throughput approaches are used to correlate drug efficacy with genetic or gene expression data.

4.2.2 FLT3 mutations that lead to A-419259 resistance

A major conclusion of our work is that in FLT3-ITD$^+$ AML, FLT3-ITD appears to be the main target of A-419259, rather than SRC family kinases. In the *de novo* resistance evolution study, we found that FLT3-ITD-N676S was the most common resistance mutation, and no mutations were found in HCK, LYN or FGR. However, engineered mutations of FLT3-ITD that are associated with resistance to other inhibitors (e.g. D835Y and F691L) also produced substantial resistance to A-419259 when expressed in TF-1 myeloid cells in the absence of HCK or other SRC-family kinases. Together these findings suggest that the presence of SRC-family kinases can influence the mutational pathway to inhibitor resistance in AML. To more deeply understand which FLT3 mutations can confer resistance to A-419259, we can apply a codon mutagenesis approach in which we select for A-419259 resistant clones of FLT3-ITD. This approach could be done in TF-1 cells where FLT3-ITD transforms the cells to cytokine independence. The selection for resistance could then either be done with a soft agar assay or by bulk selection, followed by deep sequencing of FLT3-ITD in the resistant population. The experiment could be done in parallel with cell lines co-expressing either HCK or FGR to get an idea of how expression of SRC family kinases changes the pathway to resistance.

4.2.3 Resistance to A-419259 in FLT3-WT AML

To understand the mechanism of action of A-419259 in FLT3-WT AML we need to understand how drug resistance will arise. We can employ long term evolution followed by exome sequencing to study how resistance may arise in FLT3-WT AML. The main barrier to entry for this project is that none of the FLT3-WT AML cells lines we have tested show significant sensitivity to A-419259. We would have to employ some of the approaches discussed in 4.2.1 first before pursuing this idea.

4.3 Concluding remarks

AML is still one of the deadliest cancers for adults. There are many signs of progress towards effective and durable therapies, including ATRA-ATO for PML, IDH inhibitors for IDH1/2 mutant AML, and ever improving FLT3 inhibitors. Here we described the strategy of inhibiting both FLT3-ITD and SRC family kinases. This dual inhibition seems to limit some of the canonical FLT3 inhibitor resistance mutations. We also discussed a codon mutagenesis strategy in which we found the most inhibitor-resistant HCK mutations. This study revealed that resistance against this Type-I inhibitor seems to be limited to only the gatekeeper residue. There are also other potential therapeutic strategies that should be considered.

One striking phenomenon about the FLT3 inhibitor field is the lack of any effort to make an allosteric FLT3 inhibitor. We discussed during the introduction the intramolecular regulation of the FLT3 kinase domain by the juxtamembrane domain. Addition of a peptide identical to the juxtamembrane region would theoretically reduce the kinase activity of FLT3. Therefore, one

strategy to develop an allosteric FLT3 inhibitor would be to design a small molecule to replace the important contacts between the juxtamembrane domain and the kinase domain. Starting from the peptide changes can be made to increase stability, potency and bioavailability of the small molecule. Similar strategies have been employed in the past, most famously a pro-apoptotic small molecule that antagonizes the sequestration of BH3 only proteins[464]. This allosteric inhibitor could then be combined with the most potent active site inhibitors. A similar strategy for combining an active site and allosteric inhibitor was recently employed in CML. In CML, the BCR-ABL tyrosine kinase is missing a key intramolecular regulatory interaction, which can be replaced with small molecules. The latest iteration is the small allosteric inhibitor ABL001[465], which has strong efficacy on its own. When ABL001 is combined with an active site inhibitor, two mutations would be required for resistance. The likelihood of a resistance mutation within the active site and the allosteric site is nearly statistically impossible, a prediction borne out in mouse models of CML[466].

Another strategy that could be employed is attaching ubiquitin E3 ligase ligands to FLT3 inhibitors. This strategy is known as proteolysis-targeting chimeric molecules (PROTACs). This strategy has been successfully employed to target and eliminate non-enzymatic proteins, such as transcription factors[467]. Recently, a more compact system in which a small molecule inhibitor is linked to a thalidomide analog can lead to dramatic protein degradation similar to PROTACs[468]. Both concepts have been proven to work *in vivo*. These strategies can be employed to degrade protein targets of interest in AML, such as FLT3 or HCK. Along these lines, a compound such as A-419259 may represent a viable targeting moiety, because its overall kinome-wide selectivity profile is relatively narrow and includes multiple kinases linked to AML.

Appendix A Complete KINOMEscan dataset for A-419259.

KINOMEscan values represent the percent of residual target kinase interaction with the immobilized probe compound at a A-419259 test concentration of 1.0 µM relative to control wells that contain DMSO. Therefore, a value of 0% control equals 100% probe displacement while a value of 100% control equals no binding of A-419259 to the target kinase. KINOMEscan profiling was performed by DiscoverX, which is now part of Eurofins.

KINOMEscan gene symbol	% Control
AAK1	100
ABL1(E255K)-phosphorylated	0.5
ABL1(F317I)-nonphosphorylated	2.5
ABL1(F317I)-phosphorylated	2.4
ABL1(F317L)-nonphosphorylated	4.7
ABL1(F317L)-phosphorylated	0
ABL1(H396P)-nonphosphorylated	0.2
ABL1(H396P)-phosphorylated	0.65
ABL1(M351T)-phosphorylated	1.6
ABL1(Q252H)-nonphosphorylated	0.85
ABL1(Q252H)-phosphorylated	0.5
ABL1(T315I)-nonphosphorylated	41
ABL1(T315I)-phosphorylated	83
ABL1(Y253F)-phosphorylated	0.35
ABL1-nonphosphorylated	0.1
ABL1-phosphorylated	0.25
ABL2	4.9
ACVR1	100
ACVR1B	100
ACVR2A	100
ACVR2B	100
ACVRL1	100
ADCK3	100
ADCK4	100
AKT1	100
AKT2	92

AKT3	100
ALK	29
ALK(C1156Y)	21
ALK(L1196M)	68
AMPK-alpha1	43
AMPK-alpha2	42
ANKK1	73
ARK5	90
ASK1	100
ASK2	62
AURKA	36
AURKB	100
AURKC	79
AXL	6.1
BIKE	80
BLK	0.05
BMPR1A	100
BMPR1B	92
BMPR2	97
BMX	30
BRAF	66
BRAF(V600E)	45
BRK	0.2
BRSK1	14
BRSK2	10
BTK	0.1
BUB1	100

CAMK1	92
CAMK1B	100
CAMK1D	97
CAMK1G	100
CAMK2A	88
CAMK2B	100
CAMK2D	100
CAMK2G	100
CAMK4	100
CAMKK1	100
CAMKK2	100
CASK	67
CDC2L1	61
CDC2L2	91
CDC2L5	77
CDK11	3.9
CDK2	70
CDK3	99
CDK4	91
CDK4-cyclinD1	27
CDK4-cyclinD3	81
CDK5	83
CDK7	28
CDK8	28
CDK9	65
CDKL1	99
CDKL2	70
CDKL3	100
CDKL5	100
CHEK1	54
CHEK2	40
CIT	79
CLK1	100
CLK2	100
CLK3	100
CLK4	100
CSF1R	5.8
CSF1R-autoinhibited	57
CSK	2.1
CSNK1A1	20
CSNK1A1L	64
CSNK1D	8.3

CSNK1E	1.1
CSNK1G1	80
CSNK1G2	84
CSNK1G3	100
CSNK2A1	100
CSNK2A2	66
CTK	89
DAPK1	99
DAPK2	98
DAPK3	100
DCAMKL1	43
DCAMKL2	87
DCAMKL3	100
DDR1	65
DDR2	59
DLK	54
DMPK	100
DMPK2	36
DRAK1	65
DRAK2	93
DYRK1A	99
DYRK1B	21
DYRK2	100
EGFR	26
EGFR(E746-A750del)	20
EGFR(G719C)	4.8
EGFR(G719S)	41
EGFR(L747-E749del, A750P)	57
EGFR(L747-S752del, P753S)	22
EGFR(L747-T751del,Sins)	16
EGFR(L858R)	9.7
EGFR(L858R,T790M)	29
EGFR(L861Q)	6
EGFR(S752-I759del)	6.7
EGFR(T790M)	0.2
EIF2AK1	99
EPHA1	58
EPHA2	100
EPHA3	95
EPHA4	100
EPHA5	80
EPHA6	94

EPHA7	100
EPHA8	72
EPHB1	96
EPHB2	100
EPHB3	100
EPHB4	100
EPHB6	6.8
ERBB2	2.7
ERBB3	0.2
ERBB4	0
ERK1	100
ERK2	77
ERK3	100
ERK4	56
ERK5	58
ERK8	100
ERN1	82
FAK	72
FER	100
FES	100
FGFR1	1.6
FGFR2	39
FGFR3	30
FGFR3(G697C)	27
FGFR4	62
FGR	0.85
FLT1	29
FLT3	0.65
FLT3(D835H)	12
FLT3(D835V)	0.15
FLT3(D835Y)	7.6
FLT3(ITD)	2.6
FLT3(ITD,D835V)	30
FLT3(ITD,F691L)	57
FLT3(K663Q)	5.6
FLT3(N841I)	5.3
FLT3(R834Q)	2.7
FLT3-autoinhibited	3.4
FLT4	19
FRK	5.3
FYN	5.1
GAK	69

GCN2(Kin.Dom.2,S808G)	79
GRK1	100
GRK2	100
GRK3	100
GRK4	100
GRK7	62
GSK3A	100
GSK3B	95
HASPIN	70
HCK	1.9
HIPK1	80
HIPK2	100
HIPK3	91
HIPK4	63
HPK1	44
HUNK	100
ICK	97
IGF1R	80
IKK-alpha	90
IKK-beta	90
IKK-epsilon	100
INSR	63
INSRR	86
IRAK1	98
IRAK3	89
IRAK4	90
ITK	14
JAK1(JH1domain-catalytic)	99
JAK1(JH2domain-pseudokinase)	100
JAK2(JH1domain-catalytic)	100
JAK3(JH1domain-catalytic)	65
JNK1	95
JNK2	94
JNK3	99
KIT	0.15
KIT(A829P)	5.9
KIT(D816H)	40
KIT(D816V)	70
KIT(L576P)	0
KIT(V559D)	0.05
KIT(V559D,T670I)	40
KIT(V559D,V654A)	18

KIT-autoinhibited	6.9
LATS1	30
LATS2	18
LCK	2.3
LIMK1	31
LIMK2	91
LKB1	100
LOK	20
LRRK2	98
LRRK2(G2019S)	100
LTK	36
LYN	1.7
LZK	85
MAK	100
MAP3K1	92
MAP3K15	79
MAP3K2	1.7
MAP3K3	6.3
MAP3K4	92
MAP4K2	98
MAP4K3	32
MAP4K4	83
MAP4K5	9.2
MAPKAPK2	100
MAPKAPK5	100
MARK1	82
MARK2	82
MARK3	83
MARK4	97
MAST1	64
MEK1	0.1
MEK2	0.2
MEK3	91
MEK4	89
MEK5	0.25
MEK6	98
MELK	21
MERTK	12
MET	58
MET(M1250T)	59
MET(Y1235D)	100
MINK	30

MKK7	46
MKNK1	63
MKNK2	8.3
MLCK	66
MLK1	88
MLK2	29
MLK3	100
MRCKA	98
MRCKB	100
MST1	34
MST1R	96
MST2	82
MST3	80
MST4	4.9
MTOR	90
MUSK	100
MYLK	94
MYLK2	95
MYLK4	96
MYO3A	2.7
MYO3B	17
NDR1	68
NDR2	80
NEK1	100
NEK10	100
NEK11	77
NEK2	81
NEK3	92
NEK4	100
NEK5	100
NEK6	65
NEK7	91
NEK9	90
NIK	100
NIM1	100
NLK	83
OSR1	100
p38-alpha	100
p38-beta	100
p38-delta	99
p38-gamma	100
PAK1	55

PAK2	91
PAK3	36
PAK4	93
PAK6	84
PAK7	89
PCTK1	99
PCTK2	59
PCTK3	100
PDGFRA	1.1
PDGFRB	0
PDPK1	100
PFCDPK1(P.falciparum)	0
PFPK5(P.falciparum)	78
PFTAIRE2	89
PFTK1	63
PHKG1	99
PHKG2	100
PIK3C2B	10
PIK3C2G	100
PIK3CA	100
PIK3CA(C420R)	100
PIK3CA(E542K)	85
PIK3CA(E545A)	100
PIK3CA(E545K)	95
PIK3CA(H1047L)	98
PIK3CA(H1047Y)	99
PIK3CA(I800L)	98
PIK3CA(M1043I)	100
PIK3CA(Q546K)	100
PIK3CB	64
PIK3CD	100
PIK3CG	61
PIK4CB	83
PIKFYVE	78
PIM1	100
PIM2	100
PIM3	100
PIP5K1A	100
PIP5K1C	89
PIP5K2B	94
PIP5K2C	95
PKAC-alpha	100

PKAC-beta	100
PKMYT1	100
PKN1	88
PKN2	100
PKNB(M.tuberculosis)	82
PLK1	100
PLK2	77
PLK3	72
PLK4	100
PRKCD	89
PRKCE	88
PRKCH	87
PRKCI	26
PRKCQ	66
PRKD1	63
PRKD2	63
PRKD3	17
PRKG1	100
PRKG2	100
PRKR	100
PRKX	100
PRP4	98
PYK2	88
QSK	93
RAF1	40
RET	0
RET(M918T)	0.1
RET(V804L)	24
RET(V804M)	21
RIOK1	77
RIOK2	100
RIOK3	64
RIPK1	100
RIPK2	3.6
RIPK4	84
RIPK5	7.1
ROCK1	90
ROCK2	62
ROS1	100
RPS6KA4(Kin.Dom.1-N-terminal)	66
RPS6KA4(Kin.Dom.2-C-terminal)	99
RPS6KA5(Kin.Dom.1-N-terminal)	77

RPS6KA5(Kin.Dom.2-C-terminal)	96
RSK1(Kin.Dom.1-N-terminal)	8.4
RSK1(Kin.Dom.2-C-terminal)	84
RSK2(Kin.Dom.1-N-terminal)	16
RSK2(Kin.Dom.2-C-terminal)	100
RSK3(Kin.Dom.1-N-terminal)	22
RSK3(Kin.Dom.2-C-terminal)	100
RSK4(Kin.Dom.1-N-terminal)	68
RSK4(Kin.Dom.2-C-terminal)	94
S6K1	27
SBK1	96
SGK	75
SgK110	100
SGK2	90
SGK3	77
SIK	2.1
SIK2	19
SLK	100
SNARK	26
SNRK	94
SRC	0.1
SRMS	0
SRPK1	100
SRPK2	97
SRPK3	99
STK16	100
STK33	30
STK35	27
STK36	18
STK39	100
SYK	100
TAK1	77
TAOK1	100
TAOK2	85
TAOK3	100
TBK1	100
TEC	9
TESK1	95
TGFBR1	60
TGFBR2	100
TIE1	25

TIE2	15
TLK1	93
TLK2	100
TNIK	100
TNK1	0
TNK2	1.1
TNNI3K	91
TRKA	16
TRKB	29
TRKC	45
TRPM6	100
TSSK1B	100
TSSK3	95
TTK	3.5
TXK	13
TYK2(JH1domain-catalytic)	100
TYK2(JH2domain-pseudokinase)	95
TYRO3	66
ULK1	99
ULK2	47
ULK3	84
VEGFR2	24
VPS34	63
VRK2	39
WEE1	100
WEE2	90
WNK1	73
WNK2	67
WNK3	46
WNK4	39
YANK1	30
YANK2	30
YANK3	100
YES	0
YSK1	84
YSK4	58
ZAK	13
ZAP70	100

Appendix B Sequences of all primers used in Codon mutagenesis.

All primers are listed in 5' to 3' sequence. Lowercase letters are nucleotides at the very beginning and end of the sequence that were excluded from mutagenesis. N indicated random nucleotides were inserted into those positions. Primers were designed using an automated codon tiling primers software (see methods in chapter 3).

Name of Primer	Sequence
Ravi-HCK-for-mut8,	catgaagttgaagNNNCTCCAGGTCGGAGG
Ravi-HCK-for-mut9,	gaagttgaagTTCNNNCAGGTCGGAGGCAA
Ravi-HCK-for-mut10,	agttgaagTTCCTCNNNGTCGGAGGCAATAC
Ravi-HCK-for-mut11,	ttgaagTTCCTCCAGNNNGGAGGCAATACATTCT
Ravi-HCK-for-mut12,	agTTCCTCCAGGTCNNNGGCAATACATTCTC
Ravi-HCK-for-mut13,	agTTCCTCCAGGTCGGANNNAATACATTCTCAAAAAC
Ravi-HCK-for-mut14,	CCAGGTCGGAGGCNNNACATTCTCAAAAAC
Ravi-HCK-for-mut15,	CAGGTCGGAGGCAATNNNTTCTCAAAAACTGAAA
Ravi-HCK-for-mut16,	GTCGGAGGCAATACANNNTCAAAAACTGAAACCA
Ravi-HCK-for-mut17,	GGAGGCAATACATTCNNNAAAACTGAAACCAGCG
Ravi-HCK-for-mut18,	GCAATACATTCTCANNNACTGAAACCAGCGCC
Ravi-HCK-for-mut19,	AATACATTCTCAAAANNNGAAACCAGCGCCAGC
Ravi-HCK-for-mut20,	ATTCTCAAAAACTNNNACCAGCGCCAGCC
Ravi-HCK-for-mut21,	TCAAAAACTGAANNNAGCGCCAGCCCAC
Ravi-HCK-for-mut22,	AAAACTGAAACCNNNGCCAGCCCACAC
Ravi-HCK-for-mut23,	ACTGAAACCAGCNNNAGCCCACACTGT
Ravi-HCK-for-mut24,	AAACCAGCGCCNNNCCACACTGTCC
Ravi-HCK-for-mut25,	CCAGCGCCAGCNNNCACTGTCCTGT
Ravi-HCK-for-mut26,	GCGCCAGCCCANNNTGTCCTGTGTA
Ravi-HCK-for-mut27,	CCAGCCCACACNNNCCTGTGTACGT
Ravi-HCK-for-mut28,	GCCCACACTGTNNNGTGTACGTGCC
Ravi-HCK-for-mut29,	CCACACTGTCCTNNNTACGTGCCGGAT
Ravi-HCK-for-mut30,	ACTGTCCTGTGNNNGTGCCGGATCC
Ravi-HCK-for-mut31,	TGTCCTGTGTACNNNCCGGATCCCACAT
Ravi-HCK-for-mut32,	TCCTGTGTACGTGNNNGATCCCACATCCA

Ravi-HCK-for-mut33,	TGTACGTGCCGNNNCCCACATCCAC
Ravi-HCK-for-mut34,	GTACGTGCCGGATNNNACATCCACCATCAA
Ravi-HCK-for-mut35,	TGCCGGATCCCNNNTCCACCATCAAG
Ravi-HCK-for-mut36,	CGGATCCCACANNNACCATCAAGCCG
Ravi-HCK-for-mut37,	ATCCCACATCCNNNATCAAGCCGGGG
Ravi-HCK-for-mut38,	CCACATCCACCNNNAAGCCGGGGCC
Ravi-HCK-for-mut39,	ACATCCACCATCNNNCCGGGGCCTAATA
Ravi-HCK-for-mut40,	ATCCACCATCAAGNNNGGGCCTAATAGCCA
Ravi-HCK-for-mut41,	ACCATCAAGCCGNNNCCTAATAGCCACA
Ravi-HCK-for-mut42,	ATCAAGCCGGGGNNNAATAGCCACAACA
Ravi-HCK-for-mut43,	AGCCGGGGCCTNNNAGCCACAACAG
Ravi-HCK-for-mut44,	CCGGGGCCTAATNNNCACAACAGCAAC
Ravi-HCK-for-mut45,	GGGGCCTAATAGCNNNAACAGCAACACAC
Ravi-HCK-for-mut46,	GCCTAATAGCCACNNNAGCAACACACCAG
Ravi-HCK-for-mut47,	CCTAATAGCCACAACNNNAACACACCAGGAATCA
Ravi-HCK-for-mut48,	ATAGCCACAACAGCNNNACACCAGGAATCAG
Ravi-HCK-for-mut49,	CACAACAGCAACNNNCCAGGAATCAGGG
Ravi-HCK-for-mut50,	CAACAGCAACACANNNGGAATCAGGGAGG
Ravi-HCK-for-mut51,	AGCAACACACCANNNATCAGGGAGGCA
Ravi-HCK-for-mut52,	ACACACCAGGANNNAGGGAGGCAGG
Ravi-HCK-for-mut53,	CACCAGGAATCNNNGAGGCAGGCTCT
Ravi-HCK-for-mut54,	CCAGGAATCAGGNNNGCAGGCTCTGAG
Ravi-HCK-for-mut55,	GGAATCAGGGAGNNNGGCTCTGAGGACA
Ravi-HCK-for-mut56,	GAATCAGGGAGGCANNNTCTGAGGACATCATC
Ravi-HCK-for-mut57,	GGGAGGCAGGCNNNGAGGACATCATC
Ravi-HCK-for-mut58,	GAGGCAGGCTCTNNNGACATCATCGTG
Ravi-HCK-for-mut59,	GCAGGCTCTGAGNNNATCATCGTGGTTG
Ravi-HCK-for-mut60,	GCTCTGAGGACNNNATCGTGGTTGCC
Ravi-HCK-for-mut61,	TCTGAGGACATCNNNGTGGTTGCCCTG
Ravi-HCK-for-mut62,	TCTGAGGACATCATCNNNGTTGCCCTGTATGAT
Ravi-HCK-for-mut63,	GAGGACATCATCGTGNNNGCCCTGTATGATTAC
Ravi-HCK-for-mut64,	GGACATCATCGTGGTTNNNCTGTATGATTACGAGG
Ravi-HCK-for-mut65,	TCATCGTGGTTGCCNNNTATGATTACGAGGC
Ravi-HCK-for-mut66,	TGGTTGCCCTGNNNGATTACGAGGCC
Ravi-HCK-for-mut67,	GGTTGCCCTGTATNNNTACGAGGCCATTCA
Ravi-HCK-for-mut68,	TGCCCTGTATGATNNNGAGGCCATTCACC
Ravi-HCK-for-mut69,	CCCTGTATGATTACNNNGCCATTCACCACGAA
Ravi-HCK-for-mut70,	CCTGTATGATTACGAGNNNATTCACCACGAAGACC
Ravi-HCK-for-mut71,	GATTACGAGGCCNNNCACCACGAAGAC
Ravi-HCK-for-mut72,	ATTACGAGGCCATTNNNCACGAAGACCTCAG
Ravi-HCK-for-mut73,	GAGGCCATTCACNNNGAAGACCTCAGCT
Ravi-HCK-for-mut74,	GCCATTCACCACNNNGACCTCAGCTTC
Ravi-HCK-for-mut75,	CCATTCACCACGAANNNCTCAGCTTCCAGAA
Ravi-HCK-for-mut76,	TCACCACGAAGACNNNAGCTTCCAGAAGG
Ravi-HCK-for-mut77,	CACGAAGACCTCNNNTTCCAGAAGGGGG

Ravi-HCK-for-mut78,	GAAGACCTCAGCNNNCAGAAGGGGGAC
Ravi-HCK-for-mut79,	GACCTCAGCTTCNNNAAGGGGGACCAG
Ravi-HCK-for-mut80,	CTCAGCTTCCAGNNNGGGGACCAGATG
Ravi-HCK-for-mut81,	CAGCTTCCAGAAGNNNGACCAGATGGTGG
Ravi-HCK-for-mut82,	TTCCAGAAGGGGNNNCAGATGGTGGTC
Ravi-HCK-for-mut83,	CAGAAGGGGGACNNNATGGTGGTCCTAG
Ravi-HCK-for-mut84,	AAGGGGGACCAGNNNGTGGTCCTAGAG
Ravi-HCK-for-mut85,	GGGGGACCAGATGNNNGTCCTAGAGGAATC
Ravi-HCK-for-mut86,	GGACCAGATGGTGNNNCTAGAGGAATCCG
Ravi-HCK-for-mut87,	CAGATGGTGGTCNNNGAGGAATCCGGG
Ravi-HCK-for-mut88,	GATGGTGGTCCTANNNGAATCCGGGGAGT
Ravi-HCK-for-mut89,	TGGTCCTAGAGNNNTCCGGGGAGTGG
Ravi-HCK-for-mut90,	GTCCTAGAGGAANNNGGGGAGTGGTGGA
Ravi-HCK-for-mut91,	CCTAGAGGAATCCNNNGAGTGGTGGAAGG
Ravi-HCK-for-mut92,	AGGAATCCGGGNNNTGGTGGAAGGC
Ravi-HCK-for-mut93,	AATCCGGGGAGNNNTGGAAGGCTCG
Ravi-HCK-for-mut94,	CCGGGGAGTGGNNNAAGGCTCGATC
Ravi-HCK-for-mut95,	GGGAGTGGTGGNNNGCTCGATCCCT
Ravi-HCK-for-mut96,	AGTGGTGGAAGNNNCGATCCCTGGC
Ravi-HCK-for-mut97,	GGTGGAAGGCTNNNTCCCTGGCCAC
Ravi-HCK-for-mut98,	GGAAGGCTCGANNNCTGGCCACCCG
Ravi-HCK-for-mut99,	AGGCTCGATCCNNNGCCACCCGGAA
Ravi-HCK-for-mut100,	CTCGATCCCTGNNNACCCGGAAGGAG
Ravi-HCK-for-mut101,	GATCCCTGGCCNNNCGGAAGGAGGG
Ravi-HCK-for-mut102,	CCCTGGCCACCNNNAAGGAGGGCTA
Ravi-HCK-for-mut103,	TGGCCACCCGGNNNGAGGGCTACAT
Ravi-HCK-for-mut104,	CCACCCGGAAGNNNGGCTACATCCC
Ravi-HCK-for-mut105,	ACCCGGAAGGAGNNNTACATCCCAAGC
Ravi-HCK-for-mut106,	GGAAGGAGGGCNNNATCCCAAGCAAC
Ravi-HCK-for-mut107,	GAAGGAGGGCTACNNNCCAAGCAACTATGT
Ravi-HCK-for-mut108,	GGAGGGCTACATCNNNAGCAACTATGTCG
Ravi-HCK-for-mut109,	GGCTACATCCCANNNAACTATGTCGCCC
Ravi-HCK-for-mut110,	TACATCCCAAGCNNNTATGTCGCCCGC
Ravi-HCK-for-mut111,	TCCCAAGCAACNNNGTCGCCCGCGT
Ravi-HCK-for-mut112,	CAAGCAACTATNNNGCCCGCGTTGAC
Ravi-HCK-for-mut113,	CAAGCAACTATGTCNNNCGCGTTGACTCTCT
Ravi-HCK-for-mut114,	CAACTATGTCGCCNNNGTTGACTCTCTGGA
Ravi-HCK-for-mut115,	ATGTCGCCCGCNNNGACTCTCTGGA
Ravi-HCK-for-mut116,	TCGCCCGCGTTNNNTCTCTGGAGAC
Ravi-HCK-for-mut117,	CCCGCGTTGACNNNCTGGAGACAGA
Ravi-HCK-for-mut118,	CGCGTTGACTCTNNNGAGACAGAGGAGT
Ravi-HCK-for-mut119,	CGTTGACTCTCTGNNNACAGAGGAGTGGTT
Ravi-HCK-for-mut120,	GTTGACTCTCTGGAGNNNGAGGAGTGGTTTTTC
Ravi-HCK-for-mut121,	GACTCTCTGGAGACANNNGAGTGGTTTTTCAAGG
Ravi-HCK-for-mut122,	CTCTGGAGACAGAGNNNTGGTTTTTCAAGGGC

Ravi-HCK-for-mut123,	CTGGAGACAGAGGAGNNNTTTTTCAAGGGCATC
Ravi-HCK-for-mut124,	GACAGAGGAGTGGNNNTTCAAGGGCATCAG
Ravi-HCK-for-mut125,	AGAGGAGTGGTTTNNNAAGGGCATCAGCC
Ravi-HCK-for-mut126,	GAGTGGTTTTTCNNNGGCATCAGCCGG
Ravi-HCK-for-mut127,	AGTGGTTTTTCAAGNNNATCAGCCGGAAGGAC
Ravi-HCK-for-mut128,	TTTTTCAAGGGCNNNAGCCGGAAGGAC
Ravi-HCK-for-mut129,	TCAAGGGCATCNNNCGGAAGGACGC
Ravi-HCK-for-mut130,	AGGGCATCAGCNNNAAGGACGCAGA
Ravi-HCK-for-mut131,	GCATCAGCCGGNNNGACGCAGAGCG
Ravi-HCK-for-mut132,	TCAGCCGGAAGNNNGCAGAGCGCCA
Ravi-HCK-for-mut133,	GCCGGAAGGACNNNGAGCGCCAACT
Ravi-HCK-for-mut134,	GGAAGGACGCANNNCGCCAACTGCT
Ravi-HCK-for-mut135,	AGGACGCAGAGNNNCAACTGCTGGC
Ravi-HCK-for-mut136,	ACGCAGAGCGCNNNCTGCTGGCTCC
Ravi-HCK-for-mut137,	CAGAGCGCCAANNNCTGGCTCCCGG
Ravi-HCK-for-mut138,	AGCGCCAACTGNNNGCTCCCGGCAA
Ravi-HCK-for-mut139,	GCCAACTGCTGNNNCCCGGCAACAT
Ravi-HCK-for-mut140,	AACTGCTGGCTNNNGGCAACATGCTG
Ravi-HCK-for-mut141,	TGCTGGCTCCCNNNAACATGCTGGG
Ravi-HCK-for-mut142,	TGGCTCCCGGCNNNATGCTGGGCTC
Ravi-HCK-for-mut143,	CTCCCGGCAACNNNCTGGGCTCCTT
Ravi-HCK-for-mut144,	CCGGCAACATGNNNGGCTCCTTCATG
Ravi-HCK-for-mut145,	CGGCAACATGCTGNNNTCCTTCATGATCC
Ravi-HCK-for-mut146,	AACATGCTGGGCNNNTTCATGATCCGG
Ravi-HCK-for-mut147,	TGCTGGGCTCCNNNATGATCCGGGA
Ravi-HCK-for-mut148,	CTGGGCTCCTTCNNNATCCGGGATAGC
Ravi-HCK-for-mut149,	GCTCCTTCATGNNNCGGGATAGCGAG
Ravi-HCK-for-mut150,	GCTCCTTCATGATCNNNGATAGCGAGACCAC
Ravi-HCK-for-mut151,	CTTCATGATCCGGNNNAGCGAGACCACTAA
Ravi-HCK-for-mut152,	TTCATGATCCGGGATNNNGAGACCACTAAAGGAA
Ravi-HCK-for-mut153,	TGATCCGGGATAGCNNNACCACTAAAGGAAG
Ravi-HCK-for-mut154,	ATCCGGGATAGCGAGNNNACTAAAGGAAGCTAC
Ravi-HCK-for-mut155,	GGGATAGCGAGACCNNNAAAGGAAGCTACTCT
Ravi-HCK-for-mut156,	GATAGCGAGACCACTNNNGGAAGCTACTCTTTG
Ravi-HCK-for-mut157,	AGCGAGACCACTAAANNNAGCTACTCTTTGTCC
Ravi-HCK-for-mut158,	GAGACCACTAAAGGANNNTACTCTTTGTCCGTGC
Ravi-HCK-for-mut159,	CACTAAAGGAAGCNNNTCTTTGTCCGTGCG
Ravi-HCK-for-mut160,	CTAAAGGAAGCTACNNNTTGTCCGTGCGAGAC
Ravi-HCK-for-mut161,	AAGGAAGCTACTCTNNNTCCGTGCGAGACTA
Ravi-HCK-for-mut162,	GAAGCTACTCTTTGNNNGTGCGAGACTACGAC
Ravi-HCK-for-mut163,	CTACTCTTTGTCCNNNCGAGACTACGACCC
Ravi-HCK-for-mut164,	CTCTTTGTCCGTGNNNGACTACGACCCTC
Ravi-HCK-for-mut165,	TGTCCGTGCGANNNTACGACCCTCG
Ravi-HCK-for-mut166,	CCGTGCGAGACNNNGACCCTCGGCA
Ravi-HCK-for-mut167,	TGCGAGACTACNNNCCTCGGCAGGG

Ravi-HCK-for-mut168,	CGAGACTACGACNNNCGGCAGGGAGATA
Ravi-HCK-for-mut169,	AGACTACGACCCTNNNCAGGGAGATACCG
Ravi-HCK-for-mut170,	TACGACCCTCGGNNNGGAGATACCGTG
Ravi-HCK-for-mut171,	GACCCTCGGCAGNNNGATACCGTGAAA
Ravi-HCK-for-mut172,	CTCGGCAGGGANNNACCGTGAAACAT
Ravi-HCK-for-mut173,	CTCGGCAGGGAGATNNNGTGAAACATTACAAG
Ravi-HCK-for-mut174,	CGGCAGGGAGATACCNNNAAACATTACAAGATCC
Ravi-HCK-for-mut175,	AGGGAGATACCGTGNNNCATTACAAGATCCG
Ravi-HCK-for-mut176,	GGAGATACCGTGAAANNNTACAAGATCCGGACC
Ravi-HCK-for-mut177,	GATACCGTGAAACATNNNAAGATCCGGACCCTG
Ravi-HCK-for-mut178,	CGTGAAACATTACNNNATCCGGACCCTGGA
Ravi-HCK-for-mut179,	TGAAACATTACAAGNNNCGGACCCTGGACAA
Ravi-HCK-for-mut180,	AAACATTACAAGATCNNNACCCTGGACAACGGG
Ravi-HCK-for-mut181,	TACAAGATCCGGNNNCTGGACAACGGG
Ravi-HCK-for-mut182,	AGATCCGGACCNNNGACAACGGGGG
Ravi-HCK-for-mut183,	TCCGGACCCTGNNNAACGGGGGCTT
Ravi-HCK-for-mut184,	GGACCCTGGACNNNGGGGGCTTCTA
Ravi-HCK-for-mut185,	GGACCCTGGACAACNNNGGCTTCTACATATC
Ravi-HCK-for-mut186,	CCTGGACAACGGGNNNTTCTACATATCCCC
Ravi-HCK-for-mut187,	GACAACGGGGGCNNNTACATATCCCCC
Ravi-HCK-for-mut188,	ACGGGGGCTTCNNNATATCCCCCCG
Ravi-HCK-for-mut189,	GGGGCTTCTACNNNTCCCCCCGAAG
Ravi-HCK-for-mut190,	GGCTTCTACATANNNCCCCGAAGCACCT
Ravi-HCK-for-mut191,	GCTTCTACATATCCNNNCGAAGCACCTTCAG
Ravi-HCK-for-mut192,	CTACATATCCCCCNNNAGCACCTTCAGCAC
Ravi-HCK-for-mut193,	CATATCCCCCCGANNNACCTTCAGCACTC
Ravi-HCK-for-mut194,	CCCCCCGAAGCNNNTTCAGCACTCT
Ravi-HCK-for-mut195,	CCCGAAGCACCNNNAGCACTCTGCA
Ravi-HCK-for-mut196,	CGAAGCACCTTCNNNACTCTGCAGGAG
Ravi-HCK-for-mut197,	GCACCTTCAGCNNNCTGCAGGAGCT
Ravi-HCK-for-mut198,	ACCTTCAGCACTNNNCAGGAGCTGGTG
Ravi-HCK-for-mut199,	TTCAGCACTCTGNNNGAGCTGGTGGAC
Ravi-HCK-for-mut200,	GCACTCTGCAGNNNCTGGTGGACCA
Ravi-HCK-for-mut201,	ACTCTGCAGGAGNNNGTGGACCACTACA
Ravi-HCK-for-mut202,	TCTGCAGGAGCTGNNNGACCACTACAAGA
Ravi-HCK-for-mut203,	CAGGAGCTGGTGNNNCACTACAAGAAGG
Ravi-HCK-for-mut204,	GAGCTGGTGGACNNNTACAAGAAGGGGA
Ravi-HCK-for-mut205,	CTGGTGGACCACNNNAAGAAGGGGAAC
Ravi-HCK-for-mut206,	GTGGACCACTACNNNAAGGGGAACGACG
Ravi-HCK-for-mut207,	GACCACTACAAGNNNGGGAACGACGGG
Ravi-HCK-for-mut208,	CCACTACAAGAAGNNNAACGACGGGCTCTG
Ravi-HCK-for-mut209,	ACAAGAAGGGGNNNGACGGGCTCTG
Ravi-HCK-for-mut210,	AGAAGGGGAACNNNGGGCTCTGCCA
Ravi-HCK-for-mut211,	AAGGGGAACGACNNNCTCTGCCAGAAAC
Ravi-HCK-for-mut212,	GGAACGACGGGNNNTGCCAGAAACTG

Ravi-HCK-for-mut213,	ACGACGGGCTCNNNCAGAAACTGTC
Ravi-HCK-for-mut214,	ACGGGCTCTGCNNNAAACTGTCGGT
Ravi-HCK-for-mut215,	GGCTCTGCCAGNNNCTGTCGGTGCC
Ravi-HCK-for-mut216,	TCTGCCAGAAANNNTCGGTGCCCTG
Ravi-HCK-for-mut217,	GCCAGAAACTGNNNGTGCCCTGCATG
Ravi-HCK-for-mut218,	CAGAAACTGTCGNNNCCCTGCATGTCTT
Ravi-HCK-for-mut219,	AGAAACTGTCGGTGNNNTGCATGTCTTCCAA
Ravi-HCK-for-mut220,	CTGTCGGTGCCCNNNATGTCTTCCAAG
Ravi-HCK-for-mut221,	CGGTGCCCTGCNNNTCTTCCAAGCC
Ravi-HCK-for-mut222,	TGCCCTGCATGNNNTCCAAGCCCCA
Ravi-HCK-for-mut223,	CCCTGCATGTCTNNNAAGCCCCAGAAG
Ravi-HCK-for-mut224,	GCATGTCTTCCNNNCCCCAGAAGCCT
Ravi-HCK-for-mut225,	CATGTCTTCCAAGNNNCAGAAGCCTTGGGA
Ravi-HCK-for-mut226,	TCTTCCAAGCCCNNNAAGCCTTGGGAG
Ravi-HCK-for-mut227,	CCAAGCCCCAGNNNCCTTGGGAGAAA
Ravi-HCK-for-mut228,	CAAGCCCCAGAAGNNNTGGGAGAAAGATG
Ravi-HCK-for-mut229,	CCCCAGAAGCCTNNNGAGAAAGATGCCT
Ravi-HCK-for-mut230,	CAGAAGCCTTGGNNNAAAGATGCCTGGG
Ravi-HCK-for-mut231,	AGCCTTGGGAGNNNGATGCCTGGGA
Ravi-HCK-for-mut232,	CCTTGGGAGAAANNNGCCTGGGAGATCC
Ravi-HCK-for-mut233,	CTTGGGAGAAAGATNNNTGGGAGATCCCTCG
Ravi-HCK-for-mut234,	GAGAAAGATGCCNNNGAGATCCCTCGGG
Ravi-HCK-for-mut235,	GAAAGATGCCTGGNNNATCCCTCGGGAATC
Ravi-HCK-for-mut236,	ATGCCTGGGAGNNNCCTCGGGAATC
Ravi-HCK-for-mut237,	CCTGGGAGATCNNNCGGGAATCCCTC
Ravi-HCK-for-mut238,	CTGGGAGATCCCTNNNGAATCCCTCAAGCT
Ravi-HCK-for-mut239,	GAGATCCCTCGGNNNTCCCTCAAGCTG
Ravi-HCK-for-mut240,	ATCCCTCGGGAANNNCTCAAGCTGGAGA
Ravi-HCK-for-mut241,	CCTCGGGAATCCNNNAAGCTGGAGAAGA
Ravi-HCK-for-mut242,	CTCGGGAATCCCTCNNNCTGGAGAAGAAACT
Ravi-HCK-for-mut243,	GGGAATCCCTCAAGNNNGAGAAGAAACTTGGA
Ravi-HCK-for-mut244,	GAATCCCTCAAGCTGNNNAAGAAACTTGGAGCT
Ravi-HCK-for-mut245,	CCTCAAGCTGGAGNNNAAACTTGGAGCTG
Ravi-HCK-for-mut246,	AAGCTGGAGAAGNNNCTTGGAGCTGGG
Ravi-HCK-for-mut247,	CTGGAGAAGAAANNNGGAGCTGGGCAGT
Ravi-HCK-for-mut248,	GGAGAAGAAACTTNNNGCTGGGCAGTTTGG
Ravi-HCK-for-mut249,	GAAGAAACTTGGANNNGGGCAGTTTGGGGA
Ravi-HCK-for-mut250,	AAGAAACTTGGAGCTNNNCAGTTTGGGGAAGTC
Ravi-HCK-for-mut251,	CTTGGAGCTGGGNNNTTTGGGGAAGTCT
Ravi-HCK-for-mut252,	GAGCTGGGCAGNNNGGGGAAGTCTG
Ravi-HCK-for-mut253,	AGCTGGGCAGTTTNNNGAAGTCTGGATGG
Ravi-HCK-for-mut254,	GGCAGTTTGGGNNNGTCTGGATGGC
Ravi-HCK-for-mut255,	CAGTTTGGGGAANNNTGGATGGCCACCT
Ravi-HCK-for-mut256,	GTTTGGGGAAGTCNNNATGGCCACCTACAA
Ravi-HCK-for-mut257,	GGGGAAGTCTGGNNNGCCACCTACAAC

Ravi-HCK-for-mut258,	GGGAAGTCTGGATGNNNACCTACAACAAGCAC
Ravi-HCK-for-mut259,	AGTCTGGATGGCCNNNTACAACAAGCACAC
Ravi-HCK-for-mut260,	GGATGGCCACCNNNAACAAGCACACC
Ravi-HCK-for-mut261,	ATGGCCACCTACNNNAAGCACACCAAG
Ravi-HCK-for-mut262,	GCCACCTACAACNNNCACACCAAGGTG
Ravi-HCK-for-mut263,	CACCTACAACAAGNNNACCAAGGTGGCAGT
Ravi-HCK-for-mut264,	CTACAACAAGCACNNNAAGGTGGCAGTGAA
Ravi-HCK-for-mut265,	AACAAGCACACCNNNGTGGCAGTGAAG
Ravi-HCK-for-mut266,	AAGCACACCAAGNNNGCAGTGAAGACGA
Ravi-HCK-for-mut267,	CACACCAAGGTGNNNGTGAAGACGATGA
Ravi-HCK-for-mut268,	CACCAAGGTGGCANNNAAGACGATGAAGC
Ravi-HCK-for-mut270,	GTGGCAGTGAAGNNNATGAAGCCAGGGA
Ravi-HCK-for-mut271,	CAGTGAAGACGNNNAAGCCAGGGAGC
Ravi-HCK-for-mut272,	GTGAAGACGATGNNNCCAGGGAGCATG
Ravi-HCK-for-mut273,	AAGACGATGAAGNNNGGGAGCATGTCGG
Ravi-HCK-for-mut274,	ACGATGAAGCCANNNAGCATGTCGGTG
Ravi-HCK-for-mut275,	ATGAAGCCAGGGNNNATGTCGGTGGAG
Ravi-HCK-for-mut276,	AGCCAGGGAGCNNNTCGGTGGAGGC
Ravi-HCK-for-mut277,	CAGGGAGCATGNNNGTGGAGGCCTT
Ravi-HCK-for-mut278,	GGAGCATGTCGNNNGAGGCCTTCCT
Ravi-HCK-for-mut279,	GCATGTCGGTGNNNGCCTTCCTGGC
Ravi-HCK-for-mut280,	ATGTCGGTGGAGNNNTTCCTGGCAGAG
Ravi-HCK-for-mut281,	CGGTGGAGGCCNNNCTGGCAGAGGC
Ravi-HCK-for-mut282,	TGGAGGCCTTCNNNGCAGAGGCCAA
Ravi-HCK-for-mut283,	AGGCCTTCCTGNNNGAGGCCAACGT
Ravi-HCK-for-mut285,	CCTTCCTGGCAGAGNNNAACGTGATGAAAACT
Ravi-HCK-for-mut286,	CTGGCAGAGGCCNNNGTGATGAAAACTC
Ravi-HCK-for-mut287,	GGCAGAGGCCAACNNNATGAAAACTCTGC
Ravi-HCK-for-mut288,	GAGGCCAACGTGNNNAAAACTCTGCAGC
Ravi-HCK-for-mut289,	GCCAACGTGATGNNNACTCTGCAGCATG
Ravi-HCK-for-mut290,	CCAACGTGATGAAANNNCTGCAGCATGACAA
Ravi-HCK-for-mut291,	AACGTGATGAAAACTNNNCAGCATGACAAGCTG
Ravi-HCK-for-mut292,	GTGATGAAAACTCTGNNNCATGACAAGCTGGTC
Ravi-HCK-for-mut293,	ATGAAAACTCTGCAGNNNGACAAGCTGGTCAAA
Ravi-HCK-for-mut294,	GAAAACTCTGCAGCATNNNAAGCTGGTCAAACTTC
Ravi-HCK-for-mut295,	TCTGCAGCATGACNNNCTGGTCAAACTTCA
Ravi-HCK-for-mut296,	TGCAGCATGACAAGNNNGTCAAACTTCATGC
Ravi-HCK-for-mut297,	GCATGACAAGCTGNNNAAACTTCATGCGGT
Ravi-HCK-for-mut298,	GACAAGCTGGTCNNNCTTCATGCGGTG
Ravi-HCK-for-mut299,	AAGCTGGTCAAANNNCATGCGGTGGTC
Ravi-HCK-for-mut300,	CTGGTCAAACTTNNNGCGGTGGTCACC
Ravi-HCK-for-mut301,	TGGTCAAACTTCATNNNGTGGTCACCAAGGAG
Ravi-HCK-for-mut302,	CAAACTTCATGCGNNNGTCACCAAGGAGC
Ravi-HCK-for-mut303,	TTCATGCGGTGNNNACCAAGGAGCC
Ravi-HCK-for-mut304,	ATGCGGTGGTCNNNAAGGAGCCCAT

Ravi-HCK-for-mut305,	CGGTGGTCACCNNNGAGCCCATCTAC
Ravi-HCK-for-mut306,	GGTGGTCACCAAGNNNCCCATCTACATCAT
Ravi-HCK-for-mut307,	GTGGTCACCAAGGAGNNNATCTACATCATCACG
Ravi-HCK-for-mut308,	CACCAAGGAGCCCNNNTACATCATCACGG
Ravi-HCK-for-mut309,	CAAGGAGCCCATCNNNATCATCACGGAGTT
Ravi-HCK-for-mut310,	AGGAGCCCATCTACNNNATCACGGAGTTCAT
Ravi-HCK-for-mut311,	GCCCATCTACATCNNNACGGAGTTCATGG
Ravi-HCK-for-mut312,	CCCATCTACATCATCNNNGAGTTCATGGCCAAAG
Ravi-HCK-for-mut313,	CATCTACATCATCACGNNNTTCATGGCCAAAGGAA
Ravi-HCK-for-mut314,	ACATCATCACGGAGNNNATGGCCAAAGGAAG
Ravi-HCK-for-mut315,	ATCACGGAGTTCNNNGCCAAAGGAAGCT
Ravi-HCK-for-mut316,	TCACGGAGTTCATGNNNAAAGGAAGCTTGCT
Ravi-HCK-for-mut317,	GAGTTCATGGCCNNNGGAAGCTTGCTG
Ravi-HCK-for-mut318,	GTTCATGGCCAAANNNAGCTTGCTGGACTT
Ravi-HCK-for-mut319,	TCATGGCCAAAGGANNNTTGCTGGACTTTCT
Ravi-HCK-for-mut320,	GGCCAAAGGAAGCNNNCTGGACTTTCTGA
Ravi-HCK-for-mut321,	GCCAAAGGAAGCTTGNNNGACTTTCTGAAAAGTG
Ravi-HCK-for-mut322,	CAAAGGAAGCTTGCTGNNNTTTCTGAAAAGTGATGA
Ravi-HCK-for-mut323,	GAAGCTTGCTGGACNNNCTGAAAAGTGATGAG
Ravi-HCK-for-mut324,	GCTTGCTGGACTTTNNNAAAAGTGATGAGGGC
Ravi-HCK-for-mut325,	GCTGGACTTTCTGNNNAGTGATGAGGGCAG
Ravi-HCK-for-mut326,	TGGACTTTCTGAAANNNGATGAGGGCAGCAAG
Ravi-HCK-for-mut327,	CTTTCTGAAAAGTNNNGAGGGCAGCAAGCA
Ravi-HCK-for-mut328,	TCTGAAAAGTGATNNNGGCAGCAAGCAGC
Ravi-HCK-for-mut329,	CTGAAAAGTGATGAGNNNAGCAAGCAGCCATTG
Ravi-HCK-for-mut330,	AGTGATGAGGGCNNNAAGCAGCCATTG
Ravi-HCK-for-mut331,	ATGAGGGCAGCNNNCAGCCATTGCC
Ravi-HCK-for-mut332,	GAGGGCAGCAAGNNNCCATTGCCAAAA
Ravi-HCK-for-mut333,	GGCAGCAAGCAGNNNTTGCCAAAACTC
Ravi-HCK-for-mut334,	CAGCAAGCAGCCANNNCCAAAACTCATTGA
Ravi-HCK-for-mut335,	AGCAAGCAGCCATTGNNNAAACTCATTGACTTC
Ravi-HCK-for-mut336,	GCAGCCATTGCCANNNCTCATTGACTTCTC
Ravi-HCK-for-mut337,	AGCCATTGCCAAAANNNATTGACTTCTCAGCC
Ravi-HCK-for-mut338,	ATTGCCAAAACTCNNNGACTTCTCAGCCCA
Ravi-HCK-for-mut339,	ATTGCCAAAACTCATTNNNTTCTCAGCCCAGATTG
Ravi-HCK-for-mut340,	CAAAACTCATTGACNNNTCAGCCCAGATTGCA
Ravi-HCK-for-mut341,	AAACTCATTGACTTCNNNGCCCAGATTGCAGAA
Ravi-HCK-for-mut342,	CTCATTGACTTCTCANNNCAGATTGCAGAAGGCA
Ravi-HCK-for-mut343,	TTGACTTCTCAGCCNNNATTGCAGAAGGCAT
Ravi-HCK-for-mut344,	TTCTCAGCCCAGNNNGCAGAAGGCATG
Ravi-HCK-for-mut345,	CAGCCCAGATTNNNGAAGGCATGGCC
Ravi-HCK-for-mut346,	CCCAGATTGCANNNGGCATGGCCTTC
Ravi-HCK-for-mut347,	CCAGATTGCAGAANNNATGGCCTTCATCGA
Ravi-HCK-for-mut348,	ATTGCAGAAGGCNNNGCCTTCATCGAG
Ravi-HCK-for-mut349,	TGCAGAAGGCATGNNNTTCATCGAGCAGA

Ravi-HCK-for-mut350,	AAGGCATGGCCNNNATCGAGCAGAG
Ravi-HCK-for-mut351,	GCATGGCCTTCNNNGAGCAGAGGAAC
Ravi-HCK-for-mut352,	GCATGGCCTTCATCNNNCAGAGGAACTACATC
Ravi-HCK-for-mut353,	TGGCCTTCATCGAGNNNAGGAACTACATCCA
Ravi-HCK-for-mut354,	CCTTCATCGAGCAGNNNAACTACATCCACCG
Ravi-HCK-for-mut355,	CATCGAGCAGAGGNNNTACATCCACCGAG
Ravi-HCK-for-mut356,	GAGCAGAGGAACNNNATCCACCGAGACC
Ravi-HCK-for-mut357,	CAGAGGAACTACNNNCACCGAGACCTCC
Ravi-HCK-for-mut358,	GAGGAACTACATCNNNCGAGACCTCCGAG
Ravi-HCK-for-mut359,	GAACTACATCCACNNNGACCTCCGAGCTG
Ravi-HCK-for-mut361,	TCCACCGAGACNNNCGAGCTGCCAA
Ravi-HCK-for-mut362,	ACCGAGACCTCNNNGCTGCCAACAT
Ravi-HCK-for-mut363,	CGAGACCTCCGANNNGCCAACATCTTG
Ravi-HCK-for-mut364,	GAGACCTCCGAGCTNNNAACATCTTGGTCTCT
Ravi-HCK-for-mut365,	CTCCGAGCTGCCNNNATCTTGGTCTCTG
Ravi-HCK-for-mut366,	GAGCTGCCAACNNNTTGGTCTCTGCA
Ravi-HCK-for-mut367,	GCTGCCAACATCNNNGTCTCTGCATCC
Ravi-HCK-for-mut368,	GCCAACATCTTGNNNTCTGCATCCCTGG
Ravi-HCK-for-mut369,	AACATCTTGGTCNNNGCATCCCTGGTGT
Ravi-HCK-for-mut370,	AACATCTTGGTCTCTNNNTCCCTGGTGTGTAAGA
Ravi-HCK-for-mut371,	ATCTTGGTCTCTGCANNNCTGGTGTGTAAGATTG
Ravi-HCK-for-mut372,	TGGTCTCTGCATCCNNNGTGTGTAAGATTGC
Ravi-HCK-for-mut373,	GTCTCTGCATCCCTGNNNTGTAAGATTGCTGAC
Ravi-HCK-for-mut374,	CTGCATCCCTGGTGNNNAAGATTGCTGACTT
Ravi-HCK-for-mut375,	CATCCCTGGTGTGTNNNATTGCTGACTTTGG
Ravi-HCK-for-mut376,	CTGGTGTGTAAGNNNGCTGACTTTGGCC
Ravi-HCK-for-mut377,	GGTGTGTAAGATTNNNGACTTTGGCCTGGC
Ravi-HCK-for-mut381,	CTGACTTTGGCNNNGCCCGGGTCAT
Ravi-HCK-for-mut382,	GACTTTGGCCTGNNNCGGGTCATTGAG
Ravi-HCK-for-mut383,	TTGGCCTGGCCNNNGTCATTGAGGA
Ravi-HCK-for-mut384,	GCCTGGCCCGGNNNATTGAGGACAA
Ravi-HCK-for-mut385,	TGGCCCGGGTCNNNGAGGACAACGA
Ravi-HCK-for-mut386,	GCCCGGGTCATTNNNGACAACGAGTACA
Ravi-HCK-for-mut387,	CGGGTCATTGAGNNNAACGAGTACACGG
Ravi-HCK-for-mut388,	GGTCATTGAGGACNNNGAGTACACGGCTC
Ravi-HCK-for-mut389,	ATTGAGGACAACNNNTACACGGCTCGGG
Ravi-HCK-for-mut391,	ACAACGAGTACNNNGCTCGGGAAGGG
Ravi-HCK-for-mut392,	ACGAGTACACGNNNCGGGAAGGGGC
Ravi-HCK-for-mut393,	AGTACACGGCTNNNGAAGGGGCCAAG
Ravi-HCK-for-mut394,	ACACGGCTCGGNNNGGGGCCAAGTT
Ravi-HCK-for-mut395,	CGGCTCGGGAANNNGCCAAGTTCCC
Ravi-HCK-for-mut396,	GCTCGGGAAGGGNNNAAGTTCCCCATC
Ravi-HCK-for-mut397,	GGGAAGGGGCCNNNTTCCCCATCAAG
Ravi-HCK-for-mut398,	AAGGGGCCAAGNNNCCCATCAAGTG
Ravi-HCK-for-mut399,	AGGGGCCAAGTTCNNNATCAAGTGGACAG

Ravi-HCK-for-mut400,	CCAAGTTCCCCNNNAAGTGGACAGCT
Ravi-HCK-for-mut401,	CAAGTTCCCCATCNNNTGGACAGCTCCTG
Ravi-HCK-for-mut402,	GTTCCCCATCAAGNNNACAGCTCCTGAAG
Ravi-HCK-for-mut403,	CCATCAAGTGGNNNGCTCCTGAAGCC
Ravi-HCK-for-mut404,	CCATCAAGTGGACANNNCCTGAAGCCATCAA
Ravi-HCK-for-mut405,	ATCAAGTGGACAGCTNNNGAAGCCATCAACTTT
Ravi-HCK-for-mut406,	GTGGACAGCTCCTNNNGCCATCAACTTTG
Ravi-HCK-for-mut407,	GGACAGCTCCTGAANNNATCAACTTTGGCTC
Ravi-HCK-for-mut408,	GCTCCTGAAGCCNNNAACTTTGGCTCC
Ravi-HCK-for-mut409,	TCCTGAAGCCATCNNNTTTGGCTCCTTCAC
Ravi-HCK-for-mut410,	GAAGCCATCAACNNNGGCTCCTTCACC
Ravi-HCK-for-mut411,	TGAAGCCATCAACTTTNNNTCCTTCACCATCAAGT
Ravi-HCK-for-mut412,	CCATCAACTTTGGCNNNTTCACCATCAAGTCA
Ravi-HCK-for-mut413,	ATCAACTTTGGCTCCNNNACCATCAAGTCAGAC
Ravi-HCK-for-mut414,	AACTTTGGCTCCTTCNNNATCAAGTCAGACGTC
Ravi-HCK-for-mut415,	GGCTCCTTCACCNNNAAGTCAGACGTCT
Ravi-HCK-for-mut416,	CTCCTTCACCATCNNNTCAGACGTCTGGTC
Ravi-HCK-for-mut417,	CTTCACCATCAAGNNNGACGTCTGGTCCTT
Ravi-HCK-for-mut418,	TTCACCATCAAGTCANNNGTCTGGTCCTTTGGTA
Ravi-HCK-for-mut419,	ACCATCAAGTCAGACNNNTGGTCCTTTGGTATC
Ravi-HCK-for-mut420,	ATCAAGTCAGACGTCNNNTCCTTTGGTATCCTG
Ravi-HCK-for-mut421,	GTCAGACGTCTGGNNNTTTGGTATCCTGCT
Ravi-HCK-for-mut422,	GACGTCTGGTCCNNNGGTATCCTGCTG
Ravi-HCK-for-mut423,	ACGTCTGGTCCTTTNNNATCCTGCTGATGGA
Ravi-HCK-for-mut424,	TCTGGTCCTTTGGTNNNCTGCTGATGGAGAT
Ravi-HCK-for-mut425,	TGGTCCTTTGGTATCNNNCTGATGGAGATCGTC
Ravi-HCK-for-mut426,	TCCTTTGGTATCCTGNNNATGGAGATCGTCACC
Ravi-HCK-for-mut427,	TTGGTATCCTGCTGNNNGAGATCGTCACCTAC
Ravi-HCK-for-mut428,	GTATCCTGCTGATGNNNATCGTCACCTACGG
Ravi-HCK-for-mut429,	CTGCTGATGGAGNNNGTCACCTACGGC
Ravi-HCK-for-mut430,	CTGATGGAGATCNNNACCTACGGCCGG
Ravi-HCK-for-mut431,	ATGGAGATCGTCNNNTACGGCCGGATC
Ravi-HCK-for-mut432,	AGATCGTCACCNNNGGCCGGATCCC
Ravi-HCK-for-mut433,	GATCGTCACCTACNNNCGGATCCCTTACC
Ravi-HCK-for-mut434,	GTCACCTACGGCNNNATCCCTTACCCAG
Ravi-HCK-for-mut435,	CCTACGGCCGGNNNCCTTACCCAGG
Ravi-HCK-for-mut436,	ACGGCCGGATCNNNTACCCAGGGAT
Ravi-HCK-for-mut437,	GCCGGATCCCTNNNCCAGGGATGTC
Ravi-HCK-for-mut438,	CCGGATCCCTTACNNNGGGATGTCAAACC
Ravi-HCK-for-mut439,	GGATCCCTTACCCANNNATGTCAAACCCTGAA
Ravi-HCK-for-mut440,	CCCTTACCCAGGGNNNTCAAACCCTGAAG
Ravi-HCK-for-mut441,	CTTACCCAGGGATGNNNAACCCTGAAGTGATC
Ravi-HCK-for-mut442,	CCCAGGGATGTCANNNCCTGAAGTGATCC
Ravi-HCK-for-mut443,	AGGGATGTCAAACNNNGAAGTGATCCGAGC
Ravi-HCK-for-mut444,	GATGTCAAACCCTNNNGTGATCCGAGCTCT

Ravi-HCK-for-mut445,	GTCAAACCCTGAANNNATCCGAGCTCTGGA
Ravi-HCK-for-mut446,	AACCCTGAAGTGNNNCGAGCTCTGGAG
Ravi-HCK-for-mut447,	CCTGAAGTGATCNNNGCTCTGGAGCGT
Ravi-HCK-for-mut448,	TGAAGTGATCCGANNNCTGGAGCGTGGATA
Ravi-HCK-for-mut449,	GTGATCCGAGCTNNNGAGCGTGGATACC
Ravi-HCK-for-mut450,	TCCGAGCTCTGNNNCGTGGATACCG
Ravi-HCK-for-mut451,	CGAGCTCTGGAGNNNGGATACCGGATG
Ravi-HCK-for-mut452,	CTCTGGAGCGTNNNTACCGGATGCCT
Ravi-HCK-for-mut453,	TGGAGCGTGGANNNCGGATGCCTCG
Ravi-HCK-for-mut454,	AGCGTGGATACNNNATGCCTCGCCC
Ravi-HCK-for-mut455,	GTGGATACCGGNNNCCTCGCCCAGA
Ravi-HCK-for-mut456,	GATACCGGATGNNNCGCCCAGAGAAC
Ravi-HCK-for-mut457,	TACCGGATGCCTNNNCCAGAGAACTGC
Ravi-HCK-for-mut458,	GGATGCCTCGCNNNGAGAACTGCCC
Ravi-HCK-for-mut459,	TGCCTCGCCCANNNAACTGCCCAGA
Ravi-HCK-for-mut460,	CTCGCCCAGAGNNNTGCCCAGAGGA
Ravi-HCK-for-mut461,	GCCCAGAGAACNNNCCAGAGGAGCTC
Ravi-HCK-for-mut462,	CCAGAGAACTGCNNNGAGGAGCTCTACA
Ravi-HCK-for-mut463,	CAGAGAACTGCCCANNNGAGCTCTACAACATC
Ravi-HCK-for-mut464,	GAGAACTGCCCAGAGNNNCTCTACAACATCATG
Ravi-HCK-for-mut465,	AACTGCCCAGAGGAGNNNTACAACATCATGATG
Ravi-HCK-for-mut466,	CCCAGAGGAGCTCNNNAACATCATGATGC
Ravi-HCK-for-mut467,	CAGAGGAGCTCTACNNNATCATGATGCGCTG
Ravi-HCK-for-mut468,	GAGCTCTACAACNNNATGATGCGCTGCT
Ravi-HCK-for-mut469,	CTCTACAACATCNNNATGCGCTGCTGGA
Ravi-HCK-for-mut470,	CTCTACAACATCATGNNNCGCTGCTGGAAAAAC
Ravi-HCK-for-mut471,	CTACAACATCATGATGNNNTGCTGGAAAAACCGTC
Ravi-HCK-for-mut472,	CATCATGATGCGCNNNTGGAAAAACCGTC
Ravi-HCK-for-mut473,	TGATGCGCTGCNNNAAAAACCGTCC
Ravi-HCK-for-mut474,	TGCGCTGCTGGNNNAACCGTCCGGA
Ravi-HCK-for-mut475,	GCTGCTGGAAANNNCGTCCGGAGGA
Ravi-HCK-for-mut476,	GCTGGAAAAACNNNCCGGAGGAGCG
Ravi-HCK-for-mut477,	GGAAAAACCGTNNNGAGGAGCGGCC
Ravi-HCK-for-mut478,	AAAACCGTCCGNNNGAGCGGCCGAC
Ravi-HCK-for-mut479,	ACCGTCCGGAGNNNCGGCCGACCTT
Ravi-HCK-for-mut480,	GTCCGGAGGAGNNNCCGACCTTCGA
Ravi-HCK-for-mut481,	CCGGAGGAGCGGNNNACCTTCGAATAC
Ravi-HCK-for-mut482,	GAGGAGCGGCCGNNNTTCGAATACATC
Ravi-HCK-for-mut483,	AGCGGCCGACCNNNGAATACATCCAG
Ravi-HCK-for-mut484,	CGGCCGACCTTCNNNTACATCCAGAGTG
Ravi-HCK-for-mut485,	CCGACCTTCGAANNNATCCAGAGTGTGC
Ravi-HCK-for-mut486,	GACCTTCGAATACNNNCAGAGTGTGCTGGA
Ravi-HCK-for-mut487,	ACCTTCGAATACATCNNNAGTGTGCTGGATGAC
Ravi-HCK-for-mut488,	TTCGAATACATCCAGNNNGTGCTGGATGACTTC
Ravi-HCK-for-mut489,	TCGAATACATCCAGAGTNNNCTGGATGACTTCTACAC

Ravi-HCK-for-mut490,	ATACATCCAGAGTGTGNNNGATGACTTCTACACGG
Ravi-HCK-for-mut491,	CCAGAGTGTGCTGNNNGACTTCTACACGG
Ravi-HCK-for-mut492,	GAGTGTGCTGGATNNNTTCTACACGGCCA
Ravi-HCK-for-mut493,	GTGCTGGATGACNNNTACACGGCCACA
Ravi-HCK-for-mut494,	CTGGATGACTTCNNNACGGCCACAGAGA
Ravi-HCK-for-mut495,	GGATGACTTCTACNNNGCCACAGAGAGCC
Ravi-HCK-for-mut496,	GATGACTTCTACACGNNNACAGAGAGCCAGTAC
Ravi-HCK-for-mut497,	TTCTACACGGCCNNNGAGAGCCAGTAC
Ravi-HCK-for-mut498,	TACACGGCCACANNNAGCCAGTACCAA
Ravi-HCK-for-mut499,	ACGGCCACAGAGNNNCAGTACCAACAG
Ravi-HCK-for-mut500,	GCCACAGAGAGCNNNTACCAACAGcag
Ravi-HCK-for-mut502,	GAGAGCCAGTACNNNCAGcagccatgag
Ravi-HCK-for-mut503,	GAGAGCCAGTACCAANNNcagccatgagaattc
Ravi-HCK-rev-mut8,	CCTCCGACCTGGAGNNNcttcaacttcatg
Ravi-HCK-rev-mut9,	TTGCCTCCGACCTGNNNGAActtcaacttc
Ravi-HCK-rev-mut10,	GTATTGCCTCCGACNNNGAGGAActtcaact
Ravi-HCK-rev-mut11,	AGAATGTATTGCCTCCNNNCTGGAGGAActtcaa
Ravi-HCK-rev-mut12,	GAGAATGTATTGCCNNNGACCTGGAGGAAct
Ravi-HCK-rev-mut13,	GTTTTTGAGAATGTATTNNNTCCGACCTGGAGGAAct
Ravi-HCK-rev-mut14,	GTTTTTGAGAATGTNNNGCCTCCGACCTGG
Ravi-HCK-rev-mut15,	TTTCAGTTTTTGAGAANNNATTGCCTCCGACCTG
Ravi-HCK-rev-mut16,	TGGTTTCAGTTTTTGANNNTGTATTGCCTCCGAC
Ravi-HCK-rev-mut17,	CGCTGGTTTCAGTTTTNNNGAATGTATTGCCTCC
Ravi-HCK-rev-mut18,	GGCGCTGGTTTCAGTNNNTGAGAATGTATTGC
Ravi-HCK-rev-mut19,	GCTGGCGCTGGTTTCNNNTTTTGAGAATGTATT
Ravi-HCK-rev-mut20,	GGCTGGCGCTGGTNNNAGTTTTTGAGAAT
Ravi-HCK-rev-mut21,	GTGGGCTGGCGCTNNNTTCAGTTTTTGA
Ravi-HCK-rev-mut22,	GTGTGGGCTGGCNNNGGTTTCAGTTTT
Ravi-HCK-rev-mut23,	ACAGTGTGGGCTNNNGCTGGTTTCAGT
Ravi-HCK-rev-mut24,	GGACAGTGTGGNNNGGCGCTGGTTT
Ravi-HCK-rev-mut25,	ACAGGACAGTGNNNGCTGGCGCTGG
Ravi-HCK-rev-mut26,	TACACAGGACANNNTGGGCTGGCGC
Ravi-HCK-rev-mut27,	ACGTACACAGGNNNGTGTGGGCTGG
Ravi-HCK-rev-mut28,	GGCACGTACACNNNACAGTGTGGGC
Ravi-HCK-rev-mut29,	ATCCGGCACGTANNNAGGACAGTGTGG
Ravi-HCK-rev-mut30,	GGATCCGGCACNNNCACAGGACAGT
Ravi-HCK-rev-mut31,	ATGTGGGATCCGGNNNGTACACAGGACA
Ravi-HCK-rev-mut32,	TGGATGTGGGATCNNNCACGTACACAGGA
Ravi-HCK-rev-mut33,	GTGGATGTGGGNNNCGGCACGTACA
Ravi-HCK-rev-mut34,	TTGATGGTGGATGTNNNATCCGGCACGTAC
Ravi-HCK-rev-mut35,	CTTGATGGTGGANNNGGGATCCGGCA
Ravi-HCK-rev-mut36,	CGGCTTGATGGTNNNTGTGGGATCCG
Ravi-HCK-rev-mut37,	CCCCGGCTTGATNNNGGATGTGGGAT
Ravi-HCK-rev-mut38,	GGCCCCGGCTTNNNGGTGGATGTGG
Ravi-HCK-rev-mut39,	TATTAGGCCCCGGNNNGATGGTGGATGT

Ravi-HCK-rev-mut40,	TGGCTATTAGGCCCNNNCTTGATGGTGGAT
Ravi-HCK-rev-mut41,	TGTGGCTATTAGGNNNCGGCTTGATGGT
Ravi-HCK-rev-mut42,	TGTTGTGGCTATTNNNCCCCGGCTTGAT
Ravi-HCK-rev-mut43,	CTGTTGTGGCTNNNAGGCCCCGGCT
Ravi-HCK-rev-mut44,	GTTGCTGTTGTGNNNATTAGGCCCCGG
Ravi-HCK-rev-mut45,	GTGTGTTGCTGTTNNNGCTATTAGGCCCC
Ravi-HCK-rev-mut46,	CTGGTGTGTTGCTNNNGTGGCTATTAGGC
Ravi-HCK-rev-mut47,	TGATTCCTGGTGTGTTNNNGTTGTGGCTATTAGG
Ravi-HCK-rev-mut48,	CTGATTCCTGGTGTNNNGCTGTTGTGGCTAT
Ravi-HCK-rev-mut49,	CCCTGATTCCTGGNNNGTTGCTGTTGTG
Ravi-HCK-rev-mut50,	CCTCCCTGATTCCNNNTGTGTTGCTGTTG
Ravi-HCK-rev-mut51,	TGCCTCCCTGATNNNTGGTGTGTTGCT
Ravi-HCK-rev-mut52,	CCTGCCTCCCTNNNTCCTGGTGTGT
Ravi-HCK-rev-mut53,	AGAGCCTGCCTCNNNGATTCCTGGTG
Ravi-HCK-rev-mut54,	CTCAGAGCCTGCNNNCCTGATTCCTGG
Ravi-HCK-rev-mut55,	TGTCCTCAGAGCCNNNCTCCCTGATTCC
Ravi-HCK-rev-mut56,	GATGATGTCCTCAGANNNTGCCTCCCTGATTC
Ravi-HCK-rev-mut57,	GATGATGTCCTCNNNGCCTGCCTCCC
Ravi-HCK-rev-mut58,	CACGATGATGTCNNNAGAGCCTGCCTC
Ravi-HCK-rev-mut59,	CAACCACGATGATNNNCTCAGAGCCTGC
Ravi-HCK-rev-mut60,	GGCAACCACGATNNNGTCCTCAGAGC
Ravi-HCK-rev-mut61,	CAGGGCAACCACNNNGATGTCCTCAGA
Ravi-HCK-rev-mut62,	ATCATACAGGGCAACNNNGATGATGTCCTCAGA
Ravi-HCK-rev-mut63,	GTAATCATACAGGGCNNNCACGATGATGTCCTC
Ravi-HCK-rev-mut64,	CCTCGTAATCATACAGNNNAACCACGATGATGTCC
Ravi-HCK-rev-mut65,	GCCTCGTAATCATANNNGGCAACCACGATGA
Ravi-HCK-rev-mut66,	GGCCTCGTAATCNNNCAGGGCAACCA
Ravi-HCK-rev-mut67,	TGAATGGCCTCGTANNNATACAGGGCAACC
Ravi-HCK-rev-mut68,	GGTGAATGGCCTCNNNATCATACAGGGCA
Ravi-HCK-rev-mut69,	TTCGTGGTGAATGGCNNNGTAATCATACAGGG
Ravi-HCK-rev-mut70,	GGTCTTCGTGGTGAATNNNCTCGTAATCATACAGG
Ravi-HCK-rev-mut71,	GTCTTCGTGGTGNNNGGCCTCGTAATC
Ravi-HCK-rev-mut72,	CTGAGGTCTTCGTGNNNAATGGCCTCGTAAT
Ravi-HCK-rev-mut73,	AGCTGAGGTCTTCNNNGTGAATGGCCTC
Ravi-HCK-rev-mut74,	GAAGCTGAGGTCNNNGTGGTGAATGGC
Ravi-HCK-rev-mut75,	TTCTGGAAGCTGAGNNNTTCGTGGTGAATGG
Ravi-HCK-rev-mut76,	CCTTCTGGAAGCTNNNGTCTTCGTGGTGA
Ravi-HCK-rev-mut77,	CCCCCTTCTGGAANNNGAGGTCTTCGTG
Ravi-HCK-rev-mut78,	GTCCCCCTTCTGNNNGCTGAGGTCTTC
Ravi-HCK-rev-mut79,	CTGGTCCCCCTTNNNGAAGCTGAGGTC
Ravi-HCK-rev-mut80,	CATCTGGTCCCCNNNCTGGAAGCTGAG
Ravi-HCK-rev-mut81,	CCACCATCTGGTCNNNCTTCTGGAAGCTG
Ravi-HCK-rev-mut82,	GACCACCATCTGNNNCCCCTTCTGGAA
Ravi-HCK-rev-mut83,	CTAGGACCACCATNNNGTCCCCCTTCTG
Ravi-HCK-rev-mut84,	CTCTAGGACCACNNNCTGGTCCCCCTT

Ravi-HCK-rev-mut85,	GATTCCTCTAGGACNNNCATCTGGTCCCCC
Ravi-HCK-rev-mut86,	CGGATTCCTCTAGNNNCACCATCTGGTCC
Ravi-HCK-rev-mut87,	CCCGGATTCCTCNNNGACCACCATCTG
Ravi-HCK-rev-mut88,	ACTCCCCGGATTCNNNTAGGACCACCATC
Ravi-HCK-rev-mut89,	CCACTCCCCGGANNNCTCTAGGACCA
Ravi-HCK-rev-mut90,	TCCACCACTCCCCNNNTTCCTCTAGGAC
Ravi-HCK-rev-mut91,	CCTTCCACCACTCNNNGGATTCCTCTAGG
Ravi-HCK-rev-mut92,	GCCTTCCACCANNNCCCGGATTCCT
Ravi-HCK-rev-mut93,	CGAGCCTTCCANNNCTCCCCGGATT
Ravi-HCK-rev-mut94,	GATCGAGCCTTNNNCCACTCCCCGG
Ravi-HCK-rev-mut95,	AGGGATCGAGCNNNCCACCACTCCC
Ravi-HCK-rev-mut96,	GCCAGGGATCGNNNCTTCCACCACT
Ravi-HCK-rev-mut97,	GTGGCCAGGGANNNAGCCTTCCACC
Ravi-HCK-rev-mut98,	CGGGTGGCCAGNNNTCGAGCCTTCC
Ravi-HCK-rev-mut99,	TTCCGGGTGGCNNNGGATCGAGCCT
Ravi-HCK-rev-mut100,	CTCCTTCCGGGTNNNCAGGGATCGAG
Ravi-HCK-rev-mut101,	CCCTCCTTCCGNNNGGCCAGGGATC
Ravi-HCK-rev-mut102,	TAGCCCTCCTTNNNGGTGGCCAGGG
Ravi-HCK-rev-mut103,	ATGTAGCCCTCNNNCCGGGTGGCCA
Ravi-HCK-rev-mut104,	GGGATGTAGCCNNNCTTCCGGGTGG
Ravi-HCK-rev-mut105,	GCTTGGGATGTANNNCTCCTTCCGGGT
Ravi-HCK-rev-mut106,	GTTGCTTGGGATNNNGCCCTCCTTCC
Ravi-HCK-rev-mut107,	ACATAGTTGCTTGGNNNGTAGCCCTCCTTC
Ravi-HCK-rev-mut108,	CGACATAGTTGCTNNNGATGTAGCCCTCC
Ravi-HCK-rev-mut109,	GGGCGACATAGTTNNNTGGGATGTAGCC
Ravi-HCK-rev-mut110,	GCGGGCGACATANNNGCTTGGGATGTA
Ravi-HCK-rev-mut111,	ACGCGGGCGACNNNGTTGCTTGGGA
Ravi-HCK-rev-mut112,	GTCAACGCGGGCNNNATAGTTGCTTG
Ravi-HCK-rev-mut113,	AGAGAGTCAACGCGNNNGACATAGTTGCTTG
Ravi-HCK-rev-mut114,	TCCAGAGAGTCAACNNNGGCGACATAGTTG
Ravi-HCK-rev-mut115,	TCCAGAGAGTCNNNGCGGGCGACAT
Ravi-HCK-rev-mut116,	GTCTCCAGAGANNNAACGCGGGCGA
Ravi-HCK-rev-mut117,	TCTGTCTCCAGNNNGTCAACGCGGG
Ravi-HCK-rev-mut118,	ACTCCTCTGTCTCNNNAGAGTCAACGCG
Ravi-HCK-rev-mut119,	AACCACTCCTCTGTNNNCAGAGAGTCAACG
Ravi-HCK-rev-mut120,	GAAAAACCACTCCTCNNNCTCCAGAGAGTCAAC
Ravi-HCK-rev-mut121,	CCTTGAAAAACCACTCNNNTGTCTCCAGAGAGTC
Ravi-HCK-rev-mut122,	GCCCTTGAAAAACCANNNCTCTGTCTCCAGAG
Ravi-HCK-rev-mut123,	GATGCCCTTGAAAAANNNCTCCTCTGTCTCCAG
Ravi-HCK-rev-mut124,	CTGATGCCCTTGAANNNCCACTCCTCTGTC
Ravi-HCK-rev-mut125,	GGCTGATGCCCTTNNNAAACCACTCCTCT
Ravi-HCK-rev-mut126,	CCGGCTGATGCCNNNGAAAAACCACTC
Ravi-HCK-rev-mut127,	GTCCTTCCGGCTGATNNNCTTGAAAAACCACT
Ravi-HCK-rev-mut128,	GTCCTTCCGGCTNNNGCCCTTGAAAAA
Ravi-HCK-rev-mut129,	GCGTCCTTCCGNNNGATGCCCTTGA

Ravi-HCK-rev-mut130,	TCTGCGTCCTTNNNGCTGATGCCCT
Ravi-HCK-rev-mut131,	CGCTCTGCGTCNNNCCGGCTGATGC
Ravi-HCK-rev-mut132,	TGGCGCTCTGCNNNCTTCCGGCTGA
Ravi-HCK-rev-mut133,	AGTTGGCGCTCNNNGTCCTTCCGGC
Ravi-HCK-rev-mut134,	AGCAGTTGGCGNNNTGCGTCCTTCC
Ravi-HCK-rev-mut135,	GCCAGCAGTTGNNNCTCTGCGTCCT
Ravi-HCK-rev-mut136,	GGAGCCAGCAGNNNGCGCTCTGCGT
Ravi-HCK-rev-mut137,	CCGGGAGCCAGNNNTTGGCGCTCTG
Ravi-HCK-rev-mut138,	TTGCCGGGAGCNNNCAGTTGGCGCT
Ravi-HCK-rev-mut139,	ATGTTGCCGGGNNNCAGCAGTTGGC
Ravi-HCK-rev-mut140,	CAGCATGTTGCCNNNAGCCAGCAGTT
Ravi-HCK-rev-mut141,	CCCAGCATGTTNNNGGGAGCCAGCA
Ravi-HCK-rev-mut142,	GAGCCCAGCATNNNGCCGGGAGCCA
Ravi-HCK-rev-mut143,	AAGGAGCCCAGNNNGTTGCCGGGAG
Ravi-HCK-rev-mut144,	CATGAAGGAGCCNNNCATGTTGCCGG
Ravi-HCK-rev-mut145,	GGATCATGAAGGANNNCAGCATGTTGCCG
Ravi-HCK-rev-mut146,	CCGGATCATGAANNNGCCCAGCATGTT
Ravi-HCK-rev-mut147,	TCCCGGATCATNNNGGAGCCCAGCA
Ravi-HCK-rev-mut148,	GCTATCCCGGATNNNGAAGGAGCCCAG
Ravi-HCK-rev-mut149,	CTCGCTATCCCGNNNCATGAAGGAGC
Ravi-HCK-rev-mut150,	GTGGTCTCGCTATCNNNGATCATGAAGGAGC
Ravi-HCK-rev-mut151,	TTAGTGGTCTCGCTNNNCCGGATCATGAAG
Ravi-HCK-rev-mut152,	TTCCTTTAGTGGTCTCNNNATCCCGGATCATGAA
Ravi-HCK-rev-mut153,	CTTCCTTTAGTGGTNNNGCTATCCCGGATCA
Ravi-HCK-rev-mut154,	GTAGCTTCCTTTAGTNNNCTCGCTATCCCGGAT
Ravi-HCK-rev-mut155,	AGAGTAGCTTCCTTTNNNGGTCTCGCTATCCC
Ravi-HCK-rev-mut156,	CAAAGAGTAGCTTCCNNNAGTGGTCTCGCTATC
Ravi-HCK-rev-mut157,	GGACAAAGAGTAGCTNNNTTTAGTGGTCTCGCT
Ravi-HCK-rev-mut158,	GCACGGACAAAGAGTANNNTCCTTTAGTGGTCTC
Ravi-HCK-rev-mut159,	CGCACGGACAAAGANNNGCTTCCTTTAGTG
Ravi-HCK-rev-mut160,	GTCTCGCACGGACAANNNGTAGCTTCCTTTAG
Ravi-HCK-rev-mut161,	TAGTCTCGCACGGANNNAGAGTAGCTTCCTT
Ravi-HCK-rev-mut162,	GTCGTAGTCTCGCACNNNCAAAGAGTAGCTTC
Ravi-HCK-rev-mut163,	GGGTCGTAGTCTCGNNNGGACAAAGAGTAG
Ravi-HCK-rev-mut164,	GAGGGTCGTAGTCNNNCACGGACAAAGAG
Ravi-HCK-rev-mut165,	CGAGGGTCGTANNNTCGCACGGACA
Ravi-HCK-rev-mut166,	TGCCGAGGGTCNNNGTCTCGCACGG
Ravi-HCK-rev-mut167,	CCCTGCCGAGGNNNGTAGTCTCGCA
Ravi-HCK-rev-mut168,	TATCTCCCTGCCGNNNGTCGTAGTCTCG
Ravi-HCK-rev-mut169,	CGGTATCTCCCTGNNNAGGGTCGTAGTCT
Ravi-HCK-rev-mut170,	CACGGTATCTCCNNNCCGAGGGTCGTA
Ravi-HCK-rev-mut171,	TTTCACGGTATCNNNCTGCCGAGGGTC
Ravi-HCK-rev-mut172,	ATGTTTCACGGTNNNTCCCTGCCGAG
Ravi-HCK-rev-mut173,	CTTGTAATGTTTCACNNNATCTCCCTGCCGAG
Ravi-HCK-rev-mut174,	GGATCTTGTAATGTTTNNNGGTATCTCCCTGCCG

Ravi-HCK-rev-mut175,	CGGATCTTGTAATGNNNCACGGTATCTCCCT
Ravi-HCK-rev-mut176,	GGTCCGGATCTTGTANNNTTTCACGGTATCTCC
Ravi-HCK-rev-mut177,	CAGGGTCCGGATCTTNNNATGTTTCACGGTATC
Ravi-HCK-rev-mut178,	TCCAGGGTCCGGATNNNGTAATGTTTCACG
Ravi-HCK-rev-mut179,	TTGTCCAGGGTCCGNNNCTTGTAATGTTTCA
Ravi-HCK-rev-mut180,	CCCGTTGTCCAGGGTNNNGATCTTGTAATGTTT
Ravi-HCK-rev-mut181,	CCCGTTGTCCAGNNNCCGGATCTTGTA
Ravi-HCK-rev-mut182,	CCCCCGTTGTCNNNGGTCCGGATCT
Ravi-HCK-rev-mut183,	AAGCCCCCGTTNNNCAGGGTCCGGA
Ravi-HCK-rev-mut184,	TAGAAGCCCCCNNNGTCCAGGGTCC
Ravi-HCK-rev-mut185,	GATATGTAGAAGCCNNNGTTGTCCAGGGTCC
Ravi-HCK-rev-mut186,	GGGGATATGTAGAANNNCCCGTTGTCCAGG
Ravi-HCK-rev-mut187,	GGGGGATATGTANNNGCCCCCGTTGTC
Ravi-HCK-rev-mut188,	CGGGGGGATATNNNGAAGCCCCCGT
Ravi-HCK-rev-mut189,	CTTCGGGGGGANNNGTAGAAGCCCC
Ravi-HCK-rev-mut190,	AGGTGCTTCGGGGNNNTATGTAGAAGCC
Ravi-HCK-rev-mut191,	CTGAAGGTGCTTCGNNNGGATATGTAGAAGC
Ravi-HCK-rev-mut192,	GTGCTGAAGGTGCTNNNGGGGGATATGTAG
Ravi-HCK-rev-mut193,	GAGTGCTGAAGGTNNNTCGGGGGGATATG
Ravi-HCK-rev-mut194,	AGAGTGCTGAANNNGCTTCGGGGGG
Ravi-HCK-rev-mut195,	TGCAGAGTGCTNNNGGTGCTTCGGG
Ravi-HCK-rev-mut196,	CTCCTGCAGAGTNNNGAAGGTGCTTCG
Ravi-HCK-rev-mut197,	AGCTCCTGCAGNNNGCTGAAGGTGC
Ravi-HCK-rev-mut198,	CACCAGCTCCTGNNNAGTGCTGAAGGT
Ravi-HCK-rev-mut199,	GTCCACCAGCTCNNNCAGAGTGCTGAA
Ravi-HCK-rev-mut200,	TGGTCCACCAGNNNCTGCAGAGTGC
Ravi-HCK-rev-mut201,	TGTAGTGGTCCACNNNCTCCTGCAGAGT
Ravi-HCK-rev-mut202,	TCTTGTAGTGGTCNNNCAGCTCCTGCAGA
Ravi-HCK-rev-mut203,	CCTTCTTGTAGTGNNNCACCAGCTCCTG
Ravi-HCK-rev-mut204,	TCCCCTTCTTGTANNNGTCCACCAGCTC
Ravi-HCK-rev-mut205,	GTTCCCCTTCTTNNNGTGGTCCACCAG
Ravi-HCK-rev-mut206,	CGTCGTTCCCCTTNNNGTAGTGGTCCAC
Ravi-HCK-rev-mut207,	CCCGTCGTTCCCNNNCTTGTAGTGGTC
Ravi-HCK-rev-mut208,	CAGAGCCCGTCGTTNNNCTTCTTGTAGTGG
Ravi-HCK-rev-mut209,	CAGAGCCCGTCNNNCCCCTTCTTGT
Ravi-HCK-rev-mut210,	TGGCAGAGCCCNNNGTTCCCCTTCT
Ravi-HCK-rev-mut211,	GTTTCTGGCAGAGNNNGTCGTTCCCCTT
Ravi-HCK-rev-mut212,	CAGTTTCTGGCANNNCCCGTCGTTCC
Ravi-HCK-rev-mut213,	GACAGTTTCTGNNNGAGCCCGTCGT
Ravi-HCK-rev-mut214,	ACCGACAGTTTNNNGCAGAGCCCGT
Ravi-HCK-rev-mut215,	GGCACCGACAGNNNCTGGCAGAGCC
Ravi-HCK-rev-mut216,	CAGGGCACCGANNNTTTCTGGCAGA
Ravi-HCK-rev-mut217,	CATGCAGGGCACNNNCAGTTTCTGGC
Ravi-HCK-rev-mut218,	AAGACATGCAGGGNNNCGACAGTTTCTG
Ravi-HCK-rev-mut219,	TTGGAAGACATGCANNNCACCGACAGTTTCT

Ravi-HCK-rev-mut220,	CTTGGAAGACATNNNGGGCACCGACAG
Ravi-HCK-rev-mut221,	GGCTTGGAAGANNNGCAGGGCACCG
Ravi-HCK-rev-mut222,	TGGGGCTTGGANNNCATGCAGGGCA
Ravi-HCK-rev-mut223,	CTTCTGGGGCTTNNNAGACATGCAGGG
Ravi-HCK-rev-mut224,	AGGCTTCTGGGGNNNGGAAGACATGC
Ravi-HCK-rev-mut225,	TCCCAAGGCTTCTGNNNCTTGGAAGACATG
Ravi-HCK-rev-mut226,	CTCCCAAGGCTTNNNGGGCTTGGAAGA
Ravi-HCK-rev-mut227,	TTTCTCCCAAGGNNNCTGGGGCTTGG
Ravi-HCK-rev-mut228,	CATCTTTCTCCCANNNCTTCTGGGGCTTG
Ravi-HCK-rev-mut229,	AGGCATCTTTCTCNNNAGGCTTCTGGGG
Ravi-HCK-rev-mut230,	CCCAGGCATCTTTNNNCCAAGGCTTCTG
Ravi-HCK-rev-mut231,	TCCCAGGCATCNNNCTCCCAAGGCT
Ravi-HCK-rev-mut232,	GGATCTCCCAGGCNNNTTTCTCCCAAGG
Ravi-HCK-rev-mut233,	CGAGGGATCTCCCANNNATCTTTCTCCCAAG
Ravi-HCK-rev-mut234,	CCCGAGGGATCTCNNNGGCATCTTTCTC
Ravi-HCK-rev-mut235,	GATTCCCGAGGGATNNNCCAGGCATCTTTC
Ravi-HCK-rev-mut236,	GATTCCCGAGGNNNCTCCCAGGCAT
Ravi-HCK-rev-mut237,	GAGGGATTCCCGNNNGATCTCCCAGG
Ravi-HCK-rev-mut238,	AGCTTGAGGGATTCNNNAGGGATCTCCCAG
Ravi-HCK-rev-mut239,	CAGCTTGAGGGANNNCCGAGGGATCTC
Ravi-HCK-rev-mut240,	TCTCCAGCTTGAGNNNTTCCCGAGGGAT
Ravi-HCK-rev-mut241,	TCTTCTCCAGCTTNNNGGATTCCCGAGG
Ravi-HCK-rev-mut242,	AGTTTCTTCTCCAGNNNGAGGGATTCCCGAG
Ravi-HCK-rev-mut243,	TCCAAGTTTCTTCTCNNNCTTGAGGGATTCCC
Ravi-HCK-rev-mut244,	AGCTCCAAGTTTCTTNNNCAGCTTGAGGGATTC
Ravi-HCK-rev-mut245,	CAGCTCCAAGTTTNNNCTCCAGCTTGAGG
Ravi-HCK-rev-mut246,	CCCAGCTCCAAGNNNCTTCTCCAGCTT
Ravi-HCK-rev-mut247,	ACTGCCCAGCTCCNNNTTTCTTCTCCAG
Ravi-HCK-rev-mut248,	CCAAACTGCCCAGCNNNAAGTTTCTTCTCC
Ravi-HCK-rev-mut249,	TCCCCAAACTGCCCNNNTCCAAGTTTCTTC
Ravi-HCK-rev-mut250,	GACTTCCCCAAACTGNNNAGCTCCAAGTTTCTT
Ravi-HCK-rev-mut251,	AGACTTCCCCAAANNNCCCAGCTCCAAG
Ravi-HCK-rev-mut252,	CAGACTTCCCCNNNCTGCCCAGCTC
Ravi-HCK-rev-mut253,	CCATCCAGACTTCNNNAAACTGCCCAGCT
Ravi-HCK-rev-mut254,	GCCATCCAGACNNNCCCAAACTGCC
Ravi-HCK-rev-mut255,	AGGTGGCCATCCANNNTTCCCCAAACTG
Ravi-HCK-rev-mut256,	TTGTAGGTGGCCATNNNGACTTCCCCAAAC
Ravi-HCK-rev-mut257,	GTTGTAGGTGGCNNNCCAGACTTCCCC
Ravi-HCK-rev-mut258,	GTGCTTGTTGTAGGTNNNCATCCAGACTTCCC
Ravi-HCK-rev-mut259,	GTGTGCTTGTTGTANNNGGCCATCCAGACT
Ravi-HCK-rev-mut260,	GGTGTGCTTGTTNNNGGTGGCCATCC
Ravi-HCK-rev-mut261,	CTTGGTGTGCTTNNNGTAGGTGGCCAT
Ravi-HCK-rev-mut262,	CACCTTGGTGTGNNNGTTGTAGGTGGC
Ravi-HCK-rev-mut263,	ACTGCCACCTTGGTNNNCTTGTTGTAGGTG
Ravi-HCK-rev-mut264,	TTCACTGCCACCTTNNNGTGCTTGTTGTAG

Ravi-HCK-rev-mut265,	CTTCACTGCCACNNNGGTGTGCTTGTT
Ravi-HCK-rev-mut266,	TCGTCTTCACTGCNNNCTTGGTGTGCTT
Ravi-HCK-rev-mut267,	TCATCGTCTTCACNNNCACCTTGGTGTG
Ravi-HCK-rev-mut268,	GCTTCATCGTCTTNNNTGCCACCTTGGTG
Ravi-HCK-rev-mut270,	TCCCTGGCTTCATNNNCTTCACTGCCAC
Ravi-HCK-rev-mut271,	GCTCCCTGGCTTNNNCGTCTTCACTG
Ravi-HCK-rev-mut272,	CATGCTCCCTGGNNNCATCGTCTTCAC
Ravi-HCK-rev-mut273,	CCGACATGCTCCCNNNCTTCATCGTCTT
Ravi-HCK-rev-mut274,	CACCGACATGCTNNNTGGCTTCATCGT
Ravi-HCK-rev-mut275,	CTCCACCGACATNNNCCCTGGCTTCAT
Ravi-HCK-rev-mut276,	GCCTCCACCGANNNGCTCCCTGGCT
Ravi-HCK-rev-mut277,	AAGGCCTCCACNNNCATGCTCCCTG
Ravi-HCK-rev-mut278,	AGGAAGGCCTCNNNCGACATGCTCC
Ravi-HCK-rev-mut279,	GCCAGGAAGGCNNNCACCGACATGC
Ravi-HCK-rev-mut280,	CTCTGCCAGGAANNNCTCCACCGACAT
Ravi-HCK-rev-mut281,	GCCTCTGCCAGNNNGGCCTCCACCG
Ravi-HCK-rev-mut282,	TTGGCCTCTGCNNNGAAGGCCTCCA
Ravi-HCK-rev-mut283,	ACGTTGGCCTCNNNCAGGAAGGCCT
Ravi-HCK-rev-mut285,	AGTTTTCATCACGTTNNNCTCTGCCAGGAAGG
Ravi-HCK-rev-mut286,	GAGTTTTCATCACNNNGGCCTCTGCCAG
Ravi-HCK-rev-mut287,	GCAGAGTTTTCATNNNGTTGGCCTCTGCC
Ravi-HCK-rev-mut288,	GCTGCAGAGTTTTNNNCACGTTGGCCTC
Ravi-HCK-rev-mut289,	CATGCTGCAGAGTNNNCATCACGTTGGC
Ravi-HCK-rev-mut290,	TTGTCATGCTGCAGNNNTTTCATCACGTTGG
Ravi-HCK-rev-mut291,	CAGCTTGTCATGCTGNNNAGTTTTCATCACGTT
Ravi-HCK-rev-mut292,	GACCAGCTTGTCATGNNNCAGAGTTTTCATCAC
Ravi-HCK-rev-mut293,	TTTGACCAGCTTGTCNNNCTGCAGAGTTTTCAT
Ravi-HCK-rev-mut294,	GAAGTTTGACCAGCTTNNNATGCTGCAGAGTTTTC
Ravi-HCK-rev-mut295,	TGAAGTTTGACCAGNNNGTCATGCTGCAGA
Ravi-HCK-rev-mut296,	GCATGAAGTTTGACNNNCTTGTCATGCTGCA
Ravi-HCK-rev-mut297,	ACCGCATGAAGTTTNNNCAGCTTGTCATGC
Ravi-HCK-rev-mut298,	CACCGCATGAAGNNNGACCAGCTTGTC
Ravi-HCK-rev-mut299,	GACCACCGCATGNNNTTTGACCAGCTT
Ravi-HCK-rev-mut300,	GGTGACCACCGCNNNAAGTTTGACCAG
Ravi-HCK-rev-mut301,	CTCCTTGGTGACCACNNNATGAAGTTTGACCA
Ravi-HCK-rev-mut302,	GCTCCTTGGTGACNNNCGCATGAAGTTTG
Ravi-HCK-rev-mut303,	GGCTCCTTGGTNNNCACCGCATGAA
Ravi-HCK-rev-mut304,	ATGGGCTCCTTNNNGACCACCGCAT
Ravi-HCK-rev-mut305,	GTAGATGGGCTCNNNGGTGACCACCG
Ravi-HCK-rev-mut306,	ATGATGTAGATGGGNNNCTTGGTGACCACC
Ravi-HCK-rev-mut307,	CGTGATGATGTAGATNNNCTCCTTGGTGACCAC
Ravi-HCK-rev-mut308,	CCGTGATGATGTANNNGGGCTCCTTGGTG
Ravi-HCK-rev-mut309,	AACTCCGTGATGATNNNGATGGGCTCCTTG
Ravi-HCK-rev-mut310,	ATGAACTCCGTGATNNNGTAGATGGGCTCCT
Ravi-HCK-rev-mut311,	CCATGAACTCCGTNNNGATGTAGATGGGC

Ravi-HCK-rev-mut312,	CTTTGGCCATGAACTCNNNGATGATGTAGATGGG
Ravi-HCK-rev-mut313,	TTCCTTTGGCCATGAANNNCGTGATGATGTAGATG
Ravi-HCK-rev-mut314,	CTTCCTTTGGCCATNNNCTCCGTGATGATGT
Ravi-HCK-rev-mut315,	AGCTTCCTTTGGCNNNGAACTCCGTGAT
Ravi-HCK-rev-mut316,	AGCAAGCTTCCTTTNNNCATGAACTCCGTGA
Ravi-HCK-rev-mut317,	CAGCAAGCTTCCNNNGGCCATGAACTC
Ravi-HCK-rev-mut318,	AAGTCCAGCAAGCTNNNTTTGGCCATGAAC
Ravi-HCK-rev-mut319,	AGAAAGTCCAGCAANNNTCCTTTGGCCATGA
Ravi-HCK-rev-mut320,	TCAGAAAGTCCAGNNNGCTTCCTTTGGCC
Ravi-HCK-rev-mut321,	CACTTTTCAGAAAGTCNNNCAAGCTTCCTTTGGC
Ravi-HCK-rev-mut322,	TCATCACTTTTCAGAAANNNCAGCAAGCTTCCTTTG
Ravi-HCK-rev-mut323,	CTCATCACTTTTCAGNNNGTCCAGCAAGCTTC
Ravi-HCK-rev-mut324,	GCCCTCATCACTTTTNNNAAAGTCCAGCAAGC
Ravi-HCK-rev-mut325,	CTGCCCTCATCACTNNNCAGAAAGTCCAGC
Ravi-HCK-rev-mut326,	CTTGCTGCCCTCATCNNNTTTCAGAAAGTCCA
Ravi-HCK-rev-mut327,	TGCTTGCTGCCCTCNNNACTTTTCAGAAAG
Ravi-HCK-rev-mut328,	GCTGCTTGCTGCCNNNATCACTTTTCAGA
Ravi-HCK-rev-mut329,	CAATGGCTGCTTGCTNNNCTCATCACTTTTCAG
Ravi-HCK-rev-mut330,	CAATGGCTGCTTNNNGCCCTCATCACT
Ravi-HCK-rev-mut331,	GGCAATGGCTGNNNGCTGCCCTCAT
Ravi-HCK-rev-mut332,	TTTTGGCAATGGNNNCTTGCTGCCCTC
Ravi-HCK-rev-mut333,	GAGTTTTGGCAANNNCTGCTTGCTGCC
Ravi-HCK-rev-mut334,	TCAATGAGTTTTGGNNNTGGCTGCTTGCTG
Ravi-HCK-rev-mut335,	GAAGTCAATGAGTTTNNNCAATGGCTGCTTGCT
Ravi-HCK-rev-mut336,	GAGAAGTCAATGAGNNNTGGCAATGGCTGC
Ravi-HCK-rev-mut337,	GGCTGAGAAGTCAATNNNTTTTGGCAATGGCT
Ravi-HCK-rev-mut338,	TGGGCTGAGAAGTCNNNGAGTTTTGGCAAT
Ravi-HCK-rev-mut339,	CAATCTGGGCTGAGAANNNAATGAGTTTTGGCAAT
Ravi-HCK-rev-mut340,	TGCAATCTGGGCTGANNNGTCAATGAGTTTTG
Ravi-HCK-rev-mut341,	TTCTGCAATCTGGGCNNNGAAGTCAATGAGTTT
Ravi-HCK-rev-mut342,	TGCCTTCTGCAATCTGNNNTGAGAAGTCAATGAG
Ravi-HCK-rev-mut343,	ATGCCTTCTGCAATNNNGGCTGAGAAGTCAA
Ravi-HCK-rev-mut344,	CATGCCTTCTGCNNNCTGGGCTGAGAA
Ravi-HCK-rev-mut345,	GGCCATGCCTTCNNNAATCTGGGCTG
Ravi-HCK-rev-mut346,	GAAGGCCATGCCNNNTGCAATCTGGG
Ravi-HCK-rev-mut347,	TCGATGAAGGCCATNNNTTCTGCAATCTGG
Ravi-HCK-rev-mut348,	CTCGATGAAGGCNNNGCCTTCTGCAAT
Ravi-HCK-rev-mut349,	TCTGCTCGATGAANNNCATGCCTTCTGCA
Ravi-HCK-rev-mut350,	CTCTGCTCGATNNNGGCCATGCCTT
Ravi-HCK-rev-mut351,	GTTCCTCTGCTCNNNGAAGGCCATGC
Ravi-HCK-rev-mut352,	GATGTAGTTCCTCTGNNNGATGAAGGCCATGC
Ravi-HCK-rev-mut353,	TGGATGTAGTTCCTNNNCTCGATGAAGGCCA
Ravi-HCK-rev-mut354,	CGGTGGATGTAGTTNNNCTGCTCGATGAAGG
Ravi-HCK-rev-mut355,	CTCGGTGGATGTANNNCCTCTGCTCGATG
Ravi-HCK-rev-mut356,	GGTCTCGGTGGATNNNGTTCCTCTGCTC

Ravi-HCK-rev-mut357,	GGAGGTCTCGGTGNNNGTAGTTCCTCTG
Ravi-HCK-rev-mut358,	CTCGGAGGTCTCGNNNGATGTAGTTCCTC
Ravi-HCK-rev-mut359,	CAGCTCGGAGGTCNNNGTGGATGTAGTTC
Ravi-HCK-rev-mut361,	TTGGCAGCTCGNNNGTCTCGGTGGA
Ravi-HCK-rev-mut362,	ATGTTGGCAGCNNNGAGGTCTCGGT
Ravi-HCK-rev-mut363,	CAAGATGTTGGCNNNTCGGAGGTCTCG
Ravi-HCK-rev-mut364,	AGAGACCAAGATGTTNNNAGCTCGGAGGTCTC
Ravi-HCK-rev-mut365,	CAGAGACCAAGATNNNGGCAGCTCGGAG
Ravi-HCK-rev-mut366,	TGCAGAGACCAANNNGTTGGCAGCTC
Ravi-HCK-rev-mut367,	GGATGCAGAGACNNNGATGTTGGCAGC
Ravi-HCK-rev-mut368,	CCAGGGATGCAGANNNCAAGATGTTGGC
Ravi-HCK-rev-mut369,	ACACCAGGGATGCNNNGACCAAGATGTT
Ravi-HCK-rev-mut370,	TCTTACACACCAGGGANNNAGAGACCAAGATGTT
Ravi-HCK-rev-mut371,	CAATCTTACACACCAGNNNTGCAGAGACCAAGAT
Ravi-HCK-rev-mut372,	GCAATCTTACACACNNNGGATGCAGAGACCA
Ravi-HCK-rev-mut373,	GTCAGCAATCTTACANNNCAGGGATGCAGAGAC
Ravi-HCK-rev-mut374,	AAGTCAGCAATCTTNNNCACCAGGGATGCAG
Ravi-HCK-rev-mut375,	CCAAAGTCAGCAATNNNACACACCAGGGATG
Ravi-HCK-rev-mut376,	GGCCAAAGTCAGCNNNCTTACACACCAG
Ravi-HCK-rev-mut377,	GCCAGGCCAAAGTCNNNAATCTTACACACC
Ravi-HCK-rev-mut381,	ATGACCCGGGCNNNGCCAAAGTCAG
Ravi-HCK-rev-mut382,	CTCAATGACCCGNNNCAGGCCAAAGTC
Ravi-HCK-rev-mut383,	TCCTCAATGACNNNGGCCAGGCCAA
Ravi-HCK-rev-mut384,	TTGTCCTCAATNNNCCGGGCCAGGC
Ravi-HCK-rev-mut385,	TCGTTGTCCTCNNNGACCCGGGCCA
Ravi-HCK-rev-mut386,	TGTACTCGTTGTCNNNAATGACCCGGGC
Ravi-HCK-rev-mut387,	CCGTGTACTCGTTNNNCTCAATGACCCG
Ravi-HCK-rev-mut388,	GAGCCGTGTACTCNNNGTCCTCAATGACC
Ravi-HCK-rev-mut389,	CCCGAGCCGTGTANNNGTTGTCCTCAAT
Ravi-HCK-rev-mut391,	CCCTTCCCGAGCNNNGTACTCGTTGT
Ravi-HCK-rev-mut392,	GCCCCTTCCCGNNNCGTGTACTCGT
Ravi-HCK-rev-mut393,	CTTGGCCCCTTCNNNAGCCGTGTACT
Ravi-HCK-rev-mut394,	AACTTGGCCCCNNNCCGAGCCGTGT
Ravi-HCK-rev-mut395,	GGGAACTTGGCNNNTTCCCGAGCCG
Ravi-HCK-rev-mut396,	GATGGGGAACTTNNNCCCTTCCCGAGC
Ravi-HCK-rev-mut397,	CTTGATGGGGAANNNGGCCCCTTCCC
Ravi-HCK-rev-mut398,	CACTTGATGGGNNNCTTGGCCCCTT
Ravi-HCK-rev-mut399,	CTGTCCACTTGATNNNGAACTTGGCCCCT
Ravi-HCK-rev-mut400,	AGCTGTCCACTTNNNGGGGAACTTGG
Ravi-HCK-rev-mut401,	CAGGAGCTGTCCANNNGATGGGGAACTTG
Ravi-HCK-rev-mut402,	CTTCAGGAGCTGTNNNCTTGATGGGGAAC
Ravi-HCK-rev-mut403,	GGCTTCAGGAGCNNNCCACTTGATGG
Ravi-HCK-rev-mut404,	TTGATGGCTTCAGGNNNTGTCCACTTGATGG
Ravi-HCK-rev-mut405,	AAAGTTGATGGCTTCNNNAGCTGTCCACTTGAT
Ravi-HCK-rev-mut406,	CAAAGTTGATGGCNNNAGGAGCTGTCCAC

Ravi-HCK-rev-mut407,	GAGCCAAAGTTGATNNNTTCAGGAGCTGTCC
Ravi-HCK-rev-mut408,	GGAGCCAAAGTTNNNGGCTTCAGGAGC
Ravi-HCK-rev-mut409,	GTGAAGGAGCCAAANNNGATGGCTTCAGGA
Ravi-HCK-rev-mut410,	GGTGAAGGAGCCNNNGTTGATGGCTTC
Ravi-HCK-rev-mut411,	ACTTGATGGTGAAGGANNNAAAGTTGATGGCTTCA
Ravi-HCK-rev-mut412,	TGACTTGATGGTGAANNNGCCAAAGTTGATGG
Ravi-HCK-rev-mut413,	GTCTGACTTGATGGTNNNGGAGCCAAAGTTGAT
Ravi-HCK-rev-mut414,	GACGTCTGACTTGATNNNGAAGGAGCCAAAGTT
Ravi-HCK-rev-mut415,	AGACGTCTGACTTNNNGGTGAAGGAGCC
Ravi-HCK-rev-mut416,	GACCAGACGTCTGANNNGATGGTGAAGGAG
Ravi-HCK-rev-mut417,	AAGGACCAGACGTCNNNCTTGATGGTGAAG
Ravi-HCK-rev-mut418,	TACCAAAGGACCAGACNNNTGACTTGATGGTGAA
Ravi-HCK-rev-mut419,	GATACCAAAGGACCANNNGTCTGACTTGATGGT
Ravi-HCK-rev-mut420,	CAGGATACCAAAGGANNNGACGTCTGACTTGAT
Ravi-HCK-rev-mut421,	AGCAGGATACCAAANNNCCAGACGTCTGAC
Ravi-HCK-rev-mut422,	CAGCAGGATACCNNNGGACCAGACGTC
Ravi-HCK-rev-mut423,	TCCATCAGCAGGATNNNAAAGGACCAGACGT
Ravi-HCK-rev-mut424,	ATCTCCATCAGCAGNNNACCAAAGGACCAGA
Ravi-HCK-rev-mut425,	GACGATCTCCATCAGNNNGATACCAAAGGACCA
Ravi-HCK-rev-mut426,	GGTGACGATCTCCATNNNCAGGATACCAAAGGA
Ravi-HCK-rev-mut427,	GTAGGTGACGATCTCNNNCAGCAGGATACCAA
Ravi-HCK-rev-mut428,	CCGTAGGTGACGATNNNCATCAGCAGGATAC
Ravi-HCK-rev-mut429,	GCCGTAGGTGACNNNCTCCATCAGCAG
Ravi-HCK-rev-mut430,	CCGGCCGTAGGTNNNGATCTCCATCAG
Ravi-HCK-rev-mut431,	GATCCGGCCGTANNNGACGATCTCCAT
Ravi-HCK-rev-mut432,	GGGATCCGGCCNNNGGTGACGATCT
Ravi-HCK-rev-mut433,	GGTAAGGGATCCGNNNGTAGGTGACGATC
Ravi-HCK-rev-mut434,	CTGGGTAAGGGATNNNGCCGTAGGTGAC
Ravi-HCK-rev-mut435,	CCTGGGTAAGGNNNCCGGCCGTAGG
Ravi-HCK-rev-mut436,	ATCCCTGGGTANNNGATCCGGCCGT
Ravi-HCK-rev-mut437,	GACATCCCTGGNNNAGGGATCCGGC
Ravi-HCK-rev-mut438,	GGTTTGACATCCCNNNGTAAGGGATCCGG
Ravi-HCK-rev-mut439,	TTCAGGGTTTGACATNNNTGGGTAAGGGATCC
Ravi-HCK-rev-mut440,	CTTCAGGGTTTGANNNCCCTGGGTAAGGG
Ravi-HCK-rev-mut441,	GATCACTTCAGGGTTNNNCATCCCTGGGTAAG
Ravi-HCK-rev-mut442,	GGATCACTTCAGGNNNTGACATCCCTGGG
Ravi-HCK-rev-mut443,	GCTCGGATCACTTCNNNGTTTGACATCCCT
Ravi-HCK-rev-mut444,	AGAGCTCGGATCACNNNAGGGTTTGACATC
Ravi-HCK-rev-mut445,	TCCAGAGCTCGGATNNNTTCAGGGTTTGAC
Ravi-HCK-rev-mut446,	CTCCAGAGCTCGNNNCACTTCAGGGTT
Ravi-HCK-rev-mut447,	ACGCTCCAGAGCNNNGATCACTTCAGG
Ravi-HCK-rev-mut448,	TATCCACGCTCCAGNNNTCGGATCACTTCA
Ravi-HCK-rev-mut449,	GGTATCCACGCTCNNNAGCTCGGATCAC
Ravi-HCK-rev-mut450,	CGGTATCCACGNNNCAGAGCTCGGA
Ravi-HCK-rev-mut451,	CATCCGGTATCCNNNCTCCAGAGCTCG

Ravi-HCK-rev-mut452,	AGGCATCCGGTANNNACGCTCCAGAG
Ravi-HCK-rev-mut453,	CGAGGCATCCGNNNTCCACGCTCCA
Ravi-HCK-rev-mut454,	GGGCGAGGCATNNNGTATCCACGCT
Ravi-HCK-rev-mut455,	TCTGGGCGAGGNNNCCGGTATCCAC
Ravi-HCK-rev-mut456,	GTTCTCTGGGCGNNNCATCCGGTATC
Ravi-HCK-rev-mut457,	GCAGTTCTCTGGNNNAGGCATCCGGTA
Ravi-HCK-rev-mut458,	GGGCAGTTCTCNNNGCGAGGCATCC
Ravi-HCK-rev-mut459,	TCTGGGCAGTTNNNTGGGCGAGGCA
Ravi-HCK-rev-mut460,	TCCTCTGGGCANNNCTCTGGGCGAG
Ravi-HCK-rev-mut461,	GAGCTCCTCTGGNNNGTTCTCTGGGC
Ravi-HCK-rev-mut462,	TGTAGAGCTCCTCNNNGCAGTTCTCTGG
Ravi-HCK-rev-mut463,	GATGTTGTAGAGCTCNNNTGGGCAGTTCTCTG
Ravi-HCK-rev-mut464,	CATGATGTTGTAGAGNNNCTCTGGGCAGTTCTC
Ravi-HCK-rev-mut465,	CATCATGATGTTGTANNNCTCCTCTGGGCAGTT
Ravi-HCK-rev-mut466,	GCATCATGATGTTNNNGAGCTCCTCTGGG
Ravi-HCK-rev-mut467,	CAGCGCATCATGATNNNGTAGAGCTCCTCTG
Ravi-HCK-rev-mut468,	AGCAGCGCATCATNNNGTTGTAGAGCTC
Ravi-HCK-rev-mut469,	TCCAGCAGCGCATNNNGATGTTGTAGAG
Ravi-HCK-rev-mut470,	GTTTTTCCAGCAGCGNNNCATGATGTTGTAGAG
Ravi-HCK-rev-mut471,	GACGGTTTTTCCAGCANNNCATCATGATGTTGTAG
Ravi-HCK-rev-mut472,	GACGGTTTTTCCANNNGCGCATCATGATG
Ravi-HCK-rev-mut473,	GGACGGTTTTTNNNGCAGCGCATCA
Ravi-HCK-rev-mut474,	TCCGGACGGTTNNNCCAGCAGCGCA
Ravi-HCK-rev-mut475,	TCCTCCGGACGNNNTTTCCAGCAGC
Ravi-HCK-rev-mut476,	CGCTCCTCCGGNNNGTTTTTCCAGC
Ravi-HCK-rev-mut477,	GGCCGCTCCTCNNNACGGTTTTTCC
Ravi-HCK-rev-mut478,	GTCGGCCGCTCNNNCGGACGGTTTT
Ravi-HCK-rev-mut479,	AAGGTCGGCCGNNNCTCCGGACGGT
Ravi-HCK-rev-mut480,	TCGAAGGTCGGNNNCTCCTCCGGAC
Ravi-HCK-rev-mut481,	GTATTCGAAGGTNNNCCGCTCCTCCGG
Ravi-HCK-rev-mut482,	GATGTATTCGAANNNCGGCCGCTCCTC
Ravi-HCK-rev-mut483,	CTGGATGTATTCNNNGGTCGGCCGCT
Ravi-HCK-rev-mut484,	CACTCTGGATGTANNNGAAGGTCGGCCG
Ravi-HCK-rev-mut485,	GCACACTCTGGATNNNTTCGAAGGTCGG
Ravi-HCK-rev-mut486,	TCCAGCACACTCTGNNNGTATTCGAAGGTC
Ravi-HCK-rev-mut487,	GTCATCCAGCACACTNNNGATGTATTCGAAGGT
Ravi-HCK-rev-mut488,	GAAGTCATCCAGCACNNNCTGGATGTATTCGAA
Ravi-HCK-rev-mut489,	GTGTAGAAGTCATCCAGNNNACTCTGGATGTATTCGA
Ravi-HCK-rev-mut490,	CCGTGTAGAAGTCATCNNNCACACTCTGGATGTAT
Ravi-HCK-rev-mut491,	CCGTGTAGAAGTCNNNCAGCACACTCTGG
Ravi-HCK-rev-mut492,	TGGCCGTGTAGAANNNATCCAGCACACTC
Ravi-HCK-rev-mut493,	TGTGGCCGTGTANNNGTCATCCAGCAC
Ravi-HCK-rev-mut494,	TCTCTGTGGCCGTNNNGAAGTCATCCAG
Ravi-HCK-rev-mut495,	GGCTCTCTGTGGCNNNGTAGAAGTCATCC
Ravi-HCK-rev-mut496,	GTACTGGCTCTCTGTNNNCGTGTAGAAGTCATC

Ravi-HCK-rev-mut497,	GTACTGGCTCTCNNNGGCCGTGTAGAA
Ravi-HCK-rev-mut498,	TTGGTACTGGCTNNNTGTGGCCGTGTA
Ravi-HCK-rev-mut499,	CTGTTGGTACTGNNNCTCTGTGGCCGT
Ravi-HCK-rev-mut500,	ctgCTGTTGGTANNNGCTCTCTGTGGC
Ravi-HCK-rev-mut502,	ctcatggctgCTGNNNGTACTGGCTCTC
Ravi-HCK-rev-mut503,	gaattctcatggctgNNNTTGGTACTGGCTCTC

Bibliography

1. Wiernik, P. H. *Neoplastic Diseases of the Blood*. (Cambridge University Press., 2003).

2. Bennet, J. H. Two cases of hypertrophy of the spleen and liver, in which death took place from suppuration of blood. *Edinburgh Med. Surg. J.* **64**, (1845).

3. Virchow, R. *Die Leukämie- Gesammelte Abhandlungen zur Wissenschaftlichen Medizin*. (1856).

4. W, E. Über die acute Leukämie und Pseudoleukämie. *Deutsch Arch Klin Med* **44**, (1889).

5. O, N. Über rothes Knochenmark und Myeloblasten. *Deutsch Med Wochenschr.* **26**, 287–290 (1990).

6. Yates, J.W., Wallace J., Ellison, R.R., Holland, J. F. Cytosine arabinoside (NSC-63878) and daunorubicin (NSC-83142) therapy in acute non-lymphocytic leukemia. *Cancer Chemother. Rep.* **57**, 485–488 (1973).

7. Siegel, R. L., Miller, K. D. & Jemal, A. Cancer statistics, 2018. *CA. Cancer J. Clin.* **68**, 7–30 (2018).

8. Dores, G. M., Devesa, S. S., Curtis, R. E., Linet, M. S. & Morton, L. M. Acute leukemia incidence and patient survival among children and adults in the United States, 2001-2007. *Blood* **119**, 34–43 (2012).

9. Leone, G., Mele, L., Pulsoni, A., Equitani, F. & Pagano, L. The incidence of secondary leukemias. *Haematologica* **84**, 937–45 (1999).

10. Bennett, J. M. *et al.* Proposals for the classification of the acute leukaemias. French-American-British (FAB) co-operative group. *Br. J. Haematol.* **33**, 451–8 (1976).

11. Bloomfield, C. D. & Brunning, R. D. FAB M7: acute megakaryoblastic leukemia--beyond morphology. *Ann. Intern. Med.* **103**, 450–2 (1985).

12. Lee, E. J., Pollak, A., Leavitt, R. D., Testa, J. R. & Schiffer, C. A. Minimally differentiated acute nonlymphocytic leukemia: a distinct entity. *Blood* **70**, 1400–6 (1987).

13. Duchayne, E., Demur, C., Rubie, H., Robert, A. & Dastugue, N. Diagnosis of acute basophilic leukemia. *Leuk. Lymphoma* **32**, 269–78 (1999).

14. Stasi, R. *et al.* Analysis of treatment failure in patients with minimally differentiated acute myeloid leukemia (AML-M0). *Blood* **83**, 1619–25 (1994).

15. Tallman, M. S. *et al.* Granulocytic sarcoma is associated with the 8;21 translocation in acute myeloid leukemia. *J. Clin. Oncol.* **11**, 690–7 (1993).

16. Sood, R., Kamikubo, Y. & Liu, P. Role of RUNX1 in hematological malignancies. *Blood* **129**, 2070–2082 (2017).

17. HILLESTAD, L. K. Acute promyelocytic leukemia. *Acta Med. Scand.* **159**, 189–94 (1957).

18. Coombs, C. C., Tallman, M. S. & Levine, R. L. Molecular therapy for acute myeloid leukaemia. *Nat. Rev. Clin. Oncol.* (2015). doi:10.1038/nrclinonc.2015.210

19. Adès, L. *et al.* Very long-term outcome of acute promyelocytic leukemia after treatment with all-trans retinoic acid and chemotherapy: the European APL Group experience. *Blood* **115**, 1690–6 (2010).

20. Bennett, J. M. *et al.* Proposed revised criteria for the classification of acute myeloid leukemia. A report of the French-American-British Cooperative Group. *Ann. Intern. Med.* **103**, 620–5 (1985).

21. Arthur, D. C. & Bloomfield, C. D. Partial deletion of the long arm of chromosome 16 and bone marrow eosinophilia in acute nonlymphocytic leukemia: a new association. *Blood* **61**, 994–8 (1983).

22. Hogge, D. E., Misawa, S., Parsa, N. Z., Pollak, A. & Testa, J. R. Abnormalities of chromosome 16 in association with acute myelomonocytic leukemia and dysplastic bone marrow eosinophils. *J. Clin. Oncol.* **2**, 550–7 (1984).

23. Bloomfield, C. D. *et al.* Frequency of prolonged remission duration after high-dose cytarabine intensification in acute myeloid leukemia varies by cytogenetic subtype. *Cancer Res.* **58**, 4173–9 (1998).

24. Ziemin-van der Poel, S. *et al.* Identification of a gene, MLL, that spans the breakpoint in 11q23 translocations associated with human leukemias. *Proc. Natl. Acad. Sci. U. S. A.* **88**, 10735–9 (1991).

25. Seiter, Karen (Department of Internal Medicine, Division of Oncology/Hematology, N. Y. M. C. Acute Myeloid Leukemia Staging. *Medscape* (2015). Available at: https://emedicine.medscape.com/article/2006750-overview#a1.

26. Arber, D. A. *et al.* The 2016 revision to the World Health Organization classification of myeloid neoplasms and acute leukemia. *Blood* **127**, 2391–405 (2016).

27. Larson, R. A. Therapy-related myeloid neoplasms. *Haematologica* **94**, 454–9 (2009).

28. Walter, R. B. *et al.* Significance of FAB subclassification of ‘acute myeloid leukemia, NOS’ in the 2008 WHO classification: analysis of 5848 newly diagnosed patients. *Blood* **121**, 2424–2431 (2013).

29. Yilmaz, A. F., Saydam, G., Sahin, F. & Baran, Y. Granulocytic sarcoma: a systematic review. *Am. J. Blood Res.* **3**, 265–70 (2013).

30. Roy, A., Roberts, I. & Vyas, P. Biology and management of transient abnormal myelopoiesis (TAM) in children with Down syndrome. *Semin. Fetal Neonatal Med.* **17**, 196–201 (2012).

31. Lange, B. J. *et al.* Distinctive demography, biology, and outcome of acute myeloid leukemia and myelodysplastic syndrome in children with Down syndrome: Children's Cancer Group Studies 2861 and 2891. *Blood* **91**, 608–15 (1998).

32. Yoshida, K. *et al.* The landscape of somatic mutations in Down syndrome–related myeloid disorders. *Nat. Genet.* **45**, 1293–1299 (2013).

33. Döhner, H. *et al.* Diagnosis and management of AML in adults: 2017 ELN recommendations from an international expert panel. *Blood* **129**, 424–447 (2017).

34. Ley, T. J. *et al.* DNA sequencing of a cytogenetically normal acute myeloid leukemia genome. *Nature* **456**, 66–72 (2008).

35. Marcucci, G., Haferlach, T. & Döhner, H. Molecular genetics of adult acute myeloid leukemia: Prognostic and therapeutic implications. *J. Clin. Oncol.* **29**, 475–486 (2011).

36. Patel, J. P. *et al.* Prognostic Relevance of Integrated Genetic Profiling in Acute Myeloid Leukemia. *N. Engl. J. Med.* **366**, 1079–1089 (2012).

37. Cancer Genome Atlas Research Network *et al.* Genomic and epigenomic landscapes of adult de novo acute myeloid leukemia. *N. Engl. J. Med.* **368**, 2059–74 (2013).

38. Papaemmanuil, E. *et al.* Genomic Classification and Prognosis in Acute Myeloid Leukemia. *N. Engl. J. Med.* **374**, 2209–2221 (2016).

39. Smith, C. C. *et al.* Validation of ITD mutations in FLT3 as a therapeutic target in human acute myeloid leukaemia. *Nature* **485**, 260–263 (2012).

40. Bolouri, H. *et al.* The molecular landscape of pediatric acute myeloid leukemia reveals recurrent structural alterations and age-specific mutational interactions. *Nat. Med.* **24**, 103–112 (2018).

41. Kandoth, C. *et al.* Mutational landscape and significance across 12 major cancer types. *Nature* **502**, 333–339 (2013).

42. Tyner, J. W. *et al.* Functional genomic landscape of acute myeloid leukaemia. *Nature* **562**, 526–531 (2018).

43. Chen, Z. *et al.* Fusion between a novel Krüppel-like zinc finger gene and the retinoic acid receptor-alpha locus due to a variant t(11;17) translocation associated with acute promyelocytic leukaemia. *EMBO J.* **12**, 1161–1167 (1993).

44. Di Croce, L. Chromatin modifying activity of leukaemia associated fusion proteins. *Hum. Mol. Genet.* **14**, R77–R84 (2005).

45. Saeed, S., Logie, C., Stunnenberg, H. G. & Martens, J. H. A. Genome-wide functions of PML–RARα in acute promyelocytic leukaemia. *Br. J. Cancer* **104**, 554–558 (2011).

46. Liu, P. *et al.* Fusion between transcription factor CBF beta/PEBP2 beta and a myosin heavy chain in acute myeloid leukemia. *Science (80-.).* **261**, 1041–1044 (1993).

47. Haferlach, C. *et al.* AML with CBFB–MYH11 rearrangement demonstrate RAS pathway alterations in 92% of all cases including a high frequency of NF1 deletions. *Leukemia* **24**, 1065–1069 (2010).

48. Okuda, T., Nishimura, M., Nakao, M. & Fujitaa, Y. RUNX1/AML1: A Central Player in Hematopoiesis. *Int. J. Hematol.* **74**, 252–257 (2001).

49. Lin, T.-C. *et al.* CEBPA methylation as a prognostic biomarker in patients with de novo acute myeloid leukemia. *Leukemia* **25**, 32–40 (2011).

50. El-Sharnouby, J. A., Ahmed, L. M. S., Taha, A. M. & Kamal, O. Prognostic significance of CEBPA mutations and BAALC expression in acute myeloid leukemia Egyptian patients with normal karyotype. *Egypt. J. Immunol.* **15**, 131–43 (2008).

51. Radomska, H. S. *et al.* A Cell-Based High-Throughput Screening for Inducers of Myeloid Differentiation. *J. Biomol. Screen.* **20**, 1150–1159 (2015).

52. Falini, B. *et al.* Altered nucleophosmin transport in acute myeloid leukaemia with mutated NPM1: molecular basis and clinical implications. *Leukemia* **23**, 1731–1743 (2009).

53. Falini, B. Immunohistochemistry predicts nucleophosmin (NPM) mutations in acute myeloid leukemia. *Blood* **108**, 1999–2005 (2006).

54. Jia, Y. *et al.* Negative regulation of DNMT3A de novo DNA methylation by frequently overexpressed UHRF family proteins as a mechanism for widespread DNA hypomethylation in cancer. *Cell Discov.* **2**, 16007 (2016).

55. Thol, F. *et al.* Incidence and Prognostic Influence of DNMT3A Mutations in Acute Myeloid Leukemia. *J. Clin. Oncol.* **29**, 2889–2896 (2011).

56. Gowher, H. *et al.* Mutational Analysis of the Catalytic Domain of the Murine Dnmt3a DNA-(cytosine C5)-methyltransferase. *J. Mol. Biol.* **357**, 928–941 (2006).

57. Saygin, C. *et al.* Mutations in DNMT3A, U2AF1, and EZH2 identify intermediate-risk acute myeloid leukemia patients with poor outcome after CR1. *Blood Cancer J.* **8**, (2018).

58. Ley, T. J. *et al.* DNMT3A Mutations in Acute Myeloid Leukemia. *N. Engl. J. Med.* **363**, 2424–2433 (2010).

59. Tahiliani, M. *et al.* Conversion of 5-Methylcytosine to 5-Hydroxymethylcytosine in Mammalian DNA by MLL Partner TET1. *Science (80-.).* **324**, 930–935 (2009).

60. Valinluck, V. Oxidative damage to methyl-CpG sequences inhibits the binding of the methyl-CpG binding domain (MBD) of methyl-CpG binding protein 2 (MeCP2). *Nucleic Acids Res.* **32**, 4100–4108 (2004).

61. Pastor, W. A. *et al.* Genome-wide mapping of 5-hydroxymethylcytosine in embryonic stem cells. *Nature* **473**, 394–397 (2011).

62. Ko, M. *et al.* Impaired hydroxylation of 5-methylcytosine in myeloid cancers with mutant TET2. *Nature* **468**, 839–843 (2010).

63. Mardis, E. R. *et al.* Recurring Mutations Found by Sequencing an Acute Myeloid Leukemia Genome. *N. Engl. J. Med.* **361**, 1058–1066 (2009).

64. Marcucci, G. *et al.* IDH1 and IDH2 Gene Mutations Identify Novel Molecular Subsets Within De Novo Cytogenetically Normal Acute Myeloid Leukemia: A Cancer and Leukemia Group B Study. *J. Clin. Oncol.* **28**, 2348–2355 (2010).

65. Ward, P. S. *et al.* The Common Feature of Leukemia-Associated IDH1 and IDH2 Mutations Is a Neomorphic Enzyme Activity Converting α-Ketoglutarate to 2-Hydroxyglutarate. *Cancer Cell* **17**, 225–234 (2010).

66. Dang, L. *et al.* Cancer-associated IDH1 mutations produce 2-hydroxyglutarate. *Nature* **462**, 739–744 (2009).

67. Akalin, A. *et al.* Base-Pair Resolution DNA Methylation Sequencing Reveals Profoundly Divergent Epigenetic Landscapes in Acute Myeloid Leukemia. *PLoS Genet.* **8**, e1002781 (2012).

68. Xu, W. *et al.* Oncometabolite 2-Hydroxyglutarate Is a Competitive Inhibitor of α-Ketoglutarate-Dependent Dioxygenases. *Cancer Cell* **19**, 17–30 (2011).

69. Figueroa, M. E. *et al.* Leukemic IDH1 and IDH2 Mutations Result in a Hypermethylation Phenotype, Disrupt TET2 Function, and Impair Hematopoietic Differentiation. *Cancer Cell* **18**, 553–567 (2010).

70. Chowdhury, R. *et al.* The oncometabolite 2-hydroxyglutarate inhibits histone lysine demethylases. *EMBO Rep.* **12**, 463–469 (2011).

71. Bourdon, J.-C., Surget, S. & Khoury, M. P. Uncovering the role of p53 splice variants in human malignancy: a clinical perspective. *Onco. Targets. Ther.* 57 (2013). doi:10.2147/OTT.S53876

72. Hou, H.-A. *et al.* TP53 mutations in de novo acute myeloid leukemia patients: longitudinal follow-ups show the mutation is stable during disease evolution. *Blood Cancer J.* **5**, e331–e331 (2015).

73. Ruteshouser, E. C., Robinson, S. M. & Huff, V. Wilms tumor genetics: mutations in WT1, WTX, and CTNNB1 account for only about one-third of tumors. *Genes. Chromosomes Cancer* **47**, 461–70 (2008).

74. Yang, L., Han, Y., Suarez Saiz, F., Saurez Saiz, F. & Minden, M. D. A tumor suppressor and oncogene: the WT1 story. *Leukemia* **21**, 868–76 (2007).

75. Maheswaran, S. *et al.* Physical and functional interaction between WT1 and p53 proteins. *Proc. Natl. Acad. Sci. U. S. A.* **90**, 5100–4 (1993).

76. Bansal, H. *et al.* Heat shock protein 90 regulates the expression of Wilms tumor 1 protein in myeloid leukemias. *Blood* **116**, 4591–4599 (2010).

77. Rong, Y. *et al.* Wilms' Tumor 1 and Signal Transducers and Activators of Transcription 3 Synergistically Promote Cell Proliferation: A Possible Mechanism in Sporadic Wilms' Tumor. *Cancer Res.* **66**, 8049–8057 (2006).

78. Wang, Y. *et al.* WT1 Recruits TET2 to Regulate Its Target Gene Expression and Suppress Leukemia Cell Proliferation. *Mol. Cell* **57**, 662–673 (2015).

79. Baird, P. N. & Simmons, P. J. Expression of the Wilms' tumor gene (WT1) in normal hemopoiesis. *Exp. Hematol.* **25**, 312–20 (1997).

80. Ellisen, L. W. The Wilms tumor suppressor WT1 directs stage-specific quiescence and differentiation of human hematopoietic progenitor cells. *EMBO J.* **20**, 1897–1909 (2001).

81. Svedberg, H., Richter, J. & Gullberg, U. Forced expression of the Wilms tumor 1 (WT1) gene inhibits proliferation of human hematopoietic CD34(+) progenitor cells. *Leukemia* **15**, 1914–22 (2001).

82. Miyagi, T. *et al.* Expression of the candidate Wilm's tumor gene, WT1, in human leukemia cells. *Leukemia* **7**, 970–7 (1993).

83. Menssen, H. D. *et al.* Presence of Wilms' tumor gene (wt1) transcripts and the WT1 nuclear protein in the majority of human acute leukemias. *Leukemia* **9**, 1060–7 (1995).

84. Tamaki, H. *et al.* The Wilms' tumor gene WT1 is a good marker for diagnosis of disease progression of myelodysplastic syndromes. *Leukemia* **13**, 393–9 (1999).

85. King-Underwood, L. & Pritchard-Jones, K. Wilms' tumor (WT1) gene mutations occur mainly in acute myeloid leukemia and may confer drug resistance. *Blood* **91**, 2961–8 (1998).

86. King-Underwood, L., Renshaw, J. & Pritchard-Jones, K. Mutations in the Wilms' tumor gene WT1 in leukemias. *Blood* **87**, 2171–9 (1996).

87. Rampal, R. *et al.* DNA hydroxymethylation profiling reveals that WT1 mutations result in loss of TET2 function in acute myeloid leukemia. *Cell Rep.* **9**, 1841–1855 (2014).

88. Lower, K. M. *et al.* Mutations in PHF6 are associated with Börjeson–Forssman –Lehmann syndrome. *Nat. Genet.* **32**, 661–665 (2002).

89. Voss, A. K. *et al.* Protein and gene expression analysis of Phf6, the gene mutated in the Börjeson–Forssman–Lehmann Syndrome of intellectual disability and obesity. *Gene Expr. Patterns* **7**, 858–871 (2007).

90. BORJESON, M., FORSSMAN, H. & LEHMANN, O. An X-linked, recessively inherited syndrome characterized by grave mental deficiency, epilepsy, and endocrine disorder. *Acta Med. Scand.* **171**, 13–21 (1962).

91. Van Vlierberghe, P. *et al.* PHF6 mutations in adult acute myeloid leukemia. *Leukemia* **25**, 130–134 (2011).

92. Jakovcevski, M. *et al.* Neuronal Kmt2a/Mll1 Histone Methyltransferase Is Essential for Prefrontal Synaptic Plasticity and Working Memory. *J. Neurosci.* **35**, 5097–5108 (2015).

93. Slovak, M. L. *et al.* Karyotypic analysis predicts outcome of preremission and postremission therapy in adult acute myeloid leukemia: a Southwest Oncology Group/Eastern Cooperative Oncology Group Study. *Blood* **96**, 4075–83 (2000).

94. Balgobind, B. V. *et al.* Novel prognostic subgroups in childhood 11q23/MLL-rearranged acute myeloid leukemia: results of an international retrospective study. *Blood* **114**, 2489–2496 (2009).

95. Döhner, K. *et al.* Prognostic Significance of Partial Tandem Duplications of the MLL Gene in Adult Patients 16 to 60 Years Old With Acute Myeloid Leukemia and Normal Cytogenetics: A Study of the Acute Myeloid Leukemia Study Group Ulm. *J. Clin. Oncol.* **20**, 3254–3261 (2002).

96. Steudel, C. *et al.* Comparative analysis of MLL partial tandem duplication and FLT3 internal tandem duplication mutations in 956 adult patients with acute myeloid leukemia. *Genes, Chromosom. Cancer* **37**, 237–251 (2003).

97. Whitman, S. P. *et al.* Long-term disease-free survivors with cytogenetically normal acute myeloid leukemia and MLL partial tandem duplication: a Cancer and Leukemia Group B study. *Blood* **109**, 5164–5167 (2007).

98. Meyer, C. *et al.* The MLL recombinome of acute leukemias in 2013. *Leukemia* **27**, 2165–2176 (2013).

99. Slany, R. K., Lavau, C. & Cleary, M. L. The oncogenic capacity of HRX-ENL requires the transcriptional transactivation activity of ENL and the DNA binding motifs of HRX. *Mol. Cell. Biol.* **18**, 122–9 (1998).

100. Corral, J. *et al.* An Mll-AF9 fusion gene made by homologous recombination causes acute leukemia in chimeric mice: a method to create fusion oncogenes. *Cell* **85**, 853–61 (1996).

101. Erfurth, F., Hemenway, C. S., de Erkenez, A. C. & Domer, P. H. MLL fusion partners AF4 and AF9 interact at subnuclear foci. *Leukemia* **18**, 92–102 (2004).

102. Bitoun, E., Oliver, P. L. & Davies, K. E. The mixed-lineage leukemia fusion partner AF4 stimulates RNA polymerase II transcriptional elongation and mediates coordinated chromatin remodeling. *Hum. Mol. Genet.* **16**, 92–106 (2007).

103. Mueller, D. *et al.* A role for the MLL fusion partner ENL in transcriptional elongation and chromatin modification. *Blood* **110**, 4445–4454 (2007).

104. Mueller, D. *et al.* Misguided transcriptional elongation causes mixed lineage leukemia. *PLoS Biol.* **7**, e1000249 (2009).

105. So, C. W., Lin, M., Ayton, P. M., Chen, E. H. & Cleary, M. L. Dimerization contributes to oncogenic activation of MLL chimeras in acute leukemias. *Cancer Cell* **4**, 99–110 (2003).

106. Winters, A. C. & Bernt, K. M. MLL-Rearranged Leukemias—An Update on Science and Clinical Approaches. *Front. Pediatr.* **5**, (2017).

107. Armstrong, S. A. *et al.* MLL translocations specify a distinct gene expression profile that distinguishes a unique leukemia. *Nat. Genet.* **30**, 41–47 (2002).

108. Yeoh, E.-J. *et al.* Classification, subtype discovery, and prediction of outcome in pediatric acute lymphoblastic leukemia by gene expression profiling. *Cancer Cell* **1**, 133–143 (2002).

109. Rozovskaia, T. *et al.* Expression profiles of acute lymphoblastic and myeloblastic leukemias with ALL-1 rearrangements. *Proc. Natl. Acad. Sci.* **100**, 7853–7858 (2003).

110. Li, Z. *et al.* Consistent Deregulation of Gene Expression between Human and Murine MLL Rearrangement Leukemias. *Cancer Res.* **69**, 1109–1116 (2009).

111. Kroon, E. Hoxa9 transforms primary bone marrow cells through specific collaboration with Meis1a but not Pbx1b. *EMBO J.* **17**, 3714–3725 (1998).

112. Lawrence, H. J. *et al.* Mice bearing a targeted interruption of the homeobox gene HOXA9 have defects in myeloid, erythroid, and lymphoid hematopoiesis. *Blood* **89**, 1922–30 (1997).

113. Wong, P., Iwasaki, M., Somervaille, T. C. P., So, C. W. E. & Cleary, M. L. Meis1 is an essential and rate-limiting regulator of MLL leukemia stem cell potential. *Genes Dev.* **21**, 2762–2774 (2007).

114. Lim, R. Y. H., Aebi, U. & Fahrenkrog, B. Towards reconciling structure and function in the nuclear pore complex. *Histochem. Cell Biol.* **129**, 105–116 (2008).

115. Chatel, G., Desai, S. H., Mattheyses, A. L., Powers, M. A. & Fahrenkrog, B. Domain topology of nucleoporin Nup98 within the nuclear pore complex. *J. Struct. Biol.* **177**, 81–9 (2012).

116. Oka, M. *et al.* The mobile FG nucleoporin Nup98 is a cofactor for Crm1-dependent protein export. *Mol. Biol. Cell* **21**, 1885–96 (2010).

117. Blevins, M. B., Smith, A. M., Phillips, E. M. & Powers, M. A. Complex Formation among the RNA Export Proteins Nup98, Rae1/Gle2, and TAP. *J. Biol. Chem.* **278**, 20979–20988 (2003).

118. Liang, Y., Franks, T. M., Marchetto, M. C., Gage, F. H. & Hetzer, M. W. Dynamic association of NUP98 with the human genome. *PLoS Genet.* **9**, e1003308 (2013).

119. Rosenblum, J. S. & Blobel, G. Autoproteolysis in nucleoporin biogenesis. *Proc. Natl. Acad. Sci. U. S. A.* **96**, 11370–5 (1999).

120. Kasper, L. H. *et al.* CREB binding protein interacts with nucleoporin-specific FG repeats that activate transcription and mediate NUP98-HOXA9 oncogenicity. *Mol. Cell. Biol.* **19**, 764–76 (1999).

121. Bai, X.-T. *et al.* Trans-repressive effect of NUP98-PMX1 on PMX1-regulated c-FOS gene through recruitment of histone deacetylase 1 by FG repeats. *Cancer Res.* **66**, 4584–90 (2006).

122. Gough, S. M., Slape, C. I. & Aplan, P. D. NUP98 gene fusions and hematopoietic malignancies: common themes and new biologic insights. *Blood* **118**, 6247–57 (2011).

123. Pineault, N. Induction of acute myeloid leukemia in mice by the human leukemia-specific fusion gene NUP98-HOXD13 in concert with Meis1. *Blood* **101**, 4529–4538 (2003).

124. Chou, W.-C. *et al.* Distinct clinical and biological features of de novo acute myeloid leukemia with additional sex comb-like 1 (ASXL1) mutations. *Blood* **116**, 4086–4094 (2010).

125. Cho, Y.-S., Kim, E.-J., Park, U.-H., Sin, H.-S. & Um, S.-J. Additional Sex Comb-like 1 (ASXL1), in Cooperation with SRC-1, Acts as a Ligand-dependent Coactivator for Retinoic Acid Receptor. *J. Biol. Chem.* **281**, 17588–17598 (2006).

126. Fisher, C. L., Berger, J., Randazzo, F. & Brock, H. W. A human homolog of Additional sex combs, ADDITIONAL SEX COMBS-LIKE 1, maps to chromosome 20q11. *Gene* **306**, 115–26 (2003).

127. Voisset, E. *et al.* FES kinases are required for oncogenic FLT3 signaling. *Leuk. Off. J. Leuk. Soc. Am. Leuk. Res. Fund, U.K* **24**, 721–728 (2010).

128. Yang, H. *et al.* Gain of function of ASXL1 truncating protein in the pathogenesis of myeloid malignancies. *Blood* **131**, 328–341 (2018).

129. Devaiah, B. N. *et al.* BRD4 is a histone acetyltransferase that evicts nucleosomes from chromatin. *Nat. Struct. Mol. Biol.* **23**, 540–548 (2016).

130. Pratcorona, M. *et al.* Acquired mutations in ASXL1 in acute myeloid leukemia: prevalence and prognostic value. *Haematologica* **97**, 388–392 (2012).

131. Cao, R. *et al.* Role of Histone H3 Lysine 27 Methylation in Polycomb-Group Silencing. *Science (80-.).* **298**, 1039–1043 (2002).

132. Margueron, R. & Reinberg, D. The Polycomb complex PRC2 and its mark in life. *Nature* **469**, 343–349 (2011).

133. Morin, R. D. *et al.* Somatic mutations altering EZH2 (Tyr641) in follicular and diffuse large B-cell lymphomas of germinal-center origin. *Nat. Genet.* **42**, 181–185 (2010).

134. Tanaka, S. *et al.* Ezh2 augments leukemogenicity by reinforcing differentiation blockage in acute myeloid leukemia. *Blood* **120**, 1107–1117 (2012).

135. Knutson, S. K. *et al.* A selective inhibitor of EZH2 blocks H3K27 methylation and kills mutant lymphoma cells. *Nat. Chem. Biol.* **8**, 890–896 (2012).

136. Dvinge, H. & Bradley, R. K. Widespread intron retention diversifies most cancer transcriptomes. *Genome Med.* **7**, 45 (2015).

137. Steensma, D. P. *et al.* Clonal hematopoiesis of indeterminate potential and its distinction from myelodysplastic syndromes. *Blood* **126**, 9–16 (2015).

138. Saez, B., Walter, M. J. & Graubert, T. A. Splicing factor gene mutations in hematologic malignancies. *Blood* **129**, 1260–1269 (2017).

139. Barber, T. D. *et al.* Chromatid cohesion defects may underlie chromosome instability in human colorectal cancers. *Proc. Natl. Acad. Sci.* **105**, 3443–3448 (2008).

140. Thol, F. *et al.* Mutations in the cohesin complex in acute myeloid leukemia: clinical and prognostic implications. *Blood* **123**, 914–920 (2014).

141. Thiede, C. *et al.* Analysis of FLT3-activating mutations in 979 patients with acute myelogenous leukemia: association with FAB subtypes and identification of subgroups with poor prognosis. *Blood* **99**, 4326–35 (2002).

142. Grafone, T., Palmisano, M., Nicci, C. & Storti, S. An overview on the role of FLT3-tyrosine kinase receptor in acute myeloid leukemia: biology and treatment. *Oncol. Rev.* **6**, 8 (2012).

143. Griffith, J. *et al.* The Structural Basis for Autoinhibition of FLT3 by the Juxtamembrane Domain. *Mol. Cell* **13**, 169–178 (2004).

144. Leick, M. B. & Levis, M. J. The Future of Targeting FLT3 Activation in AML. *Curr. Hematol. Malig. Rep.* 1–15 (2017). doi:10.1007/s11899-017-0381-2

145. Yamamoto, Y. *et al.* Activating mutation of D835 within the activation loop of FLT3 in human hematologic malignancies. *Blood* **97**, 2434–2439 (2001).

146. Bailey, E. *et al.* FLT3/D835Y mutation knock-in mice display less aggressive disease compared with FLT3/internal tandem duplication (ITD) mice. *Proc. Natl. Acad. Sci. U. S. A.* **110**, 21113–8 (2013).

147. Miettinen, M. & Lasota, J. Gastrointestinal stromal tumors: review on morphology, molecular pathology, prognosis, and differential diagnosis. *Arch. Pathol. Lab. Med.* **130**, 1466–78 (2006).

148. Paschka, P. *et al.* Adverse Prognostic Significance of KIT Mutations in Adult Acute Myeloid Leukemia With inv(16) and t(8;21): A Cancer and Leukemia Group B Study. *J. Clin. Oncol.* **24**, 3904–3911 (2006).

149. Beghini, A. *et al.* C-kit mutations in core binding factor leukemias. *Blood* **95**, 726–7 (2000).

150. Boissel, N. *et al.* Incidence and prognostic impact of c-Kit, FLT3, and Ras gene mutations in core binding factor acute myeloid leukemia (CBF-AML). *Leukemia* **20**, 965–970 (2006).

151. Schnittger, S. KIT-D816 mutations in AML1-ETO-positive AML are associated with impaired event-free and overall survival. *Blood* **107**, 1791–1799 (2006).

152. Galanis, A. & Levis, M. Inhibition of c-kit by tyrosine kinase inhibitors. *Haematologica* **100**, E77–E79 (2015).

153. Mulet-Margalef, N. & Garcia del Muro, X. Sunitinib in the treatment of gastrointestinal stromal tumor: patient selection and perspectives. *Onco. Targets. Ther.* **Volume 9**, 7573–7582 (2016).

154. Zhang, Z., Jiang, T., Wang, W. & Piao, D. Efficacy and safety of regorafenib for advanced gastrointestinal stromal tumor after failure with imatinib and sunitinib treatment. *Medicine (Baltimore).* **96**, e8698 (2017).

155. Siehl, J. & Thiel, E. C-kit, GIST, and imatinib. *Recent Results Cancer Res.* **176**, 145–51 (2007).

156. Downward, J. Targeting RAS signalling pathways in cancer therapy. *Nat. Rev. Cancer* **3**, 11–22 (2003).

157. Sanchez-Vega, F. *et al.* Oncogenic Signaling Pathways in The Cancer Genome Atlas. *Cell* **173**, 321-337.e10 (2018).

158. Liu, X. *et al.* RAS mutations in acute myeloid leukaemia patients: A review and meta-analysis. *Clin. Chim. Acta* **489**, 254–260 (2019).

159. Pylayeva-Gupta, Y., Grabocka, E. & Bar-Sagi, D. RAS oncogenes: weaving a tumorigenic web. *Nat. Rev. Cancer* **11**, 761–774 (2011).

160. Zhao, Y. & Adjei, A. A. The clinical development of MEK inhibitors. *Nat. Rev. Clin. Oncol.* **11**, 385–400 (2014).

161. Kolch, W. Coordinating ERK/MAPK signalling through scaffolds and inhibitors. *Nat. Rev. Mol. Cell Biol.* **6**, 827–837 (2005).

162. NITULESCU, G. M. *et al.* Akt inhibitors in cancer treatment: The long journey from drug discovery to clinical use (Review). *Int. J. Oncol.* **48**, 869–885 (2016).

163. Benjamin, D., Colombi, M., Moroni, C. & Hall, M. N. Rapamycin passes the torch: a new generation of mTOR inhibitors. *Nat. Rev. Drug Discov.* **10**, 868–880 (2011).

164. Massacesi, C. *et al.* PI3K inhibitors as new cancer therapeutics: implications for clinical trial design. *Onco. Targets. Ther.* 203 (2016). doi:10.2147/OTT.S89967

165. Lal, R., Harris, D., Postel-Vinay, S. & de Bono, J. Reovirus: Rationale and clinical trial update. *Curr. Opin. Mol. Ther.* **11**, 532–9 (2009).

166. Fu, X., Tao, L. & Zhang, X. 157. A Mutant Type 2 Herpes Simplex Virus Deleted for the Protein Kinase Domain of the ICP10 Gene Is a Potent Oncolytic Virus. *Mol. Ther.* **13**, S61–S62 (2006).

167. Chavda, B., Arnott, J. A. & Planey, S. L. Targeting protein palmitoylation: selective inhibitors and implications in disease. *Expert Opin. Drug Discov.* **9**, 1005–1019 (2014).

168. Bacher, U. Implications of NRAS mutations in AML: a study of 2502 patients. *Blood* **107**, 3847–3853 (2006).

169. Bowen, D. T. RAS mutation in acute myeloid leukemia is associated with distinct cytogenetic subgroups but does not influence outcome in patients younger than 60 years. *Blood* **106**, 2113–2119 (2005).

170. Bollu, L. R., Mazumdar, A., Savage, M. I. & Brown, P. H. Molecular Pathways: Targeting Protein Tyrosine Phosphatases in Cancer. *Clin Cancer Res.* **23**, 2136–2142 (2017).

171. Stevenson, W. S. *et al.* DNA methylation of membrane-bound tyrosine phosphatase genes in acute lymphoblastic leukaemia. *Leukemia* **28**, 787–793 (2014).

172. Motiwala, T. *et al.* Suppression of the protein tyrosine phosphatase receptor type O gene (PTPRO) by methylation in hepatocellular carcinomas. *Oncogene* **22**, 6319–6331 (2003).

173. Shimozato, O. *et al.* Receptor-type protein tyrosine phosphatase κ directly dephosphorylates CD133 and regulates downstream AKT activation. *Oncogene* **34**, 1949–1960 (2015).

174. Xu, Y., Xue, S., Zhou, J., Voorhees, J. J. & Fisher, G. J. Notch and TGF-β pathways cooperatively regulate receptor protein tyrosine phosphatase-κ (PTPRK) gene expression in human primary keratinocytes. *Mol. Biol. Cell* **26**, 1199–1206 (2015).

175. Chen, Y.-W. *et al.* Receptor-type tyrosine-protein phosphatase directly targets STAT3 activation for tumor suppression in nasal NK/T-cell lymphoma. *Blood* **125**, 1589–1600 (2015).

176. Motiwala, T. *et al.* Protein tyrosine phosphatase receptor-type O (PTPRO) exhibits characteristics of a candidate tumor suppressor in human lung cancer. *Proc. Natl. Acad. Sci.* **101**, 13844–13849 (2004).

177. Xu, R. Overexpression of Shp2 tyrosine phosphatase is implicated in leukemogenesis in adult human leukemia. *Blood* **106**, 3142–3149 (2005).

178. Tartaglia, M., Cotter, P. D., Zampino, G., Gelb, B. D. & Rauen, K. A. Exclusion of PTPN11 mutations in Costello syndrome: further evidence for distinct genetic etiologies for Noonan, cardio-facio-cutaneous and Costello syndromes. *Clin. Genet.* **63**, 423–6 (2003).

179. Díaz, M. E. *et al.* Growth hormone modulation of EGF-induced PI3K-Akt pathway in mice liver. *Cell. Signal.* **24**, 514–523 (2012).

180. Dance, M., Montagner, A., Salles, J.-P., Yart, A. & Raynal, P. The molecular functions of Shp2 in the Ras/Mitogen-activated protein kinase (ERK1/2) pathway. *Cell. Signal.* **20**, 453–459 (2008).

181. Büchner, T. *et al.* Acute Myeloid Leukemia (AML): Different Treatment Strategies Versus a Common Standard Arm—Combined Prospective Analysis by the German AML Intergroup. *J. Clin. Oncol.* **30**, 3604–3610 (2012).

182. Koreth, J. *et al.* Allogeneic Stem Cell Transplantation for Acute Myeloid Leukemia in First Complete Remission. *JAMA* **301**, 2349 (2009).

183. Yanada, M., Matsuo, K., Emi, N. & Naoe, T. Efficacy of allogeneic hematopoietic stem cell transplantation depends on cytogenetic risk for acute myeloid leukemia in first disease remission. *Cancer* **103**, 1652–1658 (2005).

184. Röllig, C. *et al.* Allogeneic Stem-Cell Transplantation in Patients With NPM1 -Mutated Acute Myeloid Leukemia: Results From a Prospective Donor Versus No-Donor Analysis of Patients After Upfront HLA Typing Within the SAL-AML 2003 Trial. *J. Clin. Oncol.* **33**, 403–410 (2015).

185. Cornelissen, J. J. *et al.* Results of a HOVON/SAKK donor versus no-donor analysis of myeloablative HLA-identical sibling stem cell transplantation in first remission acute myeloid leukemia in young and middle-aged adults: benefits for whom? *Blood* **109**, 3658–3666 (2007).

186. Schetelig, J. *et al.* Hematopoietic cell transplantation in patients with intermediate and high-risk AML: results from the randomized Study Alliance Leukemia (SAL) AML 2003 trial. *Leukemia* **29**, 1060–1068 (2015).

187. Li, D. *et al.* Efficacy of Allogeneic Hematopoietic Stem Cell Transplantation in Intermediate-Risk Acute Myeloid Leukemia Adult Patients in First Complete Remission: A Meta-Analysis of Prospective Studies. *PLoS One* **10**, e0132620 (2015).

188. Estey, E. H. Acute myeloid leukemia: 2014 Update on risk-stratification and management. *Am. J. Hematol.* **89**, 1063–1081 (2014).

189. Gong, Q. *et al.* High Doses of Daunorubicin during Induction Therapy of Newly Diagnosed Acute Myeloid Leukemia: A Systematic Review and Meta-Analysis of Prospective Clinical Trials. *PLoS One* **10**, e0125612 (2015).

190. Li, X., Xu, S., Tan, Y. & Chen, J. The effects of idarubicin versus other anthracyclines for induction therapy of patients with newly diagnosed leukaemia. *Cochrane Database Syst. Rev.* (2015). doi:10.1002/14651858.CD010432.pub2

191. Bishop, J. F. The treatment of adult acute myeloid leukemia. *Semin. Oncol.* **24**, 57–69 (1997).

192. Lichtman, M. A. A historical perspective on the development of the cytarabine (7days) and daunorubicin (3days) treatment regimen for acute myelogenous leukemia: 2013 the 40th anniversary of 7+3. *Blood Cells, Mol. Dis.* **50**, 119–130 (2013).

193. Lowenberg, B. Sense and nonsense of high-dose cytarabine for acute myeloid leukemia. *Blood* **121**, 26–28 (2013).

194. Löwenberg, B. *et al.* Cytarabine Dose for Acute Myeloid Leukemia. *N. Engl. J. Med.* **364**, 1027–1036 (2011).

195. Burnett, A. K. *et al.* Optimization of Chemotherapy for Younger Patients With Acute Myeloid Leukemia: Results of the Medical Research Council AML15 Trial. *J. Clin. Oncol.* **31**, 3360–3368 (2013).

196. Stone, R. M. *et al.* Midostaurin plus Chemotherapy for Acute Myeloid Leukemia with a *FLT3* Mutation. *N. Engl. J. Med.* **377**, 454–464 (2017).

197. Galmarini, C. M. *et al.* In vivo mechanisms of resistance to cytarabine in acute myeloid leukaemia. *Br. J. Haematol.* **117**, 860–8 (2002).

198. Drake, J. C., Hande, K. R., Fuller, R. W. & Chabner, B. A. Cytidine and deoxycytidylate deaminase inhibition by uridine analogs. *Biochem. Pharmacol.* **29**, 807–811 (1980).

199. Macanas-Pirard, P. *et al.* Resistance of leukemia cells to cytarabine chemotherapy is mediated by bone marrow stroma, involves cell-surface equilibrative nucleoside transporter-1 removal and correlates with patient outcome. *Oncotarget* **8**, (2017).

200. Schneider, C. *et al.* SAMHD1 is a biomarker for cytarabine response and a therapeutic target in acute myeloid leukemia. *Nat. Med.* **23**, 250–255 (2017).

201. Gewirtz, D. A critical evaluation of the mechanisms of action proposed for the antitumor effects of the anthracycline antibiotics adriamycin and daunorubicin. *Biochem. Pharmacol.* **57**, 727–741 (1999).

202. Cutts, S., Rephaeli, A., Nudelman, A., Ugarenko, M. & Phillips, D. Potential Therapeutic Advantages of Doxorubicin when Activated by Formaldehyde to Function as a DNA Adduct-Forming Agent. *Curr. Top. Med. Chem.* **15**, 1409–1422 (2015).

203. Marinello, J., Delcuratolo, M. & Capranico, G. Anthracyclines as Topoisomerase II Poisons: From Early Studies to New Perspectives. *Int. J. Mol. Sci.* **19**, 3480 (2018).

204. Angsutararux, P., Luanpitpong, S. & Issaragrisil, S. Chemotherapy-Induced Cardiotoxicity: Overview of the Roles of Oxidative Stress. *Oxid. Med. Cell. Longev.* **2015**, 1–13 (2015).

205. Pfizer. Cytarabine package insert. (2011). Available at: https://www.pfizer.com/sites/default/files/products/uspi_cytarabine_1000mg.pdf.

206. Laboratories, B. Daunorubicin package insert. (2013). Available at: https://docs.boehringer-ingelheim.com/Prescribing Information/PIs/Ben Venue_Bedford Labs/55390-108-01 DNOP_AQ 20mg/5539010801.

207. Zhu, J. *et al.* Retinoic acid induces proteasome-dependent degradation of retinoic acid receptor alpha (RARalpha) and oncogenic RARalpha fusion proteins. *Proc. Natl. Acad. Sci. U. S. A.* **96**, 14807–12 (1999).

208. Nervi, C. *et al.* Caspases mediate retinoic acid-induced degradation of the acute promyelocytic leukemia PML/RARalpha fusion protein. *Blood* **92**, 2244–51 (1998).

209. Lo-Coco, F. *et al.* Retinoic Acid and Arsenic Trioxide for Acute Promyelocytic Leukemia. *N. Engl. J. Med.* **369**, 111–121 (2013).

210. Wang, F. *et al.* Targeted Inhibition of Mutant IDH2 in Leukemia Cells Induces Cellular Differentiation. *Science (80-.).* **340**, 622–626 (2013).

211. Yen, K. *et al.* AG-221, a First-in-Class Therapy Targeting Acute Myeloid Leukemia Harboring Oncogenic IDH2 Mutations. *Cancer Discov.* **7**, 478–493 (2017).

212. Stein, E. M. *et al.* Enasidenib in mutant IDH2 relapsed or refractory acute myeloid leukemia. *Blood* **130**, 722–731 (2017).

213. Amatangelo, M. D. *et al.* Enasidenib induces acute myeloid leukemia cell differentiation to promote clinical response. *Blood* **130**, 732–741 (2017).

214. Kim, E. S. Enasidenib: First Global Approval. *Drugs* **77**, 1705–1711 (2017).

215. Chaturvedi, A. *et al.* Pan-mutant-IDH1 inhibitor BAY1436032 is highly effective against human IDH1 mutant acute myeloid leukemia in vivo. 2020–2028 (2017). doi:10.1038/leu.2017.46

216. Garnache-Ottou, F. Expression of the myeloid-associated marker CD33 is not an exclusive factor for leukemic plasmacytoid dendritic cells. *Blood* **105**, 1256–1264 (2004).

217. Macauley, M. S., Crocker, P. R. & Paulson, J. C. Siglec-mediated regulation of immune cell function in disease. *Nat. Rev. Immunol.* **14**, 653–666 (2014).

218. Laszlo, G. S., Estey, E. H. & Walter, R. B. The past and future of CD33 as therapeutic target in acute myeloid leukemia. *Blood Rev.* **28**, 143–153 (2014).

219. Feldman, E. J. *et al.* Phase III Randomized Multicenter Study of a Humanized Anti-CD33 Monoclonal Antibody, Lintuzumab, in Combination With Chemotherapy, Versus Chemotherapy Alone in Patients With Refractory or First-Relapsed Acute Myeloid Leukemia. *J. Clin. Oncol.* **23**, 4110–4116 (2005).

220. Borthakur, G. *et al.* Phase 1 study of an anti-CD33 immunotoxin, humanized monoclonal antibody M195 conjugated to recombinant gelonin (HUM-195/rGEL), in patients with advanced myeloid malignancies. *Haematologica* **98**, 217–221 (2013).

221. Godwin, C. D., Gale, R. P. & Walter, R. B. Gemtuzumab ozogamicin in acute myeloid leukemia. **31**, 1855–1868 (2017).

222. Rowe, J. M. & Lowenberg, B. Gemtuzumab ozogamicin in acute myeloid leukemia: a remarkable saga about an active drug. *Blood* **121**, 4838–4841 (2013).

223. Walter, R. B. Investigational CD33-targeted therapeutics for acute myeloid leukemia. *Expert Opin. Investig. Drugs* **27**, 339–348 (2018).

224. O'Hear, C., Heiber, J. F., Schubert, I., Fey, G. & Geiger, T. L. Anti-CD33 chimeric antigen receptor targeting of acute myeloid leukemia. *Haematologica* **100**, 336–344 (2015).

225. Pizzitola, I. *et al.* Chimeric antigen receptors against CD33/CD123 antigens efficiently target primary acute myeloid leukemia cells in vivo. *Leukemia* **28**, 1596–1605 (2014).

226. Li, S. *et al.* CD33-Specific Chimeric Antigen Receptor T Cells with Different Co-Stimulators Showed Potent Anti-Leukemia Efficacy and Different Phenotype. *Hum. Gene Ther.* **29**, 626–639 (2018).

227. Kenderian, S. S. *et al.* CD33-specific chimeric antigen receptor T cells exhibit potent preclinical activity against human acute myeloid leukemia. *Leukemia* **29**, 1637–1647 (2015).

228. Tasian, S. K. Acute myeloid leukemia chimeric antigen receptor T-cell immunotherapy: how far up the road have we traveled? *Ther. Adv. Hematol.* **9**, 135–148 (2018).

229. Kim, M. Y. *et al.* Genetic Inactivation of CD33 in Hematopoietic Stem Cells to Enable CAR T Cell Immunotherapy for Acute Myeloid Leukemia. *Cell* **173**, 1439-1453.e19 (2018).

230. FDA. FDA approves new combination treatment for acute myeloid leukemia. (2017). Available at: https://www.fda.gov/newsevents/newsroom/pressannouncements/ucm555778.htm.

231. FDA. No FDA approves gilteritinib for relapsed or refractory acute myeloid leukemia (AML) with a FLT3 mutationTitle. (2018). Available at: https://www.fda.gov/Drugs/InformationOnDrugs/ApprovedDrugs/ucm627045.htm?elqTrackId=59ec9d8acf7a4434859c31d4661b6dc1&elq=06b09891ba3f48f39ea6e35a5ffb1fd4&elqaid=6065&elqat=1&elqCampaignId=4918.

232. Rosnet, O. *et al.* Human FLT3/FLK2 receptor tyrosine kinase is expressed at the surface of normal and malignant hematopoietic cells. *Leukemia* **10**, 238–48 (1996).

233. Maroc, N. *et al.* Biochemical characterization and analysis of the transforming potential of the FLT3/FLK2 receptor tyrosine kinase. *Oncogene* **8**, 909–18 (1993).

234. Kikushige, Y. *et al.* Human Flt3 is expressed at the hematopoietic stem cell and the granulocyte/macrophage progenitor stages to maintain cell survival. *J. Immunol.* **180**, 7358–67 (2008).

235. Gotze, K. S. *et al.* Flt3high and Flt3low CD34+ progenitor cells isolated from human bone marrow are functionally distinct. *Blood* **91**, 1947–58 (1998).

236. Del Zotto, G., Luchetti, F. & Zamai, L. CD135. *J. Biol. Regul. Homeost. Agents* **15**, 103–6

237. Savvides, S. N., Boone, T. & Karplus, P. A. letters Flt3 ligand structure and unexpected commonalities of helical bundles and cystine knots. **7**, 486–491 (2000).

238. Lyman, S. D. Biology of flt3 ligand and receptor. *Int. J. Hematol.* **62**, 63–73 (1995).

239. Wodnar-Filipowicz, A. Flt3 ligand: role in control of hematopoietic and immune functions of the bone marrow. *News Physiol. Sci.* **18**, 247–51 (2003).

240. Lisovsky, M. *et al.* Flt3-ligand production by human bone marrow stromal cells. *Leukemia* **10**, 1012–8 (1996).

241. Yonemura, Y., Ku, H., Lyman, S. D. & Ogawa, M. In vitro expansion of hematopoietic progenitors and maintenance of stem cells: comparison between FLT3/FLK-2 ligand and KIT ligand. *Blood* **89**, 1915–21 (1997).

242. Scholl, C., Gilliland, D. G. & Fröhling, S. Deregulation of Signaling Pathways in Acute Myeloid Leukemia. *Semin. Oncol.* **35**, 336–345 (2008).

243. Gary Gilliland, D. & Griffin, J. D. The roles of FLT3 in hematopoiesis and leukemia. *Blood* **100**, 1532–1542 (2002).

244. Zhang, S., Mantel, C. & Broxmeyer, H. E. Flt3 signaling involves tyrosyl-phosphorylation of SHP-2 and SHIP and their association with Grb2 and Shc in Baf3/Flt3 cells. *J. Leukoc. Biol.* **65**, 372–80 (1999).

245. Xu, Q. Survival of acute myeloid leukemia cells requires PI3 kinase activation. *Blood* **102**, 972–980 (2003).

246. Takahashi, S. Inhibition of the MEK/MAPK signal transduction pathway strongly impairs the growth of Flt3-ITD cells. *Am. J. Hematol.* **81**, 154–155 (2006).

247. Hayakawa, F. *et al.* Tandem-duplicated Flt3 constitutively activates STAT5 and MAP kinase and introduces autonomous cell growth in IL-3-dependent cell lines. *Oncogene* **19**, 624–631 (2000).

248. Agnès, F. *et al.* Genomic structure of the downstream part of the human FLT3 gene: exon/intron structure conservation among genes encoding receptor tyrosine kinases (RTK) of subclass III. *Gene* **145**, 283–8 (1994).

249. Lyman, S. D. & Jacobsen, S. E. c-kit ligand and Flt3 ligand: stem/progenitor cell factors with overlapping yet distinct activities. *Blood* **91**, 1101–34 (1998).

250. Markovic, A., MacKenzie, K. L. & Lock, R. B. FLT-3: a new focus in the understanding of acute leukemia. *Int. J. Biochem. Cell Biol.* **37**, 1168–1172 (2005).

251. Smith, C. C. *et al.* Characterizing and Overriding the Structural Mechanism of the Quizartinib-Resistant FLT3 “Gatekeeper” F691L Mutation with PLX3397. *Cancer Discov* **5**, 668–679 (2015).

252. Zorn, J. A., Wang, Q., Fujimura, E., Barros, T. & Kuriyan, J. Crystal structure of the FLT3 kinase domain bound to the inhibitor quizartinib (AC220). *PLoS One* **10**, e0121177 (2015).

253. Yamaura, T. *et al.* A novel irreversible FLT3 inhibitor, FF-10101, shows excellent efficacy against AML cells with FLT3 mutations. *Blood* **131**, 426–438 (2018).

254. Verstraete, K. *et al.* Structural insights into the extracellular assembly of the hematopoietic Flt3 signaling complex. *Blood* **118**, 60–68 (2011).

255. Razumovskaya, E., Masson, K., Khan, R., Bengtsson, S. & Rönnstrand, L. Oncogenic Flt3 receptors display different specificity and kinetics of autophosphorylation. *Exp. Hematol.* **37**, 979–989 (2009).

256. Mol, C. D. *et al.* Structure of a c-Kit Product Complex Reveals the Basis for Kinase Transactivation. *J. Biol. Chem.* **278**, 31461–31464 (2003).

257. Lemmon, M. A. & Schlessinger, J. Cell Signaling by Receptor Tyrosine Kinases. *Cell* **141**, 1117–1134 (2010).

258. Berenstein, R. Class III Receptor Tyrosine Kinases in Acute Leukemia – Biological Functions and Modern Laboratory Analysis. *Biomark. Insights* **10s3**, BMI.S22433 (2015).

259. Zarrinkar, P. P. *et al.* AC220 is a uniquely potent and selective inhibitor of FLT3 for the treatment of acute myeloid leukemia (AML). *Myeloid Neoplasia* **114**, 2984–2992 (2009).

260. Chen, Y. *et al.* Tyrosine kinase inhibitors targeting FLT3 in the treatment of acute myeloid leukemia. 1–13 (2017). doi:10.21037/sci.2017.05.04

261. O'Donnell, M. R. *et al.* Acute Myeloid Leukemia, Version 3.2017, NCCN Clinical Practice Guidelines in Oncology. *J. Natl. Compr. Cancer Netw.* **15**, 926–957 (2017).

262. Nakao, M. *et al.* Internal tandem duplication of the flt3 gene found in acute myeloid leukemia. *Leukemia* **10**, 1911–8 (1996).

263. Abu-Duhier, F. M. *et al.* Identification of novel FLT-3 Asp835 mutations in adult acute myeloid leukaemia. *Br. J. Haematol.* **113**, 983–988 (2001).

264. Kiyoi, H., Ohno, R., Ueda, R., Saito, H. & Naoe, T. Mechanism of constitutive activation of FLT3 with internal tandem duplication in the juxtamembrane domain. *Oncogene* **21**, 2555–2563 (2002).

265. Yamaguchi, H. *et al.* Multistep pathogenesis of leukemia via the MLL-AF4 chimeric gene/Flt3 gene tyrosine kinase domain (TKD) mutation-related enhancement of S100A6 expression. *Exp. Hematol.* **37**, 701–14 (2009).

266. Kayser, S. *et al.* Insertion of FLT3 internal tandem duplication in the tyrosine kinase domain-1 is associated with resistance to chemotherapy and inferior outcome. *Blood* **114**, 2386–2392 (2009).

267. Bacher, U., Haferlach, C., Kern, W., Haferlach, T. & Schnittger, S. Prognostic relevance of FLT3-TKD mutations in AML: the combination matters--an analysis of 3082 patients. *Blood* **111**, 2527–2537 (2008).

268. Weir, M. C. *et al.* Dual inhibition of Fes and Flt3 tyrosine kinases potently inhibits Flt3-ITD+ AML cell growth. *PLoS One* **12**, e0181178 (2017).

269. Meierhoff, G. *et al.* Expression of FLT3 receptor and FLT3-ligand in human leukemia-lymphoma cell lines. *Leukemia* **9**, 1368–72 (1995).

270. Schwartz, G. W. *et al.* Classes of ITD predict outcomes in AML patients treated with FLT3 inhibitors. *Clin. Cancer Res.* clincanres.0655.2018 (2018). doi:10.1158/1078-0432.CCR-18-0655

271. Gale, R. E. *et al.* The impact of FLT3 internal tandem duplication mutant level, number, size, and interaction with NPM1 mutations in a large cohort of young adult patients with acute myeloid leukemia. *Blood* **111**, 2776–2784 (2008).

272. Schnittger, S. *et al.* Prognostic impact of FLT3-ITD load in NPM1 mutated acute myeloid leukemia. *Leuk. Off. J. Leuk. Soc. Am. Leuk. Res. Fund, U.K* **25**, 1297–1304 (2011).

273. Chu, S. H. *et al.* FLT3-ITD knockin impairs hematopoietic stem cell quiescence/homeostasis, leading to myeloproliferative neoplasm. *Cell Stem Cell* **11**, 346–358 (2012).

274. Mizuki, M. *et al.* Flt3 mutations from patients with acute myeloid leukemia induce transformation of 32D cells mediated by the Ras and STAT5 pathways. *Blood* **96**, 3907–14 (2000).

275. Bolouri, H. *et al.* The molecular landscape of pediatric acute myeloid leukemia reveals recurrent structural alterations and age-specific mutational interactions. *Nat. Med.* **24**, 103–112 (2018).

276. Smith, C. C. *et al.* Validation of ITD mutations in FLT3 as a therapeutic target in human acute myeloid leukaemia. *Nature* **485**, 260–263 (2012).

277. Daver, N., Schlenk, R. F., Russell, N. H. & Levis, M. J. Targeting FLT3 mutations in AML : review of current knowledge and evidence. *Leukemia* 299–312 (2019). doi:10.1038/s41375-018-0357-9

278. Badar, T. *et al.* Improvement in clinical outcome of FLT3 ITD mutated acute myeloid leukemia patients over the last one and a half decade. *Am. J. Hematol.* **90**, 1065–1070 (2015).

279. Smith, B. D. Single-agent CEP-701, a novel FLT3 inhibitor, shows biologic and clinical activity in patients with relapsed or refractory acute myeloid leukemia. *Blood* **103**, 3669–3676 (2004).

280. Pratz, K. W. *et al.* A pharmacodynamic study of the FLT3 inhibitor KW-2449 yields insight into the basis for clinical response. *Blood* **113**, 3938–3946 (2009).

281. Fiedler, W. et al. A phase I/II study of sunitinib and intensive chemotherapy in patients over 60 years of age with acute myeloid leukaemia and activating FLT3 mutations. *Br. J. Haematol.* **169**, 694–700 (2015).

282. Röllig, C. *et al.* Addition of sorafenib versus placebo to standard therapy in patients aged 60 years or younger with newly diagnosed acute myeloid leukaemia (SORAML): a multicentre, phase 2, randomised controlled trial. *Lancet Oncol.* **16**, 1691–1699 (2015).

283. Stone, R. M. Patients with acute myeloid leukemia and an activating mutation in FLT3 respond to a small-molecule FLT3 tyrosine kinase inhibitor, PKC412. *Blood* **105**, 54–60 (2005).

284. Levis, M. *et al.* Results from a randomized trial of salvage chemotherapy followed by lestaurtinib for patients with FLT3 mutant AML in first relapse. *Blood* **117**, 3294–3301 (2011).

285. Knapper, S. *et al.* A randomized assessment of adding the kinase inhibitor lestaurtinib to first-line chemotherapy for FLT3-mutated AML. *Blood* **129**, 1143–1154 (2017).

286. Fiedler, W. A phase 1 study of SU11248 in the treatment of patients with refractory or resistant acute myeloid leukemia (AML) or not amenable to conventional therapy for the disease. *Blood* **105**, 986–993 (2004).

287. Borthakur, G. *et al.* Phase I study of sorafenib in patients with refractory or relapsed acute leukemias. *Haematologica* **96**, 62–68 (2011).

288. Serve, H. *et al.* Sorafenib in Combination With Intensive Chemotherapy in Elderly Patients With Acute Myeloid Leukemia: Results From a Randomized, Placebo-Controlled Trial. *J. Clin. Oncol.* **31**, 3110–3118 (2013).

289. Ravandi, F. *et al.* Phase 2 study of azacytidine plus sorafenib in patients with acute myeloid leukemia and FLT-3 internal tandem duplication mutation. *Blood* **121**, 4655–4662 (2013).

290. Ravandi, F. *et al.* Final report of phase II study of sorafenib, cytarabine and idarubicin for initial therapy in younger patients with acute myeloid leukemia. *Leukemia* **28**, 1543–1545 (2014).

291. Chen, Y.-B. *et al.* Phase I Trial of Maintenance Sorafenib after Allogeneic Hematopoietic Stem Cell Transplantation for Fms-like Tyrosine Kinase 3 Internal Tandem Duplication Acute Myeloid Leukemia. *Biol. Blood Marrow Transplant.* **20**, 2042–2048 (2014).

292. Fischer, T. *et al.* Phase IIB Trial of Oral Midostaurin (PKC412), the FMS-Like Tyrosine Kinase 3 Receptor (FLT3) and Multi-Targeted Kinase Inhibitor, in Patients With Acute Myeloid Leukemia and High-Risk Myelodysplastic Syndrome With Either Wild-Type or Mutated FLT3. *J. Clin. Oncol.* **28**, 4339–4345 (2010).

293. Stone, R. M. *et al.* The Addition of Midostaurin to Standard Chemotherapy Decreases Cumulative Incidence of Relapse (CIR) in the International Prospective Randomized, Placebo-Controlled, Double-Blind Trial (CALGB 10603 / RATIFY [Alliance]) for Newly Diagnosed Acute Myeloid Le. in *The American Society of Hematology* (2017).

294. Novartis. Novartis receives FDA approval for Rydapt® in newly diagnosed FLT3-mutated acute myeloid leukemia (AML) and three types of systemic mastocytosis (SM). (2017). Available at: https://www.novartis.com/news/media-releases/novartis-receives-fda-approval-rydaptr-newly-diagnosed-flt3-mutated-acute. (Accessed: 4th September 2019)

295. Rydapt SMC. (2017). Available at: https://www.ema.europa.eu/en/documents/product-information/rydapt-epar-product-information_en.pdf.

296. Döhner, K. *et al.* Prognostic Impact of NPM1/FLT3-ITD genotypes from Randomized Patients with Acute Myeloid Leukemia (AML) Treated within the International Ratify Study. in (2017).

297. Richard F. Schlenk *et al.* Impact of Age and Midostaurin-Dose on Response and Outcome in Acute Myeloid Leukemia with FLT3-ITD: Interim-Analyses of the AMLSG 16-10 Trial. in *The American Society of Hematology* (2016).

298. Anastassiadis, T., Deacon, S. W., Devarajan, K., Ma, H. & Peterson, J. R. Comprehensive assay of kinase catalytic activity reveals features of kinase inhibitor selectivity. *Nature biotechnology* **29**, 1039–45 (2011).

299. Perl, A. E. *et al.* Selective inhibition of FLT3 by gilteritinib in relapsed or refractory acute myeloid leukaemia: a multicentre, first-in-human, open-label, phase 1–2 study. *Lancet Oncol.* **18**, 1061–1075 (2017).

300. Tallman, M. S. *et al.* Results Of a Phase 2 Randomized, Open-Label, Study Of Lower Doses Of Quizartinib (AC220; ASP2689) In Subjects With FLT3-ITD Positive Relapsed Or Refractory Acute Myeloid Leukemia (AML). *Blood* **122**, 494 (2013).

301. Smith, C. C. *et al.* Crenolanib is a selective type I pan-FLT3 inhibitor. *Proc. Natl. Acad. Sci. U. S. A.* **111**, 5319–24 (2014).

302. Levis, M. J. *et al.* Final Results of a Phase 2 Open-Label, Monotherapy Efficacy and Safety Study of Quizartinib (AC220) in Patients with FLT3-ITD Positive or Negative Relapsed/Refractory Acute Myeloid Leukemia After Second-Line Chemotherapy or Hematopoietic Stem Cell Transpl. *Blood* **120**, 673 (2012).

303. Smith, C. C. *et al.* Heterogeneous resistance to quizartinib in acute myeloid leukemia revealed by single-cell analysis. *Blood* **130**, 48–58 (2017).

304. DAIICHI SANKYO COMPANY. FDA Grants Breakthrough Therapy Designation to Daiichi Sankyo's FLT3 Inhibitor Quizartinib for Relapsed/Refractory FLT3-ITD AML. (2018). Available at: https://www.daiichisankyo.com/media_investors/media_relations/press_releases/detail/006896.html.

305. Lewis, N. L. *et al.* Phase I Study of the Safety, Tolerability, and Pharmacokinetics of Oral CP-868,596, a Highly Specific Platelet-Derived Growth Factor Receptor Tyrosine Kinase Inhibitor in Patients With Advanced Cancers. *J. Clin. Oncol.* **27**, 5262–5269 (2009).

306. Heinrich, M. C. *et al.* Crenolanib inhibits the drug-resistant PDGFRA D842V mutation associated with imatinib-resistant gastrointestinal stromal tumors. *Clin. Cancer Res.* **18**, 4375–4384 (2012).

307. Randhawa, J. K. *et al.* Results of a Phase II Study of Crenolanib in Relapsed/Refractory Acute Myeloid Leukemia Patients (Pts) with Activating FLT3 Mutations. in *The American Society of Hematology* (2014).

308. Cortes, J. E. *et al.* Crenolanib besylate, a type I pan-FLT3 inhibitor, to demonstrate clinical activity in multiply relapsed FLT3-ITD and D835 AML. *J. Clin. Oncol.* **34**, 7008–7008 (2016).

309. Lee, L. Y. *et al.* Preclinical studies of gilteritinib, a next-generation FLT3 inhibitor. *Blood* **129**, 257–260 (2017).

310. Park, I.-K. *et al.* Inhibition of the receptor tyrosine kinase Axl impedes activation of the FLT3 internal tandem duplication in human acute myeloid leukemia: implications for Axl as a potential therapeutic target. *Blood* **121**, 2064–2073 (2013).

311. Weisberg, E., Sattler, M., Ray, a & Griffin, J. D. Drug resistance in mutant FLT3-positive AML. *Oncogene* **29**, 5120–5134 (2010).

312. Heidel, F. *et al.* Clinical resistance to the kinase inhibitor PKC412 in acute myeloid leukemia by mutation of Asn-676 in the FLT3 tyrosine kinase domain. *Blood* **107**, 293–300 (2006).

313. Cools, J. *et al.* Prediction of resistance to small molecule FLT3 inhibitors: implications for molecularly targeted therapy of acute leukemia. *Cancer Res.* **64**, 6385–9 (2004).

314. Smith, C. C., Lin, K., Stecula, A., Sali, A. & Shah, N. P. FLT3 D835 mutations confer differential resistance to type II FLT3 inhibitors. *Leukemia* **29**, 2390–2392 (2015).

315. Smith, C. C. *et al.* Activity of ponatinib against clinically-relevant AC220-resistant kinase domain mutants of FLT3-ITD. *Blood* **121**, 3165–3171 (2013).

316. Zhang, W. *et al.* Reversal of acquired drug resistance in FLT3-mutated acute myeloid leukemia cells via distinct drug combination strategies. *Clin. Cancer Res.* **20**, 2363–2374 (2014).

317. Piloto, O. *et al.* Prolonged exposure to FLT3 inhibitors leads to resistance via activation of parallel signaling pathways. *Blood* **109**, 1643–1652 (2007).

318. Yang, X., Sexauer, A. & Levis, M. Bone marrow stroma-mediated resistance to FLT3 inhibitors in FLT3-ITD AML is mediated by persistent activation of extracellular regulated kinase. *Br. J. Haematol.* **164**, 61–72 (2014).

319. Traer, E. *et al.* FGF2 from Marrow Microenvironment Promotes Resistance to FLT3 Inhibitors in Acute Myeloid Leukemia. *Cancer Res.* **76**, 6471–6482 (2016).

320. Zhang, W. *et al.* Study Of Activity Of E6201, a Dual FLT3 and MEK Inhibitor, In Acute Myelogenous Leukemia With FLT3 Or RAS Mutation. in *The American Society of Hematology* (2013).

321. Fukuda, S. Flt3 ligand and the Flt3 receptor regulate hematopoietic cell migration by modulating the SDF-1 (CXCL12)/CXCR4 axis. *Blood* **105**, 3117–3126 (2005).

322. Rombouts, E. J. C. Relation between CXCR-4 expression, Flt3 mutations, and unfavorable prognosis of adult acute myeloid leukemia. *Blood* **104**, 550–557 (2004).

323. Zeng, Z. *et al.* Targeting the leukemia microenvironment by CXCR4 inhibition overcomes resistance to kinase inhibitors and chemotherapy in AML. *Blood* **113**, 6215–6224 (2009).

324. Zhang, H. *et al.* Clinical resistance to crenolanib in acute myeloid leukemia due to diverse molecular mechanisms. *Nat. Commun.* **10**, 244 (2019).

325. Piloto, O. *et al.* Inhibitory anti-FLT3 antibodies are capable of mediating antibody-dependent cell-mediated cytotoxicity and reducing engraftment of acute myelogenous leukemia blasts in nonobese diabetic/severe combined immunodeficient mice. *Cancer Res.* **65**, 1514–1522 (2005).

326. Piloto, O. *et al.* IMC-EB10, an anti-FLT3 monoclonal antibody, prolongs survival and reduces nonobese diabetic/severe combined immunodeficient engraftment of some acute lymphoblastic leukemia cell lines and primary leukemic samples. *Cancer Res.* **66**, 4843–4851 (2006).

327. Chen, L. *et al.* Targeting FLT3 by chimeric antigen receptor T cells for the treatment of acute myeloid leukemia. *Leukemia* **31**, 1830–1834 (2017).

328. Jetani, H. *et al.* CAR T-cells targeting FLT3 have potent activity against FLT3−ITD+AML and act synergistically with the FLT3-inhibitor crenolanib. *Leukemia* (2018). doi:10.1038/s41375-018-0009-0

329. LLC, I. Study of EB10 in Patients With Leukemia. *Clinical Trials GOV* (2009). Available at: https://clinicaltrials.gov/ct2/show/NCT00887926?term=IMC-EB10&rank=1.

330. Hofmann, M. *et al.* Generation, selection and preclinical characterization of an Fc-optimized FLT3 antibody for the treatment of myeloid leukemia. *Leukemia* **26**, 1228–1237 (2012).

331. Ben-Batalla, I. *et al.* Axl, a prognostic and therapeutic target in acute myeloid leukemia mediates paracrine crosstalk of leukemia cells with bone marrow stroma. *Blood* **122**, 2443–2452 (2013).

332. Park, I.-K. *et al.* Receptor tyrosine kinase Axl is required for resistance of leukemic cells to FLT3-targeted therapy in acute myeloid leukemia. *Leukemia* **29**, 2382–2389 (2015).

333. Liu, L. *et al.* Novel Mechanism of Lapatinib Resistance in HER2-Positive Breast Tumor Cells: Activation of AXL. *Cancer Res.* **69**, 6871–6878 (2009).

334. Meyer, A. S., Miller, M. A., Gertler, F. B. & Lauffenburger, D. A. The Receptor AXL Diversifies EGFR Signaling and Limits the Response to EGFR-Targeted Inhibitors in Triple-Negative Breast Cancer Cells. *Sci. Signal.* **6**, ra66–ra66 (2013).

335. Byers, L. A. *et al.* An Epithelial-Mesenchymal Transition Gene Signature Predicts Resistance to EGFR and PI3K Inhibitors and Identifies Axl as a Therapeutic Target for Overcoming EGFR Inhibitor Resistance. *Clin. Cancer Res.* **19**, 279–290 (2013).

336. Zhang, Z. *et al.* Activation of the AXL kinase causes resistance to EGFR-targeted therapy in lung cancer. *Nat. Genet.* **44**, 852–860 (2012).

337. Mahadevan, D. *et al.* A novel tyrosine kinase switch is a mechanism of imatinib resistance in gastrointestinal stromal tumors. *Oncogene* **26**, 3909–3919 (2007).

338. Dufies, M. *et al.* Mechanisms of AXL overexpression and function in Imatinib-resistant chronic myeloid leukemia cells. *Oncotarget* **2**, (2011).

339. Puissant, A. *et al.* SYK Is a Critical Regulator of FLT3 in Acute Myeloid Leukemia. *Cancer Cell* **25**, 226–242 (2014).

340. Boros, K. *et al.* Increased SYK activity is associated with unfavorable outcome among patients with acute myeloid leukemia. *Oncotarget* **6**, (2015).

341. Kuno, Y. *et al.* Constitutive kinase activation of the TEL-Syk fusion gene in myelodysplastic syndrome with t(9;12)(q22;p12). *Blood* **97**, 1050–5 (2001).

342. Zhang, J., Billingsley, M. L., Kincaid, R. L. & Siraganian, R. P. Phosphorylation of Syk Activation Loop Tyrosines Is Essential for Syk Function. *J. Biol. Chem.* **275**, 35442–35447 (2000).

343. Mansueto, M. S. *et al.* A reevaluation of the spleen tyrosine kinase (SYK) activation mechanism. *J. Biol. Chem.* jbc.RA119.008045 (2019). doi:10.1074/jbc.RA119.008045

344. Voisset, E., Lopez, S., Dubreuil, P. & De Sepulveda, P. The tyrosine kinase FES is an essential effector of KITD816V proliferation signal. *Blood* **110**, 2593–2599 (2007).

345. Rous, P. A TRANSMISSIBLE AVIAN NEOPLASM. (SARCOMA OF THE COMMON FOWL.). *J. Exp. Med.* **12**, 696–705 (1910).

346. Rous, P. A SARCOMA OF THE FOWL TRANSMISSIBLE BY AN AGENT SEPARABLE FROM THE TUMOR CELLS. *J. Exp. Med.* **13**, 397–411 (1911).

347. Martin, G. S. The hunting of the Src. *Nat. Rev. Mol. Cell Biol.* **2**, 467–475 (2001).

348. Stehelin, D., Fujita, D. J., Padgett, T., Varmus, H. E. & Bishop, J. M. Detection and enumeration of transformation-defective strains of avian sarcoma virus with molecular hybridization. *Virology* **76**, 675–684 (1977).

349. Stehelin, D., Varmus, H. E., Bishop, J. M. & Vogt, P. K. DNA related to the transforming gene(s) of avian sarcoma viruses is present in normal avian DNA. *Nature* **260**, 170–3 (1976).

350. The Nobel Prize in Physiology or Medicine 1989. *The Nobel Prize* (1989). Available at: https://www.nobelprize.org/prizes/medicine/1989/summary/.

351. Semba, K. *et al.* Location of the c-yes gene on the human chromosome and its expression in various tissues. *Science (80-.).* **227**, 1038–1040 (1985).

352. Rasheed, S., Barbacid, M., Aaronson, S. & Gardner, M. B. Origin and biological properties of a new feline sarcoma virus. *Virology* **117**, 238–244 (1982).

353. Arbesú, M. *et al.* The Unique Domain Forms a Fuzzy Intramolecular Complex in Src Family Kinases. *Structure* **25**, 630-640.e4 (2017).

354. Brown, M. T. & Cooper, J. A. Regulation, substrates and functions of src. *Biochim. Biophys. Acta* **1287**, 121–49 (1996).

355. Resh, M. D. Myristylation and palmitylation of Src family members: the fats of the matter. *Cell* **76**, 411–3 (1994).

356. Resh, M. D. Fatty acylation of proteins: new insights into membrane targeting of myristoylated and palmitoylated proteins. *Biochim. Biophys. Acta* **1451**, 1–16 (1999).

357. Takahashi, A. *et al.* Nuclear localization of Src-family tyrosine kinases is required for growth factor-induced euchromatinization. *Exp. Cell Res.* **315**, 1117–1141 (2009).

358. Shangary, S. *et al.* Lyn regulates the cell death response to ultraviolet radiation through c-Jun N terminal kinase-dependent Fas ligand activation. *Exp. Cell Res.* **289**, 67–76 (2003).

359. Kim, P. W. A Zinc Clasp Structure Tethers Lck to T Cell Coreceptors CD4 and CD8. *Science (80-.).* **301**, 1725–1728 (2003).

360. Hossain, M. I. *et al.* A Truncated Fragment of Src Protein Kinase Generated by Calpain-mediated Cleavage Is a Mediator of Neuronal Death in Excitotoxicity. *J. Biol. Chem.* **288**, 9696–9709 (2013).

361. Luciano, F., Ricci, J.-E. & Auberger, P. Cleavage of Fyn and Lyn in their N-terminal unique regions during induction of apoptosis: a new mechanism for Src kinase regulation. *Oncogene* **20**, 4935–4941 (2001).

362. Liu, X. J. *et al.* Treatment of inflammatory and neuropathic pain by uncoupling Src from the NMDA receptor complex. *Nat. Med.* **14**, 1325–1332 (2008).

363. Pérez, Y. *et al.* Lipid binding by the Unique and SH3 domains of c-Src suggests a new regulatory mechanism. *Sci. Rep.* **3**, 1295 (2013).

364. Amata, I., Maffei, M. & Pons, M. Phosphorylation of unique domains of Src family kinases. *Front. Genet.* **5**, (2014).

365. Maffei, M. *et al.* The SH3 Domain Acts as a Scaffold for the N-Terminal Intrinsically Disordered Regions of c-Src. *Structure* **23**, 893–902 (2015).

366. Tompa, P. & Fuxreiter, M. Fuzzy complexes: polymorphism and structural disorder in protein–protein interactions. *Trends Biochem. Sci.* **33**, 2–8 (2008).

367. Mayer, B. J. & Baltimore, D. Signalling through SH2 and SH3 domains. *Trends Cell Biol.* **3**, 8–13 (1993).

368. Schlessinger, J. SH2/SH3 signaling proteins. *Curr. Opin. Genet. Dev.* **4**, 25–30 (1994).

369. Whisstock, J. C. & Lesk, A. M. SH3 domains in prokaryotes. *Trends Biochem. Sci.* **24**, 132–133 (1999).

370. Saksela, K. & Permi, P. SH3 domain ligand binding: What's the consensus and where's the specificity? *FEBS Lett.* **586**, 2609–2614 (2012).

371. Berry, D. M., Nash, P., Liu, S. K.-W., Pawson, T. & McGlade, C. J. A high-affinity Arg-X-X-Lys SH3 binding motif confers specificity for the interaction between Gads and SLP-76 in T cell signaling. *Curr. Biol.* **12**, 1336–41 (2002).

372. Williams, J. C. *et al.* The 2.35 å crystal structure of the inactivated form of chicken src: a dynamic molecule with multiple regulatory interactions. *J. Mol. Biol.* **274**, 757–775 (1997).

373. Panjarian, S. *et al.* Enhanced SH3/Linker interaction overcomes Abl kinase activation by gatekeeper and myristic acid binding pocket mutations and increases sensitivity to small molecule inhibitors. *J. Biol. Chem.* **288**, 6116–6129 (2013).

374. Grover, P., Shi, H., Baumgartner, M., Camacho, C. J. & Smithgall, T. E. Fluorescence Polarization Screening Assays for Small Molecule Allosteric Modulators of ABL Kinase Function. *PLoS One* **10**, e0133590 (2015).

375. Sadowski, I., Stone, J. C. & Pawson, T. A noncatalytic domain conserved among cytoplasmic protein-tyrosine kinases modifies the kinase function and transforming activity of Fujinami sarcoma virus P130gag-fps. *Mol. Cell. Biol.* **6**, 4396–408 (1986).

376. Koytiger, G. *et al.* Phosphotyrosine Signaling Proteins that Drive Oncogenesis Tend to be Highly Interconnected. *Mol. Cell. Proteomics* **12**, 1204–1213 (2013).

377. Liu, B. A. *et al.* The SH2 Domain-Containing Proteins in 21 Species Establish the Provenance and Scope of Phosphotyrosine Signaling in Eukaryotes. *Sci. Signal.* **4**, ra83–ra83 (2011).

378. Liu, B. A. *et al.* The Human and Mouse Complement of SH2 Domain Proteins—Establishing the Boundaries of Phosphotyrosine Signaling. *Mol. Cell* **22**, 851–868 (2006).

379. Huang, H. *et al.* Defining the Specificity Space of the Human Src Homology 2 Domain. *Mol. Cell. Proteomics* **7**, 768–784 (2008).

380. Weijland, A. *et al.* Src regulated by C-terminal phosphorylation is monomeric. *Proc. Natl. Acad. Sci.* **94**, 3590–3595 (1997).

381. Bergman, M. *et al.* The human p50csk tyrosine kinase phosphorylates p56lck at Tyr-505 and down regulates its catalytic activity. *EMBO J.* **11**, 2919–24 (1992).

382. Chong, Y. P. *et al.* C-terminal Src kinase-homologous kinase (CHK), a unique inhibitor inactivating multiple active conformations of Src family tyrosine kinases. *J. Biol. Chem.* **281**, 32988–32999 (2006).

383. Sun, G. & Budde, R. J. A. Expression, Purification, and Initial Characterization of Human Yes Protein Tyrosine Kinase from a Bacterial Expression System. *Arch. Biochem. Biophys.* **345**, 135–142 (1997).

384. Briggs, S. D., Sharkey, M., Stevenson, M. & Smithgall, T. E. SH3-mediated Hck tyrosine kinase activation and fibroblast transformation by the Nef protein of HIV-1. *J. Biol. Chem.* **272**, 17899–17902 (1997).

385. Shen, K. *et al.* The Src family kinase Fgr is a transforming oncoprotein that functions independently of SH3-SH2 domain regulation. *Sci. Signal.* **11**, (2018).

386. Schreiner, S. J., Schiavone, A. P. & Smithgall, T. E. Activation of STAT3 by the Src Family Kinase Hck Requires a Functional SH3 Domain. *J. Biol. Chem.* **277**, 45680–45687 (2002).

387. Duong-Ly, K. C. & Peterson, J. R. The Human Kinome and Kinase Inhibition as a therapeutic strategy. *Curr Protoc Pharmacolo.* **60**, 2.9.1-2.9.14 (2013).

388. Hunter, T. Signaling--2000 and beyond. *Cell* **100**, 113–27 (2000).

389. Hanks, S. K. & Hunter, T. Protein kinases 6. The eukaryotic protein kinase superfamily: kinase (catalytic) domain structure and classification. *FASEB J.* **9**, 576–96 (1995).

390. Nolen, B., Taylor, S. & Ghosh, G. Regulation of Protein Kinases. *Mol. Cell* **15**, 661–675 (2004).

391. Taylor, S. S. & Kornev, A. P. Protein kinases: evolution of dynamic regulatory proteins. *Trends Biochem. Sci.* **36**, 65–77 (2011).

392. Cowan-Jacob, S. W. Structural biology of protein tyrosine kinases. *Cell. Mol. Life Sci.* **63**, 2608–2625 (2006).

393. Möbitz, H. The ABC of protein kinase conformations. *Biochim. Biophys. Acta - Proteins Proteomics* **1854**, 1555–1566 (2015).

394. Lipsick, J. A history of cancer research: Tyrosine kinases. *Cold Spring Harb. Perspect. Biol.* **11**, 1–20 (2019).

395. Sirvent, A., Benistant, C. & Roche, S. Oncogenic signaling by tyrosine kinases of the SRC family in advanced colorectal cancer. *Am. J. Cancer Res.* **2**, 357–71 (2012).

396. Hynes, N. E. Tyrosine kinase signalling in breast cancer. *Breast Cancer Res.* **2**, 154–7 (2000).

397. Yeatman, T. J. A renaissance for SRC. *Nat. Rev. Cancer* **4**, 470–480 (2004).

398. Santos, D., Prade-houdellier, N., Payrastre, B. & Re, C. A critical role for Lyn in acute myeloid leukemia compartment as revealed by the level of. *Blood* **111**, 2269–2280 (2008).

399. Dos Santos, C. *et al.* The Src and c-Kit kinase inhibitor dasatinib enhances p53-mediated targeting of human acute myeloid leukemia stem cells by chemotherapeutic agents. *Blood* **122**, 1900–13 (2013).

400. Saito, Y. *et al.* Identification of Therapeutic Targets for Quiescent, Chemotherapy-Resistant Human Leukemia Stem Cells. *Sci. Transl. Med.* **2**, 17ra9-17ra9 (2010).

401. Saito, Y. *et al.* A Pyrrolo-Pyrimidine Derivative Targets Human Primary AML Stem Cells in Vivo. *Sci. Transl. Med.* **5**, 181ra52-181ra52 (2013).

402. Koda, Y. *et al.* Identification of pyrrolo [2 , 3- d] pyrimidines as potent HCK and FLT3-ITD dual inhibitors. *Bioorg. Med. Chem. Lett.* **27**, 4994–4998 (2017).

403. Pene-Dumitrescu, T., Peterson, L. F., Donato, N. J. & Smithgall, T. E. An inhibitor-resistant mutant of Hck protects CML cells against the antiproliferative and apoptotic effects of the broad-spectrum Src family kinase inhibitor A-419259. *Oncogene* **27**, 7055–7069 (2008).

404. Pene-Dumitrescu, T. & Smithgall, T. E. Expression of a Src family kinase in chronic myelogenous leukemia cells induces resistance to imatinib in a kinase-dependent manner. *J. Biol. Chem.* **285**, 21446–21457 (2010).

405. Lyn. *The Human Protein Atlas* Available at: https://www.proteinatlas.org/ENSG00000254087-LYN/tissue.

406. Ingley, E. Functions of the Lyn tyrosine kinase in health and disease. *Cell Commun. Signal.* **10**, 21 (2012).

407. Ozawa, Y. *et al.* Src family kinases promote AML cell survival through activation of signal transducers and activators of transcription (STAT). **32**, 893–903 (2008).

408. Zhang, Q., Meng, X., Qin, G., Xue, X. & Dang, N. Lyn kinase promotes the proliferation of malignant melanoma cells through inhibition of apoptosis and autophagy via the PI3K/Akt signaling pathway. *J. Cancer* **10**, 1197–1208 (2019).

409. Weir, M. C. *et al.* Selective Inhibition of the Myeloid Src-Family Kinase Fgr Potently Suppresses AML Cell Growth in Vitro and in Vivo. *ACS Chem. Biol.* **13**, 1551–1559 (2018).

410. Zhang, W. *et al.* The dual MEK/FLT3 inhibitor E6201 exerts cytotoxic activity against acute myeloid leukemia cells harboring resistance-conferring FLT3 mutations. *Cancer Res.* (2016). doi:10.1158/0008-5472.CAN-15-1580

411. Tibes, R. *et al.* Safety, pharmacokinetics, and preliminary efficacy of E6201 in patients with advanced solid tumours, including melanoma: results of a phase 1 study. *Br. J. Cancer* **118**, 1580–1585 (2018).

412. Kim, K. *et al.* Pim-1 is up-regulated by constitutively activated FLT3 and plays a role in FLT3-mediated cell survival. **105**, 1759–1768 (2016).

413. Green, A. S. *et al.* Pim kinases modulate resistance to FLT3 tyrosine kinase inhibitors in FLT3-ITD acute myeloid leukemia. *Sci. Adv.* **1**, e1500221–e1500221 (2015).

414. Okada, K. *et al.* FLT3-ITD induces expression of Pim kinases through STAT5 to confer resistance to the PI3K/Akt pathway inhibitors on leukemic cells by enhancing the mTORC1/Mcl-1 pathway. *Oncotarget* **9**, 8870–8886 (2018).

415. Czardybon, W. *et al.* A novel, dual pan-PIM/FLT3 inhibitor SEL24 exhibits broad therapeutic potential in acute myeloid leukemia. *Oncotarget* **9**, 16917–16931 (2018).

416. Puente-Moncada, N. *et al.* Inhibition of Flt3 and Pim Kinases By Ec-70124 Exerts Potent Activity in Preclinical Models of Acute Myeloid Leukemia. *Mol. Cancer Ther.* molcanther.0530.2017 (2018). doi:10.1158/1535-7163.MCT-17-0530

417. Drexler, H. Review of alterations of the cyclin-dependent kinase inhibitor INK4 family genes p15, p16, p18 and p19 in human leukemia–lymphoma cells. *Leukemia* **12**, 845–859 (1998).

418. Wang, L. *et al.* Pharmacologic inhibition of CDK4 / 6 : mechanistic evidence for selective activity or acquired resistance in acute myeloid leukemia. **110**, 2075–2083 (2007).

419. Li, Z. *et al.* Discovery of AMG 925, a FLT3 and CDK4 dual kinase inhibitor with preferential affinity for the activated state of FLT3. *J. Med. Chem.* **57**, 3430–3449 (2014).

420. Keegan, K. *et al.* Preclinical evaluation of AMG 925, a FLT3/CDK4 dual kinase inhibitor for treating acute myeloid leukemia. *Mol. Cancer Ther.* **13**, 880–9 (2014).

421. Li, C. *et al.* AMG 925 is a dual FLT3/CDK4 inhibitor with the potential to overcome FLT3 inhibitor resistance in acute myeloid leukemia. *Mol. Cancer Ther.* **14**, 375–83 (2015).

422. Daver, N. *et al.* A Phase I Study of FLX925, a Dual FLT3 and CDK4/6 Inhibitor in Patients with Relapsed or Refractory Acute Myeloid Leukemia (AML). *The American Society of Hematology* (2017). Available at: http://www.bloodjournal.org/content/130/Suppl_1/1343.

423. Anderson, K. *et al.* Genetic variegation of clonal architecture and propagating cells in leukaemia. *Nature* **469**, 356–61 (2011).

424. Ford, A. M. *et al.* In utero rearrangements in the trithorax-related oncogene in infant leukaemias. *Nature* **363**, 358–360 (1993).

425. Mori, H. *et al.* Chromosome translocations and covert leukemic clones are generated during normal fetal development. *Proc. Natl. Acad. Sci.* **99**, 8242–8247 (2002).

426. Busque, L. *et al.* Recurrent somatic TET2 mutations in normal elderly individuals with clonal hematopoiesis. *Nat. Genet.* **44**, 1179–1181 (2012).

427. Schick, U. M. *et al.* Confirmation of the Reported Association of Clonal Chromosomal Mosaicism with an Increased Risk of Incident Hematologic Cancer. *PLoS One* **8**, e59823 (2013).

428. Takahashi, S. Current findings for recurring mutations in acute myeloid leukemia. *J. Hematol. Oncol.* **4**, 36 (2011).

429. Lichtman, M. A. A historical perspective on the development of the cytarabine (7days) and daunorubicin (3days) treatment regimen for acute myelogenous leukemia: 2013 the 40th anniversary of 7+3. *Blood Cells, Mol. Dis.* **50**, 119–130 (2013).

430. Birg, F. *et al.* Expression of the FMS/KIT-like gene FLT3 in human acute leukemias of the myeloid and lymphoid lineages. *Blood* **80**, 2584–93 (1992).

431. Parcells, B. W., Ikeda, A. K., Simms-Waldrip, T., Moore, T. B. & Sakamoto, K. M. FMS-like tyrosine kinase 3 in normal hematopoiesis and acute myeloid leukemia. *Stem Cells* **24**, 1174–1184 (2006).

432. Janke, H. *et al.* Activating FLT3 Mutants Show Distinct Gain-of-Function Phenotypes In Vitro and a Characteristic Signaling Pathway Profile Associated with Prognosis in Acute Myeloid Leukemia. *PLoS One* **9**, e89560 (2014).

433. Kottaridis, P. D. *et al.* The presence of a FLT3 internal tandem duplication in patients with acute myeloid leukemia (AML) adds important prognostic information to cytogenetic risk group and response to the first cycle of chemotherapy: analysis of 854 patients from the United King. *Blood* **98**, 1752–9 (2001).

434. Cortes, J. E. *et al.* Phase I study of quizartinib administered daily to patients with relapsed or refractory acute myeloid leukemia irrespective of FMS-like tyrosine kinase 3-internal tandem duplication status. *J. Clin. Oncol.* **31**, 3681–3687 (2013).

435. Cortes, J. *et al.* Quizartinib, an FLT3 inhibitor, as monotherapy in patients with relapsed or refractory acute myeloid leukaemia: an open-label, multicentre, single-arm, phase 2 trial. *Lancet. Oncol.* **19**, 889–903 (2018).

436. Wander, S. A., Levis, M. J. & Fathi, A. T. The evolving role of FLT3 inhibitors in acute myeloid leukemia: quizartinib and beyond. *Ther. Adv. Hematol.* **5**, 65–77 (2014).

437. Ostronoff, F. & Estey, E. The role of quizartinib in the treatment of acute myeloid leukemia. *Expert Opin. Investig. Drugs* **22**, 1659–69 (2013).

438. Sudhindra, A. & Smith, C. C. FLT3 inhibitors in AML: Are we there yet? *Curr. Hematol. Malig. Rep.* **9**, 174–185 (2014).

439. Von Bubnoff, N. *et al.* FMS-like tyrosine kinase 3-internal tandem duplication tyrosine kinase inhibitors display a nonoverlapping profile of resistance mutations in vitro. *Cancer Res.* **69**, 3032–3041 (2009).

440. Zhou, J. *et al.* Enhanced activation of STAT pathways and overexpression of survivin confer resistance to FLT3 inhibitors and could be therapeutic targets in AML. *Blood* **113**, 4052–4062 (2009).

441. Sato, T. *et al.* FLT3 ligand impedes the efficacy of FLT3 inhibitors in vitro and in vivo. *Blood* **117**, 3286–93 (2011).

442. Grundler, R. *et al.* Dissection of PIM serine/threonine kinases in FLT3-ITD-induced leukemogenesis reveals PIM1 as regulator of CXCL12-CXCR4-mediated homing and migration. *J. Exp. Med.* **206**, 1957–70 (2009).

443. Mitina, O., Warmuth, M., Krause, G., Hallek, M. & Obermeier, A. Src family tyrosine kinases phosphorylate Flt3 on juxtamembrane tyrosines and interfere with receptor maturation in a kinase-dependent manner. *Ann. Hematol.* **86**, 777–785 (2007).

444. Saito, Y. *et al.* Identification of therapeutic targets for quiescent, chemotherapy-resistant human leukemia stem cells. *Sci. Transl. Med.* **2**, 17ra9 (2010).

445. Karaman, M. W. *et al.* A quantitative analysis of kinase inhibitor selectivity. *Nat. Biotechnol.* **26**, 127–32 (2008).

446. Kitamura, T. *et al.* Establishment and characterization of a unique human cell line that proliferates dependently on GM-CSF, IL-3, or erythropoietin. *J. Cell. Physiol.* **140**, 323–34 (1989).

447. Parker, L. J. *et al.* Kinase crystal identification and ATP-competitive inhibitor screening using the fluorescent ligand SKF86002. *Acta Crystallogr. Sect. D Biol. Crystallogr.* **70**, 392–404 (2014).

448. Coffey, G. *et al.* Specific Inhibition of Spleen Tyrosine Kinase Suppresses Leukocyte Immune Function and Inflammation in Animal Models of Rheumatoid Arthritis. *J. Pharmacol. Exp. Ther.* **340**, 350–359 (2012).

449. Kiyoi, H. FLT3 inhibitors: Recent advances and problems for clinical application. *Nagoya J. Med. Sci.* **77**, 7–17 (2015).

450. Kesarwani, M., Huber, E. & Azam, M. Overcoming AC220 resistance of FLT3-ITD by SAR302503. *Blood Cancer J.* **3**, e138 (2013).

451. Fabian, M. A. *et al.* A small molecule-kinase interaction map for clinical kinase inhibitors. *Nat. Biotechnol.* **23**, 329–36 (2005).

452. Rodems, S. M. *et al.* A FRET-based assay platform for ultra-high density drug screening of protein kinases and phosphatases. *Assay Drug Dev. Technol.* **1**, 9–19 (2002).

453. Hellwig, S. *et al.* Small-molecule inhibitors of the c-Fes protein-tyrosine kinase. *Chem. Biol.* **19**, 529–540 (2012).

454. Van der Auwera, G. A. *et al.* From FastQ Data to High-Confidence Variant Calls: The Genome Analysis Toolkit Best Practices Pipeline. in *Current Protocols in Bioinformatics* **11**, 11.10.1-11.10.33 (John Wiley & Sons, Inc., 2013).

455. Bolger, A. M., Lohse, M. & Usadel, B. Trimmomatic: A flexible trimmer for Illumina sequence data. *Bioinformatics* **30**, 2114–2120 (2014).

456. Li, H. Aligning sequence reads, clone sequences and assembly contigs with BWA-MEM. *arXiv Prepr. arXiv1303.3997* (2013). doi:10.1093/bioinformatics/bts280

457. Picard. *http://broadinstitute.github.io/picard/*

458. McKenna, A. *et al.* The Genome Analysis Toolkit: a MapReduce framework for analyzing next-generation DNA sequencing data. *Genome Res.* **20**, 1297–303 (2010).

459. Cingolani, P. *et al.* A program for annotating and predicting the effects of single nucleotide polymorphisms, SnpEff: SNPs in the genome of Drosophila melanogaster strain w1118; iso-2; iso-3. *Fly (Austin).* **6**, 80–92 (2012).

460. Wong, W. C. *et al.* CHASM and SNVBox: Toolkit for detecting biologically important single nucleotide mutations in cancer. *Bioinformatics* **27**, 2147–2148 (2011).

461. Carter, H. *et al.* Mutations : computational prediction of driver missense mutations. *Cancer* **69**, 6660–6667 (2010).

462. Anastassiadis, T., Deacon, S. W., Devarajan, K., Ma, H. & Peterson, J. R. Comprehensive assay of kinase catalytic activity reveals features of kinase inhibitor selectivity. *Nature Biotechnology* **29**, 1039–1045 (2011).

463. Barretina, J. *et al.* The Cancer Cell Line Encyclopedia enables predictive modelling of anticancer drug sensitivity. *Nature* **483**, 603–607 (2012).

464. Walensky, L. D. Activation of Apoptosis in Vivo by a Hydrocarbon-Stapled BH3 Helix. *Science (80-.).* **305**, 1466–1470 (2004).

465. Schoepfer, J. *et al.* Discovery of Asciminib (ABL001), an Allosteric Inhibitor of the Tyrosine Kinase Activity of BCR-ABL1. *J. Med. Chem.* **61**, 8120–8135 (2018).

466. Wylie, A. A. *et al.* The allosteric inhibitor ABL001 enables dual targeting of BCR–ABL1. *Nature* 1–10 (2017). doi:10.1038/nature21702

467. Gu, S., Cui, D., Chen, X., Xiong, X. & Zhao, Y. PROTACs: An Emerging Targeting Technique for Protein Degradation in Drug Discovery. *BioEssays* **40**, 1700247 (2018).

468. Winter, G. E. *et al.* Phthalimide conjugation as a strategy for in vivo target protein degradation. *Science* **348**, 1376–81 (2015).